

**ISOLATION AND EVOLUTION OF NOVEL
NUCLEOSIDE PHOSPHORYLASES**

A thesis submitted in fulfilment of the requirements for the
degree of

**DOCTOR OF PHILOSOPHY
(BIOCHEMISTRY)**

at

RHODES UNIVERSITY

by

DANIEL FINSCH VISSER

August 2010

ABSTRACT

Approximately 33.4 million people are living with HIV/AIDS. Of those, 97% live in low and middle income countries, with 22.4 million in sub-Saharan Africa. Only 42% of the people who require anti-retrovirals (ARVs) in low to middle income countries are receiving anti-retroviral therapy (ART). There is a need to develop novel and cost effective methods for producing antiretroviral drugs. Stavudine and azidothymidine (AZT) were identified as potential targets because they could both be produced through a common intermediate – 5 methyluridine (5-MU). It has been established that the biocatalytic production of 5-methyluridine is possible through a reaction known as transglycosylation, in a process which has not previously been demonstrated as commercially viable.

A selection of biocatalysts were expressed either in recombinant *E. coli* strains or in the wild type organisms, purified and then screened for their ability to produce 5-MU. A combination of *Bacillus halodurans* purine nucleoside phosphorylase 1 (BHPNP1) and *E. coli* uridine phosphorylase (EcUP) gave the highest 5-MU yield (80%). This result represents the first combination of free enzymes from different organisms, giving high yields of 5-MU under high substrate conditions. Both enzymes were purified and successfully characterised. The established pH optimum was pH 7.0 for both enzymes. Temperature optima and stability data for BHPNP1 (70°C and $t_{1/2}$ at 60°C of 20.8 h) indicated that the biocatalytic step was operating within the capabilities of this enzyme and would operate well at elevated temperatures (up to 60°C). Conversely, the temperature optimum and stability data for EcUP (optimum of 40°C and $t_{1/2}$ at 60°C of 9.9 h) indicated that the enzyme remained active at 40°C for the duration of a 25 h biotransformation, but at 60°C would only be operating at

ABSTRACT

20% of its optimum activity and would lose activity rapidly. BHPNP1 and EcUP were used in a bench scale (650 ml) transglycosylation for the production of 5-MU. A 5-MU yield of 79.1% was obtained at this scale with a reactor productivity of 1.37 g.l⁻¹.h⁻¹.

Iterative saturation mutagenesis was used to rapidly evolve EcUP for improved thermostability. A moderately high throughput colorimetric method was developed for screening the mutants based on the release of *p*-nitrophenol upon phosphorolysis of a pyrimidine nucleoside analogue. By screening under 20 000 clones the mutant UPL8 was isolated. The mutant enzyme showed an optimum temperature of 60°C and improved stability at 60°C ($t_{1/2} = 17.3$ h). The increase in stability of UPL8 is due to only 2 mutations (Lys235Arg, Gln236Ala). These mutations may have caused an increase in stability due to interactions with other structural units in the protein, stabilization of the entrance to the binding pocket, or by decreasing the flexibility of the α -helix at the N-terminus.

Transglycosylation experiments showed that the mutant enzyme UPL8 is a superior catalyst for the production of 5-MU. A 300% increase in reactor productivity was noted when free enzyme preparations of UPL8 was combined with BHPNP1 at 1.5% m.m⁻¹ substrate loading. The high yield of 5-MU (75-80% mol.mol⁻¹) was maintained at 9% m.m⁻¹ substrate loading. A commercially viable productivity of 31 g.l⁻¹.h⁻¹ was thus realised.

Further optimisation of the process could produce still higher productivities. Future work in directed evolution of nucleoside phosphorylases is envisaged for improved stability and enhanced substrate range for application to other commercially relevant transglycosylation reactions.

LIST OF OUTPUTS

Publications arising directly from this study:

Published:

Visser, D.F., Hennessy, F., Rashamuse, K., Louw, M.E. and Brady, D. (2010a) Cloning, purification and characterisation of a recombinant purine nucleoside phosphorylase from *Bacillus halodurans* Alk36. *Extremophiles*. 14, 185-192.

This paper is a direct result of the research contained herein, particularly Chapters 2 and 3. My role was the production, isolation and characterisation of the enzyme. Dr Hennessy and Dr Rashamuse assisted with bioinformatics, gene isolation and cloning studies. Dr Louw supplied the organism and Dr Brady supervised the study.

Visser, D.F., Rashamuse, K.J., Hennessy, F., Gordon, G.E.R., Van Zyl, P.J., Mathiba, K., Bode, M.L. and Brady, D. (2010b) High-yielding cascade enzymatic synthesis of 5-methyluridine using a novel combination of nucleoside phosphorylases. *Biocatalysis and Biotransformation* 28, 245-253.

This paper is a direct result of the research contained herein, particularly Chapters 2 and 3. I was responsible for identifying the combination of enzymes for 5-MU production and the subsequent biotransformations. Dr Rashamuse and Dr Hennessy assisted with producing enzyme production clones and initial screening work. Dr Gordon performed the final biotransformation using my experimental design. Dr Van Zyl supervised my fermentation studies. Mr Mathiba assisted with reaction analysis. Dr Bode and Dr Brady supervised the project.

Visser, D.F., Rashamuse, K.J., Hennessy, F., Pletschke, B. and Brady, D. (2011) Stabilisation of *Escherichia coli* uridine phosphorylase by mutation and immobilisation.

Journal of Molecular Catalysis B: Enzymatic 68, 279-285

This paper is a direct result of the research contained herein, particularly Chapters 4 and 5. Dr Rashamuse and Dr Hennessy assisted me with bioinformatics and practical mutation experimental design. Prof Pletschke and Dr Brady supervised the research.

Publications arising indirectly from this study:

Gordon, G.E.R., **Visser, D.F.**, Brady, D., Raseroka, N. and Bode, M.L. (2011) Defining a process operating window for the synthesis of 5-methyluridine by transglycosylation

Journal of Biotechnology 151(1), 108-113

Dr Gordon designed and performed the majority of the experimental work in this paper. I was responsible for the supply of the biocatalysts and assisted with experimental planning and writing the publication. Mrs Raseroka assisted with sample analysis. Dr Bode and Dr Brady supervised the study.

Gordon G E R, **Visser D F**, Bode M L, Lepuru J, Zeevaart J G, Ragubeer N, Ratsaka M, Walwyn D R and Brady D (2011) An integrated chemo-enzymatic route for preparation of β -thymidine, a key intermediate in the preparation of antiretrovirals.

Organic Process Research and Development. DOI: 10.1021/op100208x

This is a paper detailing the entire process (See also Patent Below). Dr Gordon and I were responsible for aspects of 5-MU production. Dr Bode, Mr Lepuru, Dr Zeevaart, Ms Ragubeer, and Ms Ratsaka were responsible for the chemical conversion of 5-MU to thymidine. Dr Walwyn assisted with techno-economics. Dr Brady supervised the study.

Patents

Visser, D. F., Hennessy, F., Rashamuse, K., Gordon, G. E. R., Bode, M. L. and Brady, D. A biocatalytic method for synthesis of 5-methyluridine. [WO2010055369]. 2009.

Process describes the biocatalytic production of 5-methyluridine at high yields using a novel combination of enzymes. My role in this patent is as co-inventor, particularly with the biocatalysis step, and drafting of the patent.

Conference Proceedings

Visser, D.F., Rashamuse, K.J., Hennessy, F., Gordon, G.E.R., Van Zyl, P.J., Mathiba, K., Bode, M.L. Pletschke, B. and Brady, D. High yielding cascade enzymatic synthesis of 5-methyluridine using a novel Purine Nucleoside Phosphorylase, from *Bacillus halodurans* Alk36. *Poster: Biocat2010, Hamburg, Germany.*

Poster presentation relating to isolation and application of the *Bacillus halodurans* PNP. This is a direct result of this research.

Visser D F, Gordon G E R, , Bode M L, Lepuru J, Zeevaart J G, Ragubeer N, Ratsaka M, Walwyn D R and Brady D. An integrated chemo-enzymatic route for preparation of B-thymidine, a key intermediate in the preparation of antiretrovirals. *Lecture: Biocat2010, Hamburg, Germany.*

I will be presenting the technology for the production of β -thymidine. My role in this research study has been discussed above.

ACKNOWLEDGEMENTS

I would like to thank the following people and groups for their contribution and support during this research:

My Family – my wife Eve, my children Matthew and Gabrielle, thank you for all your understanding and support during this process.

My Parents – For making all of this possible!

Prof. Brett Pletschke (Supervisor) – For accepting me a student and for your assistance in compiling this thesis.

Prof Dean Brady (Co-Supervisor) – For your continued support, as a “boss”, peer and friend.

The ARVIR team:

Dr Fritha Hennessy – For your assistance in bioinformatics and protein modelling, and your endless proof reading.

Dr Justice Rashamuse – For your assistance and patience through the initial genetics and final mutation research.

Dr Moira Bode – For initiating this research and for your continued support and assistance.

Dr Greg Gordon – For your assistance in biocatalytic studies.

Dr Petrus van Zyl – For your assistance in fermentation studies.

ACKNOWLEDGEMENTS

Mr Kgama Mathiba – For dropping everything when I needed assistance with analytical work.

Dr Maureen Louw – For access to the *Bacillus halodurans* strain for gene mining.

Dr Dave Walwyn (ARVIR) – For continuing to fund the work and for sharing your knowledge and experience, particularly with techno-economic analysis.

CSIR Biosciences – For providing the platform to do this research and for funding through the Thematic and Young Researcher Establishment Funds.

LifeLab – For funding the core of the research.

Rhodes Advisory Panel – Prof Rosemary Dorrington, Prof Chris Whitely and Prof Greg Blatch for your input in to this research.

TABLE OF CONTENTS

ABSTRACT	II
LIST OF OUTPUTS	IV
ACKNOWLEDGEMENTS	VII
TABLE OF CONTENTS	IX
LIST OF FIGURES	XIV
LIST OF TABLES.....	XX
LIST OF ABBREVIATIONS.....	XXII
CHAPTER 1: GENERAL INTRODUCTION	1
1.1 The HIV/AIDS pandemic in Sub-Saharan Africa.....	1
1.2 Treatment of HIV	4
1.3 Nucleoside analogue reverse transcriptase inhibitors.....	5
1.4 Biocatalysis	10
1.5 Production nucleosides and their derivatives	12
1.6 Nucleoside Phosphorylases.....	16
1.6.1 Purine Nucleoside Phosphorylases	16
1.6.2 Pyrimidine Nucleoside Phosphorylases	22
1.7 Directed evolution	24
1.8 Immobilisation.....	33
1.9 Research Hypothesis	35
1.9.1 Problem Statement	35
1.9.2 Research Hypothesis	36
1.9.3 Aims and Objectives	36

TABLE OF CONTENTS

CHAPTER 2: IDENTIFICATION.....	37
2.1 Introduction.....	37
2.2 Methods & Materials.....	38
2.2.1 Materials	38
2.2.2 Genomic DNA Isolation	39
2.2.3 Oligonucleotides, plasmids and microbial strains	39
2.2.4 Amplification of the <i>B. halodurans</i> Alk36 PNP gene.	40
2.2.5 Native enzyme production from <i>E. coli</i>	40
2.2.6 Over-expression of nucleoside phosphorylases	41
2.2.7 Preparation of crude extracts.	42
2.2.8 Initial assessment of commercial enzymes and crude extracts for transglycosylation potential	42
2.2.9 Assessment of different nucleoside phosphorylases for production of 5-methyl uridine	43
2.2.10 Small scale biocatalytic reactions	43
2.2.11 Analytical	43
2.3 Results and Discussion.....	45
2.3.1 Assessment of nucleoside phosphorylases for production of 5-methyluridine	45
2.4 Conclusions.....	51
CHAPTER 3: PRODUCTION	53
3.1 Introduction.....	53
3.2 Materials and methods	55
3.2.1 Oligonucleotides, plasmids and microbial strains	55
3.2.2 Enzyme Production by Fermentation	55
3.2.3 Preparation of crude nucleoside phosphorylase preparations	57
3.2.4 Purification of nucleoside phosphorylases	57
3.2.5 Characterization	58
3.2.6 Bioinformatic analysis of BHPNP1	59
3.2.7 Tertiary structure confirmation	60
3.2.8 Homology Modelling	60
3.2.9 Biocatalysis Reaction	60
3.3 Results and Discussion.....	61
3.3.1 Cell Bank Validation	61
3.3.2 Enzyme Production	62
3.3.3 Enzyme Purification	64

TABLE OF CONTENTS

3.3.4	Enzyme Characterization	65
3.3.5	Sequence and homology modelling	73
3.3.6	Bench scale biocatalytic reaction	77
3.4	Conclusions	79
CHAPTER 4: STABILISATION		81
4.1	Introduction	81
4.1.1	Determining target characteristics for evolution	81
4.1.2	Selecting a suitable evolution method	81
4.1.3	Designing an effective screening method	84
4.1.4	Immobilisation	85
4.2	Methods and Materials	86
4.2.1	Determining Target Amino Acids	86
4.2.2	Preparation of <i>E. coli</i> UP template	88
4.2.3	Mutagenesis	89
4.2.4	Assay development	89
4.2.5	Screening	90
4.2.6	Iterative Mutagenesis	92
4.2.7	Growth and expression of best mutant	92
4.2.8	Production of UPL8	93
4.2.9	Characterisation of UPL8	93
4.2.10	Sequence analysis	93
4.2.11	Production of nucleoside phosphorylase Spherezymes	93
4.3	Results and discussion	97
4.3.1	Assay Development	97
4.3.2	Round 1 Mutation	98
4.3.3	Round 2 mutation	99
4.3.4	Production of UPL8 in batch fermentation	101
4.3.5	Characterisation of UPL8	103
4.3.6	Sequence and homology model analysis of the mutant UPL8	107
4.3.7	Nucleoside phosphorylase Spherezyme optimisation	110
4.3.8	Spherezyme formation	112
4.3.9	Spherezymes characterisation	112
4.4	Conclusion	116
4.4.1	Directed evolution of <i>E. coli</i> uridine phosphorylase	116
4.4.2	Immobilisation of nucleoside phosphorylases	117

TABLE OF CONTENTS

CHAPTER 5: APPLICATION	119
5.1 Introduction.....	119
5.2 Methods and materials	121
5.2.1 Materials	121
5.2.2 Proof of concept transglycosylation experiments	122
5.2.3 Comparative transglycosylation	122
5.2.4 Sampling and analysis	123
5.3 Results	123
5.3.1 5-MU production by transglycosylation using free enzyme preparations	123
5.3.2 5-MU production by transglycosylation using Spherezyme preparations	125
5.3.3 5-MU production by transglycosylation using 9% m.m ⁻¹ guanosine and 4.6% m.m ⁻¹ thymine as starting substrate concentrations	129
5.4 Conclusions.....	133
CHAPTER 6: GENERAL CONCLUSIONS	137
6.1 Screening for suitable biocatalysts	138
6.2 Production, isolation, purification and characterisation of nucleoside phosphorylase.....	138
6.3 Directed Evolution	140
6.4 Immobilisation of nucleoside phosphorylases.....	141
6.5 Application of evolved and immobilised nucleoside phosphorylases to the production of 5-MU by transglycosylation	141
6.6 General conclusion.....	142
6.7 Future Work.....	143
APPENDIX 1.....	145
APPENDIX 2.....	152
APPENDIX 3.....	158
APPENDIX 4.....	164

TABLE OF CONTENTS

APPENDIX 5..... 170

REFERENCES 172

PUBLISHED JOURNAL ARTICLES..... 184

LIST OF FIGURES

Figure 1.1	Worldwide prevalence of HIV/AIDS.	2
Figure 1.2	World wealth map.....	3
Figure 1.3	Territory sizes adjusted to represent for total expenditure in research and development	3
Figure 1.4	Territory size indicates the number of deaths directly attributable to HIV/AIDS in one year	4
Figure 1.5	Nucleoside based reverse transcriptase inhibitors (NRTIs) approved for use in the treatment of HIV (De Clercq, 2001).....	6
Figure 1.6	Commercial preparation of β -Thymidine from xylose	7
Figure 1.7	Preparation of stavudine (d4T) and zidovudine (AZT) from 5-MU.....	8
Figure 1.8	Example of chemical 5-MU synthesis.	9
Figure 1.9	Cumulative number of biocatalysis process implemented in industry	11
Figure 1.10	Distribution of biocatalytic processes across various industrial sectors	11
Figure 1.11	Biocatalytic production of thymidine by transglycosylation.	14
Figure 1.12	Biocatalytic production of 5-methyluridine by transglycosylation.	15
Figure 1.13	Scheme showing reversible phosphorolysis of a purine nucleoside to its corresponding base and pentose-1-phosphate.....	17
Figure 1.14	Schematic classification of PNPs from various sources	18
Figure 1.15	(Left) Crystal form of the low-MM <i>Thermus thermophilus</i> PNP hexamer (PDB code 1ODJ) (trimer of homodimers in a ring configuration) (Tahirov	

LIST OF FIGURES

<i>et al.</i> 2004). (Right) Model of the high-MM Calf Spleen PNP (PDB code 1LVU)(dimer of homotrimers in a stacked configuration) (Koellner <i>et al.</i> 1998).	22
Figure 1.16 (Left) Dimer conformation of the <i>E. coli</i> TP (PDB code 1TGV) in the open conformation. The two monomers are coloured differently (Pugmire and Ealick, 2002). (Right) Representation of <i>E. coli</i> uridine phosphorylase. (Accelrys).....	24
Figure 1.17 Summary of the molecular tools developed for evolution of enzymes (reproduced from Antikainen and Martin, 2005).....	25
Figure 1.18 Outline of general screening approach showing the progression from low specificity, high throughput primary screens through to highly specific characterisation assays to isolate a desired physical or biochemical trait.	31
Figure 1.19 Use of free and immobilised whole cells or enzymes in industrial processes (reproduced from Straathof <i>et al.</i> , 2002).	33
Figure 1.20 Transglycosylation reaction for the production of 5-methyluridine from guanosine and thymine.	35
Figure 2.1 Assessment of 5-MU production by individual enzyme preparations.	47
Figure 2.2 5-MU production assessment using PNP:UP ratios of 1:1 (top) and 1:2 (bottom)	48
Figure 2.3 5-MU production assessment using PNP:UP ratios of 1:5; 2:1 and 5:1 ..	49
Figure 2.4 Guanosine conversion (closed) and 5-MU production (open) for <i>E. coli</i> PNP and UP (●); and <i>B. halodurans</i> PNP and <i>E. coli</i> UP (▲).....	51
Figure 3.1. Growth (A) and nucleoside phosphorylase activity (B) profiles of <i>E. coli</i> [pMSPNP] (◆) and <i>E. coli</i> [pETUP] (■) in batch fermentations. BHPNP expression was induced at an OD _{660nm} of 7 (5h) and UP expression was induced at an OD _{660nm} of 13 (4h).	63

LIST OF FIGURES

Figure 3.2	SDS-PAGE gel image depicting the final fractions of EcUP and BHPNP1 at the end of the purification by ammonium sulphate precipitation and sequential anion exchange chromatography.	64
Figure 3.3	pH profiles of BHPNP1 (top) and EcUP (bottom).	65
Figure 3.4	Temperature profiles of BHPNP1 (top) and EcUP (bottom).	66
Figure 3.5	Representation of BHPNP1 thermal stability at 40°C(◆), 60°C(■) and 70°C(▲).	67
Figure 3.6	Representation of EcUP thermal stability at 40°C (◆) and 60°C (■)..	67
Figure 3.7	Lineweaver-Burk (top), Hanes-Woolf (middle) and Eadie-Hofstee (bottom) plots for BHPNP1 using guanosine as the substrate.	69
Figure 3.8	Lineweaver-Burk (top), Hanes-Woolf (middle) and Eadie-Hofstee (bottom) plots for EcUP using uridine as the substrate.	70
Figure 3.9	Multiple sequence alignment comparing BHPNP1 to other Type II PNPases.	74
Figure 3.10	Ribbon representation of the homology modelled three dimensional structure of BHPNP1.	76
Figure 3.11	12% SDS PAGE gel (A) and corresponding activity gel overlay (B).	77
Figure 3.12	Bench scale (650 ml) biocatalytic production of 5-MU containing thymine (1.6% m.m ⁻¹ , 127 mM), guanosine (53 mM), BHPNP1 (105 U) and EcUP (75 U) in 50 mM sodium phosphate buffer (pH 7.8) at 40°C. Guanosine conversion (◆) and 5-MU yield (■) are shown.	78
Figure 4.1	Illustration of Iterative saturation mutagenesis (reproduced from (Reetz and Carballeira,2007)).	83
Figure 4.2	Schematic representation of the variations of nucleoside analogues incorporating chromogenic substrates for rapid activity determination of nucleoside	

LIST OF FIGURES

phosphorylase activity. Also shown is the complete structure of the analogue (<i>p</i> -nitrophenol- β -D-ribofuranoside) used in this study)	85
Figure 4.3 Ribbon representation of <i>E. coli</i> uridine phosphorylase (Accelrys)	88
Figure 4.4 Experimental layout for combinatorial optimisation of nucleoside phosphorylases Spherezyme formation	95
Figure 4.5 Agar plate image showing the distinct yellow halo formation around a culture due to <i>p</i> -nitrophenol released from a ribosides moiety due to UP phosphorylation.....	97
Figure 4.6 Plot of residual activity for the best mutants from each library in the first round of mutation. Residual activity was determined after incubation for 60 min at the set temperatures (37, 50, 60, 70 and 80°C). (UPL1-2/A11 (-◆-); UPL3-1/G9 (-■-); UPL4-3/F2 (-x-); UPL5-10/F9 (-◆-); UPL6-2/H10 (-+-); Wild type UP (-●-))...	99
Figure 4.7 Plot of residual activity for mutants UPL7-2/C15 (-◆-) and UPL8-4/I5 (-■-) compared to wild type UP (-●-).	100
Figure 4.8 Thermostability comparison for mutant UPL8 (-▲-) and wild type EcUP ("■").	101
Figure 4.9 Biomass production for duplicate fermentations of <i>E. coli</i> BI21 (DE3)[pETUPL8]	102
Figure 4.10 Activity profiles for the production of UPL8 during fermentation....	102
Figure 4.11 pH activity profiles of UPL8 (▲) and EcUP (■).	103
Figure 4.12 Temperature optima profiles of UPL8 (▲) and EcUP (■).	104
Figure 4.13 Lineweaver-Burk (top), Hanes-Woolf (middle) and Eadie-Hofstee (bottom) plots for UPL8 using uridine as the substrate.	106
Figure 4.14 Nucleotide sequence alignment (bp #600 to end) of the native <i>E. coli</i> uridine phosphorylase (UP) and the mutant <i>E. coli</i> uridine phosphorylase (UPL8).	108

LIST OF FIGURES

Figure 4.15	Amino acid alignment (aa residues #150 to end) of the native <i>E. coli</i> uridine phosphorylase (UP) and the mutant <i>E. coli</i> uridine phosphorylase (UPL8).	108
Figure 4.16	Ribbon representation of UPL8.	109
Figure 4.17	Ribbon representation of amino acids chains within 15Å of the mutation site.	109
Figure 4.18	Activity maintenance for optimisation of EcUP Spherezyme formation.	110
Figure 4.19	Activity maintenance results for optimisation of UPL8 Spherezyme formation.	111
Figure 4.20	Activity maintenance results for optimisation of BHPNP1 Spherezyme formation.	111
Figure 4.21	Optimum pH curves for based on PNP activity using guanosine as substrate.	114
Figure 4.22	Optimum pH curves based on UP activity using uridine as substrate.	114
Figure 4.23	Temperature optimum curves for PNP Spherezyme preparations using guanosine as substrate.	115
Figure 4.24	Temperature optimum curves for UP Spherezyme preparations using uridine as substrate.	115
Figure 5.1	Operating window for the synthesis of 5-methyluridine by transglycosylation of guanosine and thymine (reproduced from (Gordon <i>et al.</i> , 2010)).	121
Figure 5.2	Transglycosylation experiment showing the phosphorolysis of guanosine (◆) and formation of 5-MU (■) using BHPNP1 and native EcUP as biocatalysts at 60°C (closed symbols) and 70°C (open symbols).	124

LIST OF FIGURES

Figure 5.3	Transglycosylation experiment showing the phosphorolysis of guanosine (◆) and formation of 5-MU (■) using BHPNP1 and UPL8 as biocatalysts at 60°C (closed symbols) and 70°C (open symbols).	125
Figure 5.4	Transglycosylation experiment showing the phosphorolysis of guanosine (◆) and formation of 5-MU (■) using a combination of particles of BHPNP1-SZ and EcUP-SZ as biocatalysts at 60°C (closed symbols) and 70°C (open symbols).	126
Figure 5.5	Transglycosylation experiment showing the phosphorolysis of guanosine (◆) and formation of 5-MU (■) using a combination of particles of BHPNP1-SZ and UPL8-SZ as biocatalysts at 60°C (closed symbols) and 70°C (open symbols).	127
Figure 5.6	Transglycosylation experiment showing the phosphorolysis of guanosine (◆) and formation of 5-MU (■) using BHPNP1/EcUP-SZ as biocatalyst at 60°C (closed symbols) and 70°C (open symbols).	128
Figure 5.7	Transglycosylation experiment showing the phosphorolysis of guanosine (◆) and formation of 5-MU (■) using BHPNP1/UPL8-SZ as biocatalyst at 60°C (closed symbols) and 70°C (open symbols).	129
Figure 5.8	Analysis of 5-MU yield and productivity for 1.5% m.m ⁻¹ substrate loading reactions.	130
Figure 5.9	Transglycosylation experiment showing the phosphorolysis of guanosine (◆) and formation of 5-MU (■) using free BHPNP1 and UPL8 (closed symbols) or BHPNP1-SZ and UPL8-SZ (open symbols) as biocatalysts at 65°C. ...	131
Figure 5.10	Selected transglycosylation experiment showing the 5-MU yield obtained when using free EcUP (●) or free UPL8 (■) in combination with BHPNP1. Also shown are the combinations of separately immobilised EcUP and BHPNP (◆) and co-immobilised UPL8 and BHPNP (▲).	134

LIST OF TABLES

Table 1.1	Tentative classification of PNPs from various sources.....	19
Table 2.1	Summary of results obtained for reactions	46
Table 3.1	Relevant enzyme and biomass yields from literature on expression and fermentation studies for the production of purine and pyrimidine nucleoside phosphorylases.....	54
Table 3.2	Summary of working cell bank validation for <i>E. coli</i> [pMSPNP].....	61
Table 3.3	Summary of working cell bank validation for <i>E. coli</i> [pETUP].....	61
Table 3.4	Summary of fermentation parameters for batch fermentation of <i>E. coli</i> [pMSPNP] and <i>E. coli</i> [pETUP].....	62
Table 3.5	Physical and kinetic characteristics of BHPNP1 at 40°C.....	71
Table 3.6	Physical and kinetic characteristics of EcUP at 40°C.....	72
Table 3.7	Physical and kinetic characteristics of various reported prokaryotic PNPs.	73
Table 3.8	Comparison of various PNPs to BHPNP1	75
Table 4.1	B-Fit ISM Targets for <i>E. coli</i> UP. Based on highest B-values (calculated with B-fitter based on Chain A of model 1LX7-UP), the following residues have been selected for mutations (only forward primers shown, degenerate (Ds) IUB codes in bold).	87
Table 4.2	Target and actual number of colonies picked per mutant library.	91
Table 4.3	Best hits from the first six libraries based on residual activities observed after incubation of the enzyme preparations for 1 h at 70°C.	98
Table 4.4	Best hits from libraries UP L7 and UP L8 based on residual activities observed after incubation of the enzyme preparations for 1 h at 75°C.....	100

LIST OF TABLES

Table 4.5	Physical and kinetic characteristics of UPL8 and EcUP characterised using uridine as the substrate at 40°C	105
Table 4.6	Mass and Activity recovery data for the formation of EcUP, UPL8 and BHPNP1 Spherezymes.	113
Table 4.7	Mass and Activity recovery data for the formation of co-immobilised PNP/UP Spherezymes.....	113
Table 4.8	Physical and kinetic characteristics of reported prokaryotic PyNPs	117
Table 5.1	Summary of results for guanosine conversion, 5-MU yield and reaction productivity for transglycosylation reactions using a variety of biocatalyst combinations	132
Table 5.2	Cost comparisons of 5-MU production by transglycosylation using different biocatalyst combinations. Cost model is based on raw material and operational cost for a plant producing 100 tonnes per annum	136

LIST OF ABBREVIATIONS

- 3TC - Lamivudine
- 5-MU – 5-methyluridine
- AIDS – Acquired Immune Deficiency Syndrome
- ARV – Anti-retroviral
- AZT – Zidovudine
- BLAST - Basic Local Alignment Search Tool
- BHPNP1 – PNP1 from *Bacillus halodurans*
- BhUP – UP from *Bacillus halodurans*
- BIUP – UP from *Bacillus licheniformis*
- CAST – Combinatorial active site saturation test
- d4T – Stavudine
- DCW – Dry cell weight
- dH₂O – deionised water
- DNA - Deoxyribonucleic acid
- Ds Cod – Degenerate codon
- DTT – Dithiothreitol
- EcPNP – PNP 1 from *Escherichia coli*
- EcPNP2 - PNP 2 / Xanthosine phosphorylase from *Escherichia coli*
- EcUP – UP from *Escherichia coli*
- EDA – Ethylenediamine
- EDTA – Ethylenediaminetetraacetic acid
- EFV - Efavirenz
- GC – Gas chromatography
- Glu – Gluteraldehyde
- GuA – Guanine
- GuO – Guanosine
- HAART - Highly Active Anti-Retroviral Treatment
- HIV - Human Immunodeficiency Virus
- HPLC – High performance liquid chromatography
- IPTG – Isopropyl β -D-1-thiogalactopyranoside

ABBREVIATIONS

ISM – Iterative saturation mutagenesis

kDa – kiloDaltons

K_m – Michaelis constant

K_{cat} – Turnover number

KpUP – UP from *Klebsiella pneumoniae*

LB – Luria Broth

MS – Mass spectrometry

NCBI – National centre for biotechnology information

NP – Nucleoside phosphorylase

NP-4 – Nonoxyl 4

NNRTI – Non-nucleoside reverse transcriptase inhibitor

NRT - N-deoxyribosyl transferase

NRTI – Nucleoside analogue reverse transcriptase

NVP – Navirapine

OD – Optical density

PCR – Polymerase chain reaction

PDB – Protein database

PEG – Polyethylene glycol

PEI – polyethyleneimine

P_i – Inorganic phosphate

PNP – Purine nucleoside phosphorylase

PyNP – Pyrimidine nucleoside phosphorylase

SDS-PAGE – Sodium dodecyl sulphate polyacrylamide gel electrophoresis

SZ – SphereZyme™

Thy – Thymine

TLC – Thin layer chromatography

TP – Thymidine phosphorylase

TYG – Tryptone, yeast, glucose (broth)

UP – Uridine phosphorylase

UV – Ultraviolet

V_{max} – Maximum velocity

XO – Xanthine oxidase

The IUPAC-IUBMB three and one letter codes for amino acids were used, and single letter codes were used for nucleotides.

CHAPTER 1: GENERAL INTRODUCTION

1.1 THE HIV/AIDS PANDEMIC IN SUB-SAHARAN AFRICA

Human immunodeficiency virus (HIV) is a lentivirus (a member of the retrovirus family) that causes acquired immunodeficiency syndrome (AIDS) (Weiss, 1993; Douek *et al.*, 2009), a condition in humans in which the immune system begins to fail, leading to life-threatening opportunistic infections. According to the most recent data (UNICEF/WHO/UNAIDS report, 2009) in 2008 approximately 33.4 million people were living with HIV/AIDS. Of those, 97% live in low and middle income countries, with 22.4 million in sub-Saharan Africa. Currently no cure exists for HIV and AIDS, however the use of antiretroviral treatment effectively reduces the mortality and morbidity of HIV infection, as well as reducing transmission. An estimated 4 million people in the low to middle income countries are receiving anti-retroviral therapy (ART) which represents 42% coverage of the people who require anti-retrovirals (ARVs). While this coverage is increasing (from 33% in 2007), many gaps and challenges still exist in treatment and prevention of HIV/AIDS. Access to health services, treatment programs and infrastructure are the greatest challenges in preventing, diagnosing and treating HIV/AIDS and related diseases. The cost of treatment, largely due to support from developed countries and pharmaceutical manufacturers, is becoming less of an obstacle to adequate treatment, particularly in the supply of first-line regimen drugs. Second-line regimen drugs, however, remain costly. A decrease in manufacturing costs through novel production technologies will still go a long way to supporting the ART programme.

The data depicted in Figure 1.2 to Figure 1.4 further highlight the problems faced by developing countries, particularly sub-Saharan Africa. These illustrations, adapted from data from the United Nations Development Programme's 2004 Human Development Report, show the prevalence of HIV/AIDS (Figure 1.1) and the problems associated with adequately treating the pandemic. Sub-Saharan Africa has

the highest worldwide proportion of the pandemic, yet the African regions (Southern, Central and Northern Africa) represent the three regions with the lowest purchasing power worldwide (Figure 1.2). In addition, these regions invest the least amount in research and development, which includes research in social, scientific and infrastructure development. Combined, these factors lead to the high death attributed to HIV/AIDS in these regions (Figure 1.4). If one compares Figure 1.1 to Figure 1.4, it can be noted that while there are infections in the developed countries (North America, Europe), the mortality rate due to the disease is far lower than in the developing countries. This trend continues in the most recent data. New infections numbered 55000 in North America in 2008 with 25000 deaths reported in that year out of an estimated 1.4 million people living with the condition (1.7% annual mortality). In comparison, there were an estimated 1.9 million new infections in sub-Saharan Africa and 1.4 million deaths in 2008 out of an estimated 22.4 million infected individuals (6.3% annual mortality).

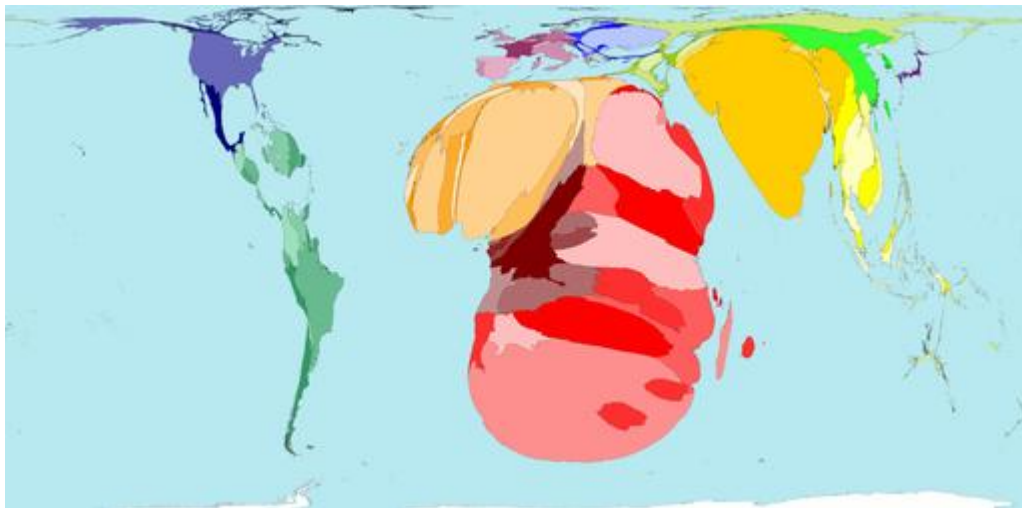


Figure 1.1 Worldwide prevalence of HIV/AIDS.

Territory size shows the proportion of people aged between 15 and 49 living with HIV/AIDS (reproduced from www.worldmapper.org/).

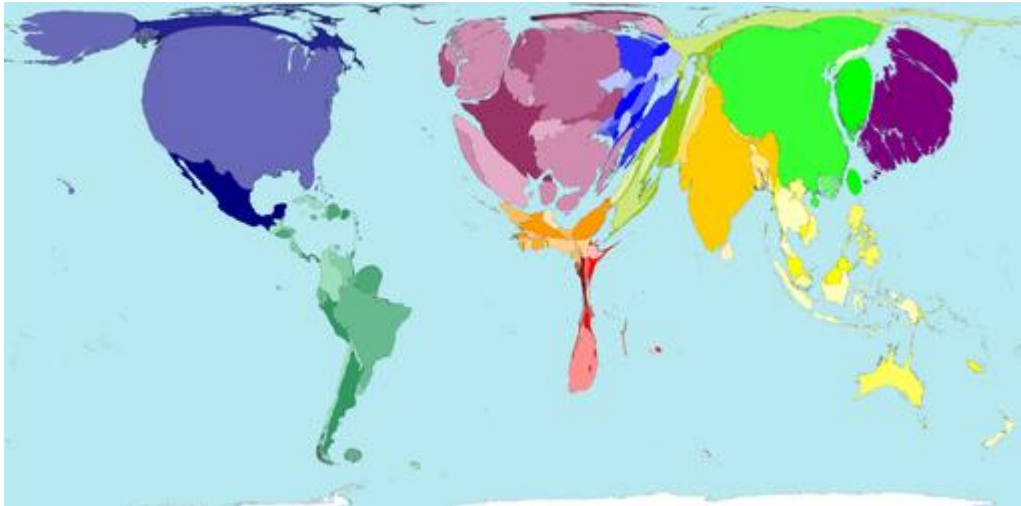


Figure 1.2 World wealth map.

Territory size represented as national purchasing power. This map indicates that Sub-Saharan Africa has the lowest purchasing power worldwide (reproduced from www.worldmapper.org/).

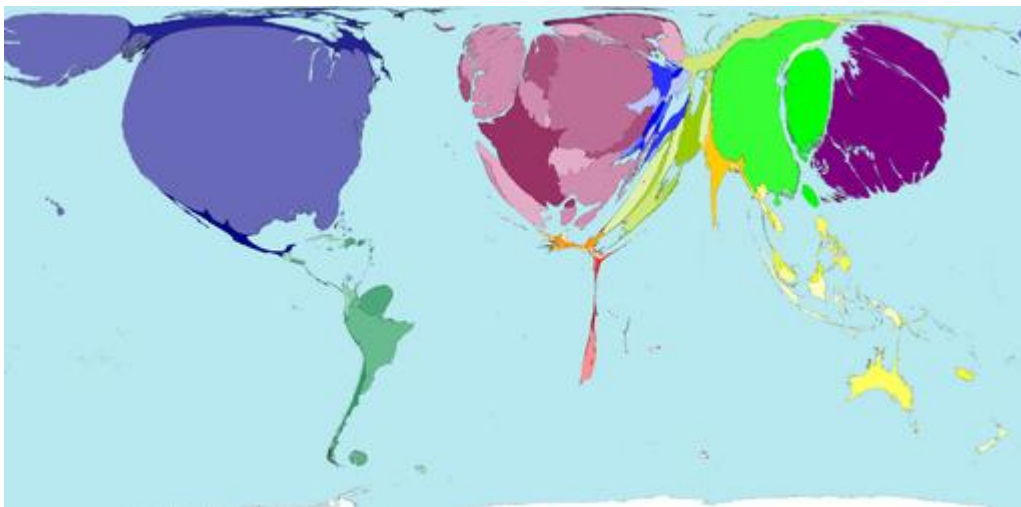


Figure 1.3 Territory sizes adjusted to represent for total expenditure in research and development

(Reproduced from www.worldmapper.org/).

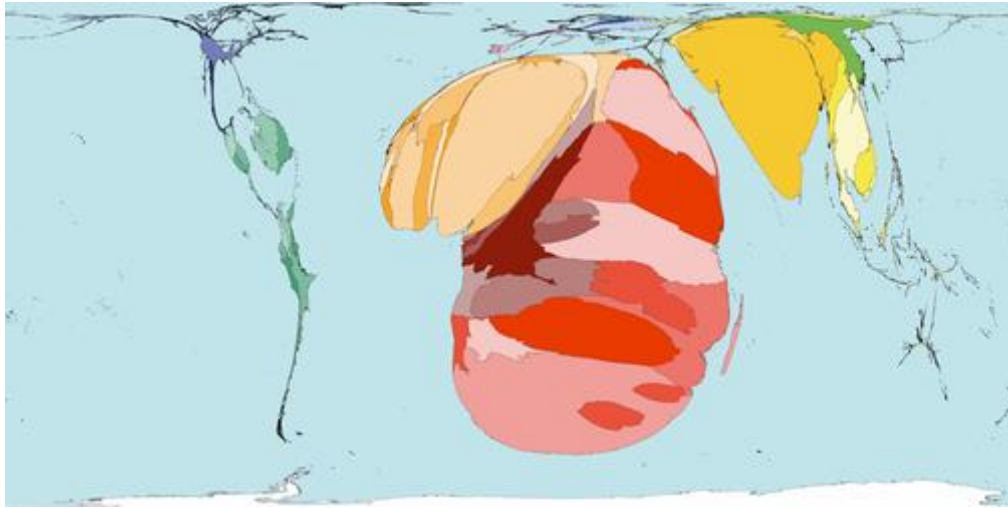


Figure 1.4 Territory size indicates the number of deaths directly attributable to HIV/AIDS in one year

(Reproduced from www.worldmapper.org/).

1.2 TREATMENT OF HIV

Currently there is no preventative vaccine (Titti *et al.*, 2007) or cure for HIV or AIDS. The only known method of prevention is avoiding exposure to the virus. The current treatment for HIV infection consists of using highly active antiretroviral therapy (HAART). HAART treatment involves combinations or “cocktails” consisting of at least three drugs belonging to two types, or “classes” of anti-retroviral agents. There are a number of points in the life cycle of HIV where it is vulnerable to interference by therapeutic agents. These agents can be classified according to where they act. The classes of antiretroviral agents include: entry and fusion inhibitors (Chantry, 2004), nucleoside reverse transcriptase inhibitors (NRTIs) (Cihlar and Ray, 2010), non-nucleoside reverse transcriptase inhibitors (NNRTIs) (De Clercq, 1998; de Bethune, 2010), integrase inhibitors (Johnson *et al.*, 2004), protease inhibitors (Huff and Kahn, 2001), transcription inhibitors (Domagala *et al.*, 1997) and nucleocapsid protein Zn finger-targeted agents (Okamoto *et al.*, 2000).

Typically the drug cocktail includes two NRTIs combined with either a NNRTI or a protease inhibitor. The use of HAART in the treatment of a patient infected with HIV

stabilizes the patient's symptoms but does not cure the patient. Irrespective of this, many HIV-infected individuals have experienced remarkable improvements in their general health and quality of life, resulting in a large reduction of HIV associated morbidity and mortality in the developed world (Palella, Jr. *et al.*, 1998). HAART treatment prevents or delays the progression of the disease from HIV to AIDS.

The majority of currently licensed antiviral drugs are analogues of naturally occurring nucleosides. The drugs inhibit viral replication by interfering with the synthesis of nucleic acids. Antiviral drugs against HIV (AZT, Stavudine, ddI) and Herpes (Acyclovir), and broad spectrum antivirals such as ribavirin have proved very effective in preventing the proliferation of the targeted virus, and therefore improve the quality of life of the infected individual. Due to the high incidence of the HIV infections in the region, the South African government is promoting the local manufacture of pharmaceutical compounds that would prolong the lives of those infected with and reduce transmission to those exposed to HIV. The traditional synthetic routes for these compounds are often complex and inefficient multi-stage processes (Lewkowicz and Iribarren, 2006). Biocatalysis represents a potential cost saving in that precursors to commonly used ARVs can be produced, more cost effectively, through biocatalytic routes.

1.3 NUCLEOSIDE ANALOGUE REVERSE TRANSCRIPTASE INHIBITORS

The NRTIs currently approved for use in the South African ARV treatment regime are depicted in Figure 1.5. All NRTIs consist of a nitrogenous base (or analogue thereof) and a sugar (or sugar-like) component linked in a stereospecific manner. Bases include purines, pyrimidines or modifications thereof. The sugar unit can be dideoxy, didehydrodideoxy- and carbocyclic sugars, or modifications thereof.

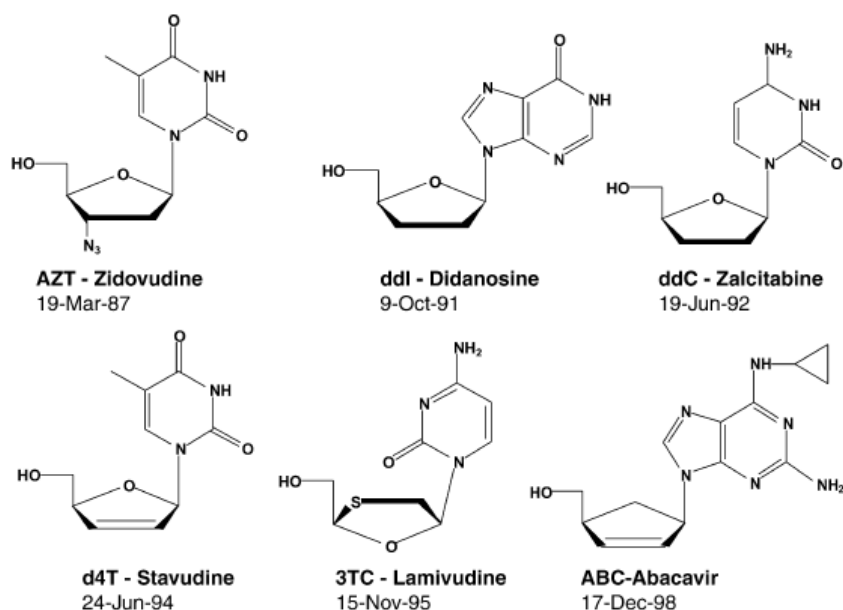
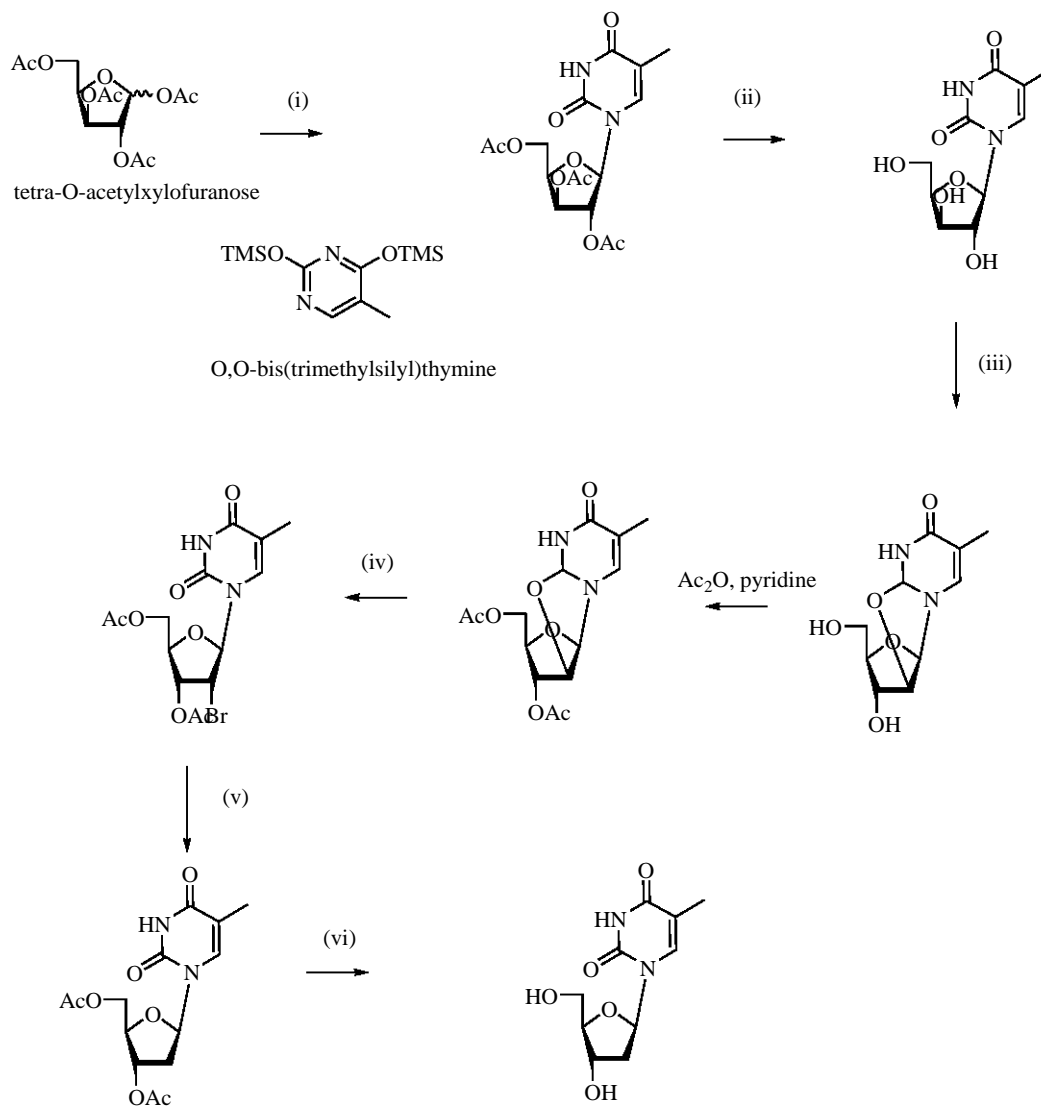


Figure 1.5 Nucleoside based reverse transcriptase inhibitors (NRTIs) approved for use in the treatment of HIV (De Clercq, 2001).

Stavudine (d4T), zidovudine (AZT), lamivudine (3TC), nevirapine (NVP) and efavirenz (EFV) are widely used during the first line regimen treatment of HIV/AIDS. The drugs may be used in single, or combination therapy, and represent 96% of the ARVs used in sub-Saharan Africa to treat HIV/AIDS (Chien, 2007). Chemical synthesis of nucleoside analogues usually involves coupling of the purine or pyrimidine base (or analogues thereof) to the sugar moiety (Ichikawa and Kato, 2001). This normally requires glycosyl activation and protection of groups on the base and the sugar residue. Stereochemistry in these structures is very important, with appreciable differences in toxicity and efficacy existing between the required compound and its stereochemical equivalent.

Both Stavudine and AZT are analogues of β -Thymidine. The nucleoside can be obtained from natural sources, such as extraction from salmon milt (Yamasa, Japan) but this is unlikely to be sustainable. Fermentation processes for the production of β -Thymidine have been developed (Lee *et al.*, 2009) producing up to 0.74 g.l⁻¹ over a 24 h fermentation. However, purification of the thymidine from this dilute fermentation stream is costly. Chemical synthesis of thymidine is also difficult and costly to produce. For example, the commercial process (Venkata *et al.*, 1997) starting from a

protected D-xylose is shown in Figure 1.6. Multiple protection and de-protection of substrates is required, leading to a lengthy process and a low overall yield of β -thymidine (32%).



(i) O,O-bis(trimethyl)thymine, SnCl_4 , CH_2CH_2 , RT, 18 h, 82.5%; (ii) NaOMe, MeOH, RT, 6 h, 94%; (iii) PhOCO_2Ph , NaHCO_3 (cat), DMF, 140-150 °C, 4 h, 55%; (iv) HBr, DMF, 90-110°C, 2 h, 95%, (v) H_2 , Ni (cat), MeOH, 45 psi/ ~ 3 bar, 4-5 h, (vi) MeOH, Na, Amberlite IR 120, 8 h, 80%

Figure 1.6 Commercial preparation of β -Thymidine from xylose

(Reproduced from Venkata *et al.*, 1997).

The difficulty in producing β -Thymidine results in a high cost, with prices between \$177/kg and \$225/kg (Yick-Vic Chemicals and Pharmaceuticals (HK) Ltd, Junwee Chemical Co. Ltd)

An alternative method for the production of stavudine and AZT using 5-methyluridine (5-MU) as a common intermediate is shown in Figure 1.7. This method was developed and commercialised by Bristol Meyers Squibb (BMS) (Chen *et al.*, 1995).

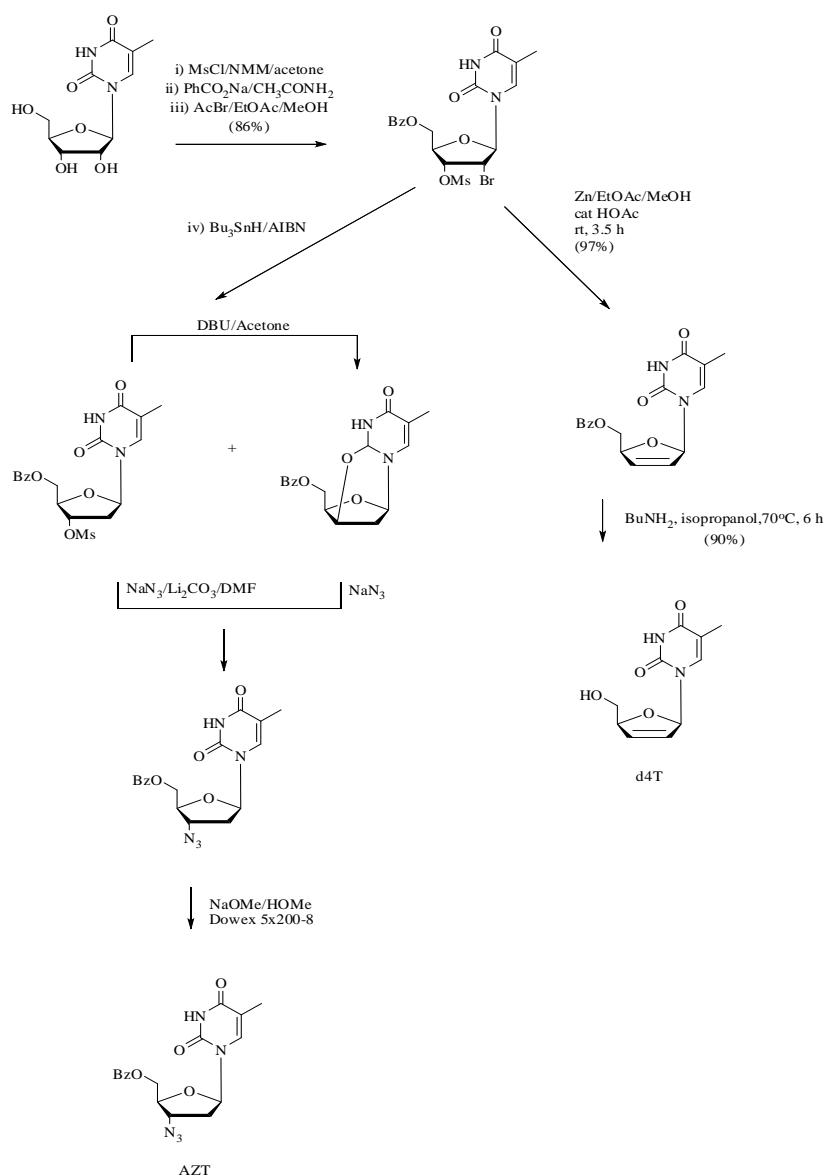


Figure 1.7 Preparation of stavudine (d4T) and zidovudine (AZT) from 5-MU.

(Reproduced from Chen *et al.* 1995)

The chemical synthesis of 5-MU is also problematic and suffers from low yields (5 – 50%), low selectivity (production of α - and β -anomers requires further chromatographic separation), and utilises a number of heavy metals, including tin or mercury (Shimizu *et al.*, 1965; Niedballa and Vorbrulêggen, 1974; Ogawa and Matsui, 1978). 5-MU can also be produced from β -thymidine, but this is not practical as the cost of 5-MU is less than that of β -thymidine.

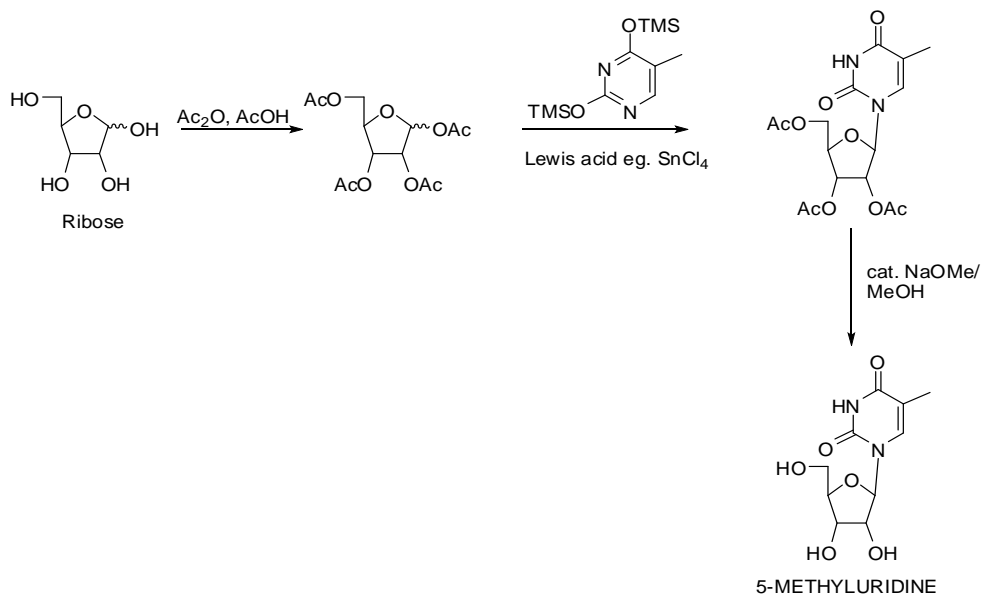


Figure 1.8 Example of chemical 5-MU synthesis.

(Adapted from Niedballa and Vorbrulêggen, 1974)

An alternative to traditional synthesis is to produce a common intermediate nucleoside through biocatalysis. Enzymatic production of a common intermediate results in a single isomer, which can then be easily modified by chemical means to give the desired compound. The enzymatic approach has the advantage of being able to produce high concentrations of the desired compound (which is not generally possible by fermentation) in mild conditions with a high degree of stereo- or regioselectivity (which is difficult with chemical synthesis). Biocatalytic production of pharmaceutical intermediates and particularly 5-MU will be discussed further.

1.4 BIOCATALYSIS

Biocatalysis is essentially the use of microorganisms or components thereof (such as enzymes) to catalyze chemical reactions. The field is becoming well established in the production of commodity and particularly fine chemicals such as pharmaceuticals and their intermediates (Straathof *et al.*, 2002; Woodley, 2006a; Pollard and Woodley, 2007). Organisms and enzymes are very efficient catalysts and generally operate in mild aqueous conditions. Enzymes are also highly selective in terms of their chemo-, regio- and enantioselectivity. Using biocatalysts therefore negates the need to protect and deprotect molecules during synthesis, resulting in fewer synthesis steps. Using whole cells or combinations of enzymes also permits one-pot multi-step reactions. This has the advantage of lower energy input in to the synthesis process and far fewer waste products than traditional chemistry, often at lower overall costs.

Limitations that previously prevented the implementation of biocatalytic reactions are steadily being overcome. Price and availability of biocatalysts have been improved by various recombinant enzyme expression technologies and more optimal fermentation technologies. Enzymes remain expensive, particularly due to development cost involved in producing large quantities, but often this cost is insignificant in the complete synthetic process. Poor operational stability of enzymes has caused limited integration of biocatalysts into existing processes, but this is being overcome by the use of enzymes from extremophiles, capable of operating in extremes of temperature, pH and pressure. Inhibition of biocatalytic activity, particularly at high substrate concentrations, is often noted in industrial applications. Some enzymes also require co-factors for activity and these can be costly.

There are a number of examples of biocatalysis in industry, and a review by Straathof *et al* (2002) discusses 134 such technologies. There has been a notable uptake of biocatalysis, particularly since the mid to late 1990s (Figure 1.9). The majority of these biocatalytic technologies are found in the pharmaceuticals industry and to a lesser extent in the agricultural and food sectors (Figure 1.10). Some of these processes are used for production of chemicals at the 100 to 100 000 ton scale. Products produced in excess of 1 ton per annum through biocatalysis include various

amino acids, nucleotides and derivatives, epoxides, hydroxyl aromatics, amines and amides.

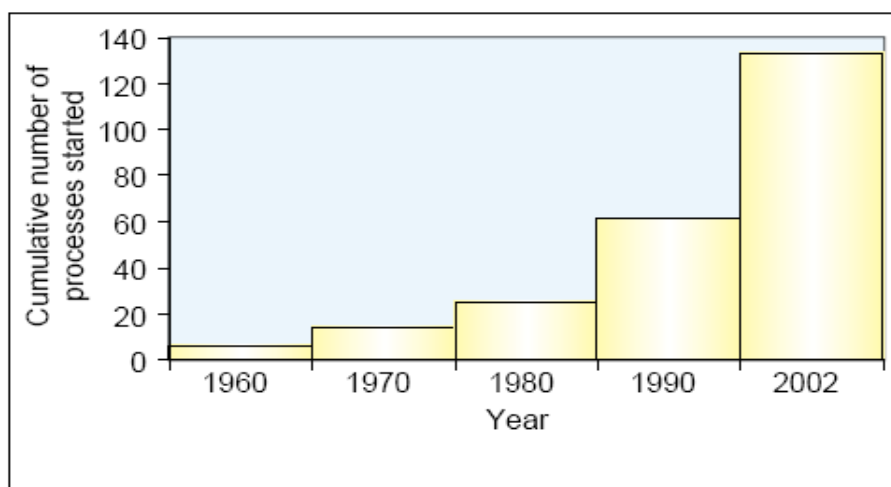


Figure 1.9 Cumulative number of biocatalysis process implemented in industry

Reproduced from (Straathof *et al.*, 2002)

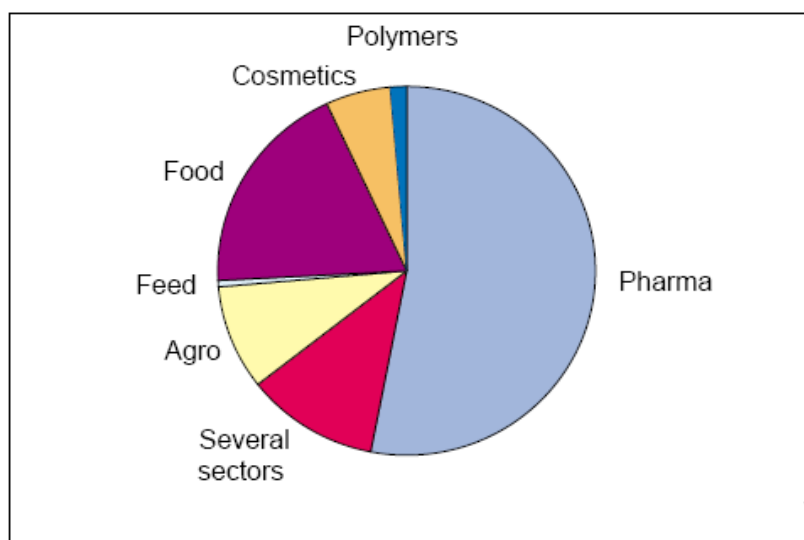


Figure 1.10 Distribution of biocatalytic processes across various industrial sectors

Reproduced from (Straathof *et al.*, 2002)

Over 35000 enzyme catalysed reactions are listed in public databases such as BioCatalysis (www.accelrys.com), and many more potential catalysts are being discovered through increased exploration of microbial diversity (through improved screening technologies and research fields such as metagenomics).

Many of these catalysts are unsuitable for industrial application for various reasons, mostly due to either limited availability of the enzymes or the low activity and stability of the catalysts in the presence of high substrate and product concentrations necessary for efficient industrial processes. However, catalyst availability can be assured through developing recombinant catalyst production organisms and improved fermentation technology. Large scale production of enzymes through these means is now becoming commonplace.

The application of the biocatalyst to an efficient industrial process can be significantly more difficult. One way of overcoming low stability and activity constraints is through reaction engineering, such as the use of biphasic and continuous mode reactors, where the catalyst is not in contact with high concentrations of either substrate or product. Immobilising the biocatalyst, be it whole cells or enzyme, also confers stability and enables recycling of the catalyst. Combinations of reaction engineering and immobilisation have been applied in a number of cases to make a process industrially viable. This approach however involves modifying the process to suit the biocatalyst. Burton *et al* (2002) suggest that this approach leads to a sub-optimal process, and that a more suitable approach is to search for or engineer a catalyst to fit in to the ideal process. Therefore, instead of developing processes that operate in very mild but comparably inefficient conditions, more biocatalysts are being discovered and developed that are capable of operating at high temperatures, in solvent based reactions, in high substrate and product conditions, and in various other conditions that were previously deemed unsuitable for biocatalysis.

1.5 PRODUCTION NUCLEOSIDES AND THEIR DERIVATIVES

Biocatalysis can provide enantio-, regio- and chemo-selective reactions in order to reduce the number of reaction steps, reduce waste, and thereby minimise synthesis costs (Araki *et al.*, 2003). Although biocatalysis can be used in many parts of the various ARV synthetic routes, it is in the area of glycosylation or transglycosylation that we may derive the most benefit.

Of particular interest in the biocatalytic production of nucleoside analogues are 2 classes of enzymes: nucleoside phosphorylases (NP) and N-deoxyribosyl transferases (NRT). Both enzymes catalyze the transfer of a glycosyl residue from a nucleoside donor to a nucleoside base. Through this reaction (transglycosylation), modified ribo- and deoxyribonucleosides have been produced such as 3-deazaadenosine (inhibits Rous sarcoma virus) and Ribavirin (general antiviral). With different combinations of these enzymes, or between different classes of the enzyme, it is possible to transfer ribose- or deoxy-ribose sugars between purine and pyrimidine bases as well as between pyrimidine or purine bases. It is also possible to transfer modified sugars between nucleoside bases or modified nucleosides, depending on the specificity of the enzyme used (Hanrahan and Hutchinson, 1992).

Nucleosides are precursors to natural nucleic acids and are involved in the structure of many coenzymes. As such, nucleoside and nucleoside derivatives play an important role in biochemistry and medicine. Their role in antiretroviral treatment has already been discussed, but they have also been identified in various other chemotherapeutic applications. As such, production of nucleosides and their analogs has been the focus of significant research in the past two decades. A recent review by Li *et al* (2010) describes the advances in this field since 2000. In this review they describe various structural modifications such as acylation, deacylation, glycosylation, halogenation and deamination of nucleosides to provide modified nucleosides with favourable clinical applications. Within the review they highlight that many of these applications are exciting, but with the exception of lipase-mediated acylation reactions, the industrial application of biocatalytic routes to nucleoside modification has not yet been seen.

In the 1980s, biocatalytic syntheses for nucleosides became the focus of research (Hanrahan and Hutchinson, 1992; Utagawa, 1999; Prasad *et al.*, 1999; Lewkowicz and Iribarren, 2006; Mikhailopulo, 2007). Transglycosylation reactions between purines and pyrimidines require the combination of pentosyltransferases such as a purine nucleoside phosphorylase, (PNP; EC 2.4.2.1) and a pyrimidine nucleoside phosphorylase (PyNP; EC 2.4.2.2), both of which catalyse the reversible phosphorolysis of nucleosides. Other enzymes that have a similar catalytic function

to PyNP are uridine phosphorylase (UP; EC 2.4.2.3) and thymidine phosphorylase (TP; EC 2.4.2.4). The equilibrium for PNP is towards nucleoside formation for natural substrates, while PyNP favours the phosphorolysis reaction (Erion *et al.*, 1997; Bzowska *et al.*, 2000; Lewkowicz and Iribarren, 2006), and hence the majority of the work to date has focused on synthesis of purine nucleosides from pyrimidine nucleosides. This represents a challenge in the synthesis of pyrimidine nucleosides.

AZT and Stavudine are thymidine (pyrimidine) analogues that are approved by regulatory bodies such as the South African Medicines Control Council as part of the HIV/AIDS treatment regimen. Chemical synthesis of both AZT and Stavudine can be achieved using 5-methyluridine or thymidine as a precursor (Chen *et al.*, 1995; Shiragami *et al.*, 1996).

It has been shown that thymidine can be produced through transglycosylation by combining thymine with 2'-deoxyribose-1-phosphate from a suitable chemical donor (Pal and Nair, 1997). As can be seen in Figure 1.11, either 2'-deoxyinosine or 2'-deoxyguanosine can be used as the deoxy-ribose donor. From an industrial perspective, though, this is not a feasible approach as the cost of these sugar donors would result in significantly higher thymidine costs.

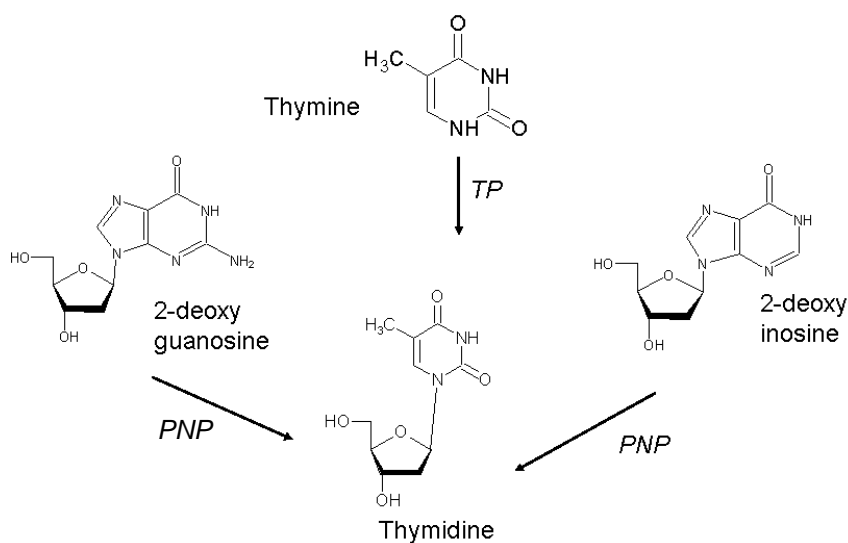


Figure 1.11 Biocatalytic production of thymidine by transglycosylation.

TP – thymidine phosphorylase. PNP – purine nucleoside phosphorylase.

5-MU itself can be synthesised by means of selective biocatalytic transglycosylation from guanosine or inosine to thymine (Figure 1.12) (Utagawa, 1999). Using inosine as the sugar donor has an advantage in that the inosine is more soluble than many other nucleosides. In order to drive the reaction toward phosphorylation or decoupling of the ribose sugar, however, it is necessary to add a second enzyme, xanthine oxidase, to remove the liberated hypoxanthine and thus drive the reaction in the desired direction. Using guanosine as the sugar donor has a disadvantage in that guanosine is fairly insoluble, and requires elevated temperature (above 60°C) for effective solubilisation even at low concentrations. The anticipated adverse reaction equilibrium and the very low solubility of the starting substrates would suggest that synthesis of this pyrimidine nucleoside would suffer from low yield and productivity.

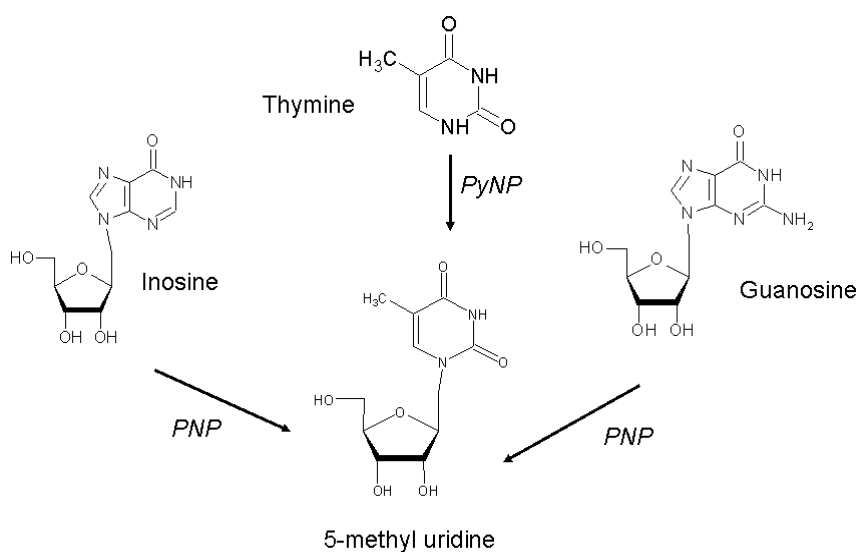


Figure 1.12 Biocatalytic production of 5-methyluridine by transglycosylation.

PyNP – pyrimidine nucleoside phosphorylase. PNP – purine nucleoside phosphorylase.

Studies using inosine as the glycosyl donor, thymine and crude enzyme were performed by Hori *et al.* (1989a; 1989b), but the reaction yielded only 22% mol.mol⁻¹ 5-MU at low substrate concentrations. Further work by the same group (Hori *et al.*,

1991) using immobilised enzymes showed improvements with a continuous conversion of inosine and thymine at an initial concentration of 75 mM in the feed to yield 24 mM 5-MU (33% molar yield). The poor equilibrium constant of 0.24 limited the conversion to 5-MU (Hori *et al.*, 1991), indicating that the reaction lacks an overall driving force towards pyrimidine synthesis. However Ishii *et al.* (1989) showed that by using guanosine as the glycosyl donor in combination with thymine and whole cells of *Erwinia carotovora* it was possible to produce 5-MU at a molar yield of 74% from high starting substrate concentrations (300 mM), albeit over a 48 h period. The substrates guanosine and thymine are only sparingly soluble in aqueous solutions and this would appear to be a potential limiting factor for enzymatic conversion. As heating the aqueous solution improves the solubility, it would be preferable to utilise moderately thermostable nucleoside phosphorylases in heated reactions. In general prokaryotic PyNP and PNP tend to be more thermostable and have broader specificity than their mammalian counterparts (Tonon *et al.*, 2004). Furthermore, a few thermostable PNPs from extremophiles such as *Sulfolobus solfataricus* (Cacciapuoti *et al.*, 2005), *Pyrococcus furiosus* (Cacciapuoti *et al.*, 2007), *Thermus thermophilus* (Almendros *et al.*, 2009) and *Geobacillus stearothermophilus* (Hori *et al.*, 1991; Hamamoto *et al.*, 1997a) have been reported and applied to the production of nucleosides.

1.6 NUCLEOSIDE PHOSPHORYLASES

1.6.1 Purine Nucleoside Phosphorylases

Purine nucleoside phosphorylase (PNP; E.C. 2.4.2.1) catalyses the cleavage of the glycosidic bond of ribo- and deoxyribonucleosides in the presence of inorganic phosphate (P_i). PNP catalyzes the reversible phosphorolysis of purine nucleosides to generate the corresponding purine base and pentose-1-phosphate (Erion *et al.*, 1997). PNP functions in the purine salvage pathway, enabling cells to utilise purine bases

recovered from metabolised purine ribo- and deoxy-ribonucleosides to synthesize purine nucleotides. They are specific for 6-oxo-purines.

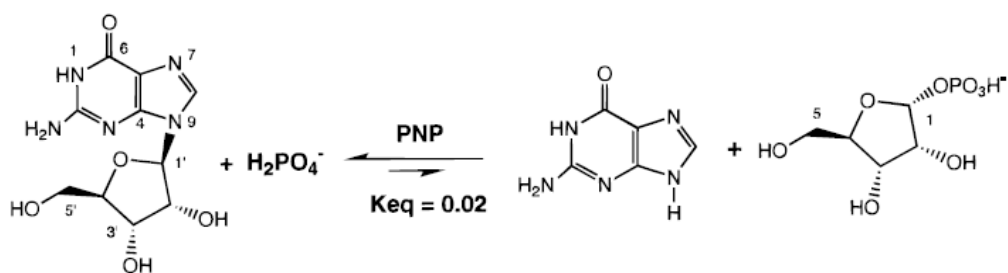


Figure 1.13 Scheme showing reversible phosphorolysis of a purine nucleoside to its corresponding base and pentose-1-phosphate.

The equilibrium is strongly towards the nucleoside synthesis reaction under natural conditions. (reproduced from Erion *et al.*, 1997).

1.6.1.1 Characterisation

PNP purified from a broad range of organisms showed different specificities. The majority of the PNPs can be classified into two main categories (

Figure 1.14 and Table 1.1):

- 1) Low-molecular-mass (low MM) homotrimers with total M_r of 80 – 100 kDa. These enzymes are specific for 6-oxo-purines (guanine and hypoxanthine), and found in higher organisms and prokaryotes.
- 2) High-molecular-mass (high MM) homohexamers with total M_r of 110 – 160 kDa. These enzymes are found in lower organisms and have broader substrate specificity, accepting both 6-amino (adenine) and 6-oxopurine nucleosides (Bennett *et al.*, 2003).

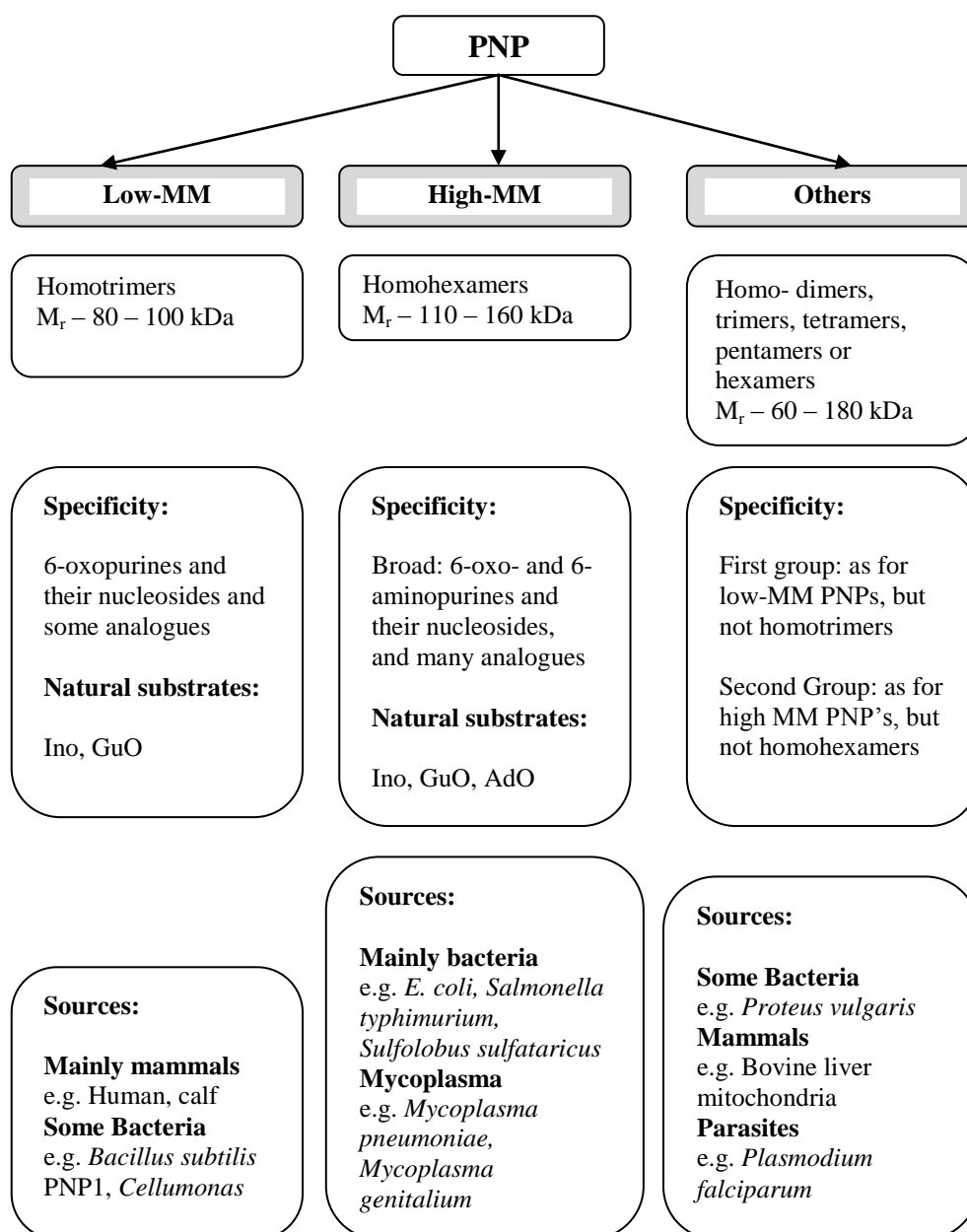


Figure 1.14 Schematic classification of PNPs from various sources

(Reproduced from Bzowska *et al.*, 2000)

Table 1.1 Tentative classification of PNPs from various sources

Source and designation	Subunit		Number of Subunits	Substrate specificity		Class, Sequence homology
	M_r (kDa)	M_r (kDa)				
<i>E. coli</i> PNP1 (<i>deoD</i> gene product)	134±14	23.7 ± 1.2	Hexamer	deoxy-inosine	100%	High-mm PNP Family 1 PNP/UDP
				deoxy-guanosine	74%	
				deoxy-adenosine	61%	
				adenosine	61%	
				guanosine	48%	
				inosine	46%	
<i>E. coli</i> PNP II xanthosine phosphorylase (<i>xapA</i> gene product)	150	25	Hexamer	deoxy-inosine	100%	Family 2 PNP/MTAP
				deoxy-guanosine	78%	
				inosine	58%	
				guanosine	37%	
				xanthosine	53%	
Human erythrocyte PNP	87-91	30 ± 0.5	Trimer	inosine guanosine		Low-mm PNP Family 2 PNP/MTAP
Calf spleen PNP	86	30 ± 0.5	Trimer	inosine guanosine		Low-mm PNP Family 2 PNP/MTAP
Mouse PNP		32.28	Trimer	inosine guanosine		Low-mm PNP Family 2 PNP/MTAP

(Adapted from Bzowska *et al.*, 2000).

All PNPs show broad pH activity optima between pH 7 and 8, with the PNP from *Geobacillus stearothermophilus* (Hori *et al.*, 1989a; 1989b) having activity optimum between neutral pH and pH 11. High-MM PNPs are more thermostable than the low-MM. *E. coli* high-MM PNP is stable at 55°C for 10 minutes (Krenitsky *et al.*, 1981), with PNP from *Sulfolobus solfataricus* still fully active after 2 h at 100°C (Cacciapuoti *et al.*, 1994). Mammalian low-MM are more temperature sensitive with calf spleen PNP losing activity after 10 min at > 35°C (Krenitsky *et al.*, 1981). Reported isoelectric points are in the pH range from 4.2 to 6.8 (Schimandle *et al.*, 1985; Haag and Lewis, 1994).

1.6.1.2 Specificity and kinetic properties

Natural substrates of low-MM PNPs are the 6-oxopurines and their ribosides and deoxyribosides, whereas the high-MM enzymes additionally accept 6-aminopurines and their nucleosides. The low-MM and high-MM PNPs can discriminate between substrates that lack either a 6-keto substituent, nitrogen N(1) or proton at this position, or have a halogen at position C(2) of the base (Bzowska *et al.*, 2000). The pentose moiety also directs specificity between the low-MM and the high-MM. Steric alteration of the hydroxyls at C(2') and / or C(3') decrease or abolish the substrate activity in the human PNP, but the enzyme is tolerant to structural diversity at the 5' position (Stoeckler *et al.*, 1982). The human enzyme also binds analogues with the pentose ring replaced by other cyclics or acyclic moieties (Montgomery *et al.*, 1993). In contrast to this, the high-MM *E. coli* enzyme is inactive towards analogues of adenosine with sterically modified pentoses, the exception being the orientation of the 5'-CH₂OH group (Doskoil and Holý, 1977). Also, the *E. coli* enzyme does not tolerate the replacement of the pentose ring by a benzyl moiety. Hence low-MM PNP exhibit higher specificity for the base moiety, and a lower one for the pentose moiety than the high-MM PNP, which shows stricter specificity for the pentose moiety.

With natural substrates, and some substrate analogues, where phosphorolysis is reversible, the equilibrium is thermodynamically in favour of nucleoside synthesis. For most unusual substrates of PNPs, the phosphorylation is irreversible, or has a K_{eq} so small that the reaction is essentially irreversible (Bzowska *et al.*, 2000; 2002). However, *in vivo*, phosphorolysis is the predominant reaction, due to coupling with other enzymes (Bzowska *et al.*, 2000).

1.6.1.3 Three-Dimensional structure

A number of PNP crystal structures have now been elucidated, many quite recently, such as *Plasmodium falciparum* (Chaikuad and Brady, 2009), *Schistosoma mansoni* (Castilho *et al.*, 2010), *Mycobacterium tuberculosis* (Lewandowicz *et al.*, 2003), *Anopheles gambiae* (Taylor *et al.*, 2007) and *Trichomonas vaginalis* (Rinaldo-Matthis *et al.*, 2007). In addition, PNPs from human erythrocytes (Ealick *et al.*, 1990), calf spleen (Bzowska *et al.*, 1995); (Koellner *et al.*, 1998), *Cellulomonas* (Bzowska *et al.*, 1998), *E. coli* (Koellner *et al.*, 1998; Dandanell *et al.*, 2005) and *Thermus thermophilus* (Tahirov *et al.*, 2004) have been elucidated.

Crystal structures have revealed that high-MM PNPs (eg. calf spleen (Figure 1.15), human erythrocyte, *Cellulomonas*) are trimers with a very similar overall structure. The calf spleen and human erythrocyte enzymes show a high degree of sequence similarity, with only ~40 residues that differ, but the sequence of the *Cellulomonas* PNP shares only 33% identity with the calf spleen enzyme. This trimer configuration has also been noted for *A. gambiae*, *S. mansoni* and *E. coli* PNPII.

The catalytically active molecule of low-MM PNPs consists of six subunits. The hexamer may be regarded as a flat cylinder ~60 Å thick and 100 Å in diameter, with an internal channel of ~20 Å diameter filled with water molecules (Koellner *et al.*, 1998). The contacts between subunits forming dimers are more extensive than between trimers of dimers forming the holoenzyme. The nature of these interactions is mainly hydrophobic, with some hydrogen bonds observed. This trimer of dimers in the ring configuration is seen with the *E. coli* PNP1, *Bacillus anthracis*, *T. thermophilus* (Figure 1.15) and *T. vaginalis* PNPs.

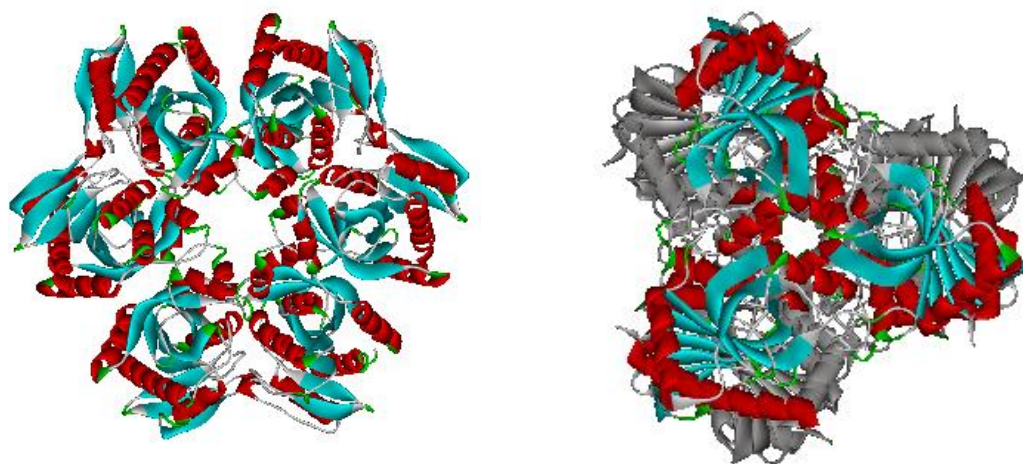


Figure 1.15 (Left) Crystal form of the low-MM *Thermus thermophilus* PNP hexamer (PDB code 1ODJ) (trimer of homodimers in a ring configuration) (Tahirov *et al.* 2004). (Right) Model of the high-MM Calf Spleen PNP (PDB code 1LVU)(dimer of homotrimers in a stacked configuration) (Koellner *et al.* 1998).

1.6.2 Pyrimidine Nucleoside Phosphorylases

1.6.2.1 Characterisation

The pyrimidine nucleoside phosphorylase activity is a function of three classes of enzymes: the thymidine nucleoside phosphorylase (TP), which is specific for a deoxyribosyl moiety, the uridine nucleoside phosphorylase (UP), which accepts deoxyuridine, deoxythymidine and uridine, and is therefore not specific for the ribosyl moiety, and pyrimidine nucleoside phosphorylase (PyNP) which catalyses the phosphorolysis of both uridine and thymidine (the PyNP from the thermophile

Geobacillus stearothermophilus shares 40% sequence identity with human thymidine phosphorylase).

1.6.2.2 Specificity and kinetic properties

Niedzwick and el Kouni (1983) tested 87 pyrimidine bases and nucleoside analogues as inhibitors towards PyNPs isolated mostly from higher organisms. Their findings provided the first structure-activity relationships for the PyNPs. Firstly, it was found that the UP had a hydrophobic region in the active site, with larger hydrophobic groups substituted at the 5'-position of uracil, dramatically enhancing binding to UP. The TP was found to be highly specific for the 2'-deoxyribosyl moiety of nucleoside ligands. It has been noted that the 5'-position of the pyrimidine ring can be occupied by a hydrogen, methyl, or amino-group with little effect on the reaction rate (Razzell and Casshyap, 1964).

1.6.2.3 Three-dimensional structures

Structures of *E. coli* (Caradoc-Davies *et al.*, 2004a), *Salmonella typhimurium* (Dontsova *et al.*, 2005), *Trypanosoma brucei* (Larson *et al.*, 2010), and *Homo sapiens* (Roosild *et al.*, 2009) uridine phosphorylases are available. Thymidine phosphorylases from *E. coli* (Walter *et al.*, 1990) and *Homo sapiens* (Norman *et al.*, 2004) have been studied. In addition, PyNPs from *Geobacillus stearothermophilus* (Pugmire and Ealick, 1998) and *Thermus thermophilus* (unpublished, DOI:10.2210/pdb2dsj/pdb) have been elucidated. The predominant subunit of UP is a dimer, with the tertiary structure being a trimer of dimers (Figure 1.15).

Structurally, TP is a dimer made up of two identical subunits with a dimeric molecular mass ranging from 90 kDa in *Escherichia coli* to 110 kDa in mammals. The fact that human TP shares 39% sequence identity with *E. coli* TP indicates similarity across prokaryotic and eukaryotic members of TP family.

The three-dimensional structure of TP reveals an S-shaped homodimer in which each subunit contains a large mixed α -helical and β -sheet domain (the α/β -domain) which is separated from a smaller α -helical domain (the α -domain) by a large cleft (Figure 1.16). The active site of each subunit consists of a thymidine binding site in the α -domain and a phosphate-binding site across the cleft in the α/β -domain (Pugmire and Ealick, 2002).

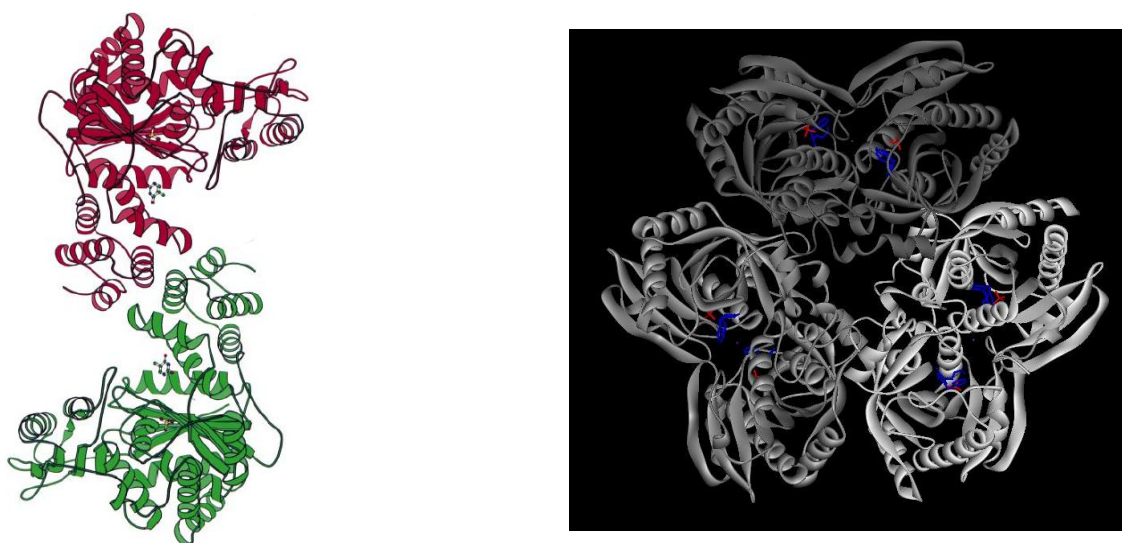


Figure 1.16 (Left) Dimer conformation of the *E. coli* TP (PDB code 1TGV) in the open conformation. The two monomers are coloured differently (Pugmire and Ealick, 2002). (Right) Representation of *E. coli* uridine phosphorylase. (Accelrys)

1.7 DIRECTED EVOLUTION

While enzymes have and are continually being discovered and have application in industrial processes, often these catalysts are not perfectly suited to an existing process or are not efficient enough for large scale processes. Natural genetic diversity is vast and it is probable that a suitable enzyme exists for a given process, but searching that vast enzyme diversity would not be feasible. The alternative is therefore to evolve a good enzyme to be more suitable for a given process. Natural

genetic evolution is a slow and tedious process whereby spontaneous errors in DNA replication occur, one of which may lead to an improved character trait. Due to natural selection, if that character trait produces a better adapted organism, then that trait will persist. This process however can be mimicked and accelerated in the lab and can be either rational or random in strategy. A number of mutation and evolution methods have been designed in this now well established field as summarised in Figure 1.17.

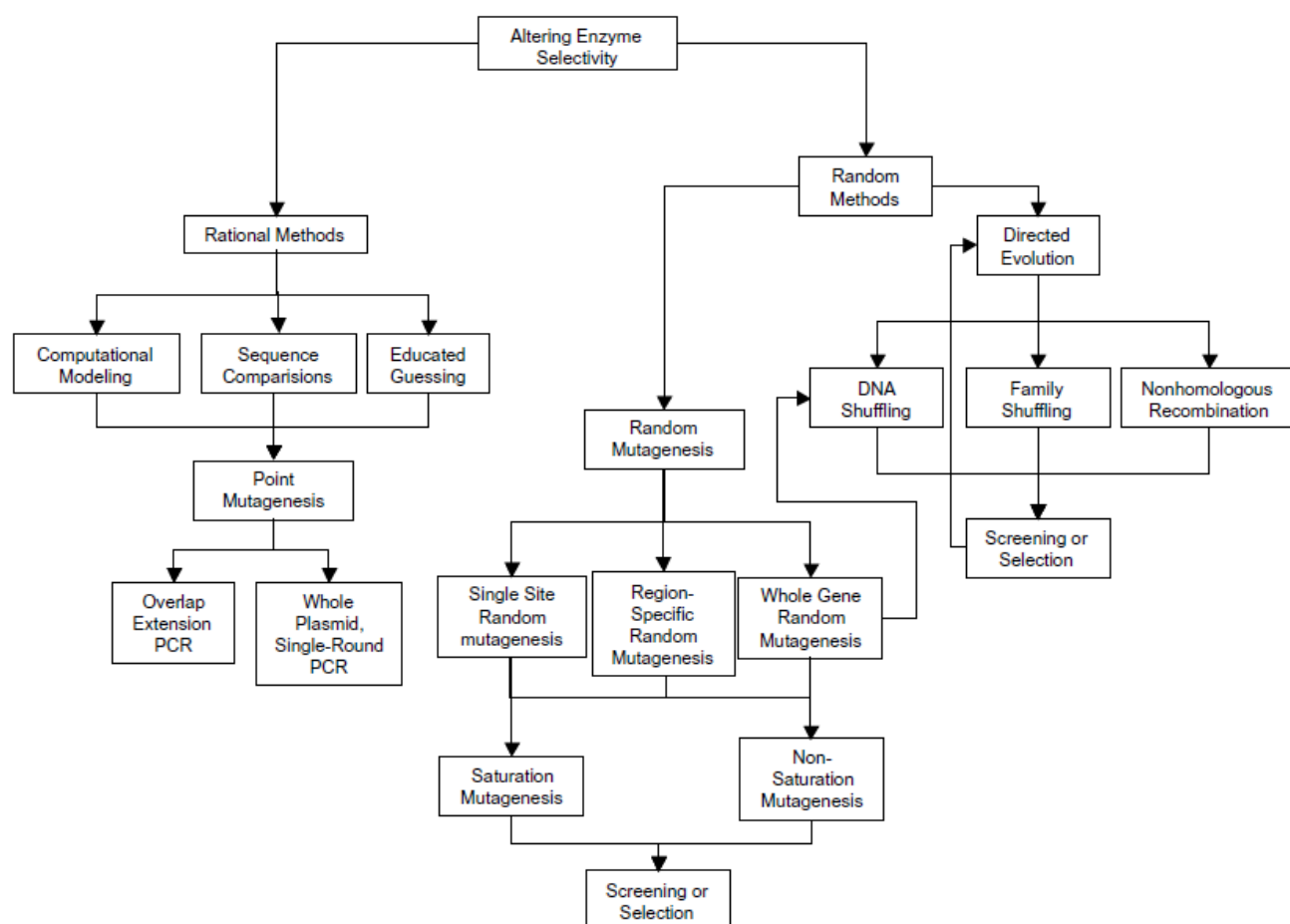


Figure 1.17 Summary of the molecular tools developed for evolution of enzymes (reproduced from Antikainen and Martin, 2005).

Rational mutagenesis requires detailed knowledge of the enzyme structure and structure-function relationships in order to define amino acid targets for mutation. It involves identification of amino acids involved in the particular trait to be modified, and then replacing those amino acids in a rational manner using site-directed mutation. The advantage of this approach is that only a small number of variants need to be screened for the improved phenotype. It is limited, however, by the need for the structure-function relationship of the enzyme to be thoroughly understood and often requires powerful computing technology to determine the best mutations to perform.

Often, however, random changes in a protein sequence can lead to unpredictable changes in tertiary structure, which can affect catalytic ability or stability of the protein. Small changes in the active site pocket, other than the catalytic amino acids, can often cause unexpected changes in specificity and activity of the enzyme (Koshland,1998). In addition, it often requires multiple mutations in different domains of the protein to improve the desired properties significantly. Hence the techniques of random mutagenesis and directed evolution are employed.

Since its inception in the early 1990s (Chen and Arnold, 1993; Stemmer, 1994), directed evolution has developed into an essential field in enzymology. Directed evolution is a powerful tool for creating molecular diversity amongst a set of proteins in order to obtain a desired phenotype (stability, catalytic activity, substrate specificity). Traditional methods such as error-prone PCR and oligonucleotide-directed randomization remain the foundations of directed evolution methodology. In addition, many new techniques have developed recently, such as codon shuffling, domain swapping and synthetic shuffling, offering more directed approaches and a higher likelihood of obtaining the desired phenotype. Along with defining a method for evolving enzyme diversity (library creation), one needs to define the methodology for determining the desired phenotype (screening methodology). Without an effective screening strategy, and therefore the ability to isolate clones with useful characteristics, the amount or quality of diversity created in the first step becomes redundant.

1.7.1.1 *Creating a directed evolution library*

Error-prone PCR methods are essentially standard PCR methods modified to enhance the natural error rate of *Taq* polymerase. Variation in the reaction composition such as increased $MgCl_2$ or adding $MnCl_2$ increases the error rate. Varying the ratio of oligonucleotides to create a nucleotide bias or adding non-natural nucleotides can also cause mutations. The frequency of mutation can be controlled by varying the initial template concentration or the number of extension cycles (Cirino *et al.*, 2003). The mutated inserts are then ligated into a suitable plasmid and transformed into a host for expression. Often this ligation step is inefficient and alternative methods such as whole plasmid PCR are employed (Miyazaki and Takenouchi, 2002). Depending on the frequency of mutation, error-prone PCR can lead to significantly large libraries, which would need to be screened to obtain the desired phenotype. The advantage, however, is that if that phenotype could exist, then this method of complete random mutation is likely to generate it.

DNA shuffling, originally developed by Stemmer *et al* (1994), is a method of creating diversity among a group of related genes collected from different organisms or created through error-prone PCR. The genes are randomly digested with either *DNase I* or a mixture of restriction endonucleases to yield a mixture of small fragments. The fragments are then reassembled in a polymerase chain reaction PCR to yield hybrid DNA strains containing combinations of each of the parent genes. A variation on the method negates the need to cleave the parent genes, but rather uses PCR to create small fragments. This has the advantage that only a small amount of the parent template is required for the reaction. In the stEP method (Zhao *et al.*, 1998) primers are used to replicate the target DNA with very short extension times, producing short fragments of replicated DNA. These fragments are then separated from the parent strand and allowed to anneal to and prime the replication of different strand. Repeated rounds of the process grow a strand of DNA with combinations of the initial parent strands. These methods can create useful recombination events, and rapid creation of a novel enzyme. The disadvantage of the methods is that the parent genes need to be sufficiently similar to allow cross priming between the sequences. Isolating a group of such sequences can be troublesome.

Saturation mutagenesis is one of the simplest forms of directed evolution. It involves mutating a single amino acid in a protein to every other natural amino acid, thereby giving every possible variation at that site. For this method, a set of forward and reverse primers are created with a mixture of C, G, A, and T nucleotides at the targeted codon site. During PCR, that site is then randomised giving codons for each of the other amino acids (Myers *et al.*, 1985).

Of particular interest are more recent developments in directed evolution based on saturation mutagenesis. The Combinatorial Active Site Saturation Test, or CAST (Reetz *et al.*, 2005), and Iterative Saturation Mutagenesis, ISM (Reetz *et al.*, 2006c), are methods which combine knowledge of the target protein's structure-function relationships with random mutagenesis. The methods require some knowledge of the target protein structure in terms of the active site or the residues potentially involved in enzyme stability. Both methods involve the creation of small, focused mutant libraries specifically around key residues involved in the target phenotype. Mutations conferring enhanced enzyme characteristics are then combined, vastly increasing the beneficial effect of individual mutations. The advantage of these methods is that dramatic improvements in the desired phenotype can be achieved with the creation of a series of relatively small mutant libraries. As an example, the enantiomeric ratio (E value) of an epoxide hydrolase from *Aspergillus niger* was increased from 4.6 to 115 after screening only 20000 clones using the CAST method. Similarly, the thermostability of a lipase from *B. subtilis* was improved from 48°C to 93°C after screening only 8000 clones using the ISM method.

Finally, one needs to define the host organism for expression of mutant enzymes. *E. coli* is most commonly used for library creation. The disadvantage of using *E. coli* it may not express functional mutants of fungal enzymes or other enzymes which are naturally glycosylated. Proteins are also not generally secreted, which may necessitate a cell breakage step in the screening protocol and also limits practical expression levels. A final limitation of *E. coli* is that the transformation of the ligation products is typically a few orders of magnitude lower than using supercoiled plasmids. This can be a problem when a large number of mutants is needed to obtain

sufficient library coverage (Tobias, 2003). The alternative is to use *Saccharomyces cerevisiae*. This would overcome the problem with expressing glycosylated genes and can allow for secretion of proteins. Transformation numbers are generally lower per unit DNA but can be improved using *in vivo* recombination of the plasmid and mutant inserts utilising the yeast's gap repair (Butler and Alcalde, 2003). In this method, open plasmid and mutant gene sequences are transformed into the yeast cells, which will then recombine the plasmid and mutant gene sequence *in vivo*. Using this method increases transformation efficiency as linear DNA rather than circular DNA is used for the transformation.

1.7.1.2 Functional screening of mutant libraries

To analyse a library of mutant enzymes adequately, a screening methodology should be designed that is accurate enough to detect small variations in enzyme function but also sensitive enough to detect the low levels of activity that are generally seen in early rounds of mutation. By the very nature of the library size created in directed evolution experiments, the assay also needs to be high throughput. Finally, the assay needs to be designed in such a way that the specific phenotype of interest can be detected (Arnold and Georgiou, 2003).

It is essential that the screening strategy is well planned before any work is performed. Wrong decisions early in the process can lead to wasting time and money, and more importantly could lead to negative or false positive results due to the wrong screening parameters. Each individual screening strategy should fit into the general screening strategy outlined in Figure 1.18. The concept is to narrow the field of test catalysts at each step while simultaneously increasing the specificity of the assays at each level. At each level the best possible assay should be identified (preferably identified for all levels) before screening takes place. In this way, primary screens can lead into secondary and subsequently tertiary screens without the need to re-formulate the cell bank for vastly different assay parameters.

Primary Screens will generally involve either selection or enrichment in liquid culture or on agar plates. Enrichment involves increasing the percentage of positive

candidates in the screening pool by applying selective pressure to the group, favouring growth of certain cells over others by, for example, supplying a nutrient that can only be accessed through the action of the desired enzyme activity. In selection screening, all the organisms will grow on the selection media, but only those with the desired phenotype will give a positive response. This response will usually either be a halo formation (through the release of a chromagen) or a zone clearance (through degradation of a turbid substrate). These methods are qualitative, giving basic yes/no answers, but do allow much higher throughput than automated screening techniques. A third alternative, if neither selection nor enrichment can be applied (where the target enzyme does not regulate growth), is to develop an agar plate screen with visual identification using either zone clearances or colour reactions. These also allow rapid visual identification of positive colonies without hindering the growth of potential catalysts. Colour reactions can be due to change in pH when a desired product is formed creating a colour change in a suitable pH indicator.

The more common method is to use a chromogenic substrate for the desired enzyme, which releases the chromogen upon enzymatic processing. If such a substrate is not available or cannot be produced, it is also possible to perform filter bound assays where the filter or a nylon membrane is saturated with the target substrate and placed over the grown colonies. If the desired activity is present, a colour reaction occurs on the filter corresponding to a single colony on the agar plate.

If a solid-phase plate assay cannot be developed, the next solution is a simple liquid based assay using soluble enzyme substrates. These methods tend to be more quantitative but do limit throughput as compared to plate assays. They require that test subjects are arrayed on microtitre plates prior to screening, as well as necessitating automation to achieve even medium throughput screens.

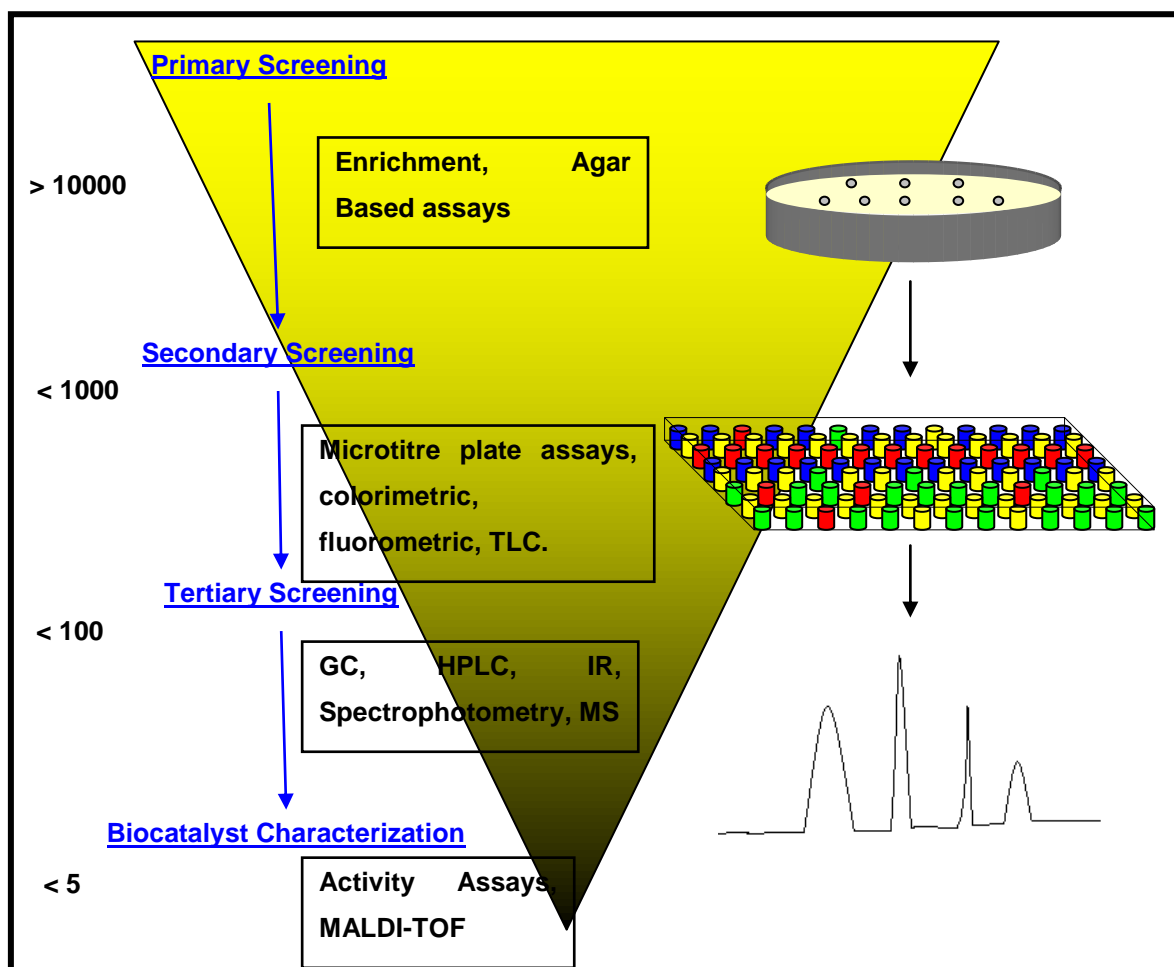


Figure 1.18 Outline of general screening approach showing the progression from low specificity, high throughput primary screens through to highly specific characterisation assays to isolate a desired physical or biochemical trait.

Substrate selection is also an important consideration when developing the primary screen. It is preferential to use the actual target substrate in the screen. Due to cost and throughput considerations this is not always possible and a substrate analogue may be required. To increase the potential of finding the activity of interest, it is essential that the analogue properties closely resemble the target substrate. If a general activity is being screened, it may be necessary to use a range of substrates at the primary level to ensure that potential positive candidates are not missed.

Screening criteria need to be considered early in the screening process. Screening criteria can affect the candidates that are identified as well as the physical and kinetic properties of identified enzymes. The ultimate goal of biocatalyst screening is to identify a catalyst for large scale production. The wrong screening criteria could identify enzymes that are not economically suitable for large scale. Screening criteria such as substrate, pH, temperature, buffer, salts and the use of co-solvents should mimic the end application as much as possible.

Secondary screening should be limited to liquid, microtitre based screens. These are semi-quantitative screens that include colorimetric screens, fluorimetric screens, luminescence and polarimetry. Developing these screens requires knowledge of the target enzyme as well as the properties of the target substrate that can be utilised in order to quantitatively analyze either the disappearance of the substrate or the formation of the desired product. Where it may not be possible to measure the activity by the methods mentioned above, one could turn to thin layer chromatography (TLC) for a solution. Alternatively, second and third coupled enzyme assays have been developed where the product(s) of a desired enzyme reaction form the substrate(s) of subsequent enzymes in the reaction mixture, which then catalyse the formation of measurable product. Secondary screening can also involve measuring variations in pH temperature, ionic and other physical assay conditions to select for enzymes activities with desirable physical characteristics.

Tertiary screening is the most complex and also the slowest of the screening steps. It is therefore only employed when there is a select group of catalysts. Recent advances in automation allow larger groups here, but due to experimental design and data manipulation considerations of dealing with a large number of catalysts at this level, it is preferential to limit the number of organisms or enzymes screened. Tertiary screens will involve gas chromatography (GC), high performance liquid chromatography (HPLC), mass spectrometry (MS) as well as spectrophotometric and fluorogenic methods using more specific substrates and reaction parameters.

1.8 IMMOBILISATION

The majority of biocatalysts used in industrial biotransformation are in the form of free whole cells (Figure 1.19). This is due to the relatively low cost involved with the development and preparation of such a catalyst. The disadvantage of using whole cells is that you can potentially get a number of side reaction and unwanted by-products, which may complicate down-stream processing. It is often therefore preferable to use partially or completely purified enzymes. The disadvantage here is that these preparations are often not stable and cannot be easily recovered to re-use. A number of processes therefore use immobilisation techniques, as they often add stability to the enzyme and enable recycle. As such, there are equivalent numbers of processes using immobilised enzymes as there are those using free enzymes, despite the cost involved in immobilizing the catalyst.

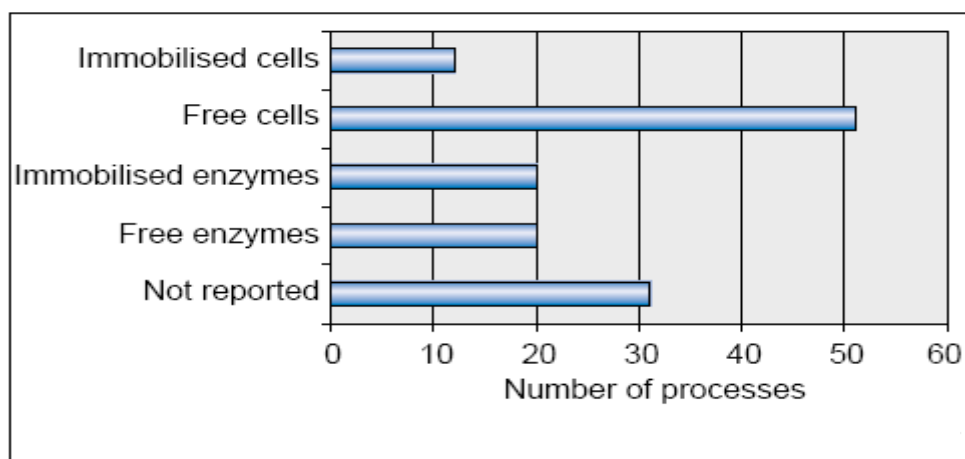


Figure 1.19 Use of free and immobilised whole cells or enzymes in industrial processes (reproduced from Straathof *et al.*, 2002).

Immobilisation methods include covalent binding to a support such as Eupergit, crosslinking or self immobilisation (CLEA, CLEC) and entrapment or encapsulation in a gel or polymer such as alginate or polyacrylamide. The relative advantages and disadvantages of each of these methodologies was reviewed by (Brady and Jordaan, 2009).

The *E. coli* UP and PNP1 have been co-immobilised by covalent linkage to epoxy-activated Sepabeads for the biocatalytic preparation of a variety of natural and modified purine nucleosides (Zuffi *et al.*, 2004). The immobilised biocatalysts showed higher thermal stability and resistance to organic solvents. The co-immobilised enzymes were recycled for more than 30 transglycosylation reactions. Similarly, nucleoside phosphorylases from *Geobacillus stearothermophilus* were covalently immobilised on aminopropylated macroporous glass (Taran *et al.*, 2009). These preparations showed increased thermal stability high and levels of activity retention (>80%) when immobilised. Simple separation of the catalysts was achieved by filtration and less than 1% activity was lost per cycle for up to 20 recycles at 70°C. Whole cells of *E. coli* BL21 were immobilised on macroporous sheets of high-density polyethelene (Trelles *et al.*, 2008). These biocatalysts were used for the production of adenosine by transglycosylation. The immobilised cells showed improved storage stability and could be reused up to 39 times with less than 50% loss in initial activity. Hori *et al* (1991) immobilised PNP and PyNP from *Geobacillus stearothermophilus* by ionic binding to DEAE-Toyopearl 650M anion exchange resin. Using the immobilised biocatalysts, they were able to design a continuous reaction for the production of 5-methyluridine from inosine and thymine which was run for 17 days at 60°C.

Use of solid supports for immobilisation (as for the nucleoside phosphorylase examples above) has the disadvantage of decreasing the volumetric and often the specific activity of the biocatalyst. Self-immobilisation techniques such as Cross-linked enzyme crystals (CLEC, St Clair and Navia, 2008)), Cross-linked enzyme aggregates (CLEA, Sheldon, 2007)) and more recently Spherezymes (Jordaan *et al.*, 2009) overcome this problem. Physically strong biocatalysts comprised of only the protein of interest can be created with high volumetric and specific activities. In addition, it has been shown by Wilson *et al.* (2004) that self immobilised enzyme can stabilise the quarternary structure of multimeric enzymes.

1.9 RESEARCH HYPOTHESIS

1.9.1 Problem Statement

It has been established that the production of 5-methyl uridine by transglycosylation is feasible (Ishii *et al.*, 1989; Hori *et al.*, 1989b; Hori *et al.*, 1991; Zoref-Shani *et al.*, 1995). However, there is no published methodology for a commercially viable biocatalytic reaction, specifically using guanosine and thymine as the starting substrates (Figure 1.20). This is largely due to the insolubility of the substrates at high concentrations (guanosine and thymine). To date, no catalysts have been discovered that suit the ideal reaction. These catalysts would need to:

- operate at temperatures above 60°C to facilitate solubilisation of the substrates
- be highly efficient catalysts in order to achieve high productivity in the reaction
- be produced cost effectively in order to not impact significantly on the process costs
- be recyclable (immobilised).

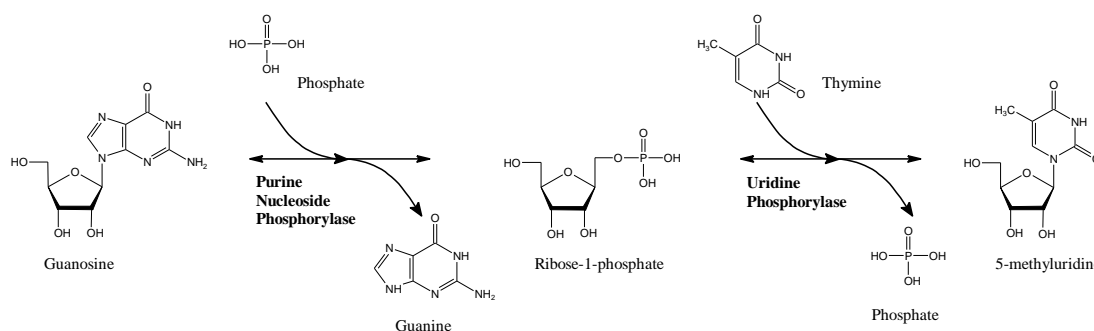


Figure 1.20 Transglycosylation reaction for the production of 5-methyluridine from guanosine and thymine.

1.9.2 Research Hypothesis

It is possible to obtain novel, highly efficient nucleoside phosphorylases for the production of 5-methyluridine through a combination of environmental screening, directed evolution and enzyme immobilisation.

1.9.3 Aims and Objectives

To prove the stated hypothesis, research will be conducted to:

- isolate suitable biocatalysts by screening environmental and commercial nucleoside phosphorylases for the ability to produce 5-MU
- determine optimal conditions for biocatalytic reactions
- determine target characteristics for biocatalyst evolution
- evolve PNP and/or UP to improve biotransformation efficiency
- stabilise biocatalysts through immobilisation

CHAPTER 2: IDENTIFICATION

SCREENING AND ISOLATION OF NUCLEOSIDE PHOSPHORYLASES

2.1 INTRODUCTION

5-Methyluridine is a non-natural nucleoside that can be used as an intermediate in the synthesis of thymidine, and in the synthesis of nucleoside analogues AZT and stavudine, both of which are used in Highly Active Anti-Retroviral Treatment (HAART) of HIV/AIDS patients. As the compound needs to be formed as a single isomer, 5-methyluridine can be synthesised through the transglycosylation of D-ribose-1-phosphate, using guanosine as a donor, and thymine as acceptor (Rocchietti *et al.*, 2004; Medici *et al.*, 2004; Ge *et al.*, 2009). However, the reagents guanosine and thymine are relatively insoluble, resulting in particulate substrates with poor reaction kinetics, and the most effective method of solubilising these materials is in hot aqueous solutions. It would therefore be preferable to utilize thermostable enzymes. Enzymes provide regio- and stereoselectivity, and hence are an ideal option for nucleoside transglycosylation (Prasad *et al.*, 1999; Utagawa, 1999). Enzymes that can be used in this transglycosylation reaction include PNP, thymidine phosphorylase (TP; EC 2.4.2.4) and uridine phosphorylase (UP; EC 2.4.2.3) (Bzowska *et al.* 2000; Pugmire and Ealick 2002). TP and UP are functionally both pyrimidine nucleoside phosphorylases (PyNP; EC 2.4.2.2.), although UP is closer in sequence identity to PNP than PyNP (Lewkowicz and Iribarren, 2006). In general, prokaryotic PNPs are more amenable to these transglycosylation reactions as they have broader specificity than their mammalian counterparts (Tonon *et al.*, 2004). In addition, thermophiles have been shown to harbour enzymes which exhibit a much greater thermostability. For example the thermophile *Geobacillus stearothermophilus* (previously *Bacillus stearothermophilus*) has two purine nucleoside phosphorylases which have been characterised (Saunders *et al.*, 1969; Hori *et al.*, 1989a) and applied in the synthesis of 5-methyluridine (Hori *et al.*, 1989b; 1991). However, although these enzymes are

thermostable, they have low levels of expression in the wild type. The genes have both been subsequently successfully expressed in *E. coli* at high levels (Okuyama *et al.*, 1996; Hamamoto *et al.*, 1997a; 1997b).

The objective of this section was to evaluate the nucleoside phosphorylases present in the moderately thermophilic and alkaliphilic organism, *Bacillus halodurans* Alk36 (Louw *et al.*, 1993; Crampton *et al.*, 2007). These enzymes will be compared to those from *E. coli*, which are known to be efficient biocatalysts for transglycosylations (Lewkowicz *et al.*, 2000; Spoldi *et al.*, 2001; Rogert *et al.*, 2002; Zuffi *et al.*, 2004; Trelles *et al.*, 2004; 2008; Ge *et al.*, 2009). In addition, nucleoside phosphorylases from *Klebsiella pneumoniae* and *Bacillus licheniformis* were identified and compared for the production of 5-methyluridine by transglycosylation.

2.2 METHODS & MATERIALS

2.2.1 Materials

All restriction enzymes and the T4 DNA ligase were purchased from Fermentas (Lithuania). The Roche High Fidelity PCR mix was used for all polymerase chain reactions. SDS-PAGE markers were purchased from Fermentas. Nucleosides and nucleoside phosphorylases were purchased from Sigma. Lysozyme, Pronase and RNase were obtained from Roche Diagnostics. Sakosyl (sodium N-lauroylsarcosinate) was obtained from Merck. General chemicals were purchased from Sigma.

2.2.2 Genomic DNA Isolation

B. halodurans Alk36 was grown overnight at 42°C in Luria Broth (LB) pH 8.5 (10 g.l⁻¹ NaCl; 10 g.l⁻¹ Tryptone, 5 g.l⁻¹ yeast extract). Similarly, *E. coli* was grown overnight at 37°C in LB at pH 7.0. Genomic DNA was isolated from both organisms according to the method of Lovett and Keggins (1979). Cells from an overnight culture (10 ml) were harvested and washed twice with TES buffer (20 mM Tris-HCl, pH 7.5, 5 mM EDTA, 100 mM NaCl). The pellet was then resuspended in 2.5 ml TES buffer. Lysozyme (500 µg.ml⁻¹) and RNase (100 µg.ml⁻¹) were added, and the suspension incubated for 25 min at 37°C. TES buffer (5 ml) was then added before adding pronase (500 µg.ml⁻¹) and sarkosyl (0.8 % m.v⁻¹). After a further 30 min incubation at 37°C, the cell debris was removed by centrifugation at 20 000 x g (30 min). The supernatant (cell lysate) was then gently shaken with an equal volume of TES saturated phenol for 10 min (room temperature). After centrifugation (15000 x g), the aqueous phase was removed and extracted twice again with phenol. The final aqueous phase was transferred to 2 volumes ethanol (4°C) and the DNA was allowed to precipitate over 30 min. The DNA precipitate was resuspended in 2 ml TES and dialysed (Snakeskin dialysis tubing, 10 000 Molecular weight cut-off, Pierce, USA) against 2 L of TES buffer overnight.

2.2.3 Oligonucleotides, plasmids and microbial strains

E. coli JM109 (DE3) was used as the expression host for *E. coli* PNP1 (EcPNP1), PNP2 (EcPNP2) and *B. halodurans* PNP1 (BHPNP1). *E. coli* BL21 (DE3) was used as the production host for *E. coli* UP (EcUP). Both the pMS470Δ8 and the pET20b plasmids conferred ampicillin resistance in the host. *Bacillus halodurans* Alk36 was used as a source of UP from that organism (BhUP). *Klebsiella pneumoniae* and *Bacillus licheniformis* were previously identified as good UP producers (Appendix 1). The PNP gene designated BHPNP1 was amplified as described below. Isolation of the *E. coli* PNP and UP genes was carried out as described by Lee *et al.* (2001) and Spoldi *et al.* (2001), respectively. The *E. coli* PNP2 (EcPNP2, product of the *xapA* gene) was amplified according to the methods of Dandanell *et al.* (2005). The

amplified PCR products were ligated initially into pGEM-T Easy and subsequently into pMS470 (EcPNP1, EcPNP2, BHPNP1) and pET20b (EcUP). The respective expression hosts were then transformed with the expression plasmids by heat shock treatment (Sambrook and Russell, 2001).

2.2.4 Amplification of the *B. halodurans* Alk36 PNP gene.

The PNP gene designated BHPNP1 was amplified using the following primers: BH1531F 5' – GGACATATGCTTAAACGTAACCTCAATTG (*Nde*I site, underlined) and BH1531R 5' – GGTAAGCTTTTACATGTCTTTAACGATTGC (*Hind*III site, underlined). PCR was performed using the High Fidelity Polymerase from Roche (Germany). The PCR amplification protocol employed was as follows: a single 10 minute hold at 95°C was followed by 25 cycles of 1 minute at 95°C, 1 minute at 55°C and 1 minute at 72°C. A final 10 minute incubation at 72°C was followed by a 4°C hold. The size of the amplified product was confirmed on a 0.8 % agarose gel and isolated using the GeneJET Gel Extraction kit (Fermentas). The PCR product was ligated into pGEM-T Easy (Promega, USA). Restriction digests were performed with *Nde*I and *Hind*III to release the BHPNP1 insert.

The BHPNP1 gene was subsequently ligated using T4 DNA ligase (Fermentas) into pMS470 Δ 8 (expression vector) (Balzer *et al.*, 1992) restricted with *Nde*I and *Hind*III. This gave plasmid pMSPNP. *E. coli* JM109 (DE3) was transformed with this plasmid for expression analysis.

2.2.5 Native enzyme production from *E. coli*

E. coli JM109 was used to provide a crude native enzyme solution for initial experiments. An inoculum culture of *E. coli* JM109 was grown in 100 ml Luria broth (LB) (10 g.l⁻¹ NaCl; 10 g.l⁻¹ Tryptone, 5 g.l⁻¹ yeast extract) overnight at 37°C with shaking at 200 rpm. Fifteen millilitres of this culture was used to inoculate 5 x 400 ml LB in Fernbach flasks. These cultures were grown for 4 h at 37°C with shaking at 220 rpm. The two litres of culture broth was centrifuged for 10 min at 17000 x g.

The resultant pellet was resuspended in 100 ml sonication buffer (20 mM Tris-HCl, pH 7.2, 5 mM EDTA, 1 mM DTT) and chilled on ice for 20 min. This suspension was sonicated for 10 min at 4°C and then centrifuged for 10 min at 17000 x g. Ammonium sulphate was added to the supernatant to 40% saturation and stirred at 4°C for 20 min. This was centrifuged as before and additional ammonium sulphate was added to the supernatant to obtain 70% saturation, which was again stirred on ice for 20 min. After centrifugation the pellet containing the enzymes of interest was resuspended in 100 ml 20 mM Tris-HCl buffer at pH 7.2. This preparation was desalted by ultrafiltration through a 10 kDa filtration membrane. The concentrated sample was washed with water and filtered to aid desalting. The resulting solution (50 ml) was lyophilized and a total of 710 mg of lyophilized material was obtained, which constituted the crude extract sample.

Similarly *B. halodurans*, *K. pneumoniae* and *B. licheniformis* were cultivated in TYG media (Tryptone, 5 g.l⁻¹; yeast extract, 2 g.l⁻¹; glucose, 1 g.l⁻¹) at 40°C with shaking at 200 rpm overnight for isolation of their specific native UP (BhUP, KpUP and BlUP, respectively).

2.2.6 Over-expression of nucleoside phosphorylases

Recombinant strains producing selected nucleoside phosphorylases were prepared at 700 ml scale using defined growth media (as used for fermentation, see section 3.2.2)(14.6 g.l⁻¹ K₂HPO₄; 2 g.l⁻¹ (NH₄)₂SO₄; 3.6 g.l⁻¹ Na₂HPO₄; 2.5 g.l⁻¹ Citric Acid; 0.25 g.l⁻¹ MgSO₄; 5 g.l⁻¹ NH₄NO₃; 10 g.l⁻¹ yeast extract; 30 g.l⁻¹ glucose and 100 µg.ml⁻¹ ampicillin). An overnight culture (100 ml) of each strain was used as the inocula for 600 ml media in 2 L Fernbach flasks. Cultures were grown for 4 h at 37°C with shaking at 200 rpm before enzyme expression was induced with a final concentration of 1 mM IPTG. Cultures were then harvested after a further 2 h growth under the same conditions.

2.2.7 Preparation of crude extracts.

UP from *B. halodurans*, *K. pneumoniae* and *B. licheniformis* was isolated according to the methods described in Appendix 2. For the over-expressed enzymes, culture broth was centrifuged for 10 min at 17000 x g. The resultant pellet was resuspended in Bugbuster HT (Novagen) containing 3 mg/ml lysozyme (USB) and incubated for 2 h at 30°C. Cell debris was removed by centrifugation (16000 x g, 10 min). The supernatant was diluted with 20 mM Tris-HCl (Sigma) buffer, pH 7.2, containing 50 mM NaCl. Samples were dialysed against the same buffer overnight. Anion exchange chromatography of each sample was performed on an AKTA Prime (Amersham Biosciences) using SuperQ 650m resin (TosohBioSep). Proteins were eluted using a linear gradient of 50 mM – 350 mM NaCl in 20 mM Tris-HCl pH 7.2, over 400 ml (4 ml.min⁻¹). PNP and UP activity were assayed on all fractions (5 ml fractions collected). Fractions identified in this step for UP and PNP activity were separately pooled and concentrated to 2 ml by ultrafiltration (Omega 30 kDa membrane, Amicon).

2.2.8 Initial assessment of commercial enzymes and crude extracts for transglycosylation potential

Reactions (3 ml) at a 2.5 mM nucleoside concentration were performed in 50 mM sodium phosphate buffer, pH 7.4 at 25°C over three hours, with agitation. TP, Bacterial PNP and xanthine oxidase (XO) (Sigma) standards were assessed, as well as a freshly prepared crude enzyme extract of *E. coli* containing both PNP and UP activity.

2.2.9 Assessment of different nucleoside phosphorylases for production of 5-methyl uridine

Enzyme stock solutions (0.02 U.ml^{-1}) were prepared in 50 mM sodium phosphate buffer, pH 8.0. Each of the enzymes were tested for their ability to produce 5-MU, firstly individually and then in ratios of PNP:UP of 5:1; 2:1; 1:1; 1:2 and 1:5. The total enzyme concentration was maintained at 0.004 U/ml for each of the experiments. Enzyme solutions and assay reagent (100 μl containing 5 mM guanosine and 5 mM thymine in 50 mM phosphate buffer, pH 8.0) were aliquoted into a 96-well microtitre plate using the EpMotion 5075 (Eppendorf). The microtitre plate was incubated for 1 h at 40°C with shaking at 900 rpm (Labsystems Thermomix). Results were analysed by TLC (5 μl spot, 85:15 chloroform:methanol mobile phase, 10 cm UV_{254} Silica plates).

2.2.10 Small scale biocatalytic reactions

EcPNP (0.85 U.mg^{-1}), EcUP (0.52 U.mg^{-1}) and BHPNP1 (1.41 U.mg^{-1}) at final concentrations of 0.15 U.ml^{-1} each were tested in 75 ml reactions at 40°C for 25 h. The reaction contained 53 mM (1.5% m.m^{-1} (mass reactant per mass reaction)) guanosine and 127 mM (1.5% m.m^{-1}) thymine in 50 mM sodium phosphate buffer (pH 7.5).

2.2.11 Analytical

2.2.11.1 Sequence confirmation of genes

Sequence data was confirmed by Inqaba Biotechnology (Pretoria, South Africa) using the PCR primers described above. *E. coli* sequences were compared to the known nucleotide and amino acid sequences (Walton *et al.*, 1989). The insert for the BH1531 gene was compared to the known nucleotide and amino acid sequence of the

gene from *B. halodurans* C-125 (BAB05250) and has been submitted to GenBank under the accession number GQ390428.

2.2.11.2 Analysis of biocatalytic reactions

Samples were prepared by dissolving the required amount of sample in sodium hydroxide (10 M, 0.5 – 1 ml) and then made up to the required volume so as to ensure the sample concentration was within the linear region of the calibration curve. Guanosine, guanine, thymine and 5-methyluridine were quantitatively analysed by HPLC, using a Waters Alliance Model 2609 instrument (Waters, USA) with a Synergi 4 μ Max-RP 150 x 4.6 mm column. Components were detected using a UV detector at 260 nm. The eluent was ammonium acetate, 25 mM, pH 4.0, flow rate of 1 ml.min⁻¹ and a run time of 20-30 minutes at 25°C. Elution times were determined to be (in minutes) 6.52 (guanine), 9.38 (thymine), 17.21 (5-MU) and 16.66 (guanosine) using pure materials from Sigma-Aldrich as reference standards.

2.2.11.3 Protein Determination

Protein concentrations were determined using the Biorad protein concentration determination assay (Biorad). Bovine Serum Albumin (BSA, Sigma-Aldrich) was used as the protein standard.

2.2.11.4 Standard colorimetric assays

The method of Hwang and Cha (1973) was modified for PNP determination wherein a suitably diluted sample (10 μ l) was added to 190 μ l of 50 mM sodium phosphate buffer, pH 8.0, containing 0.5 mM inosine and 0.2 U.ml⁻¹ xanthine oxidase, in UV compatible 96 well microtitre plates (Thermomix). The change in absorbance at 293 nm due to the liberation of uric acid was measured on a Powerwave HT microplate spectrophotometer (Biotek, USA). One unit (U) of PNP was defined as the enzyme liberating 1 μ mol of uric acid from inosine per minute, in the presence of

excess xanthine oxidase. The extinction coefficient under these conditions was determined to be $7454 \text{ M}^{-1} \cdot \text{cm}^{-1}$.

The method of Hammer-Jespersen et al. (1971) was modified for UP determination, wherein a suitably diluted sample (10 μl) was added to 190 μl of 50 mM sodium phosphate buffer containing 2.5 mM uridine, in 96-well polypropylene microtitre plates. After 10 min incubation time at 40°C , the reaction was stopped by addition of 100 μl 0.5 M perchloric acid. The samples were then incubated on ice for 20 min and centrifuged for a further 20 min (7000 x g) to remove residual protein. Sample (100 μl) was then transferred to a UV compatible microtitre plate and combined with 100 μl 1 M NaOH. The change in absorbance at 290 nm due to the liberation of uracil was measured on a Powerwave HT microplate spectrophotometer. One unit (U) of UP was defined as the enzyme required for liberation of 1 μmol of uracil from uridine in one minute. The extinction coefficient under these conditions was determined to be $3240 \text{ M}^{-1} \cdot \text{cm}^{-1}$. Nucleosides were purchased from Sigma-Aldrich.

2.3 RESULTS AND DISCUSSION

2.3.1 Assessment of nucleoside phosphorylases for production of 5-methyluridine

2.3.1.1 *Commercially available nucleoside phosphorylases and crude extract from E. coli*

The aim of the research was to develop an enzyme based high yielding synthesis for 5-methyluridine. To this end initial reactions were performed to confirm the relevant enzyme activities.

Reactions 1 and 2 (see Table 2.1) were performed as control reactions to confirm the reversibility and direction of equilibrium of the pyrimidine phosphorolysis. Reaction 3 was performed to confirm the forward (phosphorolysis) purine reaction can occur

when using XO and PNP. Xanthine oxidase was used to convert the co-product hypoxanthine to uric acid to prevent the reverse reaction. Reaction 4 was a confirmation of a transglycosylation reaction using commercial TP and PNP.

The aim was to transfer the ribose group from guanosine to thymine (i.e. from a purine to a pyrimidine), yielding 5-methyluridine, but this was unsuccessful using the commercial preparations of TP and PNP (Reaction 5). An alternative purine nucleoside, inosine, was evaluated as a ribose donor, but this was also unsuccessful (Reaction 6). Reactions 5 and 6 did not progress, presumably due to the strict requirement of TP for deoxyribose-1-phosphate rather than R-1-P, a result that was anticipated (see section 1.6.2.1), but required confirmation. However, the enzyme UP can utilise R-1-P, but was not commercially available. Through the use of native *E. coli* cell extract (which contained both PNP and UP activities 0.017 and 0.012 U.mg⁻¹), it was possible to generate 5-methyluridine (Reactions 7 and 8).

Table 2.1 Summary of results obtained for reactions

Reaction	Expected product	Starting reagents	Enzymes used	Product peak % of total peak area
1	Thymine	Thymidine	TP*	78.5
2	Thymidine	Thymine	TP*	19.5
3	Hypoxanthine, Xanthine	Inosine	XO, PNP*	61.7
4	2-deoxyinosine	Hypoxanthine, thymidine	TP, PNP*	33.4
5	5-methyluridine	Thymine, Guanosine	TP, PNP*	0
6	5-methyluridine	Inosine, thymine	XO, TP, PNP*	0
7	5-methyluridine	Inosine, thymine	Crude extract, XO	21.8
8	5-methyluridine	Guanosine, thymine (16 h)	Crude extract	8.7

Reactions were carried out at 3 ml scale in sodium phosphate buffer (50 mM, pH 7.4) with equivalent molar concentrations of thymine and guanosine (2.5 mM).

*The reactions were performed over 3 hours at 25°C using commercially available enzymes: 0.1 U of both PNP (10 U.mg⁻¹ protein) and recombinant thymidine phosphorylase from *E. coli*.

2.3.1.2 Combinations of PNP and UP from *E. coli*, *B. halodurans*, *K. pneumoniae* and *B. licheniformis*

Enzyme preparations isolated from wild type organisms were then evaluated. A number of the single enzyme preparations showed the ability to produce 5-MU (Figure 2.1). This may be explained by contaminating enzymes within the preparation as they have not been purified to homogeneity. When comparing combinations of purine and pyrimidine nucleoside phosphorylases (Figure 2.2 and Figure 2.3), it is evident that the combinations of EcPNP:EcUP (lane 1) and BHPNP1:EcUP (lane 9) consistently gave the highest 5-MU production. When comparing just these two combinations across the different ratios, one can see that higher ratios of PNP gave higher 5-MU production (Lanes 1 & 9 Figure 2.2 and Figure 2.3). A comparison of the PNPs showed here that EcPNP and BHPNP1 gave similar results throughout the experiments. EcPNP2 based enzyme combinations (Lanes 5 – 8, Figure 2.2 and Figure 2.3) showed little to no 5-MU production. Similarly, the UPs from *E. coli* (EcUP) and *B. halodurans* (BhUP) seemed to be superior catalysts when compared to those from *K. pneumoniae* (KpUP) and *B. licheniformis* (BIUP).

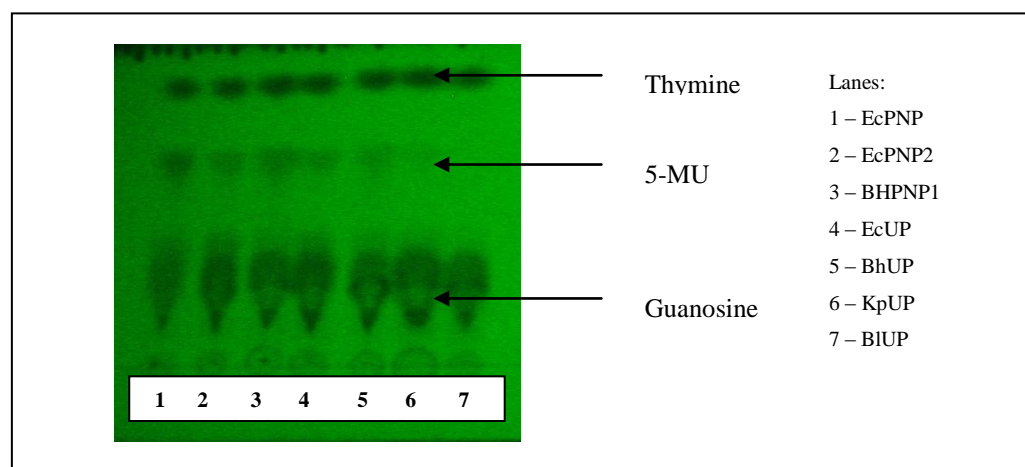


Figure 2.1 Assessment of 5-MU production by individual enzyme preparations.

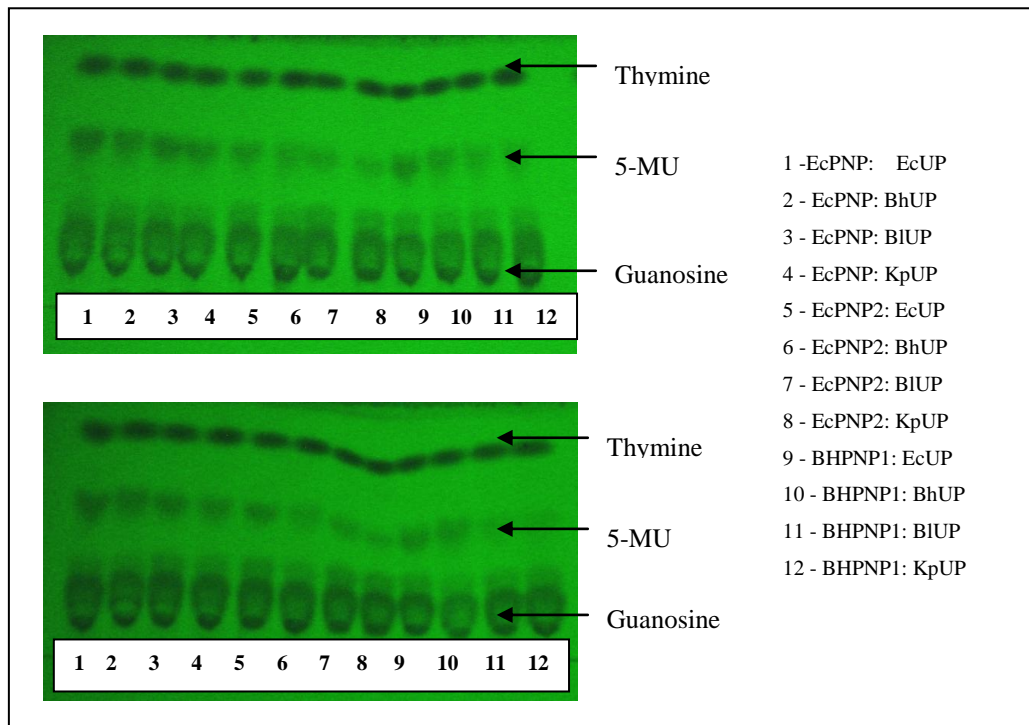


Figure 2.2 5-MU production assessment using PNP:UP ratios of 1:1 (top) and 1:2 (bottom)

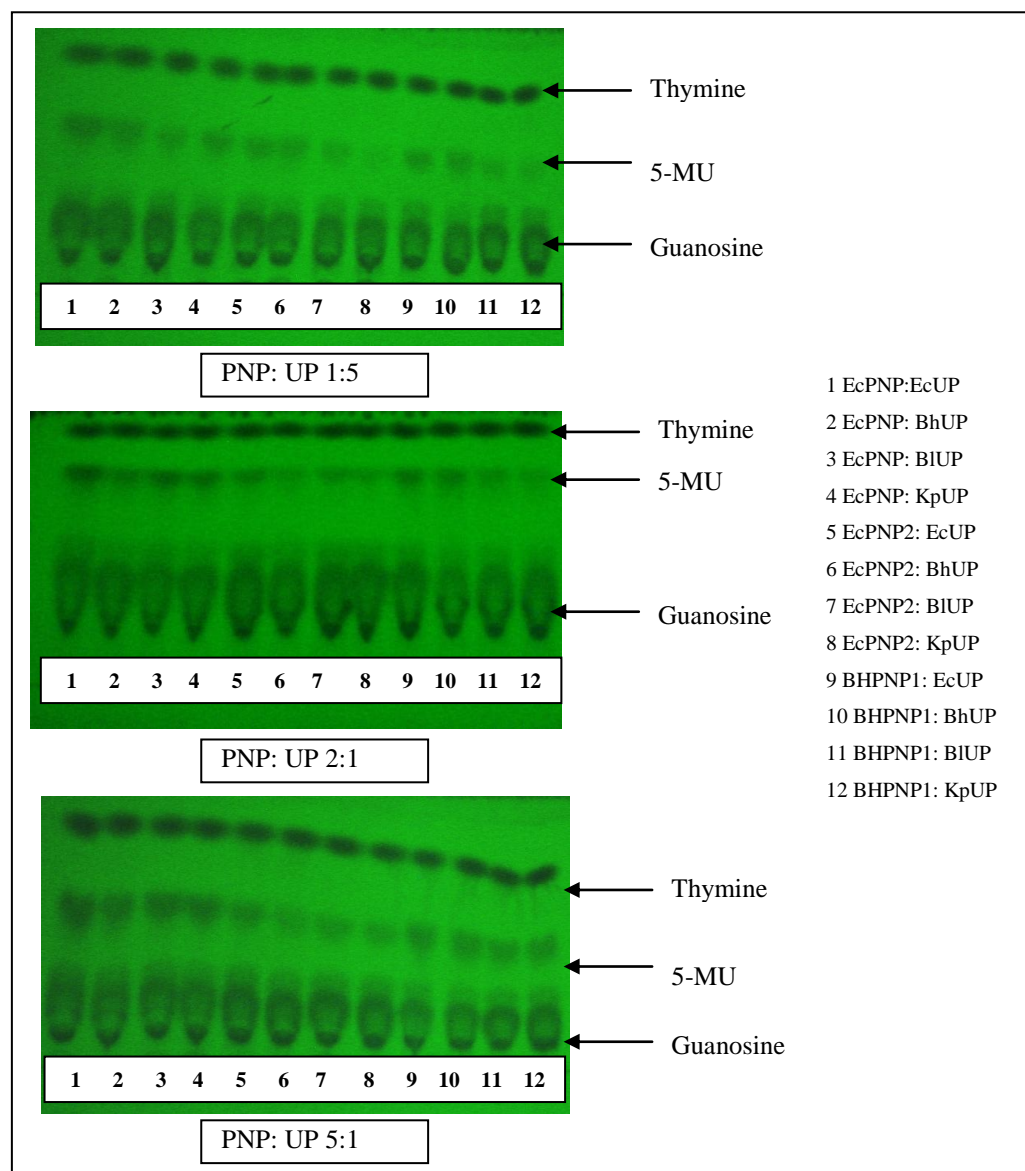


Figure 2.3 5-MU production assessment using PNP:UP ratios of 1:5; 2:1 and 5:1

While all combinations tested demonstrated some 5-methyl uridine production, reactions containing EcPNP, BHPNP1 and EcUP showed the highest production levels. This observation is most likely due to base and sugar moiety specificities. The UPs isolated from *K. pneumoniae* or *B. licheniformis* have previously been shown to be active towards uridine, indicating that they are specific towards the dioxy sugar moiety (Ribose-1-phosphate), but the low activity seen in this experiment indicates that they are not active towards the 5-methylated pyrimidine base. Similarly, the UPs from *E. coli* and *B. halodurans* are active towards the dioxy sugar moiety, but show

good activity towards both the methylated (5-methyluracil) and non-methylated (uracil) pyrimidine base. These results also indicate that the PNP1 from *E. coli*, and PNP1 from *B. halodurans*, are more active towards guanosine than PNP2 from *E. coli*. This was expected as PNP2 has been characterised as being more specific towards xanthosine than other purine substrates (Dandanell *et al.*, 2005). It was decided therefore to perform larger scale tests using EcPNP, BHPNP1 and EcUP.

A series of experiments was then conducted to identify which enzyme system (EcPNP : EcUP or BHPNP1 : EcUP) provided the best 5-MU yield. The enzymes were over-expressed as stated in the methods section by shake-flask cultivation. EcPNP (0.85 U.mg⁻¹), EcUP (0.52 U.mg⁻¹) and BHPNP1 (1.41 U.mg⁻¹) at final concentrations of 0.15 U.ml⁻¹ each were tested in 75 ml reactions at 40°C for 25 h. Improved molar yields to 51% on 53 mM (1.5% m.m⁻¹) guanosine in the presence of 127 mM (1.5% m.m⁻¹) thymine were observed for the combination of the *E. coli* enzymes. However, a combination of BHPNP1 and EcUP gave an improved molar yield of 80% (Figure 2.4). At these concentrations the substrates for the transglycosylation were well above their solubilities and therefore formed slurries. The guanine co-product was also highly insoluble and contributed to the slurry as it formed.

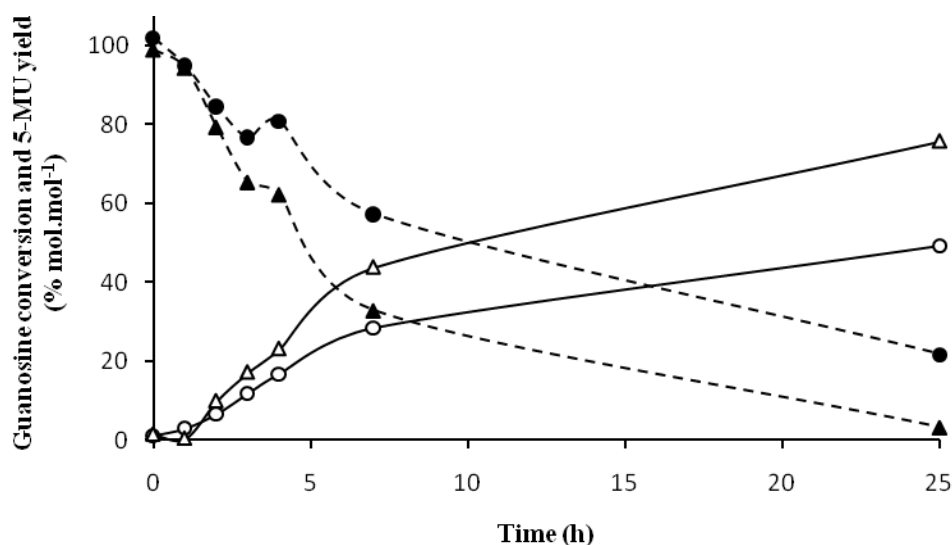


Figure 2.4 Guanosine conversion (closed) and 5-MU production (open) for *E. coli* PNP and UP (●); and *B. halodurans* PNP and *E. coli* UP (▲).

Reactions were run over 25 h with 1.5% m.m⁻¹ substrate (guanosine and thymine) loading and 0.15 U.ml⁻¹ biocatalyst loading. Molar conversion and yield is based on moles of guanosine loaded.

2.4 CONCLUSIONS

In this section it was shown that the commercially available nucleoside phosphorylases do not exhibit the substrate specificities required for the production of 5-methyluridine by transglycosylation. This is due to the base and sugar specificities of those enzymes. Screening for and combination of PNPs and UPs from a variety of other organisms, however, did show the ability to produce 5-MU. These studies showed that enzymes isolated for high activity towards uridine, did not necessarily have high activity for 5-methyl uridine production. Similarly, screening needs to be targeted towards the purine nucleoside of interest (guanosine), as the PNPs tend to have a preference for specific base and sugar combinations. Of particular interest is the PNP from *B. halodurans*, which will now be further characterised.

Combination of PNP and UP from *E. coli* proved very promising for the targeted reaction. Published transglycosylation research using *E. coli* (or expressed PNP and UP from *E. coli*) have focused on the production of purine nucleosides such as adenosine. The combination of the *E. coli* enzymes in this study therefore represents a novel transglycosylation for the production of a pyrimidine nucleoside. More promising though is the combination of *B. halodurans* PNP with *E. coli* UP. A 5-MU yield of 80% was achieved under high substrate conditions using this combination. The yield achieved in this un-optimised reaction is higher than the best overall yield quoted for this reaction (74%, (Ishii *et al.*, 1989), albeit at a lower substrate concentration (127 mM thymine and 53 mM guanosine compared to 300 mM starting substrate concentrations used by Ishii and co-workers). The molar yield achieved is also higher than both the batch and continuous reactions performed by Hori and co-workers (Hori *et al.*, 1989b; 1991). The 5-MU productivity, however, of the transglycosylation reaction in this study ($0.44 \text{ g.l}^{-1}.\text{h}^{-1}$) is lower than that of the reaction reported by Ishii and co-workers ($1.19 \text{ g.l}^{-1}.\text{h}^{-1}$) and the continuous reaction described by Hori and co-workers ($6.20 \text{ g.l}^{-1}.\text{h}^{-1}$, Hori *et al.*, 1991). Optimization of enzyme and substrate loading may further improve productivity and will thus be studied further.

CHAPTER 3: PRODUCTION

EXPRESSION, PURIFICATION, CHARACTERISATION AND APPLICATION OF *E. COLI* UP AND *B. HALODURANS* PNP

3.1 INTRODUCTION

Nucleoside analogues are widely used as antiviral and anticancer drugs, where they act as inhibitors of viral replication or cellular DNA replication. The traditional synthetic routes for these compounds are often complex and inefficient multi-stage processes (Lewkowicz and Iribarren, 2006). In Chapter 2 it was demonstrated that a combination of the purine nucleoside phosphorylase (BHPNP1) from the thermotolerant alkalophile *Bacillus halodurans*; (previously *B. brevis*, Louw *et al.*, 1993) with the uridine phosphorylase (UP) (EC 2.4.2.3) from *E. coli* in a one-pot cascade reaction can produce 5-methyluridine in high yield.

The uridine phosphorylase has previously been characterised (Leer *et al.*, 1977) as well as overexpressed in *E. coli* (Esipov *et al.*, 2002). Purine nucleoside phosphorylases from *E. coli* (Lee *et al.*, 2001; Esipov *et al.*, 2002) and *Geobacillus stearothermophilus* (Hamamoto *et al.*, 1997a) have been expressed in *E. coli*.

A number of fermentation studies have been performed on wild type and recombinant organisms for the production of nucleosides phosphorylases. These have been summarised in Table 3.1

Table 3.1 Relevant enzyme and biomass yields from literature on expression and fermentation studies for the production of purine and pyrimidine nucleoside phosphorylases

Host Strain	Expressed Enzyme	Enzyme Yield		Biomass Yield	Reference
		U.l ⁻¹	U.g ⁻¹ wet cells	g.l ⁻¹	
<i>E. coli</i> K12	<i>E. coli</i> PyNP	34600		ND	Leer <i>et al.</i> 1977
<i>E. coli</i> DH5 α	<i>E. coli</i> PyNP	-	10400	ND	Bestetti <i>et al.</i> , 2000
	<i>E. coli</i> PyNP	-	6200	ND	
	<i>E. coli</i> PyNP	-	3100	ND	
<i>E. coli</i> MG1655	<i>E. coli</i> PyNP	-	6000	ND	
	<i>E. coli</i> PNP	-	1000	ND	
<i>E. coli</i> DH5 α	<i>E. coli</i> PNP	-	600	ND	
	<i>E. coli</i> PNP	-	996	ND	
<i>E. coli</i> MG1655	<i>E. coli</i> PNP	-	643	ND	
	<i>E. coli</i> PyNP	-	2760	27.8 ¹	
<i>E. coli</i> DH5 α	<i>E. coli</i> PNP	-	600	28.5 ¹	Zuffi <i>et al.</i> , 2004
<i>B. stearo-thermophilus</i>	<i>B. stearo-thermophilus</i> PNP	5100	-	13.3 ²	Hori <i>et al.</i> 1989
<i>Klebsiella</i> sp	<i>Klebsiella</i> PNP	86.5	-	1.2 ²	Ling <i>et al.</i> , 1990
	<i>Klebsiella</i> PyNP	121.8	-	1.2 ²	
<i>E. coli</i> HS533	<i>E. coli</i> PNP	17386	-	11.3 ²	Lee <i>et al.</i> 2001
<i>E. coli</i> BL21	<i>E. coli</i> PyNP	300000	-		
<i>E. coli</i> BL21	<i>E. coli</i> PNP	15120	-		
<i>E. coli</i> ATCC 10536	N/A (Fed-batch fermentation)			110	Cutayar and Poillon, 1989
<i>E. coli</i> B	N/A (Batch fermentation)			9.3	Luli and Strohl, 1990
<i>E. coli</i> JM 105	N/A (Batch fermentation)			10.8	van de Wahl and Shiloach, 1998
<i>E. coli</i> JM109	N/A (Batch fermentation)			48.3	
<i>E. coli</i> BL21	N/A (Batch fermentation)			60.15	
<i>E. coli</i> JM109	N/A (Batch fermentation)			48.3	
<i>E. coli</i> BL21	N/A (Batch fermentation)			76.9	

¹ Biomass yield reported as wet cell mass, converted to dry cell mass using a conversion factor of 6

² Biomass yield report in OD 600, converted to dry cell mass using a conversion factor of 1.3

The focus of this chapter was to optimize recombinant *E. coli* fermentation conditions for the production of the enzymes. EcUP and BHPNP1 were purified and characterised. The biocatalytic production of 5-MU was then investigated in a bench-scale reaction.

3.2 MATERIALS AND METHODS

3.2.1 Oligonucleotides, plasmids and microbial strains

E. coli JM109 (DE3) [pMSBHPNP1] and *E. coli* BL21 (DE3) [pETUP] were prepared as described in Chapter 2.

3.2.2 Enzyme Production by Fermentation

3.2.2.1 Organism maintenance

Cell banks of *E. coli* JM109 [pMSPNP] and *E. coli* BL21 [pETUP] were maintained as cryopreserved cultures at -70°C . Detailed methodologies for cell bank creation and validation are given Appendix 3.

3.2.2.2 Inoculum train

Fernbach flasks containing 650 ml LB media with $100\ \mu\text{g}\cdot\text{ml}^{-1}$ ampicillin were inoculated with 2 ml of cell bank cultures. The cultures were grown overnight and used as the inocula for the fermentations.

3.2.2.3 Batch fermentations

Batch fermenters (Braun Biostat C) containing 9.3 l GMO 20 medium (Ramchuran *et al.*, 2002) was inoculated with 700 ml inoculum (overnight culture of the respective strains grown in LB media at 37°C). The composition of the GMO 20 medium was as follows: K_2HPO_4 , $14.6\ \text{g}\cdot\text{l}^{-1}$; $(\text{NH}_4)_2\text{SO}_4$ $2\ \text{g}\cdot\text{l}^{-1}$; Na_2HPO_4 , $3.6\ \text{g}\cdot\text{l}^{-1}$; Citric Acid, $2.5\ \text{g}\cdot\text{l}^{-1}$; MgSO_4 , $1.2\ \text{g}\cdot\text{l}^{-1}$; NH_4NO_3 , $5\ \text{g}\cdot\text{l}^{-1}$ and Yeast extract, $20\ \text{g}\cdot\text{l}^{-1}$. Glucose ($17.5\ \text{g}\cdot\text{l}^{-1}$) and trace element solution, ($5\ \text{ml}\cdot\text{l}^{-1}$) was sterilized separately and added to the fermenters before inoculation. Ampicillin, $100\ \mu\text{g}\cdot\text{ml}^{-1}$, was aseptically added to the flasks containing the glucose and trace element solution. The trace element solution consisted of the following: $\text{CaCl}_2\cdot 2\text{H}_2\text{O}$, $0.4\ \text{g}\cdot\text{l}^{-1}$; $\text{FeCl}_3\cdot 6\text{H}_2\text{O}$, $16.7\ \text{g}\cdot\text{l}^{-1}$;

MnCl₂·4H₂O, 0.15 g.l⁻¹; ZnSO₄·7H₂O, 0.18 g.l⁻¹; CuCl₂·2H₂O, 0.125 g.l⁻¹; CoCl₂·6H₂O, 0.18 g.l⁻¹; Na₂EDTA, 20.1 g.l⁻¹.

The pH of the fermentations was controlled at pH 7.2 with 33% m.v⁻¹ NH₄OH or 20% m.v⁻¹ H₂SO₄ diluted in dH₂O. The temperature was controlled at 37°C and the aeration set to 1 v.v.m⁻¹. The starting agitation was set at 300 rpm and ramped up manually to control the pO₂ above 30% saturation. Growth, enzyme activity and glucose utilisation were monitored by taking 10 ml samples at 1 hourly intervals. Initially, *E. coli* JM109 [pMSPNP] fermentations were induced at a residual glucose concentration of between 1 and 3 g.l⁻¹ at an IPTG concentration of 1.0 mM. Upon further investigation at 1 l scale (Appendix 4), it was determined that targeting induction at mid-log growth phase based on measurements at 660 nm (OD ~ 7) and at an IPTG concentration of 0.5 mM was more effective. Induction of the *E. coli* BL21 [pETUP] fermentations was at an OD of approximately 13, which was reached at 4 h.

3.2.2.4 Sampling, growth and analysis.

Growth was measured by determining the optical density at 660 nm (using suitably diluted samples to obtain accurate OD readings) and dry cell weight (DCW) in triplicate. A volume of 2 ml of the sample was centrifuged, washed with 0.1 M HCl to remove precipitated salts, and the pellet was then used for dry cell weight determination by drying to constant weight at 110°C. Glucose concentration was measured using Accutrend[®] (Boehringer Mannheim).

For determination of the enzyme activity of the biomass, triplicate samples of 1 ml were centrifuged and resuspended in a minimum volume of the cell disruption solution B-Per (Pierce, USA) and vortexed briefly to re-suspend the pellet. After incubation at room temperature for 5 min the samples were centrifuged and the supernatant analysed for nucleoside phosphorylase activity using the standard enzyme assays (See Chapter 2).

3.2.3 Preparation of crude nucleoside phosphorylase preparations

After fermentation, the broth was harvested and allowed to settle overnight at 4°C. The biomass was separated from the supernatant by decanting, and subjected to a freeze-thaw cycle alternating between +20°C and -20°C. Liberated soluble protein was stored at 4°C, after separation by centrifugation (14000 x g, 10 min, Beckman Avante, Beckman Coulter, Inc. CA, USA). The pelleted biomass was resuspended in 1 l deionised water and further disrupted using a pressure based cell disruptor (2 Plus, Constant Systems, UK) with 1 pass at 40 kpsi to release additional enzyme. Cellular debris was again removed by centrifugation. The combined resultant protein solutions (supernatants from freeze-thaw and cell disruption processes) were concentrated and simultaneously washed with dH₂O by ultrafiltration using a Prostack cross-flow filtration unit (30 kDa cut-off membrane, Waters USA). The final preparation was lyophilized in the presence of 1% m.m⁻¹ maltose and 1% m.m⁻¹ polyethylene glycol PEG 8000 (Virtis Genesis 25 L freeze drier).

3.2.4 Purification of nucleoside phosphorylases

Crude enzyme preparations of EcUP and BHPNP1 (lyophilised material) were used for further purification. Resuspended material was first fractionated by ammonium sulphate precipitation (30% and 70% saturation). The pellet from the 70% saturation was resuspended in a minimum volume of Buffer A (20 mM Tris-HCl, pH 7.2). Residual ammonium sulphate was removed by ultrafiltration (100 kDa membrane) and washing with Buffer A. Anion exchange chromatography of each sample was performed on an AKTA Prime (Amersham Biosciences, UK) using Toyopearl SuperQ 650m anion exchange resin (Tosoh BioSep, USA). Protein was first eluted from the column using a linear salt gradient of between 50 mM – 500 mM NaCl in 20 mM Tris-HCl, pH 7.2, over 400 ml at a flow rate of 4 ml/min. PNP activity was assayed in all fractions (5 ml fractions collected) and those containing activity were separately pooled and concentrated by ultrafiltration (30 kDa membrane, Millipore USA). Excess NaCl was removed by diafiltration on the same membrane. This sample was then re-applied to the anion exchange column and eluted over a linear salt gradient of

150 – 400 mM NaCl. Active fractions were pooled and concentrated by ultrafiltration as above.

3.2.5 Characterization

3.2.5.1 *pH Profiling*

For BHPNP1, reaction mixtures (1 ml) contained 1 mM guanosine in 50 mM Universal buffer (50 mM Tris, 50 mM Boric Acid, 33 mM Citric acid; 50 mM Na₂PO₄) adjusted with either HCl or NaOH to pH values between 3 and 11. PNP (0.025 U) was added to initiate the reaction. After a 10 min incubation at 40°C, the reaction was stopped by the addition of 0.5 ml of a 5 M NaOH solution. Guanosine conversion and guanine formation were analysed by HPLC on a Waters 2690 HPLC (interfaced with Waters Millennium Software) equipped with Waters 996 Photodiode Array Detector at 260nm and a Phenomenex Synergi 4µm Max-RP 80A, 150 x 4.60 mm column at 22°C. The mobile phase was a 25 mM ammonium acetate buffer (pH 4.0), at a flow rate of 1.0 ml/min.

EcUP pH profiling was performed using the standard assay. The phosphate buffer in the standard assay was replaced with Universal buffer (as for BHPNP1 profile) adjusted to pH values between 3 and 11.

3.2.5.2 *Temperature Profiling*

For BHPNP1, reaction mixtures (1 ml) contained 1 mM guanosine in 50 mM sodium phosphate buffer, pH 8.0. PNP (0.025 U) was added to initiate the reaction. After a 10 min incubation at temperatures between 30°C and 90°C, the reaction was stopped by the addition of 0.5 ml of a 5 M NaOH solution. Guanosine conversion and guanine formation were analysed by HPLC as above. EcUP temperature profiling was performed using the standard assay between temperatures of 30°C and 90°C.

3.2.5.3 *Thermostability*

Enzyme solutions were incubated at 40°C, 60°C and 70°C (PNP only) respectively. Samples were analysed at room temperature for activity (standard methods – section 2.2.11.4) over a 19 hour period.

3.2.5.4 *Kinetic Parameters*

Kinetic parameters for PNP were determined for both inosine (standard assay) and guanosine (assay as described for temperature optimum study) as starting substrates. Initial substrate concentrations were varied between 0.05 mM and 1.0 mM.

EcUP kinetic parameters were determined using the standard assay, with uridine initial concentrations varying between 0.1 mM and 5.0 mM. The reaction was stopped at 1, 2, 3, 4, 6 and 10 min for selection of data within the linear range. Michaelis-Menten plots and the linear transformations (Lineweaver–Burk, Hanes-Woolf and Eadie-Hofstee) were used to determine kinetic parameters.

3.2.6 **Bioinformatic analysis of BHPNP1**

Due to the high level of sequence identity between the genomes of *B. halodurans* Alk36 and *B. halodurans* C-125 the genome sequence of *B. halodurans* C-125 (Takami *et al.*, 2000) (NC_002570) as published in the DNA Data Bank of Japan (<http://gib.genes.nig.ac.jp>) was searched for novel nucleoside phosphorylase gene sequences using the genomic BLAST (Basic Local Alignment Search Tool; (Altschul *et al.*, 1990) located at the National Centre for Biotechnology Information (NCBI) to confirm that no other PNPs or PyNPs were present apart from the annotated ones. Two PNP and one PyNP genes were identified. The two PNPs are BH1531 and BH1532, and the PyNP was designated BH1533. Primers for the amplification of the PNP gene BH1531 were designed based on the genome sequence. Isolation and characterisation of the gene corresponding to BH1531 from *B. halodurans* strain Alk36 was subsequently performed. This gene was termed BHPNP1.

3.2.7 Tertiary structure confirmation

Denatured (5 min, 95°C) and non-denatured preparations of the enzyme were analysed on a 12% SDS –PAGE gel. The gel was overlaid with a 0.5% agarose solution to determine the position of active subunits. The agarose solution contained 10 mM inosine, 0.2 U.ml⁻¹ xanthine oxidase and 10 mM INT (iodonitrotetrazolium violet) in 20 mM sodium phosphate buffer, pH 7.5. Active PNP is indicated by a red/pink band on the gel due to the cascade action of the PNPase and xanthine oxidase leading to the reduction of INT to its tetrazolium salt. Positions of active and non-active units were then confirmed by staining the gel with Coomassie.

3.2.8 Homology Modelling

Multiple sequence alignments were performed using ClustalW (Larkin *et al.*, 2007). Homology modelling was performed using Accelrys Discovery Studio 2.0. The model was based on the bovine structure 1LVU (Bzowska *et al.*, 2004). Bovine PNP and BHPNP1 have 49 % sequence identity and 63 % sequence similarity.

3.2.9 Biocatalysis Reaction

To demonstrate the overall reaction at bench scale an experiment was conducted at 650 ml using an enzyme load of 105 U BHPNP1 and 75 EcUP and a thymine to guanosine mole ratio of 2.3 : 1 (1.5% m.m⁻¹ (53 mM) guanosine and 1.6% m.m⁻¹ (127 mM) thymine) performed at 40°C over 23 h, with Trizma Base (50 mM) and sodium phosphate buffer (50 mM) at pH 7.8 to ensure both adequate buffering while providing catalytic amounts of phosphate for the reaction.

3.3 RESULTS AND DISCUSSION

3.3.1 Cell Bank Validation

A summary of the validation parameters for both strains is given in Table 3.2 and Table 3.3 below. Percentage variation between experiments for each parameter were generally below 10 % (excluding cell counts), which indicates a high degree of reproducibility within the working cell banks.

Table 3.2 Summary of working cell bank validation for *E. coli* [pMSPNP]

Parameter	μ_{\max}	Doubling Time H	Viable Cell Counts CFU.ml ⁻¹	Final [Protein] g.l ⁻¹	Final Activity U	Final Specific Activity U.g ⁻¹ (protein)	Productivity U.h ⁻¹ .l ⁻¹
Average	0.799	0.873	2.57 x 10 ⁷	0.414	6580	7592	696.30
SD	0.084	0.086	1.27 x 10 ⁷	0.023	243	652	25.66
%CV	10.46%	9.90%	49.30%	5.57%	3.69%	8.58%	3.69%

Table 3.3 Summary of working cell bank validation for *E. coli* [pETUP]

Parameter	μ_{\max}	Doubling Time H	Viable Cell Counts CFU.ml ⁻¹	Final [Protein] g.l ⁻¹	Final Activity U	Final Specific Activity U.g ⁻¹ (protein)	Productivity U.h ⁻¹ .l ⁻¹
Average	0.8873	0.785	1.432 x 10 ⁸	0.262	6587	11989	836.44
SD	0.0736	0.067	1.59 x 10 ⁷	0.012	44	580	5.55
%CV	8.29%	8.53%	11.08%	4.50%	0.66%	4.85%	0.66%

3.3.2 Enzyme Production

In order to prepare sufficient enzyme for larger scale reactions, optimised fermentations (10 l) were performed for the production of BHPNP1 and EcUP (Figure 3.1). High levels of enzyme were produced within 8 to 10 h of fermentation. The fermentation results are summarised in Table 3.4. Data presented are averages of duplicate fermentations in each case. The expression of EcUP was 37.7 kU.l⁻¹, which was 10 fold that of the wild type. The lyophilised BHPNP1 activity (5.41 U.mg⁻¹) was similar to the preparation used previously (5.14 U.mg⁻¹), while the EcUP preparation (4.3 U.mg⁻¹) showed a more than 20-fold improvement in specific activity when compared to the previous preparations (0.2 U.mg⁻¹).

Table 3.4 Summary of fermentation parameters for batch fermentation of *E. coli* [pMSPNP] and *E. coli* [pETUP]

Value	BHPNP1	EcUP
Maximum OD (660 nm)	14.4	20.59
μ_{\max}	0.43	0.60
Yield (g _{DCW} ·g ⁻¹ _{glucose})	0.53	0.55
Biomass (g.l ⁻¹)	9.45	12.37
Productivity (g _{DCW} ·l ⁻¹ ·h ⁻¹)	1.16	1.62
Enzyme Yield (kU.l ⁻¹)	26.9	37.7
Enzyme productivity (kU.l ⁻¹ ·h ⁻¹)	3.3	5.8
Enzyme Yield (kU)*	215	211
Specific Activity (kU.g ⁻¹) [†]	5.41	4.30

*Total recovered units after downstream processing

[†]Units per gram dry product after lyophilisation

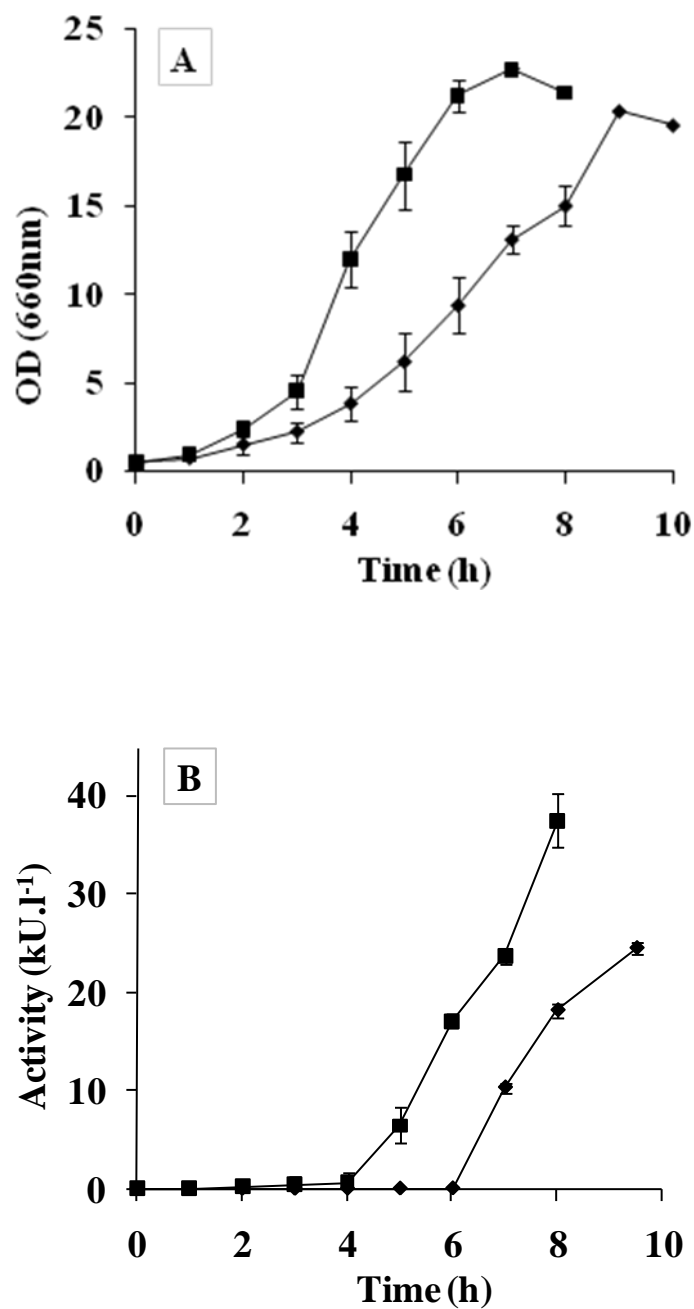


Figure 3.1. Growth (A) and nucleoside phosphorylase activity (B) profiles of *E. coli* [pMSPNP] (◆) and *E. coli* [pETUP] (■) in batch fermentations. BHPNP expression was induced at an OD_{660nm} of 7 (5h) and UP expression was induced at an OD_{660nm} of 13 (4h).

Standard deviation indicated is calculated from duplicate fermentations.

3.3.3 Enzyme Purification

PNP was purified to a 42% purity (by density analysis on Biorad gel analysis software) and a specific activity of 26.28 U.mg^{-1} total protein. EcUP was purified to 84% purity with a specific activity of 30.69 U.mg^{-1} . The SDS-PAGE results are depicted in Figure 3.2.

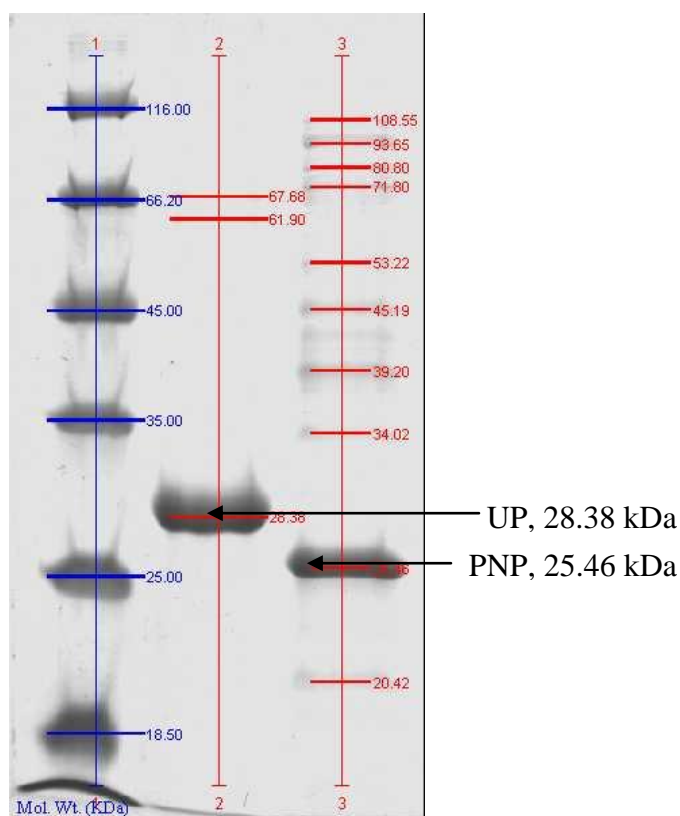


Figure 3.2 SDS-PAGE gel image depicting the final fractions of EcUP and BHPNP1 at the end of the purification by ammonium sulphate precipitation and sequential anion exchange chromatography.

Lane 1 – molecular weight marker (Fermentas #SM0431); Lane 2 – UP; Lane 3 – PNP.

3.3.4 Enzyme Characterization

3.3.4.1 *pH Optima*

BHPNP1 showed a pH optimum of 7.0, retaining 60% activity between pH 5.7 and 7.4 (Figure 3.3). EcUP also showed an optimum of 7.0, retaining 60% activity between pH 6.0 and 8.2 (Figure 3.4).

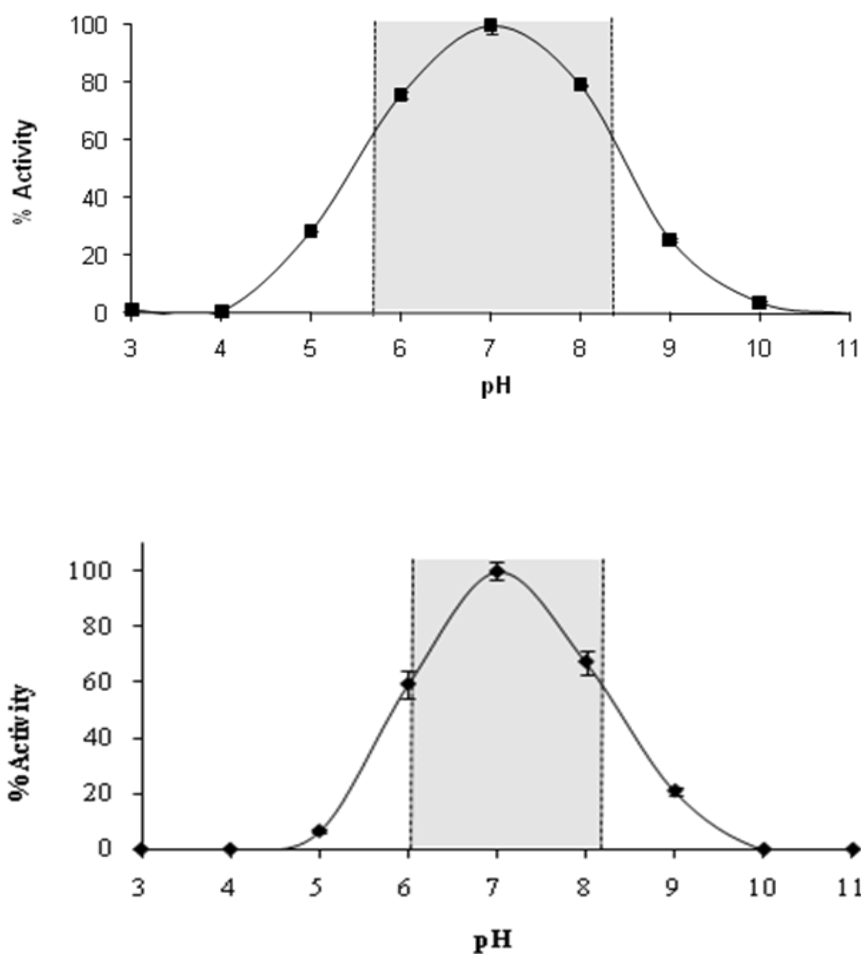


Figure 3.3 pH profiles of BHPNP1 (top) and EcUP (bottom).

Shaded areas indicate the pH range in which the enzymes retain 60% activity. Standard deviation indicated is calculated from triplicate assays.

3.3.4.2 *Temperature Optima*

BHPNP1 had optimal activity at 70°C and a broad activity range, retaining 60% activity between 30 and 74°C. In contrast, EcUP had an optimum of 40°C with a narrow activity range (retaining 60% activity) between 30 and 52°C (Figure 3.4).

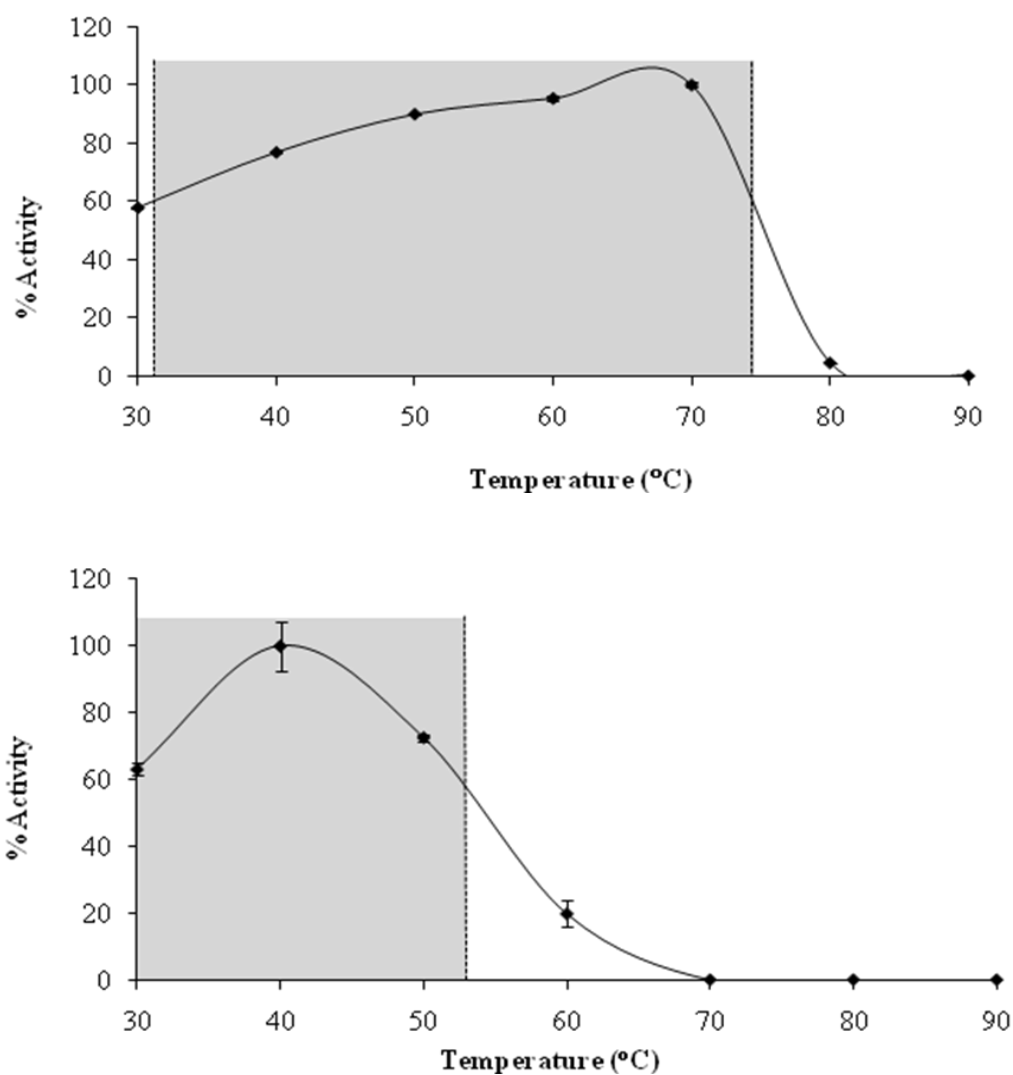


Figure 3.4 Temperature profiles of BHPNP1 (top) and EcUP (bottom).

Shaded areas indicate the temperature range in which the enzymes retain 60% activity. Standard deviation indicated is calculated from triplicate assays.

3.3.4.3 *Temperature Stability*

Although the optimum temperature of PNP was shown to be 70°C, stability at this temperature was less than 30 min (Figure 3.5). PNP did however show good stability at 60°C ($t_{1/2}$ – 20.8 h) and excellent stability at 40°C, with no change in activity over the time period (19 h) investigated. UP showed a half life of 9.9 h at 60°C, albeit at 20% of its optimum activity. At 40°C, the half-life was 37 h (Figure 3.6).

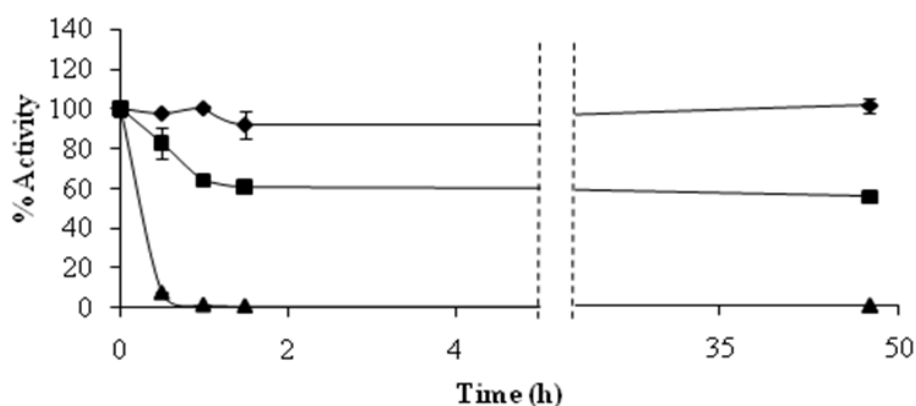


Figure 3.5 Representation of BHPNP1 thermal stability at 40°C(♦), 60°C(■) and 70°C(▲).

Standard deviations represented were calculated from triplicate assays.

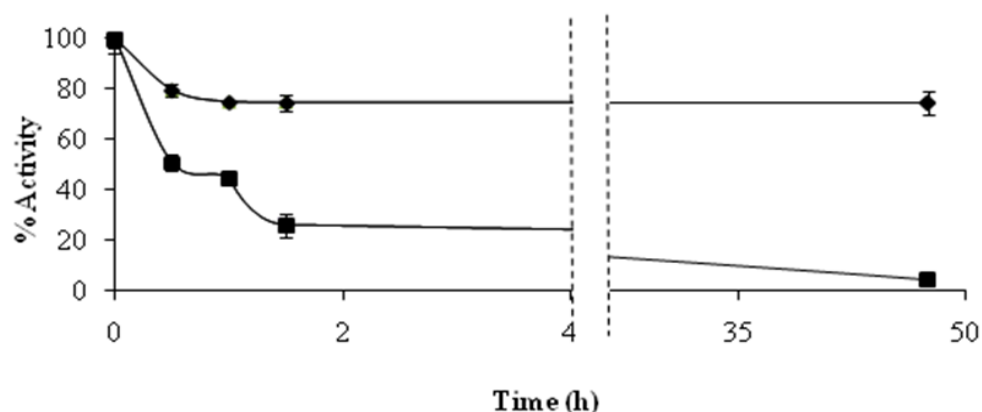
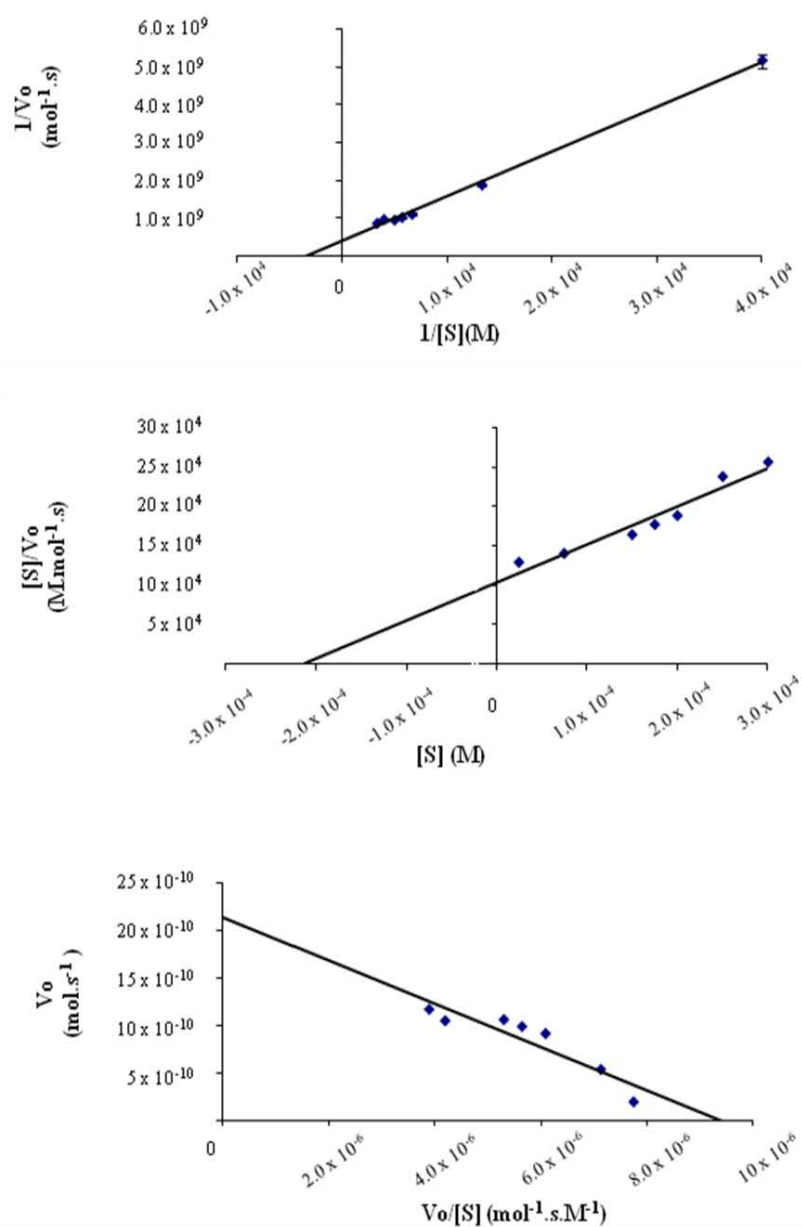


Figure 3.6 Representation of EcUP thermal stability at 40°C (♦) and 60°C (■).

Standard deviations represented were calculated from triplicate assays.

3.3.4.4 Kinetic Characterisation

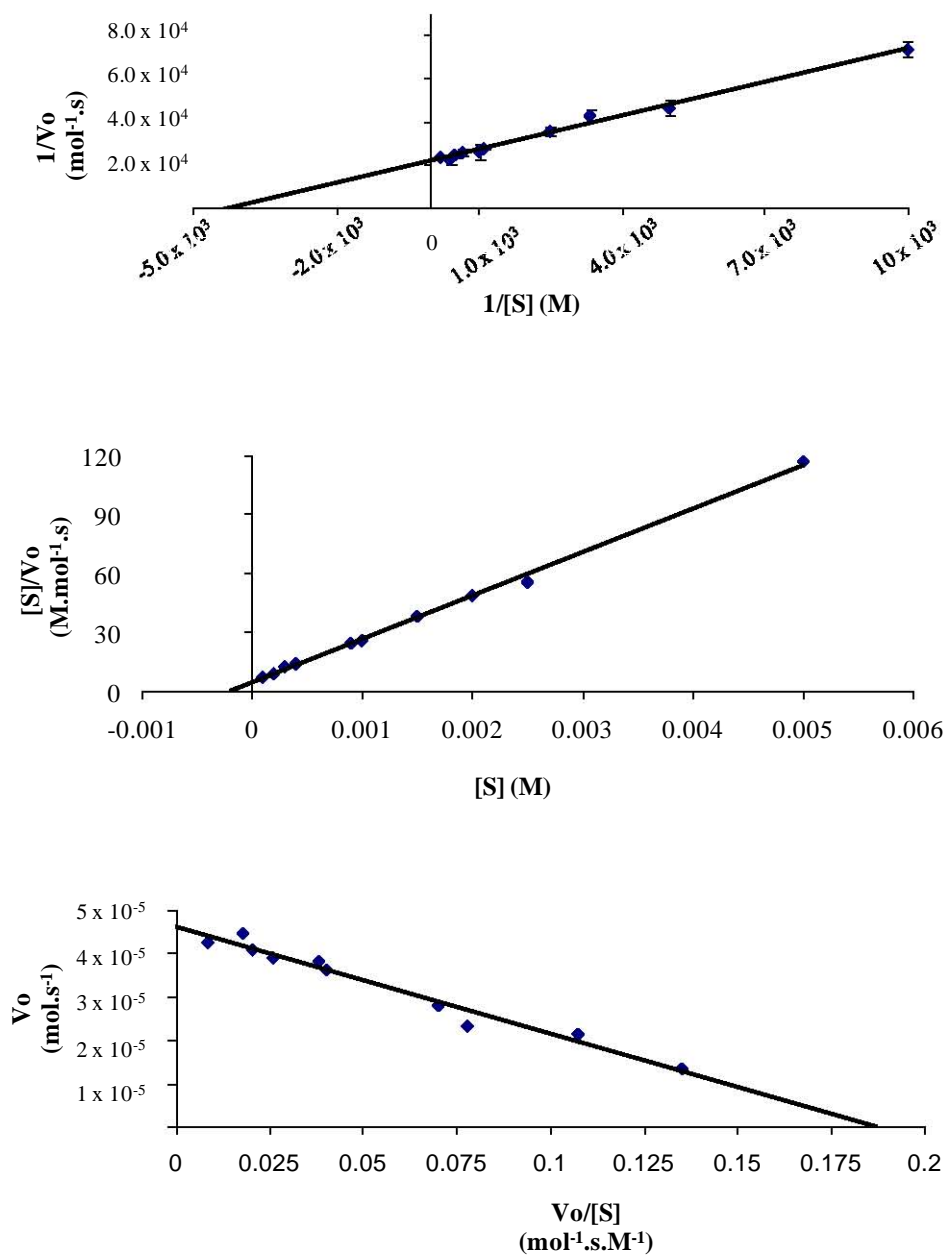
Linear transformation of velocity data obtained for BHPNP1 with varying initial substrate concentrations showed good linear regression fit where inosine was used ($R^2 > 99\%$ for all plots) and adequate fit for guanosine experiments ($R^2 > 94\%$) (Figure 3.7). Data obtained for varying uridine concentrations also showed good linear regression fit ($>99\%$). From the plots (Lineweaver-Burk, Eadie-Hofstee and Hanes-Woolf), K_M and V_{max} were determined with less than 7% deviation in the values calculated from the three plots (Figure 3.7). Subsequently the turnover number (k_{cat}) and the specificity constant were calculated. These values are summarised in Table 3.5 (BHPNP1) and Table 3.6 (EcUP) below.



Parameter	Lineweaver-Burk	Hanes- Woolf	Eadie-Hofstee	Average	Stdev	%CV
R^2	0.9976	0.939	0.84	0.93	0.08	8.61%
K_m (M)	3.18×10^{-4}	2.14×10^{-4}	2.26×10^{-4}	2.527×10^{-4}	5.73×10^{-5}	22.67%
V_{max} (mol.s ⁻¹)	2.68×10^{-9}	2.06×10^{-9}	2.13×10^{-9}	2.291×10^{-9}	3.37×10^{-10}	14.70%

Figure 3.7 Lineweaver-Burk (top), Hanes-Woolf (middle) and Eadie-Hofstee (bottom) plots for BHPNP1 using guanosine as the substrate.

Insert table indicates calculation of K_m and V_{max} from the 3 plots.



Parameter	Lineweaver-Burk	Hanes- Woolf	Eadie-Hofstee	Average	Stdev	%CV
R^2	0.9918	0.9975	0.9685	0.99	0.02	1.56%
K_m (M)	2.39×10^{-4}	2.17×10^{-4}	2.45×10^{-4}	2.34×10^{-4}	1.46×10^{-5}	6.24%
V_{max} (mol.s ⁻¹)	4.56×10^{-5}	4.52×10^{-5}	4.61×10^{-5}	5.57×10^{-5}	4.41×10^{-7}	0.96%

Figure 3.8 Lineweaver-Burk (top), Hanes-Woolf (middle) and Eadie-Hofstee (bottom) plots for EcUP using uridine as the substrate.

Insert table indicates calculation of K_m and V_{max} from the 3 plots.

Kinetic and physical characteristics of both BHPNP1 and EcUP have been determined (summarised in Table 3.5 and Table 3.6). Data obtained for EcUP agreed with published data (pH optimum: 7.3, pH range 6.0 – 8.5, K_m – 150 μM (uridine, Leer *et al.*, 1997). BHPNP1 showed similar substrate affinity towards both inosine and guanosine (K_m value of 236 and 208 μM respectively) and similar substrate affinity as *E. coli* PNP (K_m of 234 μM).

Table 3.5 Physical and kinetic characteristics of BHPNP1 at 40°C

Parameter	Unit	Inosine	Guanosine
Specific Activity	U.mg ⁻¹	26.28	
K_M	μM	236	206
V_{max}	mol.s ⁻¹	4.76×10^{-6}	2.03×10^{-9}
k_{cat}	s ⁻¹	2.844×10^2	1.214×10^1
Specificity Constant	M ⁻¹ .s ⁻¹	1.203×10^8	5.869×10^4
pH Optimum	-	7.0	
pH range (60%)	-	5.7 - 8.4	
Temp Optimum	°C	70	
Temp Range (60%)	°C	32 - 74	
Temp Stability ($t_{1/2}$ @ 60°C)	h	20.8	
Temp Stability ($t_{1/2}$ @ 40°C)	h	ND	

Table 3.6 Physical and kinetic characteristics of EcUP at 40°C

Parameter	Unit	Uridine
Specific Activity	U.mg ⁻¹	30.69
K_M	μM	233.91
V_{max}	mol.s ⁻¹	4.57 x 10 ⁻⁵
k_{cat}	s ⁻¹	4.55 x 10 ⁴
Specificity Constant	M ⁻¹ .s ⁻¹	1.94 x 10 ⁸
pH Optimum	-	7.0
pH range (60%)	-	6.0-8.2
Temp Optimum	°C	40
Temp Range (60%)	°C	30-52
Temp Stability ($t_{1/2}$ @ 60°C)	h	9.89
Temp Stability ($t_{1/2}$ @ 40°C)	h	37

The PNP1 from the thermophile *G. stearothermophilus* has been previously expressed and characterised (Hori *et al.* 1989a; Hamamoto *et al.* 1997a). The *G. stearothermophilus* enzyme has a pI of 4.7, with an optimal pH range between 7.5 and 11, in contrast to the optimal pH range of BHPNP1 of between 5.7 and 8.4 and a predicted pI of 5.1. The *G. stearothermophilus* PNP is more thermostable than BHPNP1 as it is stable at 70°C for more than 30 hours. In contrast, the half life of BHPNP1 at 60°C is 20 hours. The K_m for *G. stearothermophilus* PNP using inosine was similar at 0.22 mM, but had a greater affinity for guanosine at K_m 0.14 mM. Characteristics of prokaryote PNPs that have been characterized are listed in Table 3.7

Table 3.7 Physical and kinetic characteristics of various reported prokaryotic PNPs

Organism	K_M (mM)		k_{cat}	pH Optimum	Temperature Optimum	Reference
	Inosine	Guanosine				
<i>E. coli</i>	0.34	0.155	105	7.5	60	Leer <i>et al.</i> 1997
<i>B. stearo-thermophilus</i>	0.22	0.34	-	8	80	Hori <i>et al.</i> 1989; Hamamoto <i>et al.</i> 1996
<i>B. halodurans</i>	0.236	0.14	284	7	70	Visser <i>et al.</i> , 2010 Wielgus-Kutrowska <i>et al.</i> , 2002
<i>Cellulomonas sp.</i>	0.043	0.11	28	8	-	Cacciapuoti, 2007
<i>P. furiosus</i>	0.322	0.122	-	-	120	Shirae and Yokozeki, 1991
<i>E. carotovora</i>	1.92	1.85	84	8.5	40	Utagawa <i>et al.</i> 1985
<i>E. aerogenes</i>	2.2	-	-	6.8	60	Cacciapuoti 2005
<i>S. solfataricus</i>	0.084	0.114	132	-	120	

3.3.5 Sequence and homology modelling

B. halodurans is unusual among the bacilli that have been completely sequenced so far, in that it contains two Type II (low-MM) PNPs as opposed to the Type I (High-MM) and Type II PNPs present in other *Bacillus* species (BLAST analysis, Hennessy, personal communication). The gene sequence of BHPNP1 was identical to that of BH1531 from *B. halodurans* C-125 except for a silent substitution at nucleotide 519 (C to T), and hence the protein sequence was identical to that found in *B. halodurans* C-125. BLAST analysis indicated that the closest related structure deposited in the protein data base (PDB) was that of the bovine PNP (Table 3.8; Figure 3.9) which is 47 % identical to BHPNP1. BH1531 is a member of the Type II PNPs.

Bovine	MANGYTYEDYQDTAKWLLSHTEQ-----RPQVAVICGSLGGLVKNLTKQAQTFDYSEIPN	55
Human	MENGYTYEDYKNTAEWLLSHTKH-----RPQVAICGSLGGLTKDLTKQAQIFDYGEIPN	55
<i>B. halodurans</i>	---MLNVTQLQEATTFIQQQIET-----KPTIGLILGSLGILADEIEQPVKVPYSIDIPH	52
<i>G. stearothermophilus</i>	----MNRTAIEQAAQFLKEKFP-----SPQIGLILGSLGVLADEIEQAIKIPYSIDIPN	51
<i>B. subtilis</i>	----MKDRIERAAAFIKQNLPE-----SPKIGLILGSLGILADEIENPVKLYEDIPE	50
BH1532	--MENIREKVKQSAEYLLGKIKN-----KPAIGLILGSLGELANEIEEAVHIPYEQIPN	53
<i>E. coli</i>	----MSQVQFVSHNPLFCIDI IKTYKPDFTPRVAFILGSLGALADQIENAVAI SYEKLPG	56
	. . . : * :..* ***** *.: : . . * .:*	
Bovine	FPPESTVPGHAGRLVFGILNGRACVMMQGRFHM ^Y EGY ^P FWKVTFPVRFLLGVETLVVVTN	115
Human	FPRSTVPGHAGRLVFGILNGRACVMMQGRFHM ^Y EGY ^P LWKVTFPVRFHLLGVDTLVVTN	115
<i>B. halodurans</i>	FPVSTVQGHAGQLVIGMLEGKQVIAMQGRFHF ^Y EGY ^S LEVVTFPVRFVMMKALGVEQIVTN	112
<i>G. stearothermophilus</i>	FPVSTVEGHAGQLVYGQLEGATVVVMQGRFHY ^Y EGY ^S FDKVTFPVRFVMMKALGVEQLIVTN	111
<i>B. subtilis</i>	FPVSTVEGHAGQLVLTGTEGVSVIAMQGRFHF ^Y EGY ^S MEKVTFPVRFVMMKALGVEALIVTN	110
BH1532	FPVSTVEGHAGQLVIGTLHGKVVAMQGRFHY ^Y EGY TM QEVTFPVRFVMEIGVELIVTN	113
<i>E. coli</i>	FPVSTVHGHAGELVLGH ^{LQ} GVVCMKGRGH ^F YEG ^{RG} MTIMTDAIRTFKLLGCELLFCTN	116
	** *** ***** ** * * * : * : ** * *** : : * .: .: : * : . : **	
Bovine	<u>AAGGLNPNFEVGDIMLIRDHINLPGFSGENPLRGPNEERFGVRF</u> PAMSDAYDRDMRQKAH	175
Human	<u>AAGGLNPKFEVGDIMLIRDHINLPGFSGQNPLRGPNDERFGDRF</u> PAMSDAYDRDMRQRAL	175
<i>B. halodurans</i>	<u>AAGGVNESFEAGDLMIIRDHINN</u> ---MAQNPLIGPNEAFGVRFPDMSNAYSERLRLTAK	169
<i>G. stearothermophilus</i>	<u>AAGGVNESFEAGDLMIISDHINN</u> ---MGGNPLIGPNSALGVRFPDMSSEAYSKRLRQLAK	168
<i>B. subtilis</i>	<u>AAGGVNTEFRAGDLMIITDHINF</u> ---MGTNPLIGPNEADFGARFPDMSAYDKDLSLAE	167
BH1532	<u>ACGGMNKNFAPGDLMIITDHLNM</u> ---TGDNPLIGPNVEEWGPRFPDMSHAYTPELVEFVE	170
<i>E. coli</i>	<u>AAGSLRPEVAGSLVALKDHINT</u> ---MPGTPMVGLNDDRFGERFFSLANAYDAEYRALLQ	173
	*. *. : . . * .: : * : * . : * : * * * * * : : * * .: * *	
Bovine	STWKQMGEQRELQEGTYVMLGGPNFETVAECRLLRNLGADAVGMSTVPEVIVARHCGLRV	235
Human	STWKQMGEQRELQEGTYVMVAGPSFETVAECRVLQKLGADAVGMSTVPEVIVARHCGLRV	235
<i>B. halodurans</i>	EKGNTLN--LKLQEGVYVANTGPVYETPAEVRMIRKLGDAVGMSTVPEVIVARHAGLEV	227
<i>G. stearothermophilus</i>	DVANDIG--LRVREGVYVANTGPAYETPAEIRMI ^R VMGGDAVGMSTVPEVIVARHAGMEV	226
<i>B. subtilis</i>	KIAKDLN--IPIQKGVYTAVTGPSYETPAEVRFLRTMGSDAVGMSTVPEVIVANHAGMRV	225
BH1532	ETANRLD--IKVQKGVYAGITGPTYMTGAELIMLRNLGGDVI ^G MSTVPEVIVARHAGMKV	228
<i>E. coli</i>	KVAKEEG--FPLTEGVFVSYPGPNFETA ^E IRMMQIIGGDVVGMSVVPVEISARHC ^{DL} KV	231
	. : . : : : * : . . * * * .: : * .: .: * * * * * * .: .: .: *	
Bovine	FGFSLITNKVIMDYESQGANHEEVLEAGKQAAQKLEQFVSLMASIPVSGHTG	289
Human	FGFSLITNKVIMDYESLEKANHEEVLAAGKQAAQKLEQFVSI ^L MASIPVDPKAS	289
<i>B. halodurans</i>	LGISCI ^S NMAAGILDPQ--L ^S HDEVIETTERVRQDFLNLVKAIVKDM-----	272
<i>G. stearothermophilus</i>	LGISCI ^S NMAAGILDQP--L ^T HDEVIETTEKVKADFLRFVKAIVRNMAKN----	274
<i>B. subtilis</i>	LGISCI ^S NAAAGILDQP--L ^S HDEVMEVTEKVKAGFLKLVKAIVAQYE-----	271
BH1532	IGISCI ^T DMAIGEEIAG--I ^T HEEVAVANKTKPKFIKLVKEIVANVNV-----	275
<i>E. coli</i>	VAVSAITNMAEGLSDVK--L ^S HAQT ^L AAAE ^L SKQNFINLIGFLR ^K IA-----	277
	... * * : : . . * * : : : : : : : : : : : : : : . . : : : .	

Figure 3.9 Multiple sequence alignment comparing BHPNP1 to other Type II PNP_s.

The alignment was generated using ClustalW (Larkin *et al.*, 2007; <http://www.ebi.ac.uk/clustalw>). Residues shown to be important in the binding site of bovine and human PNP_s are underlined (Montgomery, 1993; Mao *et al.*, 1997; Narayana *et al.*, 1997). Dots (. and :) indicate partial similarity and asterisks (*) indicate a 100% match.

Table 3.8 Comparison of various PNPs to BHPNP1

Protein	% protein identity	% protein similarity	PNP Type	Accession number
<i>E. coli</i> PNP	17.0	33.0	I	P0ABP8
<i>E. coli</i> XapA	44.0	61.0	II	NP_416902
<i>G. stearothermophilus</i> PNP1	74.9	86.2	II	P77834
Bovine PNP	47.1	61.1	II	P55859
Human PNP	45.2	58.5	II	P00491
<i>B. halodurans</i> BH1532	57.1	75.6	II	BAB05251
<i>B. subtilis</i> PNP	69.6	78.8	II	P46354
<i>G. stearothermophilus</i> PNP2	18.3	32.2	I	P77835

BHPNP1 was aligned with *G. stearothermophilus* PNP1 (P77834) (Hamamoto *et al.* 1997a), Bovine PNP (P55859) (Bzowska *et al.*, 1995), Human PNP (P00491) (Williams *et al.*, 1984), *B. subtilis* PNP (P46354) (Schuch *et al.*, 1999), the second *B. halodurans* PNP (BH1532, BAB05251) (Takami *et al.* 2000) and *E. coli* XapA (NP_416902) (Dandanell *et al.* 2005).

BHPNP1 has low levels of identity to Type I PNPs, such as *E. coli* PNP and *G. stearothermophilus* PNP2 (17 % and 18.3 % identity respectively). It has higher levels of identity to Type II PNPs. Selected Type II PNPs were aligned using ClustalW. Amino acids known to be involved in the activity of the bovine and human enzymes (Lewcowicz and Iribarren, 2006; Ealick *et al.*, 1990) were generally conserved, with the exception of Tyr192, Ser234, Met236 and Ala237. These were all conservative substitutions with the exception of Met236 (BHPNP1). Hence, it is likely that the active site, and overall tertiary structure, of BHPNP1 will resemble the bovine and human PNPs and is therefore likely to be a homo-trimer. The structure of BHPNP1 was hence modelled based on the structure of the bovine PNP (Figure 3.10).

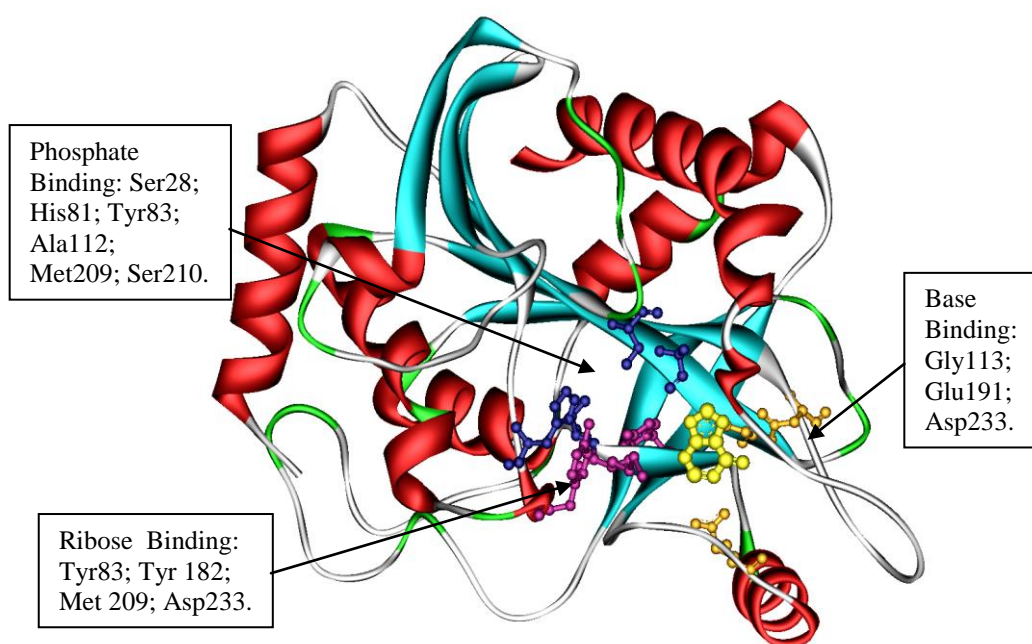


Figure 3.10 Ribbon representation of the homology modelled three dimensional structure of BHPNP1.

Modelling of the BHPNP1 structure was performed using the bovine structure 1VFN (Bzowska *et al.* 2004) as a template. The monomeric subunit was modelled with a substrate (Hypoxanthine, yellow Ball and Stick) using Accelrys Discovery Studio 2.0. Highlighted are the predicted phosphate (blue), ribose (purple) and purine base (orange) binding amino acids.

BHPNP1 and *G. stearothermophilus* PNP1 are 74.9 % identical. These proteins are likely to have similar structural characteristics. As already mentioned by Hamamoto *et al.* (1997b), the high level of sequence identity between the *G. stearothermophilus* PNP1 and the eukaryotic PNPs strongly suggests structural similarity. This would also apply to the BHPNP1 protein. However SDS-PAGE analysis of a non-denatured protein (not boiled)(Figure 3.11) gave an apparent molecular weight of 50 kDa, potentially indicating a dimeric protein. This result would need to be confirmed by gel filtration.

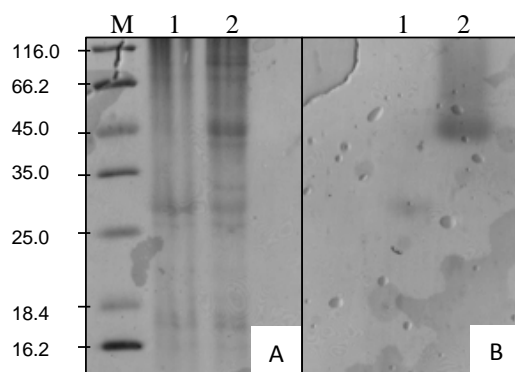


Figure 3.11 12% SDS PAGE gel (A) and corresponding activity gel overlay (B).

The experiment indicates that the predominant tertiary confirmation is a dimer. The expected denatured subunit is visible in both the denatured and non-denatured samples at approximately 27 kDa. Another dominant band at approximately 50 kDa on the coomassie stained gel (Lane B2) relates to the active band on the overlay (Lane B2). M – Marker (Fermentas #SM0431); 1 – Denatured BHPNP1 (95°C, 5 min); 2 – non-denatured BHPNP1.

3.3.6 Bench scale biocatalytic reaction

The results obtained showed a guanosine molar conversion of 94.7% and a 5-methyluridine molar yield of 79.1% (Figure 3.12) within 7 hours, at a 5-MU productivity of $1.37 \text{ g.l}^{-1}\text{h}^{-1}$. The yield of this non-optimised reaction was comparable to those reported by Ishii *et al.* (1989) (74% mol/mol 5-MU) using whole cells of an *Erwinia* wild type organism. This also demonstrated that cell free extracts are tolerant of high substrate concentrations as slurries, using starting substrate concentrations in excess of 0.1 M, which has previously only been applied in whole cell biocatalytic reactions (Ishii *et al.* 1989).

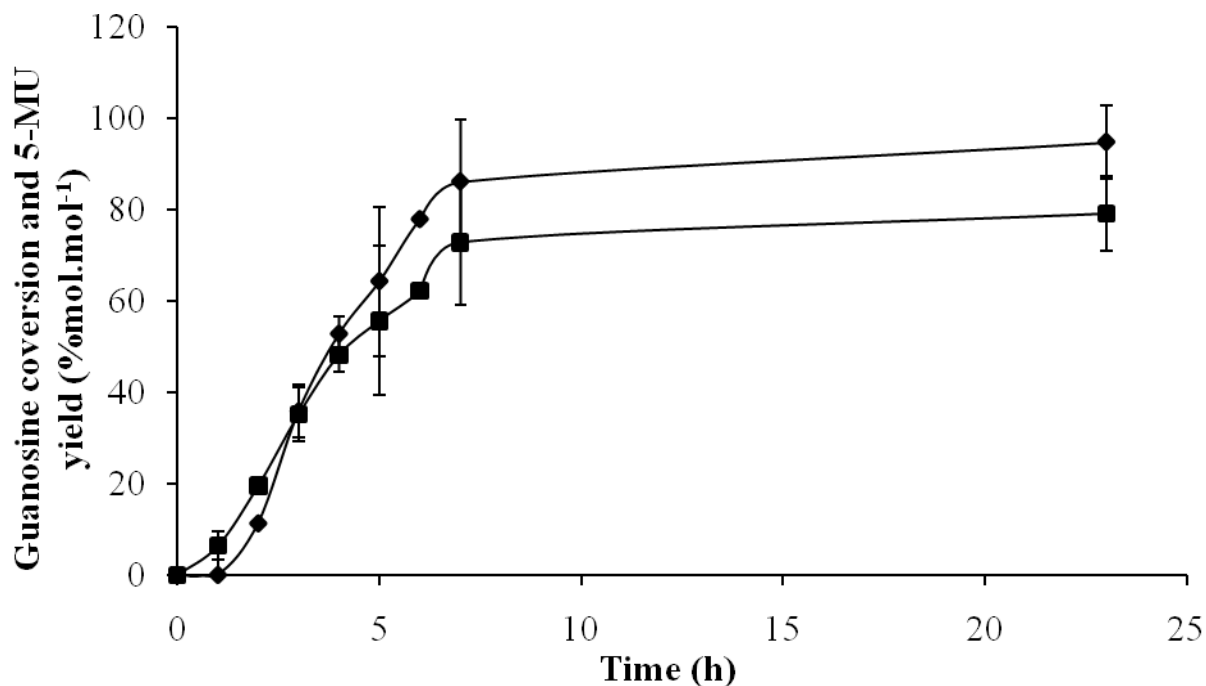


Figure 3.12 Bench scale (650 ml) biocatalytic production of 5-MU containing thymine (1.6% m.m⁻¹, 127 mM), guanosine (53 mM), BHPNP1 (105 U) and EcUP (75 U) in 50 mM sodium phosphate buffer (pH 7.8) at 40°C. Guanosine conversion (◆) and 5-MU yield (■) are shown.

Error bars are calculated from the mole balance of the complete reaction.

To confirm the structure of the reaction product, a sample was washed with hot isopropyl alcohol, filtered, and vacuum dried. The proton NMR (Appendix 5) was determined to be: δ H (400 MHz, D₂O) 7.69 (1 H, s), 5.89 (1 H, d, J 4.7), 4.33 (1 H, t, J 5.1), 4.23 (1 H, t, J 5.4), 4.11 (1 H, dd, J 4.2, 8.2), 3.91 (1 H, dd, J 2.9, 12.8), 3.81 (1 H, dd, J 4.2, 12.8), 1.87 (3 H, s), which was identical to that of a commercial standard. The carbon data was ¹³C NMR (100 MHz, D₂O) δ 166.3, 151.6, 137.2, 111.2, 88.8, 84.0, 73.4, 69.2, 60.5, 11.4.

3.4 CONCLUSIONS

Production of *B. halodurans* purine nucleoside phosphorylase and *E. coli* uridine phosphorylase, which were required for the synthesis of 5-methyluridine, was demonstrated in batch fermentations using the production strains *E. coli* JM109 [pMSPNP] and *E. coli* BL21 [pETUP] resulting in enzyme yields of 26.9 and 37.7 kU.l⁻¹ for BHPNP1 and EcUP, respectively.

Both catalysts were purified and successfully characterised. The established pH optima indicate that it may be advantageous to operate the biocatalytic step at pH 7.0 as this is the optimum for both enzymes. Effects of the difference in pH (particularly regarding substrate solubility and availability) would need to be tested further. Temperature optima and stability data for PNP (70°C and $t_{1/2}$ at 60°C of 20.8 h) indicate that the biocatalytic step is operating within the capabilities of this enzyme and would operate well at elevated temperatures (up to 60°C). Conversely, the temperature optimum and stability data for UP (optimum of 40°C and $t_{1/2}$ at 60°C of 9.9 h) indicate that, while the enzyme remains active at 40°C for the duration of a 25 h biotransformation, at 60°C the enzyme would only be operating at 20% of its optimum activity and would lose activity rapidly. Physical and kinetic parameters determined for the *E. coli* UP agree with published data for this enzyme (Leer *et al.*, 1977). BHPNP1 showed similar characteristics as the PNP isolated from *G. stearothermophilus* (Hori *et al.* 1989a) in terms of substrate affinity, catalytic activity, pH optimum and temperature optimum. The *G. stearothermophilus* PNP however exhibits better temperature stability and a wider pH range.

The biocatalytic reaction described here indicates that a novel combination of nucleoside phosphorylases (*B. halodurans* PNP and *E. coli* UP) can facilitate the production of pyrimidine nucleosides from purine nucleosides in high yields. Partially purified enzyme preparations were applied in a two step transglycosylation reaction for the production of 5-methyluridine in a one-pot synthesis step with a yield of 79.1% mol/mol on guanosine. This represents the first example of a free-enzyme transglycosylation giving high yields in a slurry-based reaction. The productivity observed here (1.37g.l⁻¹h⁻¹) is now comparable to the work done by Ishii and co-

workers (1989) who achieved $1.19 \text{ g.l}^{-1}\text{h}^{-1}$ in a whole-cell catalysed reaction. This productivity however is still lower than the $6.20 \text{ g.l}^{-1}\text{.h}^{-1}$, achieved by Hori and co-workers (1991), and an order of magnitude below the general commercially viable productivity defined by Straathof *et al.* (2002). The productivity can be potentially improved through reaction engineering to optimize the reactions conditions to best suit the current enzyme characteristics. An alternative would be to tailor the current enzymes to better suit the reaction. For this approach, the most likely target would be to improve the thermostability of the *E. coli* UP. Improved thermostability would ensure that the enzyme remains optimally active throughout the reaction, thus improving the productivity of the reaction. The following chapter will focus on the evolution of EcUP for this purpose.

CHAPTER 4: STABILISATION

EVOLUTION OF *E. COLI* UP AND BIOCATALYST IMMOBILISATION

4.1 INTRODUCTION

4.1.1 Determining target characteristics for evolution

Characterisation of the two biocatalysts in the previous chapter has shown that both enzymes are suitably active against the desired substrates (guanosine, thymine and ribose-1-phosphate). The biocatalytic reaction showed that high guanosine conversion (>90%) and high 5-methyluridine yield (>75%) could be achieved in mild conditions. This reaction is equivalent or better than those described in literature (Ishii *et al.*, 1989; Hori *et al.*, 1989b; 1991). This process is however not suitable for industrial application due to the low reaction productivity. In order to increase the productivity, one would need to increase the reaction temperature. This would increase the substrate solubility and therefore increase the availability of the substrates to the enzymes. BHPNP1 has been shown to be stable at 60°C while *E. coli* UP has very low stability at that temperature. The target for evolution therefore would be to increase the thermostability of the *E. coli* UP.

4.1.2 Selecting a suitable evolution method

Rational design mutagenesis has produced some useful catalysts, but the process requires detailed knowledge of the structural and mechanistic properties of the enzyme. Additionally, while it may be possible to predict the effects of a mutation at the active site, it is difficult to determine those mutations which may affect the overall protein structure. The same can be said for mutations on the surface of a protein.

Saen-Oon *et al.* (2008) reported that two mutations to surface residues of human purine nucleoside phosphorylase enhanced the catalytic activity of the enzyme, even though they were remote from the active site.

Rational design is particularly difficult when the character trait being targeted is stability of the enzyme as this is not as straightforward as modifying catalytic or related amino acids in the active site. Mutations that introduce disulphide bonds, modify the surface charges or rigidifying mutations such as removing glycines or introducing proline residues can be engineered into a protein to improve stability and has been successfully applied (Eijsink *et al.*, 2005).

The alternative is random mutation, which indiscriminately mutates the gene sequence creating molecular diversity. A library of randomised genes is then expressed in a suitable host organism and screened for the desirable trait. In random mutation however, very large numbers of variants need to be screened to adequately cover the generated diversity. This screening is costly and laborious. It is advantageous therefore to direct the mutation towards certain areas of the protein, thereby focusing the evolution and minimising the required library size. Methods of directed evolution, described in Chapter 1, include error-prone PCR, gene shuffling and saturation mutagenesis. More recent methodologies are variations or combinations of these basic methods.

Of particular interest for rapid evolution of enzyme stability is the method developed by Reetz and co-workers (Reetz *et al.*, 2006a; Reetz *et al.*, 2006b; Reetz and Carballeira, 2007) known as iterative saturation mutagenesis (ISM). The method combines the randomization of saturation mutagenesis with rational design in that the saturation is targeted at an area or areas of the protein that are likely to create an enhanced phenotype based on structural or catalytic information. In addition, this method represents a “rapid” form of evolution in that the libraries created are small and focused and therefore do not require extensive screening programs. The key to the method is the iterative nature of the mutation where the mutated gene giving the most improved trait from the first round of mutation, is used as the primer for a second round of mutation using the next best target. This iteration is repeated until the desired target enhancement is reached (Figure 4.1).

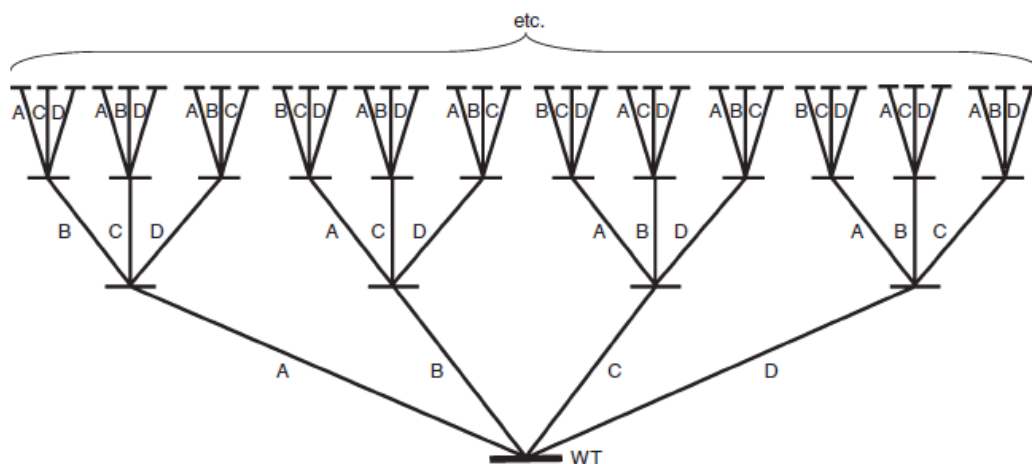


Figure 4.1 Illustration of Iterative saturation mutagenesis (reproduced from (Reetz and Carballeira,2007).

In this example, 4 randomization sites are chosen and used as the first round of mutation. The best mutation from the first round of mutation (eg from library A) is then used as the primer for the next mutation with one of the other chosen sites (B, C or D) and so forth until the desired phenotype is developed.

Selecting the amino acids or areas of the protein to target represents a challenge. Analysis of mesophilic and thermophilic enzymes show that extremophilic enzymes have a higher degree of surface rigidity. Reetz and co-workers therefore targeted amino acids with the highest degree of flexibility indicated by atomic displacement parameters available from X-ray data, namely B-factors (also called B-values). They developed a method called B-Factor Iterative Test (B-FIT), which highlights the amino acids with the highest flexibility and thereby creates targets for mutagenesis. Using the ISM method, Reetz and co-workers increased the thermostability of *Bacillus subtilis* lipase from 48°C to 93°C after screening only 8 000 clones (Reetz *et al.*, 2006b). Similarly, the same group applied ISM to amino acids of interest in the active site (rather than amino acids predicted by B-fit) of *Aspergillus niger* epoxide hydrolase. After a total screening of 20 000 clones, they managed to increase the enantioselectivity from an E value of 4.6 to a value of 115.

E. coli uridine phosphorylase is a good candidate for directed evolution through ISM. It is a multimeric protein, which further complicates rational design; the crystal structure of uridine phosphorylase has been determined (Morgunova *et al.*, 1995; Caradoc-Davies *et al.*, 2004b), which simplifies the process of determining saturation targets; and, as a native *E. coli* enzyme, expression of mutants is well suited for an *E. coli* expression system. The only reports of mutagenesis on PyNPs is directed at discovering residues critical to folding (Oliva *et al.*, 2004) and for determining active site residues (Chebotaev *et al.*, 2001). To date no mutagenesis studies have been reported for the specific enhancement of physical or catalytic characteristics of uridine phosphorylases.

4.1.3 Designing an effective screening method

The current protocol for uridine phosphorylase determination (see Chapter 2) would not be suitable for assaying large numbers of clones due to the number of steps involved. It would be preferable to develop a simple method for confirming activity.

Schramm *et al.* (2002) described a number of nucleoside analogues incorporating chromogenic substrates (Figure 4.2). Of particular interest for pyrimidine nucleoside phosphorylase screening is a ribose sugar linked to a pyrimidine-like structure such as α -naphthol, *p*-nitrophenol or 2-hydroxy-5-nitropyridine. When cleaved the chromogenic substrate gives a measurable response either alone or by interaction with other assay components (such as a diazonium salt for α -naphthol). Using a second substrate (such as a diazonium salt) is often a rate limiting step and only gives an accurate result within a narrow substrate or enzyme concentration range. Use of 2-hydroxy-5-pyridine as the chromagen would be limited in that the reaction would need to be made alkaline to intensify the colour formation. This secondary step would limit the application of the substrate for on-line kinetic measurement. It was therefore decided to produce the *p*-nitrophenol analogue. This compound would adequately mimic uridine and release of *p*-nitrophenol is routinely used for lipase, esterase and amylase activity determinations in our labs. Additionally, *p*-nitrophenol substrates are generally thermotolerant and would therefore be well suited to assays at elevated temperatures.

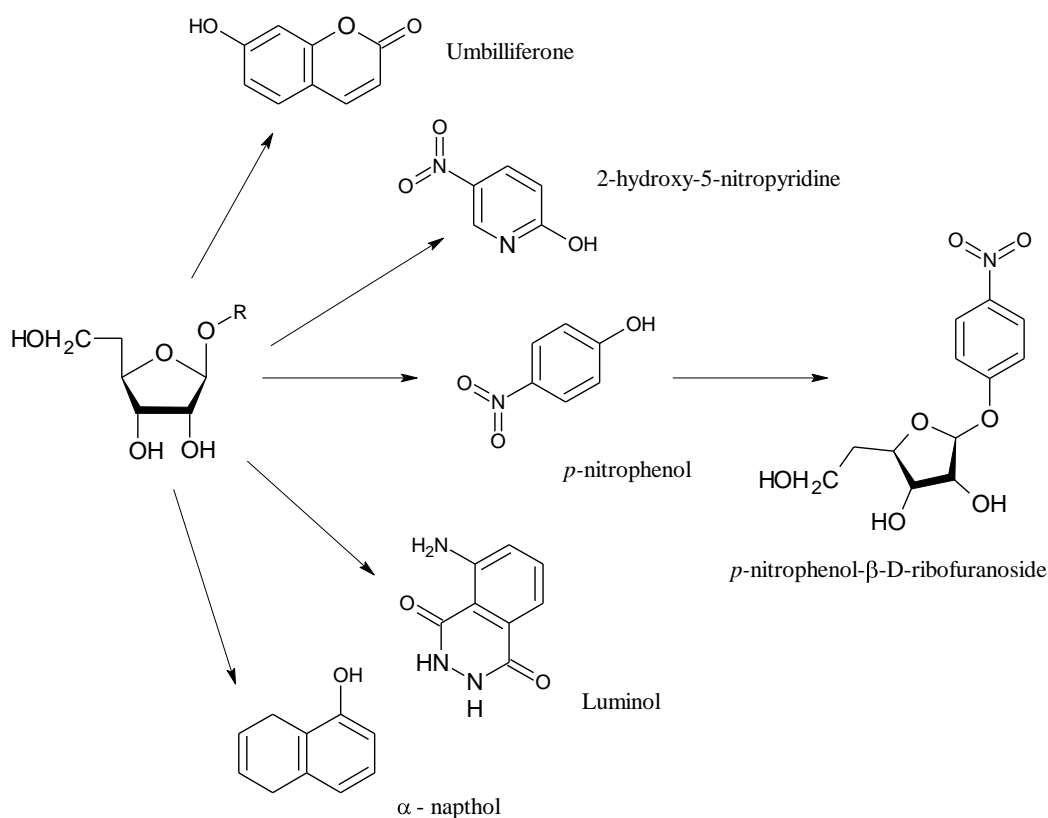


Figure 4.2 Schematic representation of the variations of nucleoside analogues incorporating chromogenic substrates for rapid activity determination of nucleoside phosphorylase activity. Also shown is the complete structure of the analogue (*p*-nitrophenol-β-D-ribofuranoside) used in this study)

4.1.4 Immobilisation

The advantages of immobilisation for these biocatalysts would be stabilization of the native *E. coli* UP or further stabilisation of any mutant and BHPNP1. In addition, immobilisation may enable enzyme recyclability, which would be advantageous from a process cost point of view. The transglycosylation reaction for 5-MU production however presents a problem for immobilised enzyme recovery. The co-product, guanine, is highly insoluble in aqueous solutions. At the end of the reaction therefore, it would be difficult to separate any suspended particles (immobilised enzyme) from the guanine by-product. This may be overcome by reactor design or by immobilising

the enzyme on a solid support which can be easily separated from the reaction solution.

The *E. coli* UP and PNP1 have been co-immobilised by covalent linkage to epoxy-activated Sepabeads for the biocatalytic preparation of a variety of natural and modified purine nucleosides (Zuffi *et al.*, 2004). Similarly, nucleoside phosphorylase from *Geobacillus stearothermophilus* were covalently immobilised on aminopropylated macroporous glass (Taran *et al.*, 2009). These preparations showed increased thermal stability high levels of activity retention (>80%) when immobilised. Of particular interest is the work done by Hori and co-workers, who immobilised PNP and PyNP from *Geobacillus stearothermophilus* by ionic binding to DEAE-Toyopearl 650M anion exchange resin (Hori *et al.*, 1991). Using the immobilised biocatalysts, they were able to design a continuous reaction for the production of 5-methyluridine from inosine and thymine which was run for 17 days at 60°C.

This study aims to show whether these multimeric enzymes can be immobilised using the Spherezyme technology (Brady *et al.*, 2008) and the effects of that immobilisation.

4.2 METHODS AND MATERIALS

4.2.1 Determining Target Amino Acids

To determine the B-value, the structure of *E. coli* UP (1LX7) was opened in “B-fitter” (Freeware from the Manfred Reetz research group (http://www.mpi-muelheim.mpg.de/kofo/institut/arbeitsbereiche/reetz/englisch/reetz_research1.html)).

The programme automatically determines the surface residues with highest B-values. ISM Libraries 1 to 6 in Table 4.1 are combinations of 1, 2 or 3 of the targets from a distinct region on the surface of the enzyme (Figure 4.3).

Table 4.1 B-Fit ISM Targets for *E. coli* UP. Based on highest B-values (calculated with B-fitter based on Chain A of model 1LX7-UP), the following residues have been selected for mutations (only forward primers shown, degenerate (Ds) IUB codes in bold).

			Library		
	aa	B-Value	Ds Cod	Size (95% coverage)	Primers
1	MET38/ LYS40	38.68 36.51	NNK/ NNK	3066	UP1F: AAGATCGCCGCGCTG NNK GAT NNK CCG GTAAAGCTG
2	LYS 60	34.29	NNK	100	UP2F: AGCTGGATGGT NNK CCTGTTATCGT
3	LYS 145	35.19	NNK	100	UP3F: TTGAAGCTGCG NNK TCCATTG
4	PRO229/ ASN230/ ALA231	37.77 53.85 58.08	DNK/ VDK/ NRT	10352	UP4F: CAAGAGATC DNKVDKNRT GAGACGATG AAACAA
5	LYS235/ GLN236	54.12 45.40	NNK/ NNK	3066	UP5F: AATGCTGAGACGATG NNKNNK ACCGAA AGCCATGCG
6	GLU232/ MET234	63.23 63.12	NNK/ NNK	3066	UP6F: CAAGAGATCCCGAATGCT NNK ACG NNK AAACAAACC

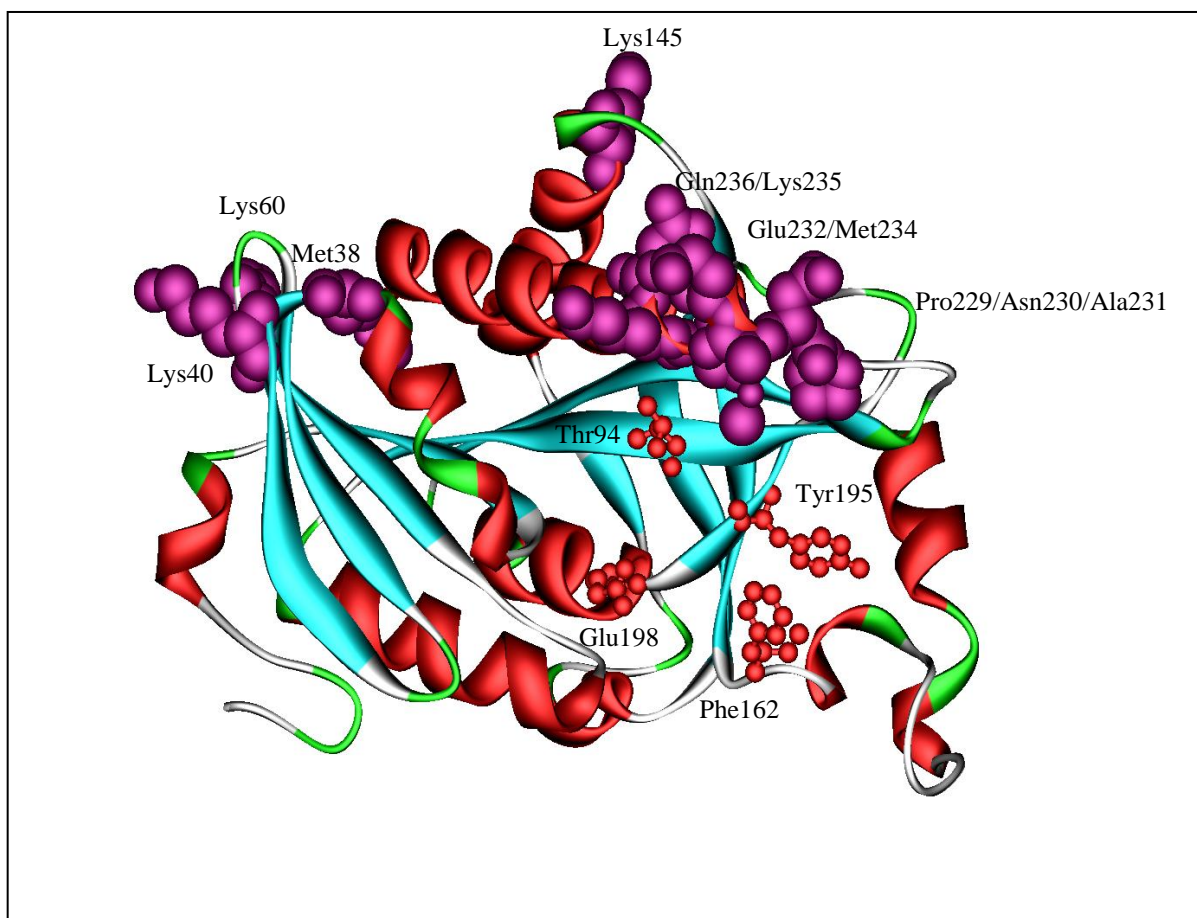


Figure 4.3 Ribbon representation of *E. coli* uridine phosphorylase (Accelrys)

Catalytic residues are shown in red (ball and stick format) and residues targeted of ISM in purple (CPK format) based on the 1LX7 structure (Burling *et al.*, 2003).

4.2.2 Preparation of *E. coli* UP template

The pETUP plasmid was sequenced (Inqaba Biotech) to confirm the sequence of the UP insert. Results showed that there were no frame shifts or mutations in the stock plasmid.

4.2.3 Mutagenesis

A Stratagene QuikChange II Mutagenesis Kit (Stratagene, USA) was used to perform plasmid based mutagenesis. Primers were obtained from Inqaba Biotech (Pretoria, South Africa). To initiate the reaction, 1 μ l of *PfuTurbo* DNA polymerase (2.5 U/ μ l) was added to the reaction mixes. The PCR reaction was as follows: A single cycle at 95°C for 1 minute, 18 cycles at 95°C for 50 seconds, 55°C for 50 seconds, and 68°C for 1 minute per kb of plasmid length, followed by a cycle at 68°C for 7 minutes. *DpnI* restriction enzyme (5 μ l) was then added to each reaction and incubated for 5 hours at 37°C to digest the parental (i.e., the nonmutated) supercoiled dsDNA. The mutated plasmid was then cleaned and concentrated (Zymogen DNA clean up kit, Fermentas). Between 100 and 250 ng of this material was used to transform competent *E. coli* XL1 Blue cells by heat shock (42°C, 45 s).

4.2.4 Assay development

4.2.4.1 Synthesis of 4-nitrophenol- β -D-ribofuranoside

A suspension of 10 g 1-O-acetyl-2,3,5-tri-O-benzoyl- β -D-ribofuranose, 5.6 g *p*-nitrophenol, 1.2 ml boron trifluoride diethyl etherate in 100 ml dry CHCl₂ was allowed to stir overnight at room temperature. The solution was washed with aq. bicarbonate (to remove unreacted 4-nitrophenol). The aqueous phase was separated and the resultant organic portion was reduced to half the initial volume under reduced pressure before separation of the *p*-nitrophenol-2,3,5-tri-O-benzoyl- β -D-ribofuranoside from the reactants by flash chromatography (1:2:8 EtOAc:CHCl₃:Hexane). Fractions showing the desired product (measured by TLC on UV_{254nm}, R_f = 0.8 in the above mobile phase) were pooled yields and dried under vacuum. This product was then suspended in 100 ml methanol, adjusted to pH 10 with NaOH and left to stir overnight. The solution was then concentrated under reduced pressure. The residue was dissolved in dissolved in 1:1 MeOH/CH₂Cl₂ and filtered through a silica pad. The eluate was concentrated and purified (to remove methyl benzoate contaminant) by EtOAc trituration. A yield of 3.88 g of product (*p*-

nitrophenol- β -D-ribofuranoside) was achieved. The product and its purity were confirmed by $^1\text{H-NMR}$ (Appendix 5).

4.2.4.2 Application of 4-nitrophenol- β -D-ribofuranoside to determination of uridine phosphorylase activity

Two methods of UP detection were tested. First, 0.1% m.v⁻¹ of the substrate was incorporated into Luria agar. Cultures separately expressing UP and PNP were streaked onto the agar plates and allowed to grow overnight at 37°C. The substrate was also tested in liquid culture to determine if kinetic analysis was possible. An amount equivalent to 0.01% m.v⁻¹ of the substrate was dissolved in a minimal volume of warm methanol, and made up to volume with 50 mM sodium phosphate buffer (pH 7.5). For 96-well and 384-well microtitre plates a volume of 240 μl or 40 μl respectively was added to 10 μl of a known enzyme solution (0.25 U.ml⁻¹). The change in absorbtion due to the release of *p*-nitrophenol was measured at 410 nm using a Powerwave HT microtitreplate reader.

4.2.5 Screening

4.2.5.1 Preparation of mutant screening libraries

Mutant libraries were plated on to Luria agar (100 $\mu\text{g.ml}^{-1}$ ampicillin) in Q-trays and incubated overnight at 37°C. Colonies were picked and inoculated into Luria broth (60 μl , 384 well plates) using the QPix2 colony picker (Genetix, UK). The number of colonies picked per library is given in Table 4.2. After an overnight incubation, duplicate plates were prepared using the replication function of the QPix2. The replicate plates were incubated overnight and served as the back-up cultures. To the master plates, IPTG was added to a final concentration of 1 mM. These plates were incubated for a further 20 h to facilitate mutant protein expression. Cells were then harvested by centrifugation (3000 x g, 20 min). The cells were broken by the addition

of 15 μ l B-Per directly to the cell pellet followed by a 60 min incubation at room temperature. Cell debris was removed by centrifugation (3000 x g, 20 min).

Table 4.2 Target and actual number of colonies picked per mutant library.

	Targeted Library Size	Colonies Picked
UP L1	3000	3500
UP L2	100	600
UP L3	100	600
UP L4	10000	1100
UP L5	3000	3500
UP L6	3000	3000

Colonies were picked using the Genetix Qpix2. Target library sizes were calculated according the number of clones required to obtain 95% coverage of all possible mutation. The library size is dependant on the number of amino acids mutated and the degenerate codon utilized. Libraries with lower than targeted number of colonies picked was due to low transformation efficiency.

4.2.5.2 Primary Screening

Cellular extracts (5 μ l) from each of four wells were pooled to single destination wells on each of two plates using an EpMotion 5025 liquid handling station. Activity of the pooled samples was measured before and after incubation at 70°C for 15 min. The native *E. coli* UP showed 10% residual activity under these conditions. Hits from each of the libraries were selected based on the highest percentage residual activity. The original four samples corresponding to the hits were then assayed in the same way to determine the original culture giving the highest residual activity.

4.2.5.3 Secondary Screening

Single culture hits were re-inoculated into 5 ml cultures and incubated overnight. The plasmid harbouring the mutated gene was then extracted (Fermentas plasmid miniprep kit). This plasmid was used to re-transform *E. coli* XL1 blue. This new culture was then grown at 37°C to an OD of 1.0 (50 ml Luria broth, 100 µg.ml⁻¹ ampicillin) and protein expression induced (0.1 mM IPTG, 3.5 h). Cells were harvested by centrifugation (3000 x g, 20 min) and disrupted by addition of B-Per (4 ml per gram wet weight). After removal of cellular debris, the expressed protein was further purified by ultrafiltration through a 100 kDa membrane (Amicon). The resultant protein solutions were then incubated at temperatures between 40 and 80°C degrees for 60 min to determine the temperature at which 50% of the initial activity was retained ($T_{50(\%)}^{60(\text{min})}$ value).

4.2.6 Iterative Mutagenesis

The strain containing the mutated enzyme showing the highest stability after the first round of screening was used as the template for the second round of screening. In this case a strain from library 5 showed the highest residual activity after a 15 min incubation at 70°C (95% activity retained). The plasmid harbouring this mutated gene was used in PCR reaction with the mutation primers for library UP4 and UP6, which gave next two best hits, respectively. Saturation mutagenesis and subsequent screening was performed as described above.

4.2.7 Growth and expression of best mutant

The plasmid for the best mutant (UPL8 from library UP 8) was isolated from the *E. coli* XL1 blue strain (QIAprep Spin Miniprep Kit, Qiagen) and retransformed by heat shock (Sambrook and Russell,2001) into competent *E. coli* BL21 (DE3) for over expression and production of the mutant enzyme. The strain thus created was named *E. coli* BL21 (DE3)[pETUPL8].

4.2.8 Production of UPL8

The mutant enzyme was produced in two 10 l fermentations according to the protocols described in Chapter 3 (3.2.2). The UPL8 enzyme was purified as per section 3.2.4

4.2.9 Characterisation of UPL8

Kinetic and physical characteristics of UPL8 were determined according to the methods described for wild type UP in section 3.2.5. Temperature optimum, pH optimum and kinetic properties were determined.

4.2.10 Sequence analysis

The mutant gene sequences present in the best strains isolated from each of the mutation experiments were sequenced (Inqaba Biotech).

4.2.11 Production of nucleoside phosphorylase Spherezymes

4.2.11.1 Preparation of nucleoside phosphorylases

Lyophilised crude extracts of the original and mutant nucleoside phosphorylases produced in sections 3.2.2 and 4.2.8 were dissolved in 50 mM Tris-HCL buffer (pH 8.0). The nucleoside phosphorylases were partially purified by ammonium sulphate precipitation (30% saturation to remove the majority of the contaminating proteins and 70% saturation to precipitate PNP and UP). The resultant pellet was resuspended, in the same buffer, before ultrafiltration (30 kDa cut-off membrane, Pall minimate TFF) to remove excess $\text{NH}_2(\text{SO}_4)_2$ and concentrate the enzyme. Final protein concentrations of 170 mg.ml^{-1} , 110 mg.ml^{-1} and 70 mg.ml^{-1} were obtained for UPL8, EcUP and BHPNP1, respectively.

4.2.11.2 *Spherezyme optimisation*

A combinatorial optimisation experiment was designed to determine optimal cross-linking and Spherezyme formation parameters for each of the enzymes. The parameters investigated included protein concentration (50 or 100 mg.ml⁻¹ for UP and 35 or 70 mg.ml⁻¹ for PNP), cross linker (25% m/v glutaraldehyde (Glu) with either 0.33 M ethylenediamine (EDA) or 5% m/v Polyethyleneimine (PEI)), cross linker ratio (1:1 Glu:EDA, 1:2 Glu:EDA, 1:1 Glu:PEI), and cross linker concentration (8%, 16% and 24% v/v). The experimental layout is given in Figure 4.4.

The oil phase was prepared by adding the surfactant nonoxynol-4 (NP-4) (CHC Group, South Africa) to a concentration of 0.05% v/v in mineral oil and stirring for 10 min to ensure adequate dispersion. Aliquots of the oil phase (0.5 ml) were then placed in a 2.2 ml deep well microtitre plate. The wells contained 4 mm cylindrical magnetic stirrer bars to facilitate mixing. The Glu:EDA solution were prepared 5 to 10 min before addition to the enzyme preparation and the Glu:PEI were prepared 1 -2 min before addition. Sufficient cross-linker solution was then added to a 50 µl aliquot of the respective enzyme solution. This preparation was mixed briefly and then added directly to the oil phase. The emulsions were allowed to react overnight at room temperature.

After incubation, the emulsion was broken by centrifugation (Beckman Avante centrifuge, 1000 x g, 20 min) the oil phase was removed before washing the spheres 4 times with 1 ml 50 mM Tris-HCl pH 8.0 containing 1 mM ethanolamine to quench excess glutaraldehyde. The spheres were then washed with just the buffer to remove excess ethanolamine. The final preparations were suspended in 1 ml buffer for determining PNP and UP activities using the standard colorimetric assays described previously.

Figure 4.4 Experimental layout for combinatorial optimisation of nucleoside phosphorylases Spherezyme formation

	1	2	3	4	5	6	7	8	9	10	11	12
A		Cross Linker Concentration (% v/v)										
		4%	16%	24%	4%	16%	24%	4%	16%	24%		
B	Cross linker type	Glu:EDA 1:1	Glu:EDA 1:1	Glu:EDA 1:1	Glu:EDA 1:1	Glu:EDA 1:1	Glu:EDA 1:1	Glu:EDA 1:1	Glu:EDA 1:1	Glu:EDA 1:1	Protein Concentration (mg/ml)	
		50 mg/ml	50 mg/ml	50 mg/ml	50 mg/ml	50 mg/ml	50 mg/ml	35 mg/ml	35 mg/ml	35 mg/ml		
C		Glu:EDA 1:2	Glu:EDA 1:2	Glu:EDA 1:2	Glu:EDA 1:2	Glu:EDA 1:2	Glu:EDA 1:2	Glu:EDA 1:2	Glu:EDA 1:2	Glu:EDA 1:2		
		50 mg/ml	50 mg/ml	50 mg/ml	50 mg/ml	50 mg/ml	50 mg/ml	35 mg/ml	35 mg/ml	35 mg/ml		
D		Glu:PEI 1:1	Glu:PEI 1:1	Glu:PEI 1:1	Glu:PEI 1:1	Glu:PEI 1:1	Glu:PEI 1:1	Glu:PEI 1:1	Glu:PEI 1:1	Glu:PEI 1:1		
		50 mg/ml	50 mg/ml	50 mg/ml	50 mg/ml	50 mg/ml	50 mg/ml	35 mg/ml	35 mg/ml	35 mg/ml		
E		Glu:EDA 1:1	Glu:EDA 1:1	Glu:EDA 1:1	Glu:EDA 1:1	Glu:EDA 1:1	Glu:EDA 1:1	Glu:EDA 1:1	Glu:EDA 1:1	Glu:EDA 1:1		
		100 mg/ml	100 mg/ml	100 mg/ml	100 mg/ml	100 mg/ml	100 mg/ml	70 mg/ml	70 mg/ml	70 mg/ml		
F		Glu:EDA 1:2	Glu:EDA 1:2	Glu:EDA 1:2	Glu:EDA 1:2	Glu:EDA 1:2	Glu:EDA 1:2	Glu:EDA 1:2	Glu:EDA 1:2	Glu:EDA 1:2		
		100 mg/ml	100 mg/ml	100 mg/ml	100 mg/ml	100 mg/ml	100 mg/ml	70 mg/ml	70 mg/ml	70 mg/ml		
G	Glu:PEI 1:1	Glu:PEI 1:1	Glu:PEI 1:1	Glu:PEI 1:1	Glu:PEI 1:1	Glu:PEI 1:1	Glu:PEI 1:1	Glu:PEI 1:1	Glu:PEI 1:1			
	100 mg/ml	100 mg/ml	100 mg/ml	100 mg/ml	100 mg/ml	100 mg/ml	70 mg/ml	70 mg/ml	70 mg/ml			
H		Ec UP			UPL8			BhPNP				
		Enzyme Preparation										

4.2.11.3 Preparation of nucleoside phosphorylase Spherezymes

Solutions (2 ml) of EcUP (100 mg.ml⁻¹), UPL8 (100 mg.ml⁻¹) and BHPNP1 (70 mg.ml⁻¹) were prepared. In addition, mixtures (2 ml) of EcUP and BHPNP1 (60 and 70 mg respectively) as well as UPL8 and BHPNP1 (85 and 70 mg respectively) were prepared for co-immobilisation studies. Active site protectants (50 mM inosine and/or 50 mM uridine) were added to the solution directly prior to cross linking. To these solutions, 320 µl of the cross linker (1:1 Glu:5% PEI) was added, mixed and then directly added to 20 ml of the oil phase (mineral oil with 0.05% NP-4). The solutions were stirred at 700 rpm with a magnetic stirrer for 1 min to ensure a proper emulsion. Stirring was then decreased and the emulsion was allowed to incubate overnight at 4°C. The emulsion was then broken and the spheres recovered by centrifugation (Beckman J-21, 1000 x g, 10 min). Immobilised enzyme particles were washed 4 times with 50 mM Tris HCl, pH 8.0, containing 1 mM ethanolamine. Excess ethanolamine was washed off with Tris buffer. Finally, the immobilised enzyme particles were recovered by filtration under vacuum (Whatman #1). The immobilised enzyme particles were then dried at room temperature under high vacuum (Virtis Genesis 25L freeze dryer).

4.2.11.4 Spherezyme characterisation

Each of the Spherezyme preparations was resuspended in 50 mM sodium phosphate buffer (pH 7.5) for further analysis. PNP and UP activities were determined using the standard colorimetric assays (section 2.2.11.4). Temperature and pH optima as well as stability data at 60°C was determined according to the methods defined in section 3.2.5.

4.3 RESULTS AND DISCUSSION

4.3.1 Assay Development

Incorporation of the *p*-nitrophenol- β -D-ribofuranoside into agar gave a positive result for the detection of uridine phosphorylase. A distinct yellow halo was noted around the strain expressing UP as opposed to a faint halo around the control organism (expressing PNP) (Figure 4.5). Further analysis using a library of mutant UP clones showed that a high expression level is required for distinction from background activity. Use of the *p*-nitrophenol- β -D-ribofuranoside as a substrate for agar-based screening is therefore feasible, but only where high expression levels are present.

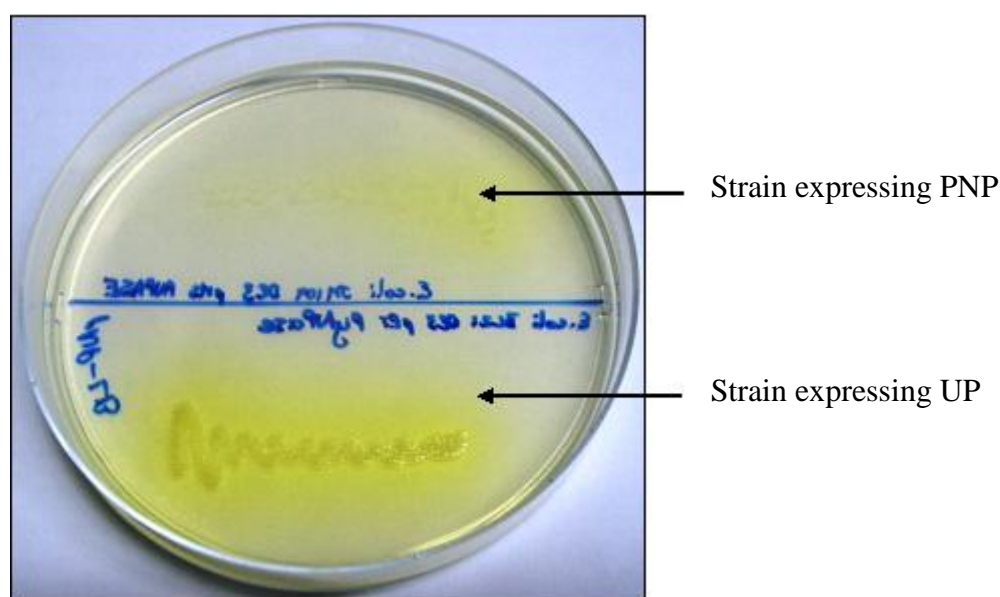


Figure 4.5 Agar plate image showing the distinct yellow halo formation around a culture due to *p*-nitrophenol released from a ribosides moiety due to UP phosphorylation.

The control culture (above), *E. coli* expressing PNP showed low level halo formation while the experiment (below), *E. coli* expressing UP showed more distinct halo formation.

Use of *p*-nitrophenol- β -D-ribofuranoside in liquid colorimetric assay proved effective. Although slightly lower activities ($0.2 \text{ U}\cdot\text{ml}^{-1}$ for a $0.25 \text{ U}\cdot\text{ml}^{-1}$ preparation) were noted, the result was sufficient to enable the use of the assay for distinguishing superior activities amongst a range of mutants. In addition, the colorimetric assay is a rapid method for comparing activities for thermostability and optima studies. Substrate control reactions showed little or no natural degradation of the substrate at elevated temperatures. Unfortunately, due to the pH sensitivity of *p*-nitrophenol, the substrate is not suitable for pH optima studies.

4.3.2 Round 1 Mutation

All mutation targets seemed to show some degree of improvement of thermostability. The best hits after the primary screening are given in Table 4.3. These values were used as the basis for the best hit selection, as the T_{50}^{60} (Figure 4.6) proved inconclusive for determining differences between the mutants. No activity was observed after incubation at 80°C regardless of the stability of the enzyme at 70°C , a result which skewed the potential stability values.

Table 4.3 Best hits from the first six libraries based on residual activities observed after incubation of the enzyme preparations for 1 h at 70°C .

Library	Mutant	Mutation	% Residual Activity
WT	Wild Type	None	10.0%
1	UPL1-2/A11	Met38Leu; Lys40Ser	31.7%
2	UPL2-2/G15	Lys60Lys	12.2%
3	UPL3-1/G9	Lys145Lys	12.9%
4	UPL4-3/F2	Pro229Ter; Asn230Asn; Ala231Asp	51.1%
5	UPL5-10/F9	Lys235Arg; Gln236Ala	95.5%
6	UPL6-2/H10	Glu232Glu; Met234*	30.9%

*Sequence inconclusive

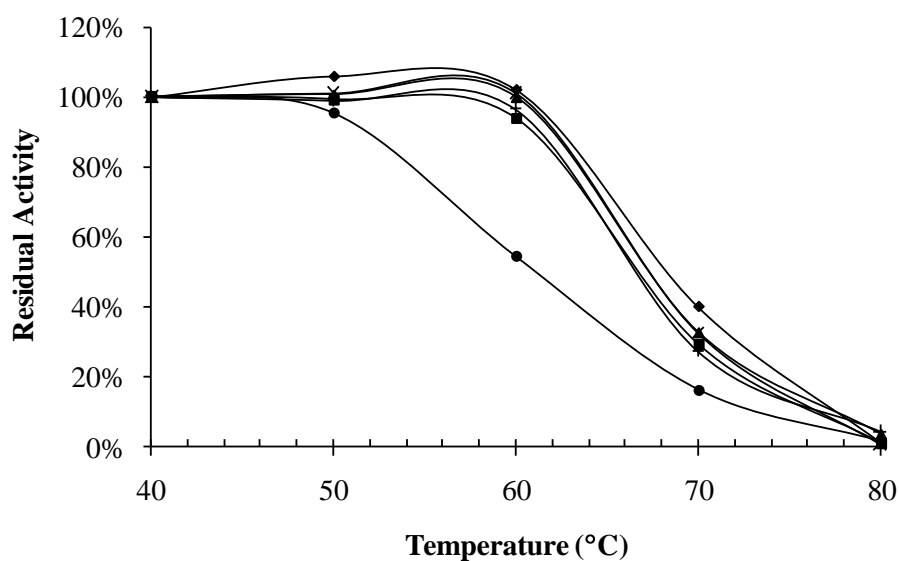


Figure 4.6 Plot of residual activity for the best mutants from each library in the first round of mutation. Residual activity was determined after incubation for 60 min at the set temperatures (37, 50, 60, 70 and 80°C). (UPL1-2/A11 (-♦-); UPL3-1/G9 (-■-); UPL4-3/F2 (-x-); UPL5-10/F9 (-◆-); UPL6-2/H10 (-+-); Wild type UP (-●-)).

4.3.3 Round 2 mutation

Mutation of the best hit from library 5 (round 1) with the primers for library UP L1 (giving library UP L7) and library UP L6 (giving library UP L8) again gave positive results in initial screening (Table 4.4). Screening, however, was now performed at 75°C for 15 min.

Table 4.4 Best hits from libraries UP L7 and UP L8 based on residual activities observed after incubation of the enzyme preparations for 1 h at 75°C

Library	Mutant	Mutation	% Residual Activity
7	UPL7-2/C15	Met38Val; Lys40Asp Lys235Arg; Gln236Ala	88.5%
8	UPL8-4/I5	Lys235Arg; Gln236Ala	80.2%

Determination of T_{50}^{60} values (Figure 4.7) showed good stability at 70°C but again no activity at 80°C, skewing the final values. It was decided to determine the stability of the enzyme from library 8 at 60 and 70°C to get a better indication of improved stability (Figure 4.8). These results showed marked improvements in stability at both 60 and 70°C.

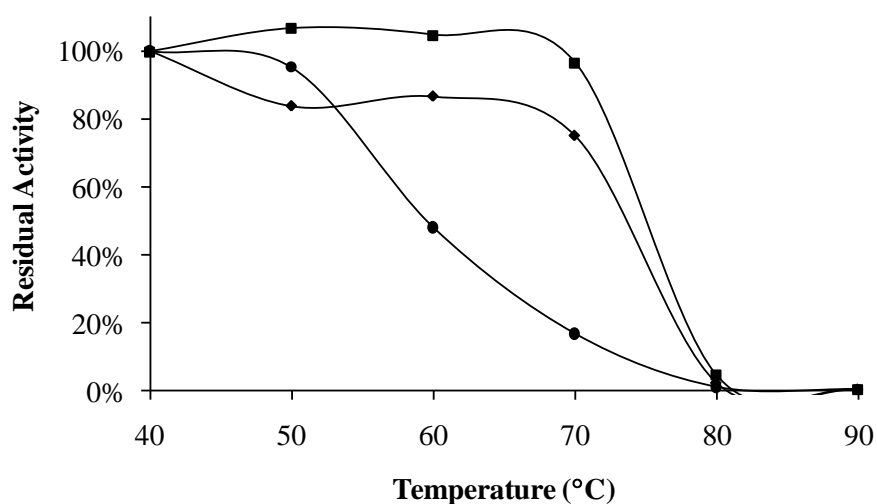


Figure 4.7 Plot of residual activity for mutants UPL7-2/C15 (-♦-) and UPL8-4/I5 (-■-) compared to wild type UP (-●-).

Residual activity was determined after incubation for 60 min at the set temperatures (37, 50, 60, 70 and 80°C)

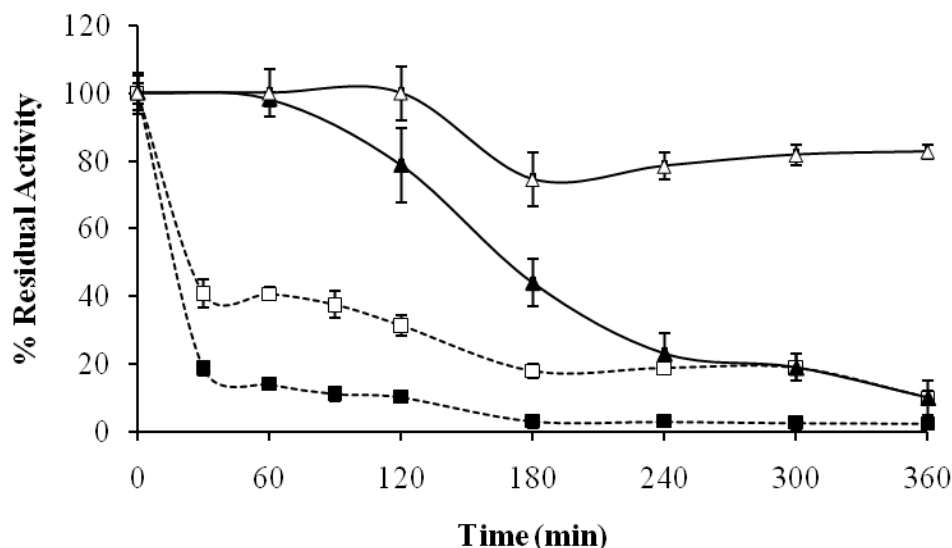


Figure 4.8 Thermostability comparison for mutant UPL8 (-▲-) and wild type EcUP ("■").

Enzyme preparations were incubated at 60°C (open symbols) and 70°C (closed symbols) for 6 h.

The aim of the directed evolution was to increase the thermostability of *E. coli* UP. The characterisation in Chapter 3 indicated that BHPNP1 would operate best at 60°C for the duration of the biocatalytic reaction. The target for this evolution was therefore to enhance EcUP thermostability at 60°C. The results in Figure 4.8 clearly show that this has been achieved. While further stabilisation could be achieved by further rounds of mutation, it is not necessary at this point since further enhancements in stability would then out perform BHPNP1 and thus be redundant. It was therefore decided to continue with production and characterisation of this mutant.

4.3.4 Production of UPL8 in batch fermentation

Fermentation characteristics of *E. coli* BL21(DE3)[pETUPL8] were similar to those seen for *E. coli* BL21(DE3)[pETUP]. Biomass production reached a level of $8.28 \pm 0.43 \text{ g.l}^{-1}$ (Figure 4.9) compared to the 12.4 g.l^{-1} previously obtained. The maximum UPL8 expression level (Figure 4.10) was significantly higher at $52.6 \pm 6.9 \text{ kU.l}^{-1}$ (compared to 37.7 kU.l^{-1}).

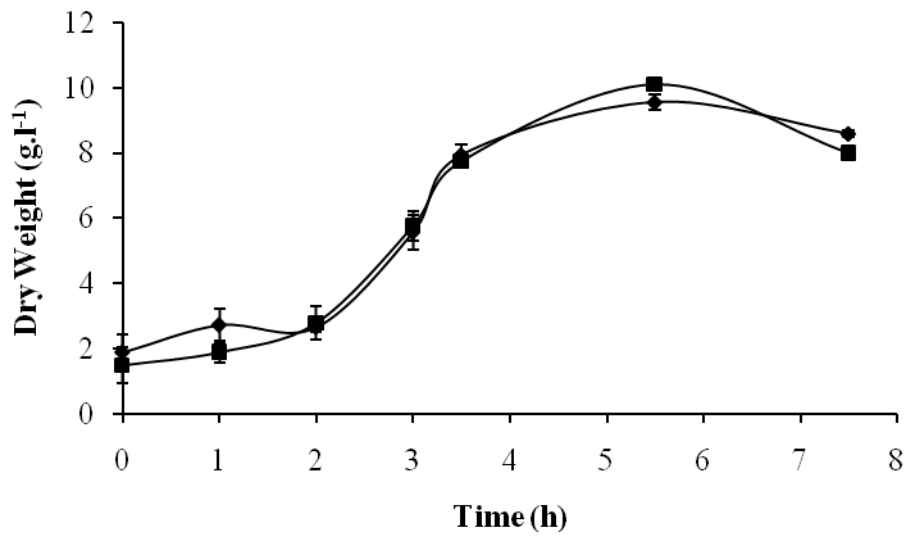


Figure 4.9 Biomass production for duplicate fermentations of *E. coli* B121 (DE3)[pETUPL8]

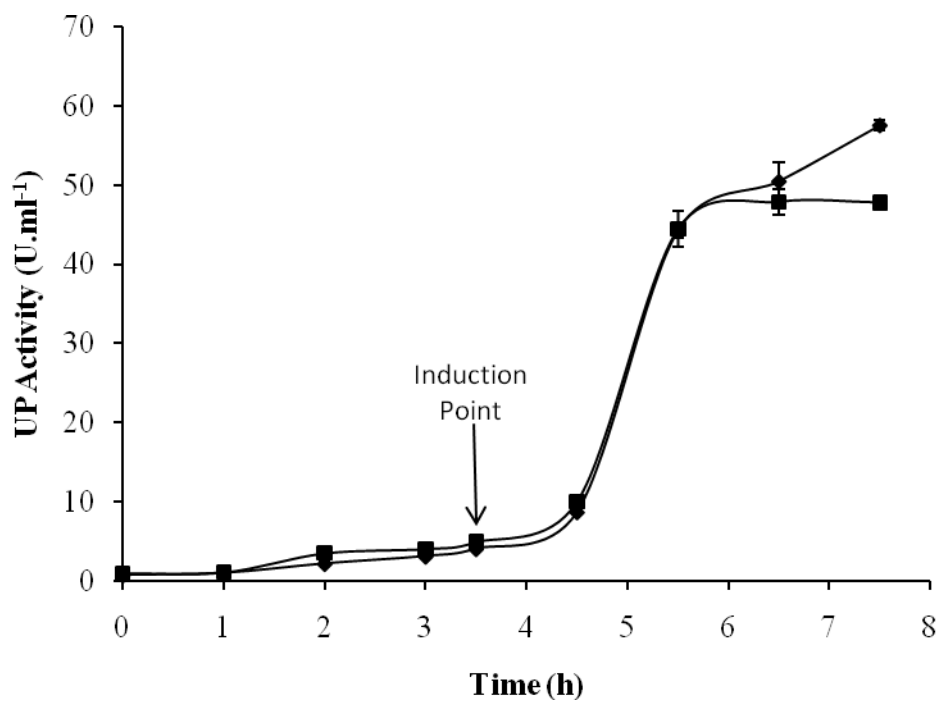


Figure 4.10 Activity profiles for the production of UPL8 during fermentation

4.3.5 Characterisation of UPL8

4.3.5.1 pH Optima

UPL8 showed a pH optimum of 7.0, retaining 60% activity between pH 5.6 and 8.4 (Figure 4.11), which is similar to the wild type UP (optimum of 7.0, retaining 60% activity between pH 6.0 and 8.2).

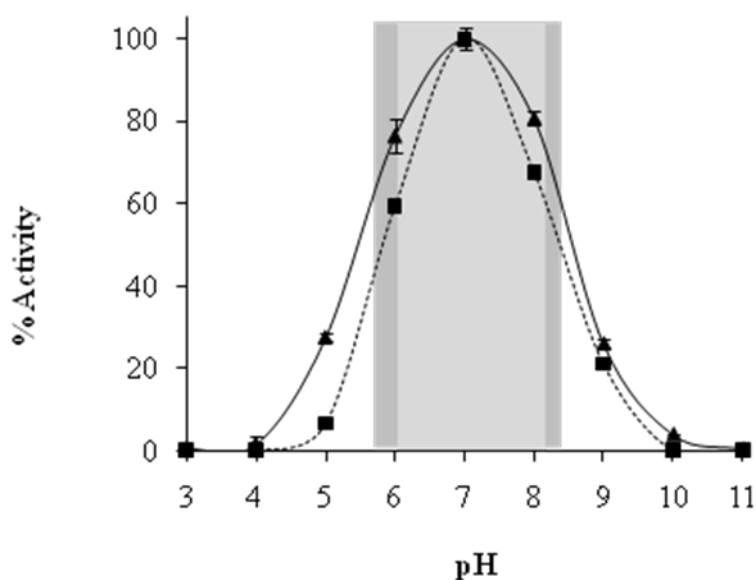


Figure 4.11 pH activity profiles of UPL8 (▲) and EcUP (■).

The shaded areas indicate the pH range of the enzymes (> 60% activity). A moderate increase in the pH range (darker shading) is noted for UPL8 while pH optima remain the same at pH 7.0.

4.3.5.2 Temperature Optima

UPL8 has a significantly improved temperature optimum (60°C) and a broader activity range, retaining 60% activity between 37 and 67°C (Figure 4.12). In contrast, native UP had an optimum of 40°C with a narrow activity range (retaining 60% activity) between 30 and 52°C. The thermal characteristics of the modified enzyme were now similar to those of BHPNP1 (optimum of 70°C, range of 30 to 74°C).

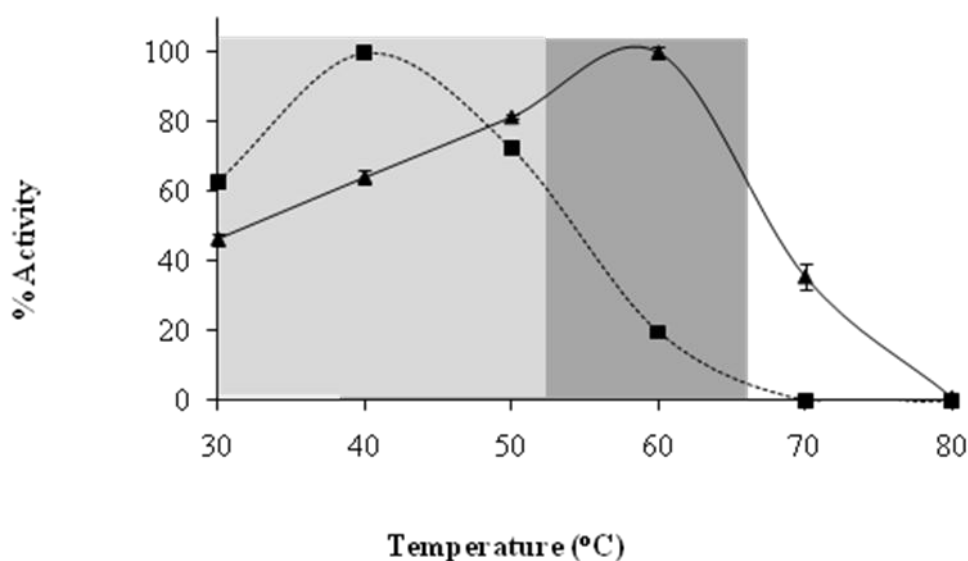


Figure 4.12 Temperature optima profiles of UPL8 (▲) and EcUP (■).

The shaded areas indicate the temperature range of the enzymes (> 60% activity). A significant increase in the temperature range and optimum is noted for UPL8.

4.3.5.3 Temperature Stability

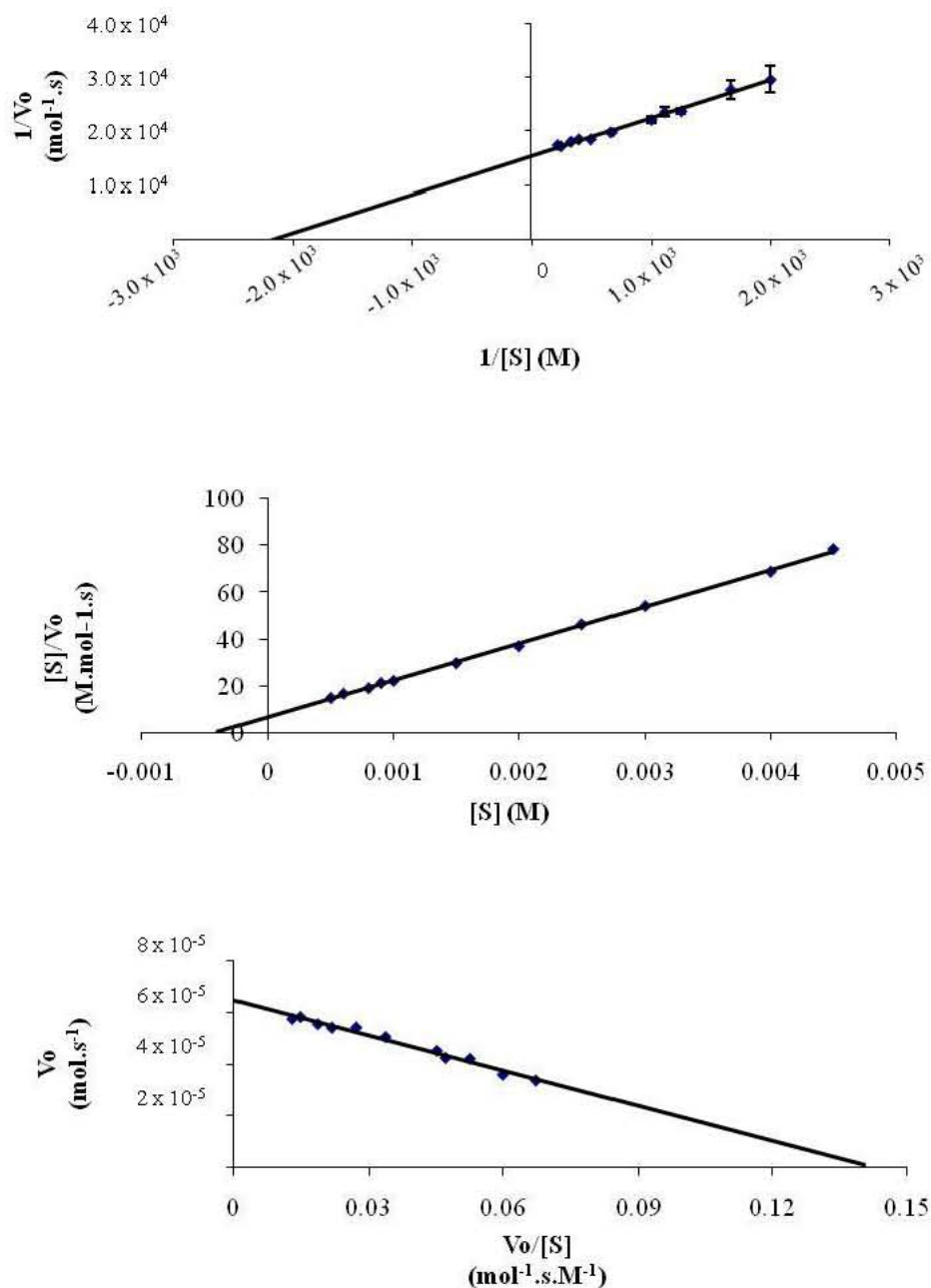
Wild type UP showed a half life of 9.9 h at 60°C, albeit at 20% of its optimum activity. At 40°C, the half-life was 37 h. The mutant enzyme has a half life at 60°C of 17.3 h and 3.3 h at 70°C (Figure 4.8). This again is comparable to the stability data for BHPNP1.

4.3.5.4 Kinetic Characterisation

Data obtained for varying uridine concentrations also showed good linear regression fit ($R^2 \geq 0.95$). From the plots (Lineweaver-Burk, Eadie-Hofstee and Hanes-Woolf, Figure 4.13), K_m and V_{max} were determined with less than 5% deviation in the values calculated from the three plots. Subsequently the turnover number (k_{cat}) and the specificity constant were calculated. The values are summarised in Table 4.5

Table 4.5 Physical and kinetic characteristics of UPL8 and EcUP characterised using uridine as the substrate at 40°C

Parameter	Unit	UPL8	EcUP
Specific Activity	U.mg ⁻¹	19.18	30.69
K_M	μM	464.3	233.9
V_{max}	mol.s ⁻¹	2.85 x 10 ⁻⁵	6.46 x 10 ⁻⁵
k_{cat}	s ⁻¹	2.73 x 10 ⁷	2.81 x 10 ⁷
Specificity Constant	M ⁻¹ .s ⁻¹	1.17 x 10 ¹¹	6.28 x 10 ¹⁰
pH Optimum	-	7.0	7.0
pH range (60%)	-	5.6 - 8.4	6.0-8.2
Temp Optimum	°C	60	40
Temp Range (60%)	°C	38-67	30-52
Temp Stability (t _{1/2} @ 60°C)	h	17.3	9.89
Temp Stability (t _{1/2} @ 70°C)	h	37	3.3



Parameter	Lineweaver-Burk	Hanes-Woolf	Eadie-Hofstee	Average	Stdev	%CV
R^2	0.9922	0.9992	0.9824	0.99	0.01	0.85%
K_m (M)	4.64×10^{-4}	4.23×10^{-4}	4.53×10^{-4}	4.47×10^{-4}	2.09×10^{-5}	4.67%
V_{max} ($\text{mol} \cdot \text{s}^{-1}$)	6.521×10^{-5}	6.39×10^{-5}	6.48×10^{-5}	6.46×10^{-5}	6.87×10^{-7}	1.06%

Figure 4.13 Lineweaver-Burk (top), Hanes-Woolf (middle) and Eadie-Hofstee (bottom) plots for UPL8 using uridine as the substrate.

Insert table indicates calculation of K_m and V_{max} from the 3 plots.

4.3.6 Sequence and homology model analysis of the mutant UPL8

The best mutant identified from the first round of mutation was from library UP5, which targeted Lys235 and Gln236. The subsequent mutations (those from libraries UP4 and UP6) targeted Pro229, Asn230, Ala231; and Glu232, Met234 in two separate experiments, respectively. The expectation therefore would be to achieve between 2 and 7 mutations in the final mutants. The best mutant from library UP7 showed a total of 4 mutations (Table 4.4). These additional mutations were not necessarily beneficial as the UPL8 mutant showed only the original mutations at position 235 (Lys→Arg) and 236 (Gln→Ala) (Figure 4.14 to Figure 4.17). Yet UPL8 was shown to be the superior mutant. The Lys235Arg mutation should not have had a dramatic affect as they are both basic amino acids. The larger arginine should also have increased flexibility at the site due to it being a longer side chain. This longer side chain however may be interacting with the neighbouring α -helix (Particularly Thr94, Figure 4.17), thereby conferring rigidity to the overall structure. The Gln236Ala mutation however does fit with the theory of decreased flexibility due to Ala having a smaller side chain and being non-polar as opposed to the polar Gln. Why just these two amino acid changes should have such a marked effect on the stability of the protein is unknown. Both are positioned on the α -helix leading to the N-terminal of the protein. This entire domain may have created instability in the native protein and it is plausible that these mutations stabilised that region, possibly through introduced H-bonding to neighbouring helices. This is further confirmed by the mutation in library 4, where removal of the entire α -helix yielded good thermostability characteristics. The mutations are also situated in close proximity to the entrance of the binding pocket. It is plausible that an increase in rigidity at this point would limit flexibility and therefore conformational changes during binding of the substrate.

The data obtained show that a relatively small, unpredictable mutation can have a marked effect on the physical characteristics of an enzyme. While it would be of interest to further study the effects of the observed mutation and further mutations, the desired increase in thermostability has been achieved. It was decided, therefore, to

continue with immobilisation studies to determine whether mutation or immobilisation, alone or in combination, would lead to a vastly improved biocatalyst.

```

Up          601 ACCCTGCTGACCATGTGTGCAAGTCAGGGCCTGCGTGCCGGTATGGTAGC      650
          |||
UPL8       601 ACCCTGCTGACCATGTGTGCAAGTCAGGGCCTGCGTGCCGGTATGGTAGC      650

Up          651 GGGTGTATATCGTTAACCGCACCCAGCAAGAGATCCCGAATGCTGAGACGA      700
          |||
UPL8       651 GGGTGTATATCGTTAACCGCACCCAGCAAGAGATCCCGAATGCTGAGACGA      700

Up          701 TGAACAACCGAAAGCCATGCGGTGAAAATCGTGGTGGAAGCGGCGCT      750
          |||
UPL8       701 TCGTGCACCGAAAGCCATGCGGTGAAAATCGTGGTGGAAGCGGCGCT      750

Up          751 CGTCTGCTGTAA      762
          |||
UPL8       751 CGTCTGCTGTAA      762

```

Figure 4.14 Nucleotide sequence alignment (bp #600 to end) of the native *E. coli* uridine phosphorylase (UP) and the mutant *E. coli* uridine phosphorylase (UPL8).

Mutated bases are highlighted.

```

UP      151  THVGV TASSDTFYPGQERYDTYSGRVVRHFKGSMEEWQAMGVMNYEMESA  200
          |||
UPL8   151  THVGV TASSDTFYPGQERYDTYSGRVVRHFKGSMEEWQAMGVMNYEMESA  200

Up      201  TLLTMCASQGLRAGMVAGVIVNRTQQEIPNAETMKQTESHAVKIVVEAAR  250
          |||
UPL8   201  TLLTMCASQGLRAGMVAGVIVNRTQQEIPNAETMRATESHAVKIVVEAAR  250

Up      251  RLLX  254
          |||
UPL8   251  RLLX  254

```

Figure 4.15 Amino acid alignment (aa residues #150 to end) of the native *E. coli* uridine phosphorylase (UP) and the mutant *E. coli* uridine phosphorylase (UPL8).

Mutated amino acids are highlighted.

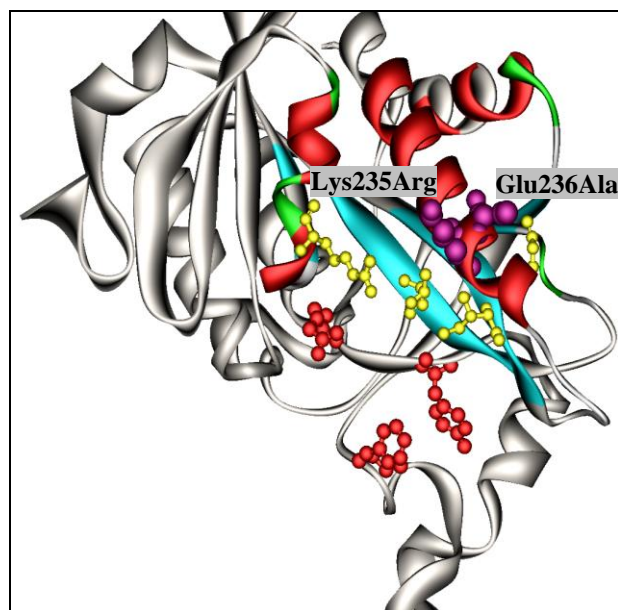


Figure 4.16 Ribbon representation of UPL8.

Amino acid chains within 15 Å of the mutation (purple, CPK) are coloured by secondary type (Ribbon) while the remainder of the protein is coloured grey. Catalytic amino acids are shown in red (Ball and stick) while amino acids within 7 Å (See Figure 4.17) of the mutation site are shown in yellow (Ball and stick).

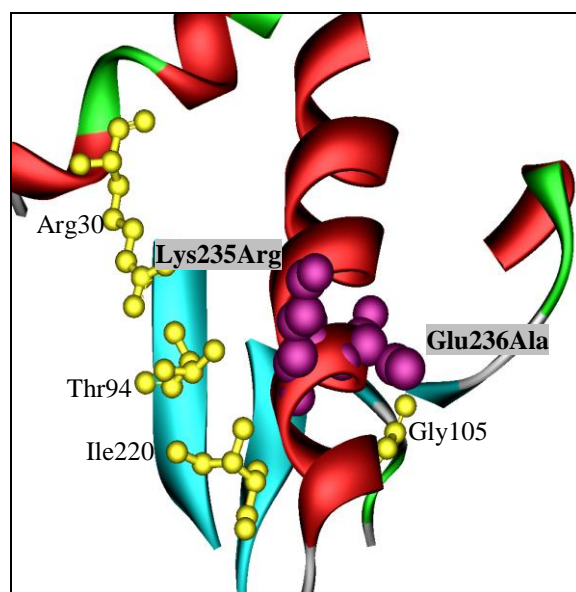


Figure 4.17 Ribbon representation of amino acids chains within 15Å of the mutation site.

Mutations are shown in bold (Purple CPK) and amino acids within 7 Å of the mutation are represented in yellow (Ball and stick).

4.3.7 Nucleoside phosphorylase Spherezyme optimisation

The combinatorial experimental design proved effective for preparing small scale emulsions for Spherezyme preparations. Active Spherezymes were produced in 52 of the 54 experiments. For UPL8 and EcUP (Figure 4.18 and Figure 4.19) a decrease in activity retention was noted with an increase in cross-linker concentration. The higher protein concentration showed higher retention of activity indicating better cross-linking efficiency. The best activity retention was obtained when using 4% 1:2 Glu:EDA (29 and 39% retention of activity for UPL8 and EcUP, respectively). For BHPNP1, 16% cross-linker generally gave better results (Figure 4.20) and Glu:5% PEI showed better cross-linking efficiency than Glu:EDA. The best result was obtained with 16% Glu:5%PEI at 70 mg.ml⁻¹.

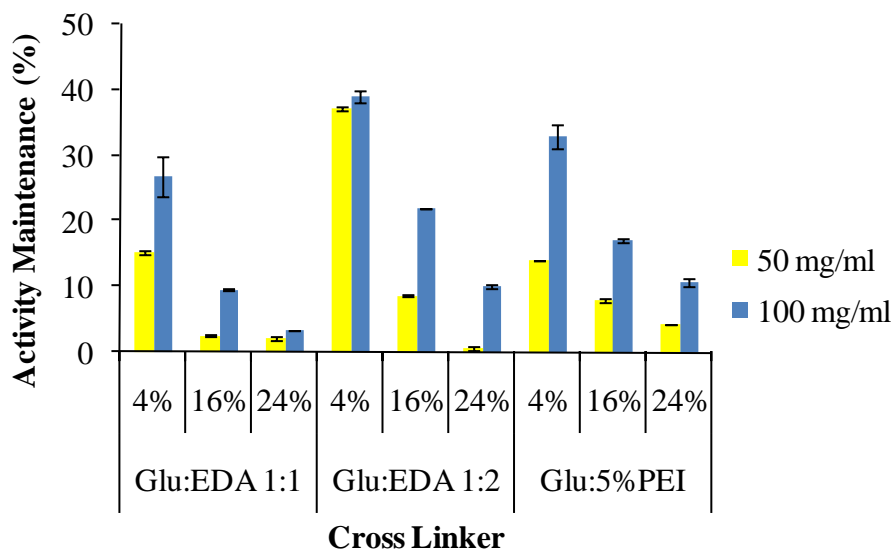


Figure 4.18 Activity maintenance for optimisation of EcUP Spherezyme formation.

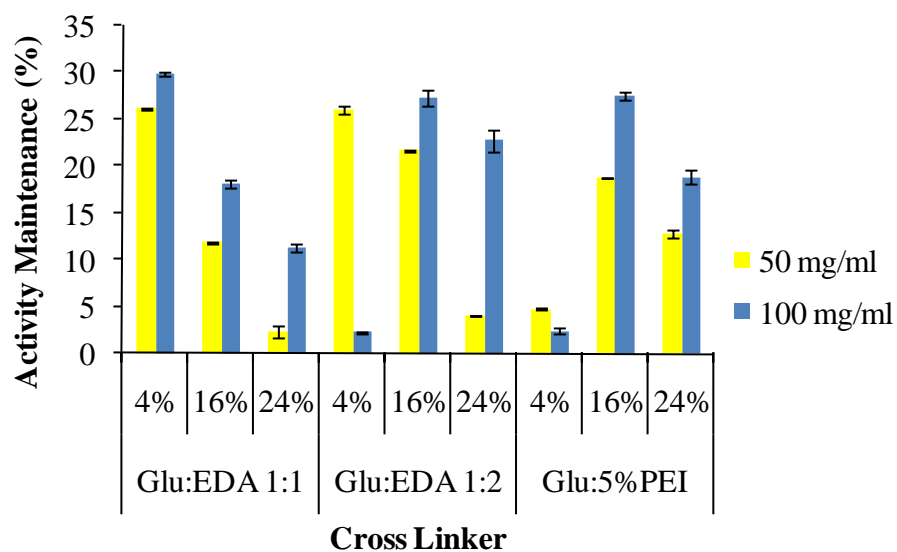


Figure 4.19 Activity maintenance results for optimisation of UPL8 Spherezyme formation.

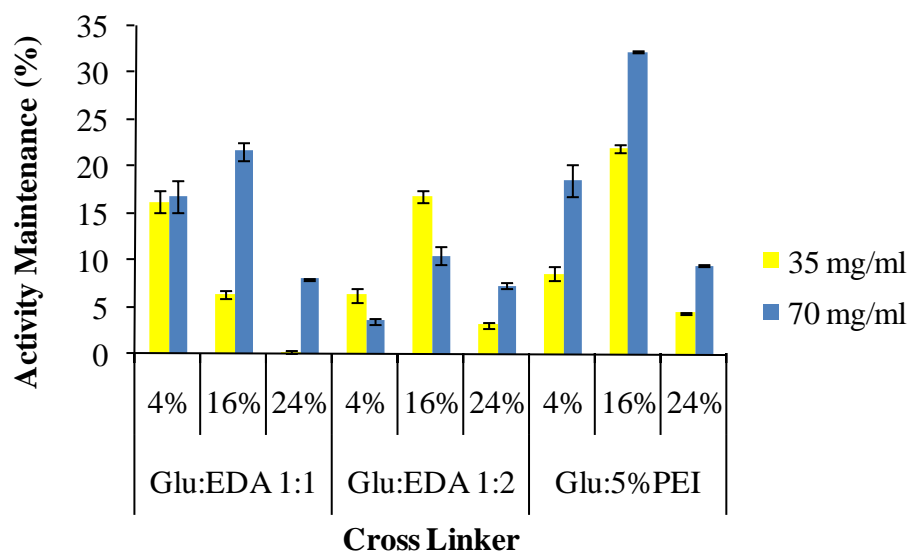


Figure 4.20 Activity maintenance results for optimisation of BHPNP1 Spherezyme formation.

4.3.8 Spherozyme formation

Initial preparations of UPL8 and EcUP Spherozymes at larger scale gave poor activity and mass retention results using the optimum cross linker identified above. Since Glu:5% PEI showed good results for both PNP and EcUP preparations, it was decided to use this cross linker instead for larger scale preparations. The retention of activity and yield of remained low at larger scale using this cross-linker, but sufficient (mass and activity) Spherozyme was produced for analysis. The Glu:5% PEI was also used for co-immobilisation studies. The activity and mass recovery data is given in Table 4.6 and Table 4.7.

4.3.9 Spherozymes characterisation

Spherozyme formation had no effect on pH optima for both the EcUP and UPL8 preparations (Figure 4.21 and Figure 4.22). For PNP preparations, the pH range appeared broader than that of the free enzyme (Figure 4.21). Spherozymes of native EcUP showed an increase of 20°C in optimum temperature, Spherozymes of UPL8 retained a temperature optimum of 60°C. The range of activity for all the UP Spherozymes appeared to have improved with all the spheres having activity at 70 and 80°C compared to the free enzymes which show no activity at 80°C. Temperature optima for the BHPNP1 sphere preparations appeared to have decreased by 10 to 20°C. However the spheres exhibited activity at 80°C, which was not seen with the free enzyme (Figure 4.23 and Figure 4.24)

Table 4.6 Mass and Activity recovery data for the formation of EcUP, UPL8 and BHPNP1 Spherezymes.

Sphere	Amount Immobilised		Mass Recovery		Activity Recovery					
	Units	mg	mg	%	PNP activity			UP Activity		
					U.ml ⁻¹	Total Units	% Recovery	U.ml ⁻¹	Total Units	% Recovery
EcUP-SZ	3375	184	57	30.88%	0.13	1.5		13.3	151.3	4.48%
UPL8-SZ	2506	203	30	14.55%	0.03	0.2		9.1	53.9	2.15%
BHPNP1-SZ	746	86	187	217.91%	10.12	189.6	25.41%	0.8	15.6	

Table 4.7 Mass and Activity recovery data for the formation of co-immobilised PNP/UP Spherezymes.

Sphere	Amount Immobilised			Mass Recovery		Activity Recovery						
	Units PNP	Units UP	mg	mg	%	PNP activity			UP Activity			UP:PNP ratio
						U.ml ⁻¹	Total Units	% Recovery	U.ml ⁻¹	Total Units	% Recovery	
EcUP/BHPNP1-SZ	373	938	94	77	82.13%	7.47	57.6	15.45%	16.9	130.2	13.88%	2.26
UPL8/BHPNP1-SZ	373	1044	128	165	129.57%	6.01	99.3	26.62%	25.8	426.5	40.86%	4.30

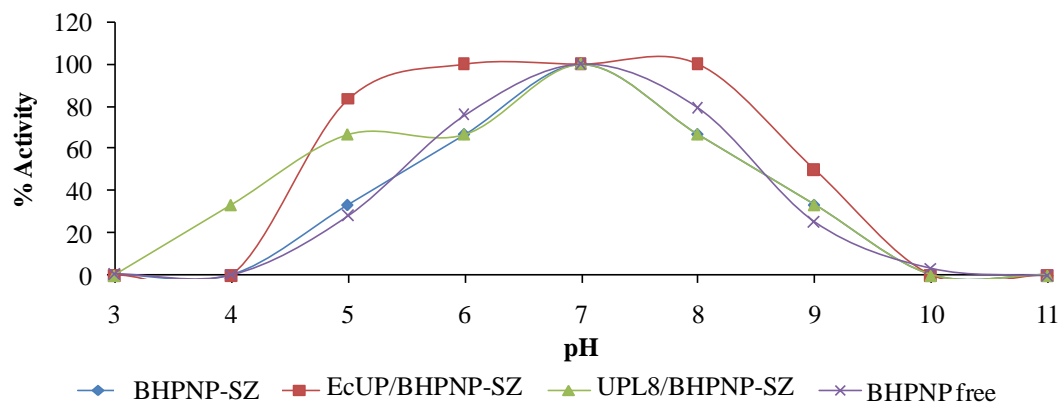


Figure 4.21 Optimum pH curves for based on PNP activity using guanosine as substrate.

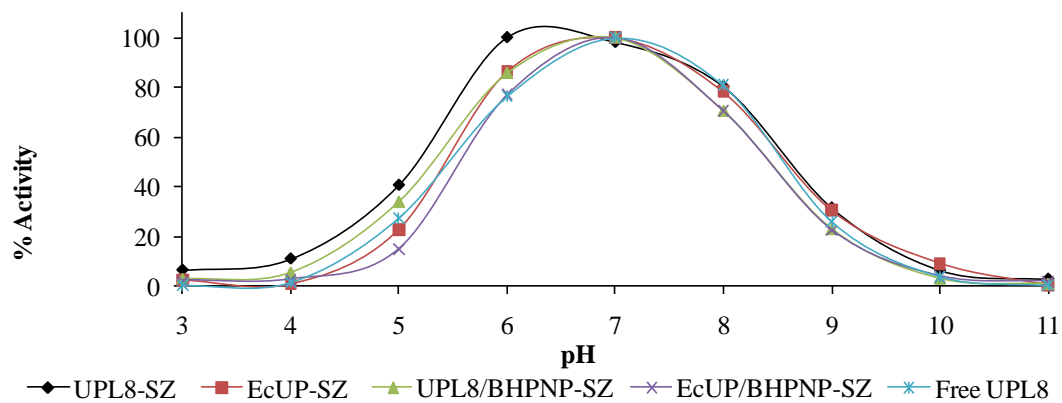


Figure 4.22 Optimum pH curves based on UP activity using uridine as substrate.

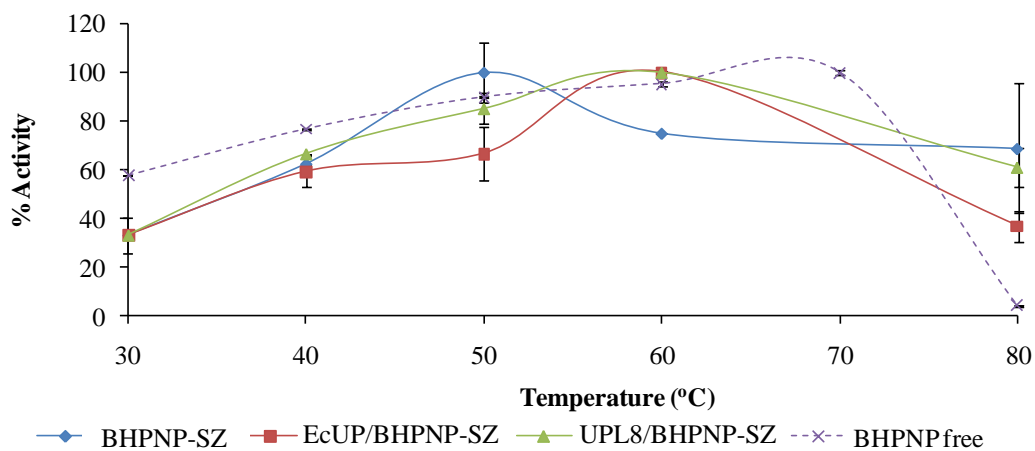


Figure 4.23 Temperature optimum curves for PNP Spherezyme preparations using guanosine as substrate.

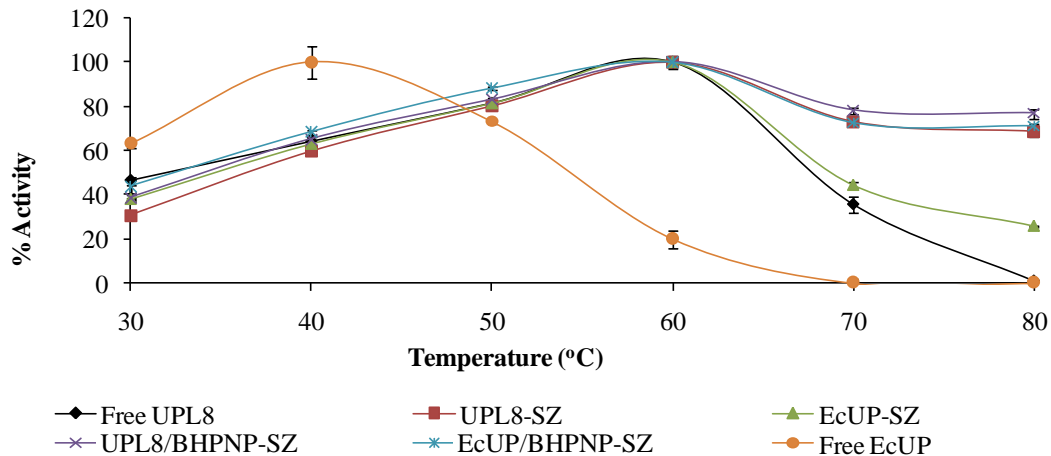


Figure 4.24 Temperature optimum curves for UP Spherezyme preparations using uridine as substrate

4.4 CONCLUSION

4.4.1 Directed evolution of *E. coli* uridine phosphorylase

Iterative saturation mutagenesis proved to be an effective method for rapid evolution of a multimeric enzyme. Under 20 000 clones were screened across 8 libraries of mutants to obtain an enzyme with a 20°C shift in optimum temperature and vastly improved stability at 60°C and 70°C compared to the wild type enzyme. The mutant enzyme retained its pH activity characteristics but showed a moderate drop in substrate specificity (Increased K_M). UPL8 was successfully produced by batch fermentation to high expression levels (52 kU.l⁻¹) and was subsequently purified using the methodology established for the wild type enzyme. There have been no reports of engineering for enhanced physical characteristics on any prokaryotic UPs. It is only therefore possible to compare this mutant UP to other wild type enzymes, as listed in Table 4.8. Very few PyNPs and particularly UPs from prokaryote sources have been fully characterised. Other than those listed, PyNP from *B. subtilis* (Gao *et al.*, 2006) and *T. thermophilus* (Shimizu and Kunishima, 2007) have been purified for crystallography studies, but no characterization was reported. The PyNP from *G. stearothermophilus* has the highest temperature optimum and thermal stability reported to date. *E. coli* UPL8 is then the next most stable UP. The substrate affinity of the mutant enzyme ($K_m = 0.46$ mM) is lower than both the native *E. coli* and the *G. stearothermophilus* enzymes, but is still within the micromolar range, making it significantly active towards uridine. The pH optimum for most reported PyNPs is around 7.0.

Sequence analysis of the UPL8 has shown that only two mutations occurred relating to a single round of mutation (UP5). This indicates that the screening methodology may not have been sensitive enough to isolate this clone in the first round of mutation. Subsequent rounds of mutation did not add any beneficial mutations. The methods for selection of positive clones would need to be improved for further research.

Table 4.8 Physical and kinetic characteristics of reported prokaryotic PyNPs

Organism	K_m (mM) Uridine	pH Optimum	Temperature Optimum	Reference
<i>E. coli</i>	0.15	7.5	37	Leer <i>et al.</i> 1997
<i>L. casei</i>	3.8	7.0	-	Avraham <i>et al.</i> , 1988
<i>E. carotovora</i>	-	-	60	Zaks and Dodds, 1997
<i>E. coli</i> UPL8	0.46	7.0	60	This study
<i>E. aerogenes</i>	0.7	8.52	65	Utagawa <i>et al.</i> 1985
<i>B. stearo- thermophilus</i>	0.19	7.2	70	Hori <i>et al.</i> 1989; Hamamoto <i>et al.</i> 1996

4.4.2 Immobilisation of nucleoside phosphorylases

EcUP, UPL8 and BHPNP1 were all successfully immobilised with varying degrees of activity retention. The UPs showed less cross-linking efficiency (indicated by mass recovery) as well as lower activity retention, which would indicate that the immobilisation affects the substrate binding capacity of the enzyme. Immobilisation however did have a stabilising effect on both EcUP and UPL8. EcUP-SZ and showed a new temperature optimum at 60°C and activity at 70 and 80°C which was not noted with the free enzyme. UPL8-SZ did not show an increase in the optimum temperature but did exhibit a broader activity range, maintaining significant activity at 70 and 80°C. Both preparations maintained the pH optimum profiles seen for the free enzymes. The BHPNP1 showed higher cross-linking efficiency as well as activity retention. No significant changes were noted in either the temperature or pH optimum, although the preparation did show greater activity at 80°C than that noted for the free enzyme. In addition to the single enzyme preparations, co-immobilised combinations were also developed. Co-immobilising UP with BHPNP1 seemed to increase the cross-linking efficiency and activity retention of the UPs, with UPL8 and

EcUP showing increases of 9% and 38% in activity retention, respectively, when immobilised with BHPNP1. The physical characteristics of the co-immobilised enzymes were similar to that of the single-immobilised preparations.

Hori and co-workers (1991) immobilised 0.42 units of crude enzyme from *G. stearothermophilus* on anion exchange resin for production of 5-MU and showed no loss on activity through immobilisation. The PNP and PyNP from *G. stearothermophilus* were immobilised on a glass solid support (Taran *et al.*, 2009) with only 30% loss in initial activity. Similar activity loss was noted for the immobilisation of *E. coli* PNP and PyNP on Sepabeads (Zuffi *et al.*, 2004). In contrast, between 80 and 90 % of the activity was lost on Spherezyme formation. This figure may be improved upon further optimisation of the immobilisation process. The advantage of immobilisation by Spherezymes, however, is the high specific activity compared to other preparations. In the study by Zuffi and co-workers, specific activities (per mg of immobilised biocatalyst) were 0.18 and 0.04 U.mg⁻¹ for UP and PyNP, respectively. In comparison, co-immobilised BHPNP1 and UPL8 showed specific activities (per mg Spherezyme) of 2.6 and 0.6 U.mg⁻¹, respectively, which is approximately 15 fold higher.

We have shown here that it is possible to increase the thermal stability of *E. coli* UP by directed evolution in a relatively short period time, without the need for extensive screening. We have shown too that immobilisation of EcUP also increases thermal stability. The biocatalysts prepared in this study (free enzyme and immobilised preparations) will now be tested for their ability to improve the productivity in the biocatalytic production of 5-MU.

CHAPTER 5: APPLICATION

USE OF ENHANCED NUCLEOSIDE PHOSPHORYLASE BIOCATALYSTS FOR THE PRODUCTION OF 5- METHYLURIDINE BY ONE-POT TRANSGLYCOSYLATION

5.1 INTRODUCTION

The previous best transglycosylation reaction for the preparation of 5-MU using thymine and guanosine in the presence of PNP and UP was described by Ishii *et al.* (1989). Reasonable yields of 5-MU (74%) were achieved at relatively high guanosine and thymine concentrations of 300 mM each. The reactions were carried out at 60°C using whole cells of *Erwinia carotovora*. The chief disadvantage of this process was the long reaction time which resulted in a low reactor productivity of 1.19 g.l⁻¹.h⁻¹; an order of magnitude below an economically desirable level (Straathof *et al.* 2002). This may have been due to the limited transfer of substrates and products through the cell wall. Enzyme preparations generally have higher specific activities than whole cells and do not have the limitations associated with membrane transport (Woodley, 2006b), potentially leading to higher mass transfer rates and therefore higher reaction productivities.

In parallel to the work presented here, research was conducted in our labs to define a process operating window for the economically viable production of 5-MU from guanosine and thymine by transglycosylation using EcUP and BHPNP1 as described in Chapters 2 and 3. This optimisation was first carried out on a small scale (2 ml) and then scaled up to one litre. Due to the low solubility of the reaction components the biocatalytic reaction medium is a slurry system, which is likely to be operating under limited solid-liquid mass transfer conditions. This makes solid-liquid mixing

an important factor in reaction success, and hence key variables such as solids loading and reactor configuration were assessed. The most important process variable considered during the investigation was improvement of reaction volumetric productivity ($\text{g.l}^{-1}.\text{h}^{-1}$) to match requirements for an average economically viable process of around $15.5 \text{ g.l}^{-1}.\text{h}^{-1}$ (Straathof *et al.* 2002), while maintaining or improving upon previous reaction yields of 79% (Chapter 3).

The study defined a process operating window for the biocatalytic production of 5-MU from guanosine and thymine (Figure 5.1). Parameters investigated include pH, temperature, solids loading and reactor configuration. The optimal operating conditions were found to be a loading of 378 mM (9% m.m^{-1}) guanosine and 439 mM (4.7% m.m^{-1}) thymine at 60°C at an enzyme loading of 2000 U.l^{-1} operating in a low shear environment. Under these conditions a guanosine conversion of $> 95\%$ and a 5-MU yield of 85% were achieved. An overall productivity of $10 \text{ g.l}^{-1}.\text{h}^{-1}$ was obtained with a final product concentration of 84 g.l^{-1} . The increased temperature of 60°C proved possible despite the optimal native UP stability being 40°C , which may be partly attributable to using higher enzyme loading, allowing the rate of thermal deactivation to be offset. This is the first demonstration of an economically viable isolated enzyme transglycosylation for the synthesis of 5-MU from guanosine and thymine and has subsequently been patented (Visser *et al.*, 2009).

While the parallel study showed the efficacy of the native enzymes, it also showed the limitations of biocatalysts, particularly EcUP. While an adequate process has been developed, a large amount of enzyme is required to perform the reaction adequately due to the poor stability at 60°C . In this chapter the aim was to show that application of the stabilized catalysts (modified by mutation, immobilisation or both) can vastly improve the transglycosylation efficiency.

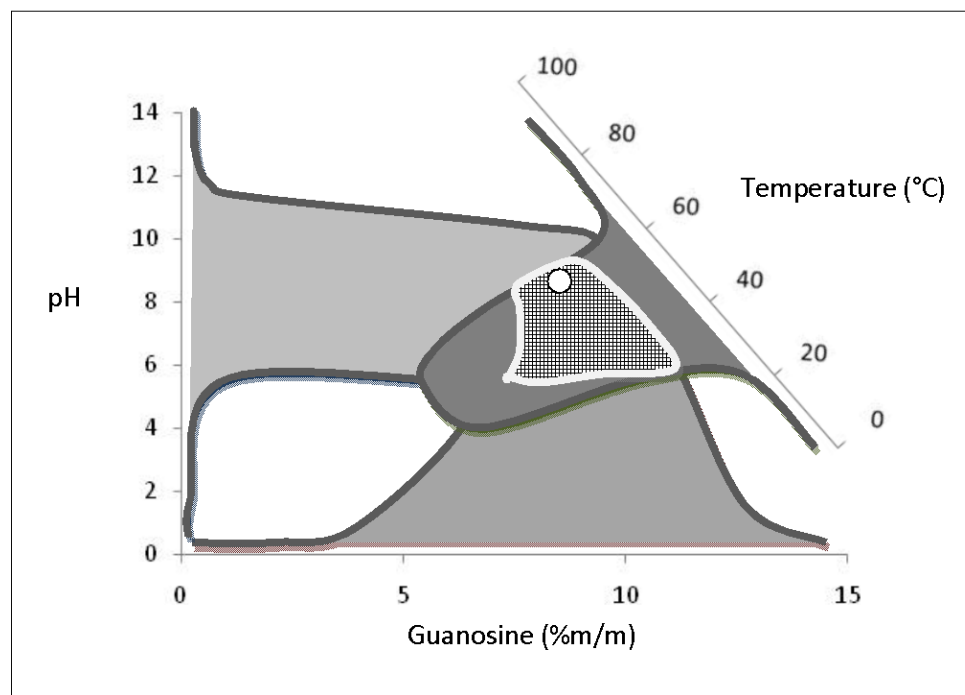


Figure 5.1 Operating window for the synthesis of 5-methyluridine by transglycosylation of guanosine and thymine (reproduced from (Gordon *et al.*, 2010). Operating window (chequered area) shows the range in which the reaction is possible based on biocatalyst and reaction characteristics. Clear area in operating window depicts the current optimal conditions (60°C, 9% m.m⁻¹ substrate loading, pH 8).

5.2 METHODS AND MATERIALS

5.2.1 Materials

Thymine, guanosine, 5-methyl uridine and guanine standards were purchased from Sigma. The enzymes purine nucleoside phosphorylase (PNP) from *Bacillus halodurans*, uridine phosphorylase (UP) from *Escherichia coli*, and mutant *E. coli* UP (UPL8) were expressed in *E. coli* as *E. coli* JM109[pMSPNP], *E. coli* BL21(DE3)[pETUP] and *E. coli* BL21(DE3)[pETUPL8], respectively. The enzymes were produced by fermentation and prepared as previously described (Chapters 3 and 4). Spherezyme preparations (BHPNP1-SZ, EcUP-SZ, UPL8-SZ, BHPNP1/EcUP-SZ, BHPNP1/UPL8-SZ) were prepared as described in Chapter 4.

5.2.2 Proof of concept transglycosylation experiments

A series of transglycosylation experiments were performed to compare various combinations of biocatalysts. Reactions (100 ml) contained 1.5% m.m⁻¹ loading of guanosine and thymine in 50 mM sodium phosphate buffer (pH 8.0) with 200 U.l⁻¹ of each of the biocatalysts. Reactions were performed at 60°C and 70°C in round bottomed flasks immersed in an oil bath controlled at the set temperatures. Flasks were fitted with condensers to negate the effects of evaporation. Mixing was achieved with magnetic stirrers at 500 rpm. The following biocatalyst combinations were tested:

Free enzyme combinations:	EcUP and BHPNP1 (control reaction) UPL8 and BHPNP1
Single-immobilised enzymes:	EcUP-SZ and BHPNP1-SZ UPL8-SZ and BHPNP1-SZ
Co-immobilised enzymes:	BHPNP1/EcUP-SZ BHPNP1/UPL8-SZ

5.2.3 Comparative transglycosylation

To show the advantage of using the modified biocatalysts, an experiment was performed at the optimum substrate load determined during the reaction optimisation study. The reaction (100 ml) contained 9.0 % m.m⁻¹ guanosine and 4.7 % m.m⁻¹ thymine suspended in 50 mM sodium phosphate buffer pH 8.0 in a round bottomed flask fitted with a condenser. In previous studies (Gordon *et al.*, 2010) 2000 U.l⁻¹ biocatalyst loading was used at this substrate loading. Here only 1000 U.l⁻¹ biocatalyst loading was used as the increased thermal stability of the mutant meant that the UP would not deteriorate over the time course of the reaction as noted for the wild type UP. Temperature was maintained at 65°C throughout the biotransformation study. Combinations of free as well as immobilised UPL8 and BHPNP1 were tested.

5.2.4 Sampling and analysis

Transglycosylation reactions were run for a period of 8 h. Samples (100 μ l) were removed (in triplicate) hourly. The sample was diluted in 900 μ l 10 M NaOH to stop the reaction and fully dissolve the nucleosides. This solution was then further diluted in 1 M NaOH for analysis so as to ensure that the sample concentration was within the linear region of the calibration curve. Guanosine, guanine, thymine and 5-MU were quantitatively analysed by HPLC, using a Waters Alliance Model 2609 instrument with a Synergi 4 μ m Max-RP 150 x 4.6 mm column and compared to pure standards (Sigma). Components were detected using a UV detector at 260 nm. The eluent was ammonium acetate, 25 mM, pH 4.0, at a flow rate of 1 ml.min⁻¹ and a run time of 20 - 30 minutes at 25°C.

5.3 RESULTS

In Chapter 2 it was shown that a unique combination of uridine phosphorylase from *E. coli* combined with the purine nucleoside phosphorylase from *B. halodurans* could lead to 5-MU yields of above 75% mol.mol⁻¹ using 1.5% m.m⁻¹ guanosine and thymine as starting substrate. This reaction was successfully scaled up to a 650 ml reaction using the same substrate concentrations. Here we compare those initial reactions with reaction performed with the modified biocatalysts produced during this study (Chapter 4).

5.3.1 5-MU production by transglycosylation using free enzyme preparations

The control reaction (using BHPNP1 and EcUP at 60°C) showed similar results to those previously obtained indicating that the reaction conditions were similar to those used previously. As expected, minimal guanosine was converted and no 5-MU was produced at 70°C (Figure 5.2). Use of the mutant uridine phosphorylase (UPL8, Figure 5.3) however showed a marked improvement in reaction productivity

($5.0 \text{ g.l}^{-1}.\text{h}^{-1}$ compared to $1.29 \text{ g.l}^{-1}.\text{h}^{-1}$ for the control) while maintaining the same yield (73% yield compared to 75% for the control, see Table 5.1). The result at 70°C , however, was unexpected. Physical characterisation of both the BHPNP1 (Chapter 3) and UPL8 (Chapter 4) enzymes showed that they exhibited activity and stability at 70°C . It was therefore expected that there would be a measure of 5-MU production. While 44% of the guanosine was converted (mostly within the first hour of the reaction) no 5-MU was produced. Increased localised shear (due to mixing in a high slurry environment compared to the low shear conditions used for enzyme characterisation) at high temperature may have led to the enzyme denaturation.

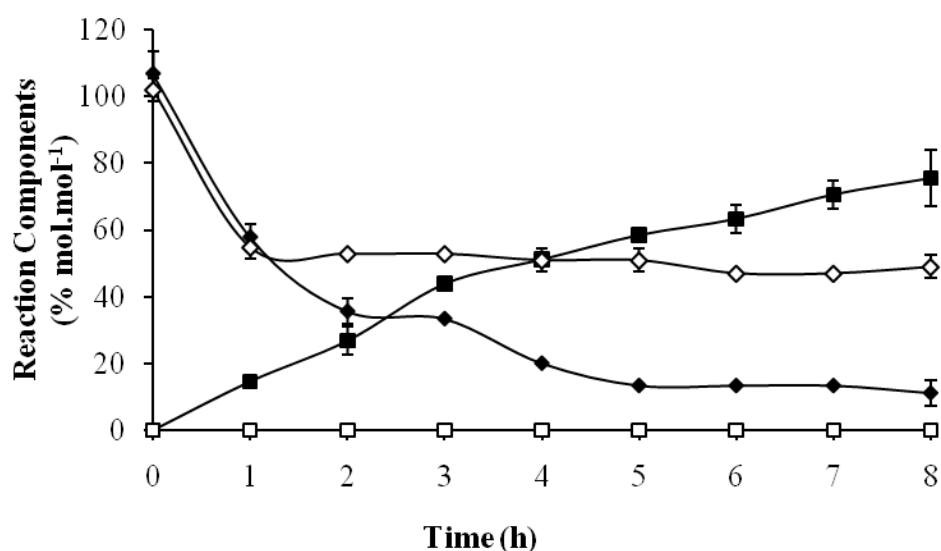


Figure 5.2 Transglycosylation experiment showing the phosphorolysis of guanosine (\blacklozenge) and formation of 5-MU (\blacksquare) using BHPNP1 and native EcUP as biocatalysts at 60°C (closed symbols) and 70°C (open symbols).

Error bars generated from analysis of time point samples in triplicate.

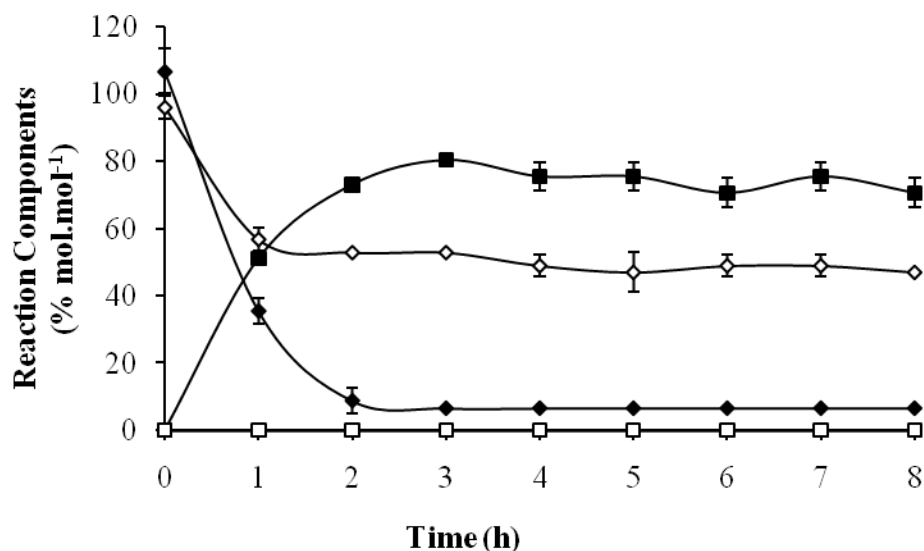


Figure 5.3 Transglycosylation experiment showing the phosphorolysis of guanosine (\blacklozenge) and formation of 5-MU (\blacksquare) using BHPNP1 and UPL8 as biocatalysts at 60°C (closed symbols) and 70°C (open symbols).

Error bars generated from analysis of time point samples in triplicate.

5.3.2 5-MU production by transglycosylation using Spherezyme preparations

5.3.2.1 Single immobilised enzymes

The use of immobilised enzymes for this reaction could potentially have two advantages; namely an increase in stability of mesophilic enzymes allowing a higher reaction temperature, and recycling of the biocatalyst to decrease the catalyst cost. The results obtained for the use of single immobilised enzymes (Figure 5.4 and Figure 5.5) show that the immobilised enzymes conferred increased stability to the native *E. coli* UP, indicated by the production of 5-MU at 70°C. This increased stability however did not lead to a significant increase in reaction productivity at 60°C (1.50 g.l⁻¹.h⁻¹ compared to 1.29 g.l⁻¹.h⁻¹ for the free enzyme control). Similar results were obtained when using the immobilised mutant enzyme (UPL8-SZ, Figure 5.5) where production of 5-MU was noted at both 60°C and 70°C, but at reaction productivities

lower than those seen for the free enzyme control reaction. Higher 5-MU yield was noted when using UPL8-SZ (69%) compared to using EcUP-SZ (29 %) at 70°C.

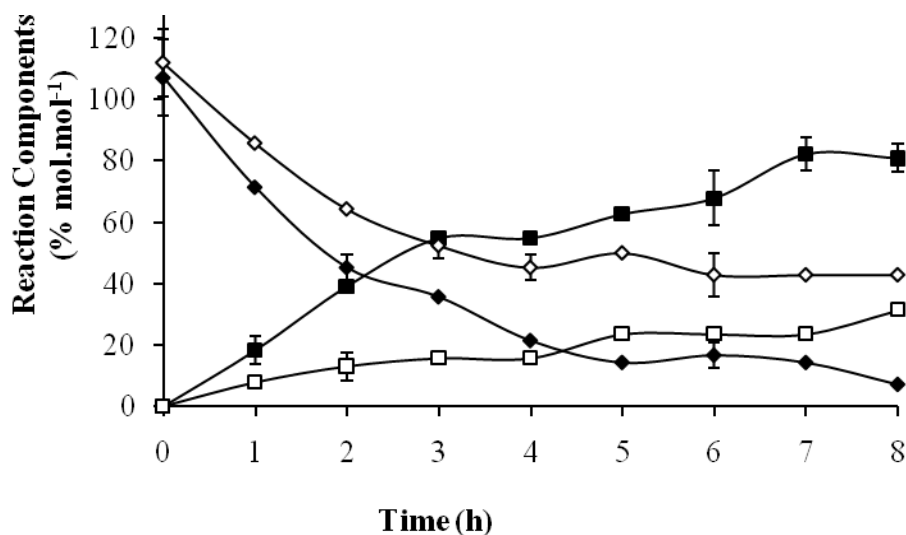


Figure 5.4 Transglycosylation experiment showing the phosphorolysis of guanosine (◆) and formation of 5-MU (■) using a combination of particles of BHPNP1-SZ and EcUP-SZ as biocatalysts at 60°C (closed symbols) and 70°C (open symbols).

Error bars generated from analysis of time point samples in triplicate.

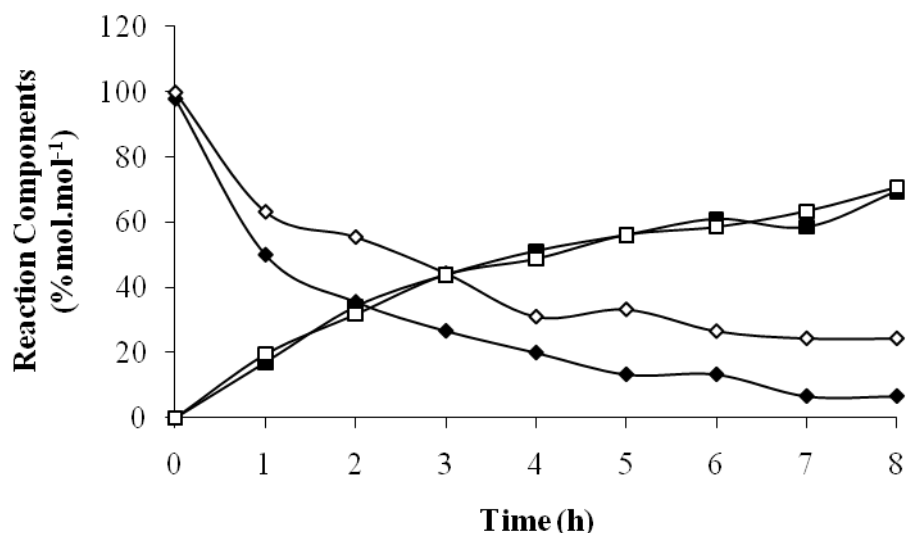


Figure 5.5 Transglycosylation experiment showing the phosphorolysis of guanosine (◆) and formation of 5-MU (■) using a combination of particles of BHPNP1-SZ and UPL8-SZ as biocatalysts at 60°C (closed symbols) and 70°C (open symbols).

Error bars generated from analysis of time point samples in triplicate.

5.3.2.2 Co-immobilised Spherezymes

Co-immobilising enzymes could be advantageous in that the proximity of the two enzymes could enhance the mass transfer characteristics of the system, thereby increasing the reaction rate while maintaining the other potential advantages discussed above. However, low yields were seen for EcUP co-immobilised with BHPNP1 (Figure 5.6) at reactor productivities similar to the free enzyme and lower than the single immobilised enzyme system at 60°C. The results at 70°C did show higher yields and productivities than the single immobilised enzyme which would indicate a higher degree of stability in the co-immobilised system. The results however were still lower than the free enzyme at 60°C.

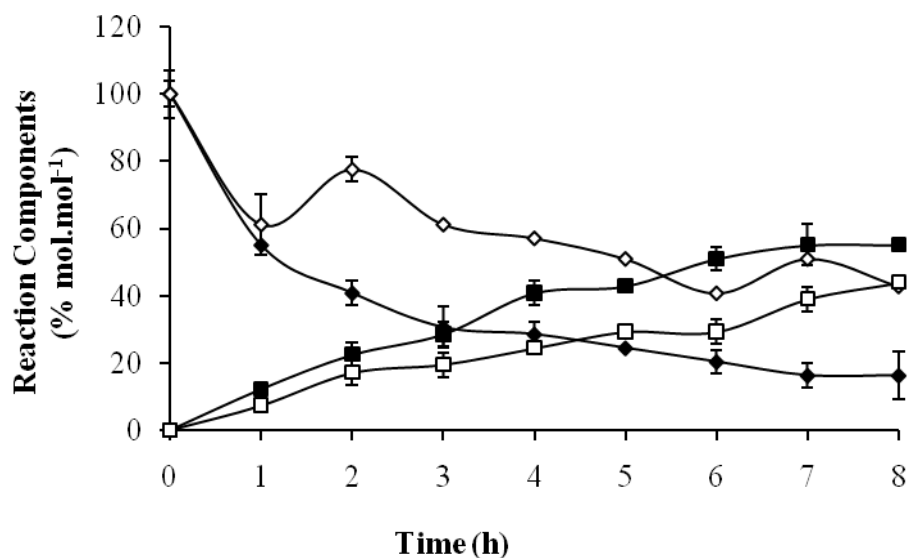


Figure 5.6 Transglycosylation experiment showing the phosphorolysis of guanosine (◆) and formation of 5-MU (■) using BHPNP1/EcUP-SZ as biocatalyst at 60°C (closed symbols) and 70°C (open symbols).

Error bars generated from analysis of time point samples in triplicate.

The UPL8 enzyme co-immobilised with BHPNP1 (Figure 5.7) gave good yields at both 60°C (70.2%) and 70°C (51.2%). This indicates that this system had a high degree of stability. The reaction productivities however (1.38 and 0.88 g.l⁻¹.h⁻¹ at 60°C and 70°C, respectively) were still not significantly different or higher than the free enzyme control reaction.

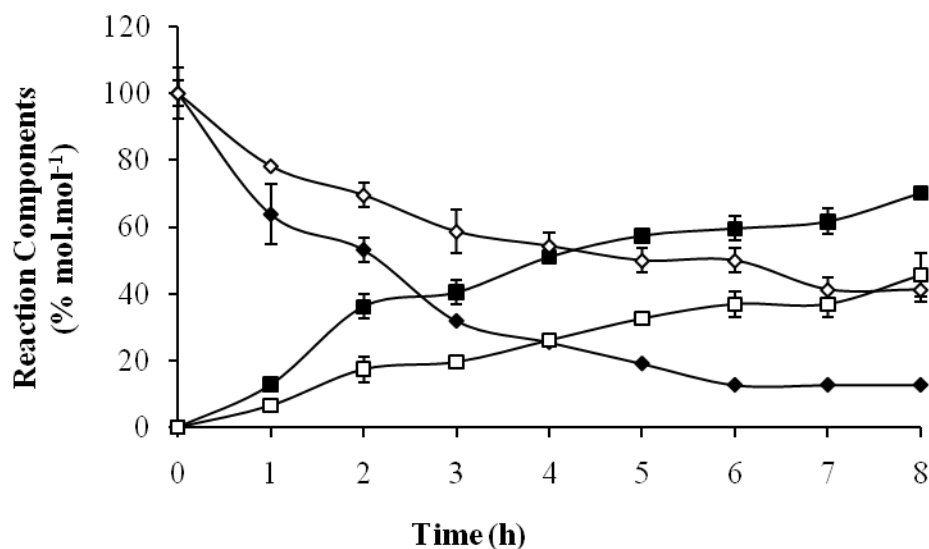


Figure 5.7 Transglycosylation experiment showing the phosphorolysis of guanosine (\blacklozenge) and formation of 5-MU (\blacksquare) using BHPNP1/UPL8-SZ as biocatalyst at 60°C (closed symbols) and 70°C (open symbols).

Error bars generated from analysis of time point samples in triplicate.

5.3.3 5-MU production by transglycosylation using 9% m.m^{-1} guanosine and 4.6% m.m^{-1} thymine as starting substrate concentrations

The previous section showed that free UPL8 with BHPNP1 and co-immobilised UPL8 with BHPNP1 gave the highest productivities for free and immobilised biocatalyst systems respectively (Figure 5.8).

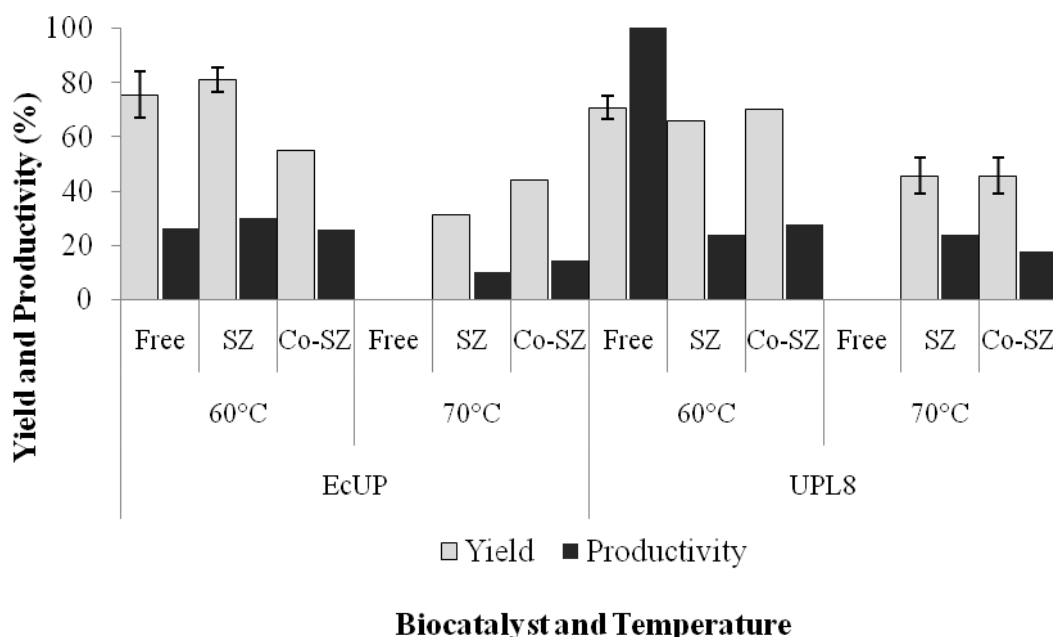


Figure 5.8 Analysis of 5-MU yield and productivity for 1.5% m.m^{-1} substrate loading reactions.

Yield is expressed as % mol.mol^{-1} . Productivity is expressed as a percentage of the highest achieved value. Different biocatalyst configurations: Free – free enzyme; SZ – Single immobilised enzyme; Co-SZ – co-immobilised enzymes. See text for further reaction details.

These systems were therefore tested under the optimum reaction conditions determined for this process, namely using 9% m.m^{-1} guanosine, 4.6% m.m^{-1} thymine as starting substrate concentration with increased enzyme loading. In this experiment however, the temperature was increased slightly to 65°C as previous results had shown that all the biocatalysts would be stable at this temperature. In addition, the enzyme load was decreased to 1000 U.l^{-1} as it was felt that the high enzyme load used in the optimised reaction was not necessary due to the increased stability of the mutant enzyme.

The results in Figure 5.9 and Table 5.1 (Reactions 13 and 14) show that use of UPL8 as free enzyme biocatalysts leads to similar 5-MU yields (76.8%) at much higher reactor productivities. The reaction was essentially complete within 2 h leading to a

productivity of $31.5 \text{ g.l}^{-1}.\text{h}^{-1}$, which is a 3-fold improvement on the optimised reaction using the native EcUP ($10 \text{ g.l}^{-1}.\text{h}^{-1}$). This result confirms the reaction at $1.5\% \text{ m.m}^{-1}$ (Figure 5.3) in that a 6 fold higher productivity (5.0 to $31.5 \text{ g.l}^{-1}.\text{h}^{-1}$) was seen when the substrate loading was increased proportionately (1.5 to $9.0\% \text{ m.m}^{-1}$). The co-immobilised enzyme system also showed a good yield of 5-MU (75.1%) but at a lower productivity ($7.7 \text{ g.l}^{-1}.\text{h}^{-1}$) as was seen at lower substrate loading.

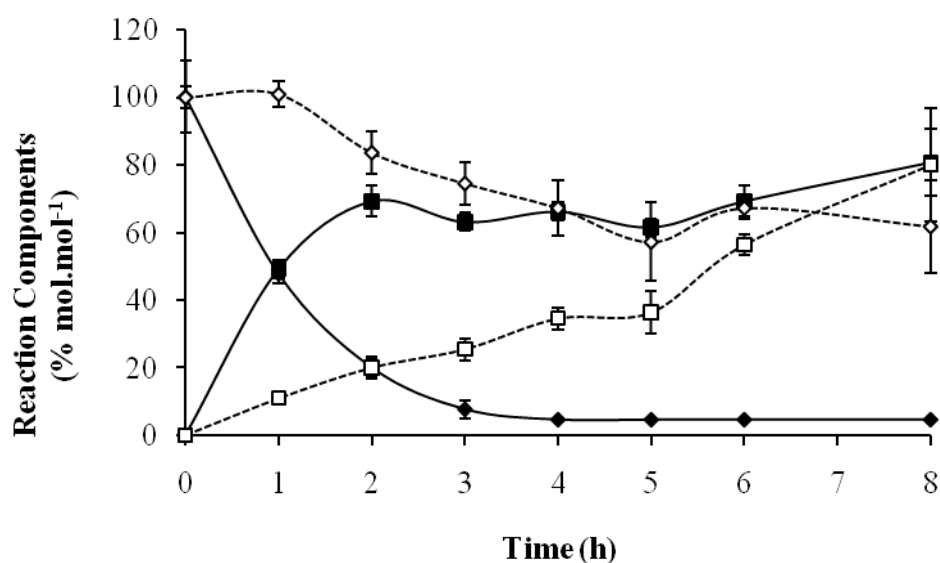


Figure 5.9 Transglycosylation experiment showing the phosphorolysis of guanosine (◆) and formation of 5-MU (■) using free BHPNP1 and UPL8 (closed symbols) or BHPNP1-SZ and UPL8-SZ (open symbols) as biocatalysts at 65°C .

Table 5.1 Summary of results for guanosine conversion, 5-MU yield and reaction productivity for transglycosylation reactions using a variety of biocatalyst combinations

Rxn [†]	Biocatalysts*		Temp °C	Reaction time h	GuO Conversion % mol/mol	5-MU Yield % mol/mol	5-MU Productivity g.l ⁻¹ .h ⁻¹
	PNP	UP					
1	BHPNP1	EcUP	60	8	88.9	75.6	1.29
2	BHPNP1	EcUP	70	8	44.4	0.0	0.00
3	BHPNP1	UPL8	60	2	91.1	73.1	5.00
4	BHPNP1	UPL8	70	8	44.4	0.0	0.00
5	BHPNP1- SZ	EcUP-SZ	60	7	86.7	76.8	1.50
6	BHPNP1- SZ	EcUP-SZ	70	8	57.8	29.2	0.50
7	BHPNP1- SZ	UPL8-SZ	60	8	93.3	69.5	1.19
8	BHPNP1- SZ	UPL8-SZ	70	8	75.6	69.5	1.19
9	BHPNP1/EcUP-SZ		60	7	82.2	65.8	1.29
10	BHPNP1/EcUP-SZ		70	8	53.3	41.4	0.71
11	BHPNP1/UPL8-SZ		60	8	86.7	70.2	1.38
12	BHPNP1/UPL8-SZ		70	8	57.8	51.2	0.88
13	BHPNP1	UPL8	65	2	79.8	76.8	31.50
14	BHPNP1- SZ	UPL8-SZ	65	8	47.1	75.1	7.70

[†]Reactions 1 – 12 contained 1.5% m.m⁻¹ (53 mM) GuO and 1.5% m.m⁻¹ (119 mM) Thy. Reactions 13 and 14 contained 9.0% m.m⁻¹ (318 mM) GuO and 4.6% m.m⁻¹ (365 mM) Thy.

*Biocatalyst loading for Reactions 1 – 12 was 200 U.l⁻¹ of each. For reactions 13 and 14, 1000 U.l⁻¹ was used.

5.4 CONCLUSIONS

Small scale experiments showed that the mutant enzyme UPL8 is a superior catalyst for the production of 5-MU. As expected, the increase in stability of the mutant enzyme lead to a significant (3-fold) increase in reactor productivities while maintaining the high yields (75- 80 %) in the free enzyme system. The increase in productivity was achieved within the constraints of the reaction operating window (Figure 5.1), implying that no further reaction optimisation would be necessary to implement the mutant enzyme. This productivity achieved was nearly 30 fold higher than the process described by Ishii *et al.* (1989). The biotransformation demonstrated here also compares well to other commercial biotransformations (summarised in Straathof *et al.* 2002). Within the 64 biotransformations for the production of fine chemicals analysed in that study, the average productivity was 15.5 g.l⁻¹.h⁻¹, the average product yield was 78 % and the average final product concentration was 108 g.l⁻¹. The transglycosylation reaction in this study has an above average productivity (31.5 g.l⁻¹.h⁻¹) and an acceptable yield (77%). The final product concentration (74 g.l⁻¹) is lower than the commercial average, but is equivalent to the average for commercial nucleotide production (65 g.l⁻¹). Figure 5.2 gives a comparison of the best stabilised enzyme preparations (mutated, immobilised and co-immobilised) with respect to 5-MU yield.

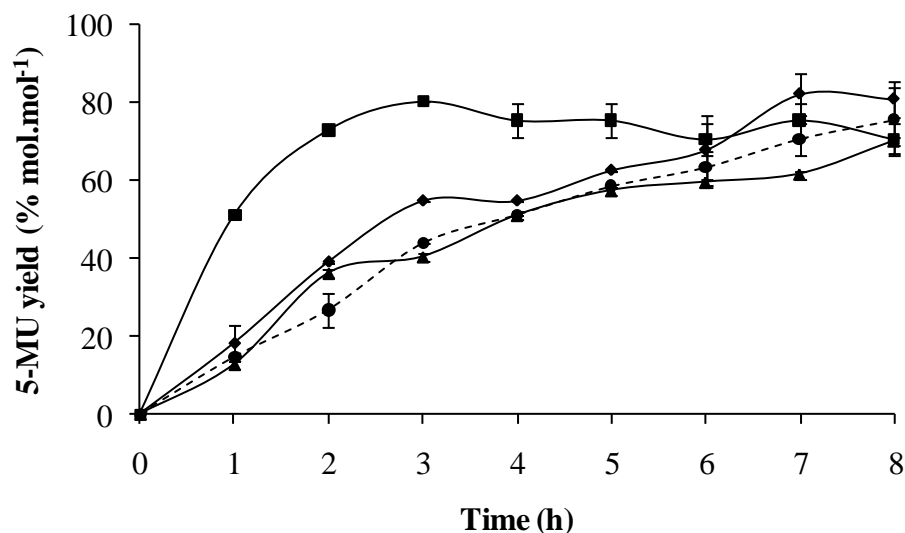


Figure 5.10 Selected transglycosylation experiment showing the 5-MU yield obtained when using free EcUP (●) or free UPL8 (■) in combination with BHPNP1. Also shown are the combinations of separately immobilised EcUP and BHPNP (◆) and co-immobilised UPL8 and BHPNP (▲).

All reactions were performed using 1.5 % m.m⁻¹ substrate loading at 60°C. Data was averaged from triplicate samples.

Immobilisation of the enzyme did lead to the expected increase in stability for both EcUP and UPL8, but this did not lead to increased reactor productivity. This could only be explained by the immobilisation having a detrimental effect on mass transfer in the slurry system. This was further confirmed with the use of co-immobilised enzymes, where higher yields were noted at 70°C, but no improvements on reaction productivity were observed for the reactions run at 60°C or 70°C. The only advantage therefore of using the immobilised enzyme would be through the re-use of the biocatalyst.

Table 5.2 gives a comparison of 5-MU production costs. These costs were calculated using a techno-economic model developed for large scale production of 5-MU. The model is based on a production plant producing 100 tonnes per annum. It takes into account the cost of production of the biocatalyst, bulk substrate costs and operational

costs. The operational and plant costs vary according to the reactor productivity and yields based on the presumption that higher productivities would require smaller reactor vessels and shorter reaction times to achieve the same outputs. Using the performance values for the optimised reaction (BHPNP1 and EcUP) as a baseline, cost savings per annum were calculated for the modified biocatalyst systems. The values in Table 5.2 show that the free enzyme system using UPL8 would lead to significant cost saving (\$ 530, 000 per annum), which was the goal of this technology.

The immobilised biocatalysts showed an increase in the cost of 5-MU production. The increase in cost is due to the lower productivity but also due to the increase in biocatalysts cost. Factors such as activity retention (see Chapter 4), the relative increases in fermentation costs due to need to produce more enzyme before immobilisation, and the cost of immobilised enzyme manufacture were taken into account. In addition, a cost reduction was factored in assuming that the immobilised catalyst could be recycled 10 times. Only the co-immobilised UPL8 and BHPNP1 showed a drop in 5-MU production costs. This is largely due to the high degree of activity retention noted when preparing these catalysts. This cost saving, however is largely dependent on the ability to recycle the catalysts, which is technically challenging due to the presence of solids in the slurry reaction, and has as yet not been demonstrated.

Table 5.2 Cost comparisons of 5-MU production by transglycosylation using different biocatalyst combinations. Cost model is based on raw material and operational cost for a plant producing 100 tonnes per annum

Reaction	Biocatalysts		5-MU Yield % mol.mol ⁻¹	5-MU Productivity g.l ⁻¹ .h ⁻¹	Required	Required	5-MU Cost \$.kg ⁻¹	Cost Saving per year \$M	Saving on 5MU Cost %
	PNP	PyNP			Fermenter Size m ³	Bioreactor Size m ³			
Current	BHPNP	EcUP	85%	10	0.32	3.0	35.9	0.000	0.0
Free Enzyme System with UPL8	BHPNP	UPL8	80%	31.5	0.19	1.0	30.6	0.530	14.8
Immobilised Enzymes (Native UP)	BHPNP-SZ	EcUP-SZ	77%	11.6	0.72	3.0	83.5	-4.760	-132.6
Immobilised Enzymes (UPL8)	BHPNP-SZ	UPL8-SZ	75%	7.7	0.72	4.0	104.66	-6.876	-191.5
Co- immobilised enzymes	BHPNP/EcUP-SZ		66%	10	0.58	3.0	55.51	-1.961	-54.6
Co- immobilised enzymes	BHPNP/UPL8-SZ		80%	10.65	0.12	3.0	27.58	0.832	23.2

CHAPTER 6: GENERAL CONCLUSIONS

There is a need to develop novel and cost effective methods for producing antiretroviral drugs, particularly those utilised in the treatment of HIV/AIDS. Stavudine and AZT were identified as potential targets because they could both be produced through a common intermediate, namely 5-methyluridine. It has been established that the production of 5-methyluridine by biocatalysis is possible through a reaction known as transglycosylation. A number of transglycosylation processes have been described for the production of 5-MU, but none of them represent a truly commercially viable process.

The most likely biocatalytic route is through transfer of ribose-1-phosphate from guanosine to thymine utilising a combination of purine (PNP) and pyrimidine nucleoside phosphorylase (PyNP). The reaction would need to be performed at high substrate concentration where the substrates (guanosine and thymine) would be largely insoluble. To increase the solubility of the substrates, it would be necessary to heat the reaction to above 60°C. The ideal biocatalysts would therefore need to be able to operate at 60°C, be highly specific and active towards guanosine, ribose-1-phosphate and thymine, and be tolerant of high substrate loading. From a process point of view, the production of these catalysts would need to be cost-efficient and the biocatalysts should potentially be immobilised to facilitate catalyst recycle.

This study was initiated to isolate and develop biocatalysts (a combination of purine and pyrimidine nucleoside phosphorylases) suitable for the large scale production of 5-MU. The research hypothesis was that it was possible to obtain novel, highly efficient nucleoside phosphorylases for the production of 5-methyl uridine, through a combination of environmental screening and directed evolution.

6.1 SCREENING FOR SUITABLE BIOCATALYSTS

A set of commercially available nucleosides phosphorylases was tested and shown not have the substrate specificities required for 5-MU production by transglycosylation. A selection of organisms, identified in literature, through bioinformatic studies or through previous screening exercises, was then tested. Enzymes were produced either in recombinant *E. coli* strains or in the wild type organisms, isolated and then screened in a combinatorial experiment for their ability to produce 5-MU. Combinations of each of the purine and pyrimidine nucleoside phosphorylases were tested. This screen showed that the PNP1 from *E. coli* and PNP from *B. halodurans* in combination with UP from *E. coli* gave the highest yield of 5-MU. A quantitative analysis of these biocatalyst combinations showed that the combination of *B. halodurans* PNP (BHPNP1) and *E. coli* UP gave the highest 5-MU yield (80%). This result represents the first combination of free enzymes from different organisms, giving high yields of 5-MU under high substrate conditions.

6.2 PRODUCTION, ISOLATION, PURIFICATION AND CHARACTERISATION OF NUCLEOSIDE PHOSPHORYLASE

The genes encoding BHPNP1 (*BH1531*) and EcUP (*deoD*) were isolated and cloned into *E. coli* production hosts. These strains showed excellent expression characteristics. Production of *B. halodurans* purine nucleoside phosphorylase and *E. coli* uridine phosphorylase was demonstrated in high density batch fermentations using the production strains *E. coli* JM109 [pMSPNP] and *E. coli* BL21 [pETUP]. Fermentations were performed up to 20 l scale in less than 8 h total fermentation time. Expression of the phosphorylases was achieved by addition of 0.5 mM IPTG at during the mid-log phase of growth (3.5 – 4 h). Maximum enzyme activity was achieved 3 - 4 h after induction. Enzyme yields of 26.9 and 37.7 kU.l⁻¹ for BHPNP1 and EcUP respectively. These levels are above previously published results for PNP production (5 – 17 kU.l⁻¹, Table 3.1, Chapter 3) but fall below the maximum reported UP production levels (300 kU.l⁻¹) (Lee *et al.*, 2001), which indicates that higher production levels could be achieved through further fermentation optimisation.

Both catalysts were purified and successfully characterised. The established pH optimum was pH 7.0 for both enzymes. Temperature optima and stability data for BHPNP1 (70°C and $t_{1/2}$ at 60°C of 20.8 h) indicated that the biocatalytic step was operating within the capabilities of this enzyme and would operate well at elevated temperature (up to 60°C). Conversely, the temperature optimum and stability data for EcUP (optimum of 40°C and $t_{1/2}$ at 60°C of 9.9 h) indicated that while the enzyme remained active at 40°C for the duration of a 25 h biotransformation, it would only be operating at 20% of its optimal activity at 60°C and would lose activity rapidly. Kinetic characterisation of both enzymes was performed. Results for EcUP correlated well with those quoted in literature for this enzyme (Leer *et al.*, 1977).

The novel PNP from *B. halodurans* was functionally similar to that of *G. stearothermophilus* characterised by Hori and co-workers (Hori *et al.*, 1989a) in terms of temperature optimum, substrate specificity and affinity, pH optimum and predicted pI. The *G. stearothermophilus* PNP showed higher stability at 70°C (>30 h).

Bioinformatic analysis of BHPNP1 showed that it is most similar to the *G. stearothermophilus* PNP II (79 % similarity) and bovine PNP (47 % identical). This classifies BHPNP1 as a Type II (low-MM) PNP. Amino acids known to be involved in the activity of the bovine and human enzymes were generally conserved. Hence it is likely that the active site, and overall tertiary structure, of BHPNP1 will resemble the bovine and human PNPs and is therefore likely to be a homotrimer. Homology modelling of BHPNP1 was based on the bovine structure 1LVU (Bzowska *et al.* 2004) and showed good fit. Analysis, however, showed that the predominant active form of the enzyme is a dimer rather than a trimer as noted for *G. stearothermophilus* (Hori *et al.*, 1989a). Tertiary structure of BHPNP1 will need to be confirmed by gel filtration and crystallography.

The biocatalysts were then used in a bench scale (650 ml) transglycosylation for the production of 5-MU. A 5-MU yield of 79.1% was obtained at this scale with a reactor productivity of 1.37 g.l⁻¹.h⁻¹. While this showed a good yield and represents the

highest reported productivity for a free enzyme system, the productivity still falls short of industrially acceptable levels.

Other research in our group showed that this productivity could be increased to 10 g.l⁻¹.h⁻¹ using increased substrate and enzyme loading, as well as reactor design optimisation at larger scale.

6.3 DIRECTED EVOLUTION

EcUP was selected as a target for directed evolution, specifically for improving thermostability. Iterative saturation mutagenesis was used to rapidly mutate EcUP. A moderately high throughput colorimetric method was developed for screening the mutants based on the release of *p*-nitrophenol upon phosphorolysis of a pyrimidine nucleoside analogue. By screening less than 20 000 clones across 8 libraries of mutants, the mutant UPL8 was isolated. The mutant enzyme showed a temperature optimum of 60°C, which is 20°C higher than for the wild type enzyme. An improved stability at 60°C ($t_{1/2} = 17.3$ h) and 70°C ($t_{1/2} = 3.3$ h) was observed, compared to that of the wild type enzyme (9.9 h and 0 h respectively). The mutant enzyme retained its pH activity characteristics and showed a moderate drop in substrate specificity. UPL8 was successfully produced by batch fermentation to high expression levels (52 kU.l⁻¹) and was subsequently partially purified using the methodology established for the wild type enzyme.

The increase in stability of UPL8 is due to only two mutations (Lys235Arg, Gln236Ala). These mutations may have caused an increase in stability due to interaction with other structural units in the protein, stabilization of the entrance to the binding pocket, or by decreasing the flexibility of the α -helix at the N-terminus.

6.4 IMMOBILISATION OF NUCLEOSIDE PHOSPHORYLASES

EcUP, UPL8 and BHPNP1 were all successfully immobilised. The UPs showed less cross-linking efficiency and lower activity retention. EcUP-SZ exhibited a new temperature optimum at 60°C and activity at both 70 and 80°C, which was not noted with the free enzyme. UPL8-SZ displayed a broader activity range, maintaining activity at 70 and 80°C. Both preparations had similar pH optimum profiles as those seen in the free enzymes. The BHPNP1 showed higher cross-linking efficiency. No significant changes were noted in the temperature or pH optima, but the preparation did show greater activity at 80°C than that noted for the free enzyme. Co-immobilised combinations were also implemented. Co-immobilising UP with BHPNP1 increased the cross-linking efficiency of the UPs, with UPL8 and EcUP showing increases of 9% and 38% in activity retention, respectively. The physical characteristics of the co-immobilised enzymes were similar to that of the single-immobilised preparations.

6.5 APPLICATION OF EVOLVED AND IMMOBILISED NUCLEOSIDE PHOSPHORYLASES TO THE PRODUCTION OF 5-MU BY TRANSGLYCOSYLATION

Transglycosylation experiments showed that the mutant enzyme UPL8 was a superior catalyst for the production of 5-MU. A 300% increase in reactor productivity was noted when free enzyme preparations of UPL8 were combined with BHPNP1 at 1.5% m.m⁻¹ substrate loading. Furthermore, only half the enzyme loading was required to achieve the same result at 9% m.m⁻¹ loading, which are the optimal conditions determined for this reaction. The high yield of 5-MU (75-80% mol.mol⁻¹) was maintained in all the experiments.

Immobilisation of the enzyme did not lead to increased reactor productivity. This could only be explained by the fact that immobilisation may have a detrimental effect on mass transfer in the slurry system. Higher yields were noted for the immobilised enzymes at 70°C than those for the free enzyme preparations, but at low productivities.

A cost analysis was performed to determine the beneficial affect of increased productivity. The costs were calculated using a techno-economic model developed for large scale production of 5-MU, which was based on a production plant producing 100 tonnes per annum (approximately 50% of the global thymidine market) and took into account the cost of production of the biocatalyst, bulk substrate costs and operational costs. The free enzyme system using UPL8 would lead to significant cost saving (\$ 0.5 million per annum) or alternatively would decrease the price of 5-MU production, which was the goal of this research.

6.6 GENERAL CONCLUSION

The hypothesis of this study was that novel and highly efficient biocatalysts for the production of 5-methyluridine could be identified through a combination of natural screen and directed evolution. Through screening natural sources, a novel purine nucleoside phosphorylase was isolated. Combination of this enzyme with a known pyrimidine nucleoside phosphorylase gave a biocatalyst combination that produced 5-methyluridine at a high yield but low productivity. Engineering the pyrimidine nucleoside phosphorylase to suit the ideal biocatalytic conditions, through directed evolution, yielded an enzyme suitable for a large scale biocatalytic production of 5-methyluridine.

Commercial scale biocatalytic production of 5-MU would lead to cheaper ARV production, since 5-MU is a critical common intermediate. This in turn, from a cost point of view, would make drugs like Stavudine and AZT more accessible to people in lower income groups, who make up the majority of the HIV/AIDS infections in

sub-Saharan Africa. Increasing the percentage of people receiving ARV treatment will go a long way to eradicating the disease.

The impact of this study however could be expanded to the production of other natural and non-natural nucleosides which have anti-retroviral activity. The combination and subsequent screening of nucleosides phosphorylases from different sources can be applied to a variety of transglycosylation reactions. Subsequent biocatalyst engineering should then lead to commercially viable reactions, as seen in this research.

6.7 FUTURE WORK

The research depicted here shows promise for a commercially viable process for the production of 5-MU by transglycosylation. To realise this goal, further optimisation would need to be performed at larger scale. Specifically, the parameters tested in the biocatalytic reaction were the maximum parameters found to be suitable for the native UP. It may be possible that UPL8 is capable of high reaction rates with higher substrate loading ($> 9\% \text{ m.m}^{-1}$). In addition, the more stable UPL8 may be able to handle higher agitation rates which would improve mass transfer and hence productivity characteristics of the reaction. These parameters would need to be tested.

Fermentation studies for both enzymes were successful. Higher volumetric activity, however, has been reported for the recombinant production of *E. coli* UP. Further fermentation optimisation would be beneficial in decreasing the cost of the biocatalyst.

The directed evolution studies produced a UP with elevated temperature optimum and increased thermal stability. This result was shown to be the result of only two mutations in one of the target regions. Further mutation and structural analysis may create a more stable biocatalyst. This could also be applied to increasing the stability of BHPNP1. Nucleoside phosphorylases are also used in the production of other nucleosides and nucleoside derivatives. Further mutation work directed at the binding pocket of both PNP and UP may yield mutants that are highly active towards non-

natural nucleoside bases and sugar moieties. The knowledge gained through this research could then be rapidly applied to the development of other biocatalytic reactions.

Finally, while the cost of the free enzyme (UPL8 or BHPNP1) does not contribute significantly to the overall cost of the process, it would still be preferable to have a recyclable biocatalyst. Further immobilisation studies, either as Spherezymes or other alternatives, are envisaged.

Appendix 1

Screening for Novel Thermostable Uridine, Purine, and Thymidine Phosphorylases

A1.1 Introduction

In this study a collection of bacteria isolated from deep terrestrial environments was screened for the presence of PNP, UP or TP. The environment in which these organisms exist consists of high temperatures (>40°C), and either acidic or alkaline conditions. Both whole cell and cellular extracts were screened against a number of substrates to determine the presence of both purine and pyrimidine nucleoside phosphorylases. In addition, transglycosylation reactions were tested in these organisms for the ability to produce thymidine (from deoxyinosine and thymine) and 5-methyl uridine (from guanosine and thymine).

A1.2 Methods and Materials

All materials were analytical grade purchased from either Sigma Chemicals or Merck, unless otherwise indicated in the text.

A1.2.1 Growth and preparation of organisms

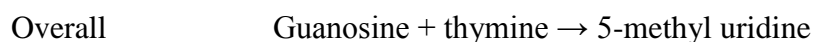
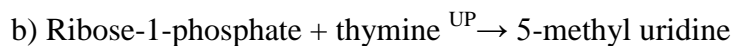
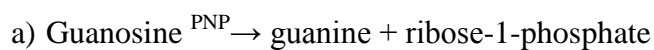
The organisms were a loan from Prof Derek Litthauer at the University of the Free State (UFS). A library of 42 unidentified strains was screened. For the initial whole cell studies, cultures were grown according to pre-defined cultivation methods supplied by UFS. When sufficient biomass for each culture was achieved, the organisms were harvested by centrifugation (3000 rpm, 20 min, Sorval RT 7) and then resuspended in 20% glycerol solution to make up a 50% (m/m) cell suspension. These cultures were aliquoted in to 96 well test plates and frozen before screening. Organisms selected for nucleoside

phosphorylase activity were later cultivated in TYG media (5 g/L Tryptone, 2 g/L yeast extract, 1 g/L glucose) at 37°C.

A1.2.2 Primary Screening

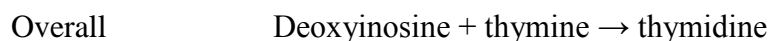
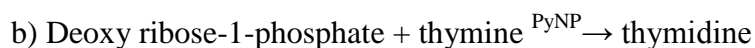
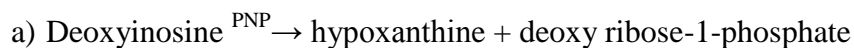
For primary screening, test cultures in 96 well test plates were centrifuged (Sorvall RT7, 3000 rpm, 10 min), the supernatant was discarded and the cultures were resuspended in 100 µl phosphate buffer (pH 7.4) containing substrates to test for the following enzymes and/or reactions:

A PNP and UP



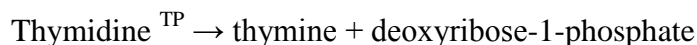
The appearance of 5-methyl uridine indicates the presence of both PNP and UP

B PNP and UP



Production of thymidine indicates the presence of PNP and/or TP

C TP



Production of thymine indicates the presence of TP.

The above assays were initiated by the addition of 10 mM each of guanosine and thymine for reaction (A), deoxyinosine and thymine for reaction (B) and 10 mM thymidine for reaction (C). Substrates were added to the bacterial cultures which had been preheated to 60°C, to make a final reaction volume of 100 µl. Reactions were run with shaking at 1500 rpm in a

Labsystems Thermomix (Finland) at 60°C for 20 hours. The solutions were then centrifuged at 3600 rpm for 15 min in Sorvall RT7 to separate the cells from the aqueous layer.

Chemical controls for the substrates were treated in the same manner. The stock nucleosides were added to phosphate buffer to give a final volume of 100 µl. These samples were also incubated at 60°C for 20 hours to observe degradation of the substrates.

Reaction products were qualitatively observed by direct application of 5 µl of the aqueous layer to Silica UV_{254nm} TLC plates. Products of reaction (A) were separated using an 85:15 chloroform to methanol mixture while products of reactions (B) and (C) were separated using a 5:1 chloroform to methanol mixture. All substrates and products were viewed under UV_{266nm}.

A1.2.3 Organism Identification by 16S RNA analysis

Organisms showing the most significant nucleoside phosphorylase activities were grown on TYG agar plates and submitted for 16S RNA analysis (Inqaba Biotech, Pretoria, South Africa).

A1.3 Results

A1.3.1 Primary Screening

Primary screening results show that four of the strains contained both PNP and UP capable of producing 5-methyluridine from guanosine and thymine (Figure A1.1). Fourteen of the strains were able to break thymidine down to thymine indicating the presence of a thermostable thymidine phosphorylase (Figure A1.2, not all results shown). A further two strains showed the ability to produce thymidine from deoxyinosine and thymine indicating the presence of a thermostable PNP (Figure A1.3).

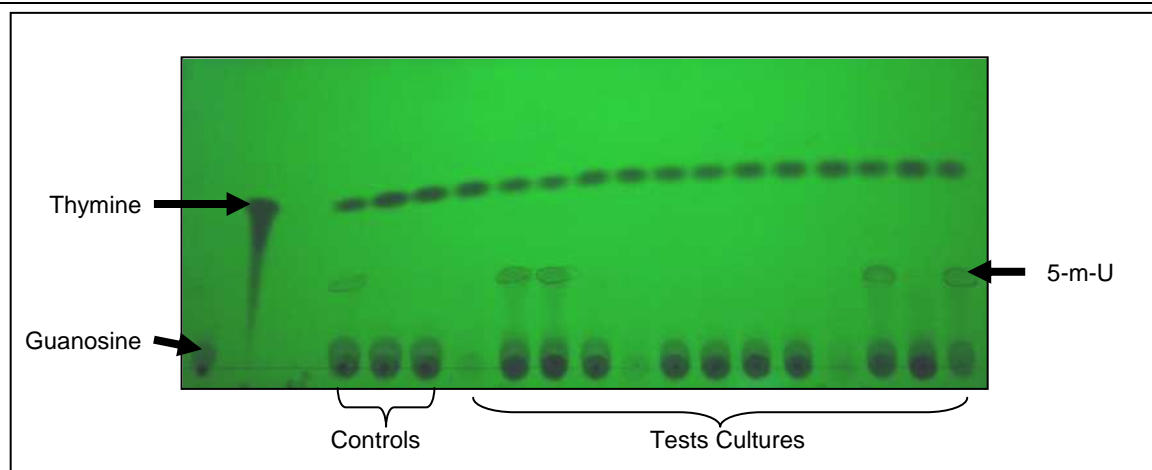


Figure A1.1 Image of TLC plate under UV_{266nm} from reaction (A) (Production of 5-methyl uridine (5-m-U)).

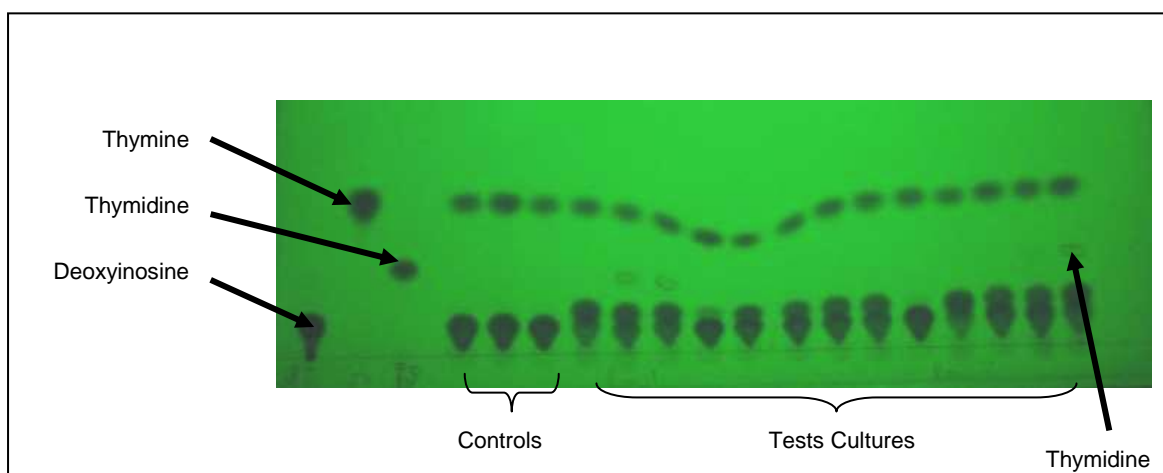


Figure A1.2 Image of TLC plate under UV_{266nm} from reaction (B) (Production of thymidine)

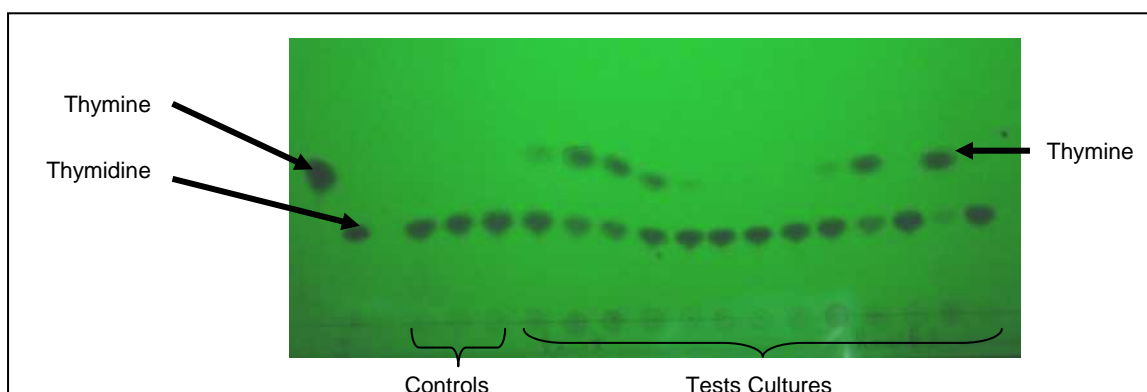


Figure A1.3 Image of TLC plate under UV_{266nm} from reaction (C) (Production of thymine)

The following strains were selected for their respective nucleoside phosphorylase activity:

UV 2 - UP, TP, PNP

UV 5 - UP, TP, PNP

UV 23 - UP, PNP

UV 24 - UP, PNP

UV 25 - TP

UV 18 - TP

Four of these strains (UV 02, UV 05, UV 18 and UV 23) were cultured for 48 h at 37°C or 45°C in Luria broth and then harvested by centrifugation. The resultant pellet was resuspended to 50% cell suspensions in a 20% glycerol solution for storage. Crude extracts were prepared from a portion of the solutions by adding 1:1 (v/v) lysis buffer (2 mg/ml lysozyme, 2 mM DTT, 2 mM MgCl₂, 1% CHAPS, 0.01% PEI) and incubating for 2 h at 30°C. Cultures were then further disrupted by sonication. Cellular debris was separated by centrifugation at 13000 rpm for 5 min. The supernatant (cytosolic fraction), was separated and the pellet (membrane fraction) was resuspended in 50 mM sodium phosphate buffer (pH 7.4). The fractions (whole cell, cytosolic, membrane) were tested for activity against uridine and guanosine to show the presence of UP and PNP, respectively.

Under these conditions, UP activity was not noted for UV02 or UV05 but was noted for UV18 and UV23. PNP activity was noted for all cultures.

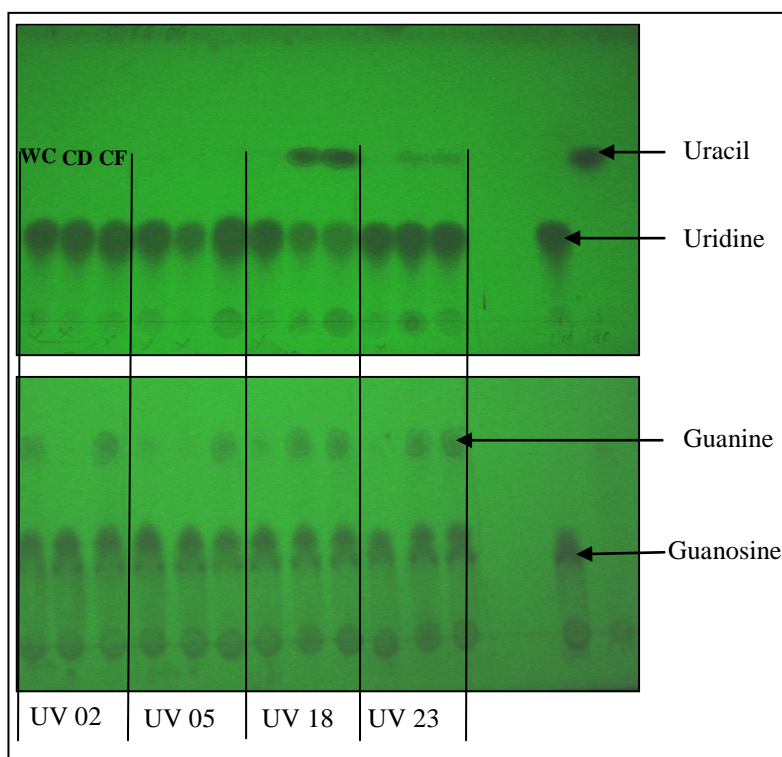


Figure A1.4 TLC image showing PNP (guanosine) and UP (uridine) activity after cell disruption by sonication.

WC = whole cell, CD = cellular debris and CF – Cytosolic fraction. The same pattern is repeated for each sample.

A1.3.2 16S RNA analysis

UV02 - Bacillus cereus (100% identity)

The genomic sequence for this organism is available (Ivanova *et al.*, 2003) and indicates that the organisms contains 2 PNPs and a PyNP. This would confirm results obtained during primary screening where a PyNP was noted.

UV23 - Bacillus licheniformis (99% identity)

Here too the genomic sequence is available (Rey *et al.*, 2004) and also indicates 2 PNPs and a PyNP.

UV05 and UV18 - Klebsiella pneumoniae (99% identity)

This is a class II pathogen whose genomic sequence has been completed but is not yet published. The available data does suggest that the organism contains a PNP, a distinct UP and a PyNP. This does correlate with data obtained throughout this screening process.

A1.4 Conclusions

The organisms that were screened in here do show some promise as sources of alternative nucleoside phosphorylases. They are however not significantly different to mesophilic organisms (*E. coli*) or moderately thermophilic organisms (*B. halodurans*) already investigated, particularly with regard PNP activity towards guanosine. The UP activity noted for UV18 and UV23 however do show promise as an alternative to the *E. coli* or *B. halodurans* UPs and will thus be used for further testing.

Appendix 2

Isolation of PNP and PyNP from wild type organisms

A2.1 Introduction

A study was performed to identify the most effective methods for the isolation of both PNPs and PyNPs identified from the wild type organisms. A number of disruption methods were tested including Yeast Buster (Novagen), Y-Per (Pierce), Bug Buster (Novagen), lysozyme (USB), Lytozyme (Sigma-Aldrich) and release of the cytosolic fraction through free-thaw cycles, sonication or grinding with liquid nitrogen.

A2.2 Methods and Materials

Freeze-thaw cycles were performed on the samples by 2 cycles of slow freeze and thaw at -20°C and room temperature, respectively. For liquid nitrogen grinding, 1 ml of a 40% (m/v) cell solution was subjected to 3 x 2 min cycles of freezing and grinding in a mortar and pestle (cryo-impacting). Sonication was performed in a Sonics Vibra Cell, power setting 3, for 10 min (10 ml sample, 20% cell solution). After each treatment, the cellular debris was separated by centrifugation (13000 rpm, 10 min). The supernatant was transferred to a fresh tube and the pellet was resuspended in an equal volume of 50 mM Tris-HCl buffer, pH8.0.

For chemical and enzyme treatments, cell mass from 200 µl of a 40% solution was harvested by centrifugation (13000 rpm, 10 min) and resuspended in 200 µl Y-PER, Yeast Buster, Bug Buster with 2 mg/ml lysozyme, or 10 U/ml Lytozyme. Solutions were incubated for 1 h at 30°C with shaking at 600 rpm (Boeco TS-100 Thermo Shaker) then centrifuged (13000 rpm, 10 min). Supernatants were transferred to a fresh tube and pellets were resuspended in 200 µl of 50 mM Tris-HCl buffer pH 8.0.

PNP and PyNP activities were determined by the standard assays (Section 2.2.11.4). Protein concentrations were determined using the Biorad microtitre plate assay in the Biotek Instruments Powerwave HT.

A1.3 Comparison of Extraction Methods

Results for sonication and lysozyme alone are not presented here as it was noted in the primary screening experiments that these methods were not effective for releasing nucleoside phosphorylases. Here we present alternative cell disruption methods investigated to obtain effective release of the enzymes.

Figures A2.1 and A2.2 show the release of PNP from all 4 cultures. From these graphs it was noted that a combination of Bug Buster and lysozyme was effective for extraction of the PNP, giving up to 75% release of active protein when compared to the cellular debris. Cryo-impacting also showed above 40% release of the PNP in all the cultures. Conversely, UP extraction from UV18 and UV23 (Figure A2.3) was most effective with Y-Per treatment and very ineffective with the Bug Buster and Lysozyme combination. This may be due to the larger size of the perforation in the cell wall due to the Y-Per when compared to the Bug Buster. The PyNPs are generally larger protein complexes and therefore may only be released through larger perforations. However, if this were the case, then the PNP would have been effectively released with Y-per. It is therefore possible that the components of the Y-Per affect PNP activity, or conversely that the components of Bug Buster adversely effect PyNP activity. Again, cryo-impacting gave more than 50% release of the PyNP.

The specific activity results were then normalised to compare the amount of active protein that would be available in a 10 ml sample (taking total protein released in to account). These results (Figure A2.4) indicate that although cryo-impacting consistently gave more than 50% release of active protein compared to that which remained with the cellular debris, the total available active protein was a lot lower than other treatments. A large amount of PNP and PyNP is therefore denatured during cryo-impacting. Y-per treatment is the most effective method of protein extraction and may in fact enhance the activity for PyNP. A combination of Bug Buster and lysozyme is the most effective method of extraction for PNP.

APPENDIX 2

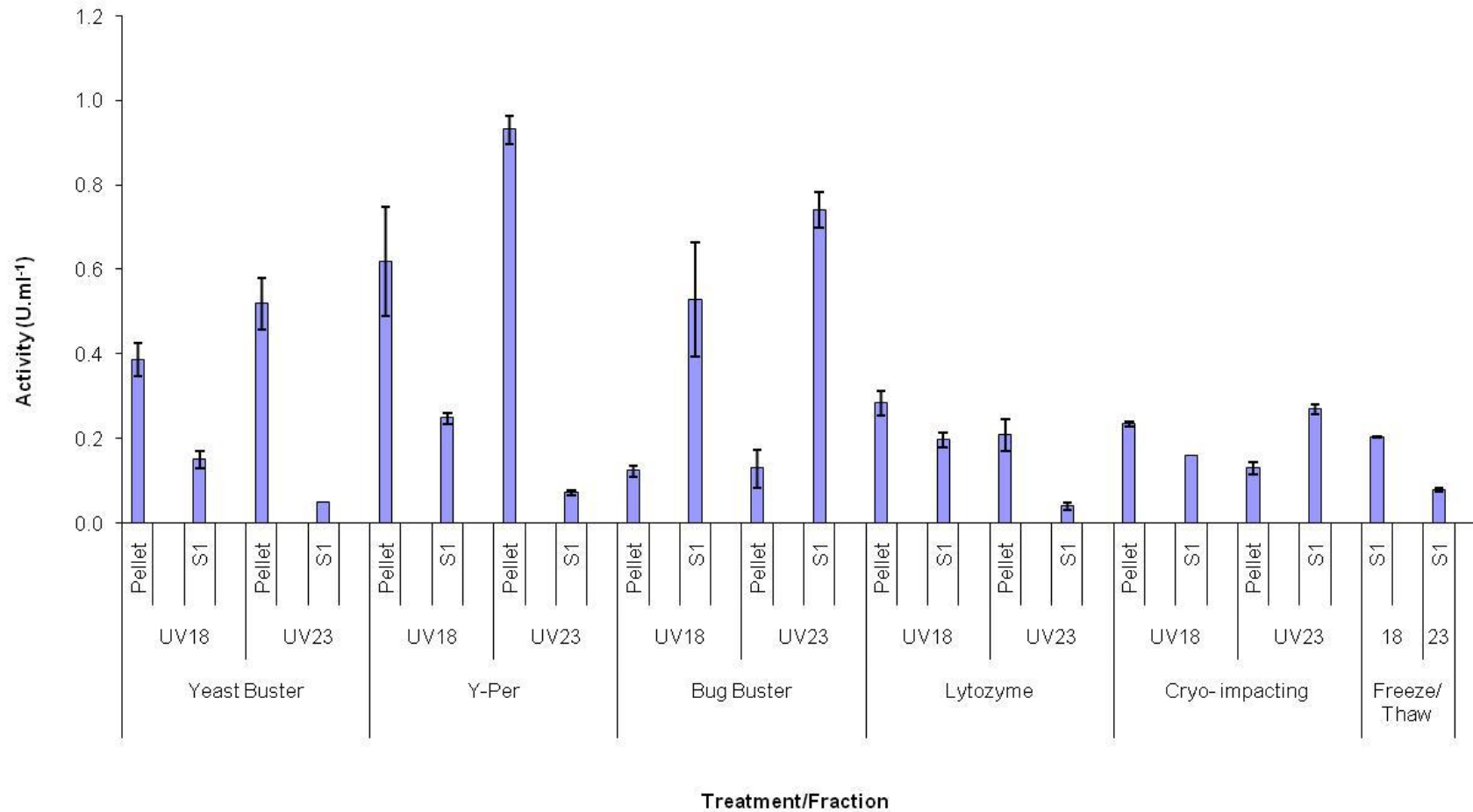


Figure A2.1 Comparison of release of PNP from UV18 and UV23 using different methods of protein extraction.

Pellet indicates the cellular debris while S1 indicates the solubilised cytosolic fraction. Error bars represent standard deviation observed on triplicate analysis.

APPENDIX 2

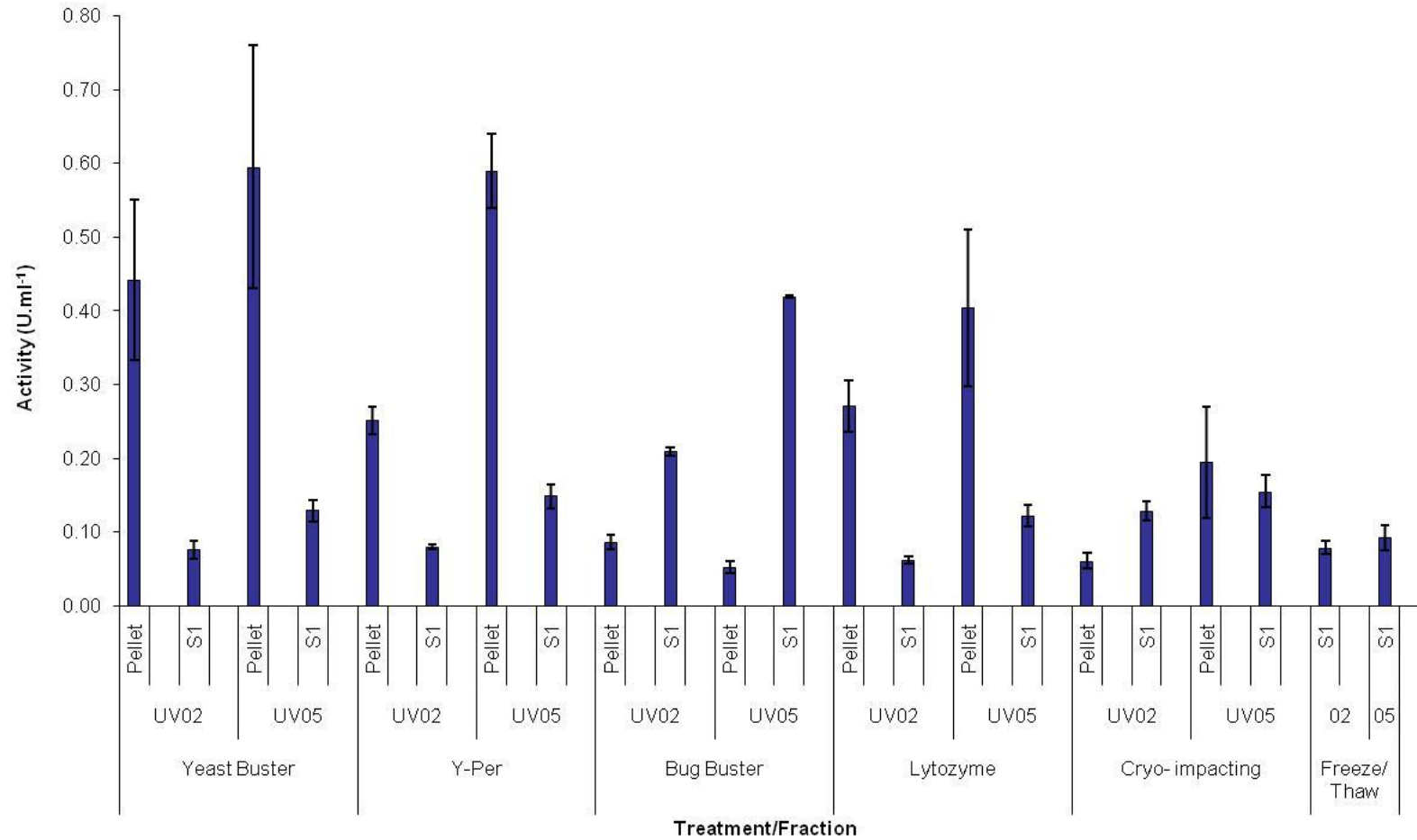


Figure A2.2 Comparison of release of PNP from UV02 and UV05 using different methods of protein extraction.

Pellet indicates the cellular debris while S1 indicates the solubilised cytosolic fraction. Error bars represent standard deviation observed on triplicate analysis.

APPENDIX 2

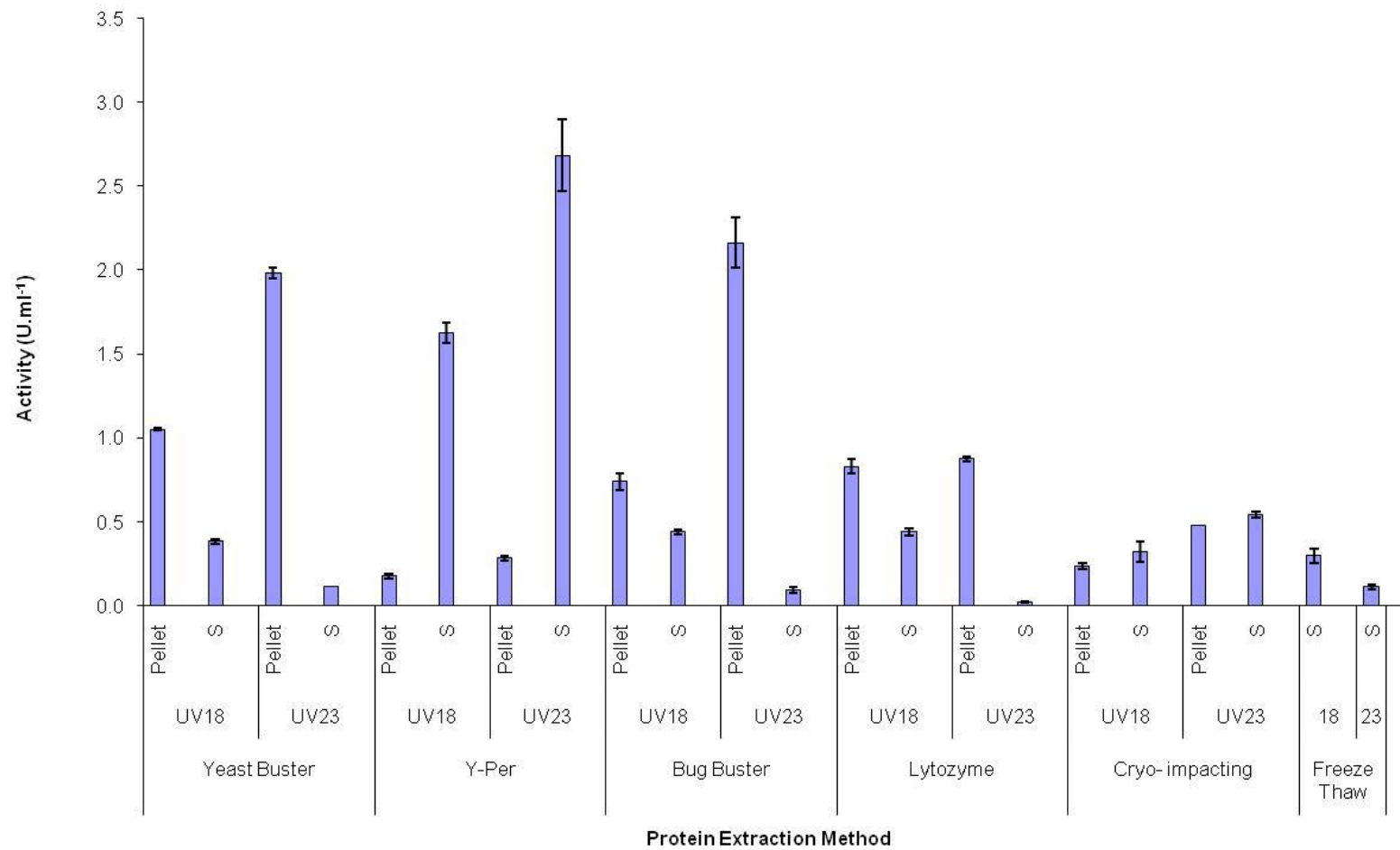


Figure A2.3 Comparison of release of PyNP from UV18 and UV23 using different methods of protein extraction.

Pellet indicates the cellular debris while S indicates the solubilised cytosolic fraction. Error bars represent standard deviation observed on triplicate analysis.

APPENDIX 2

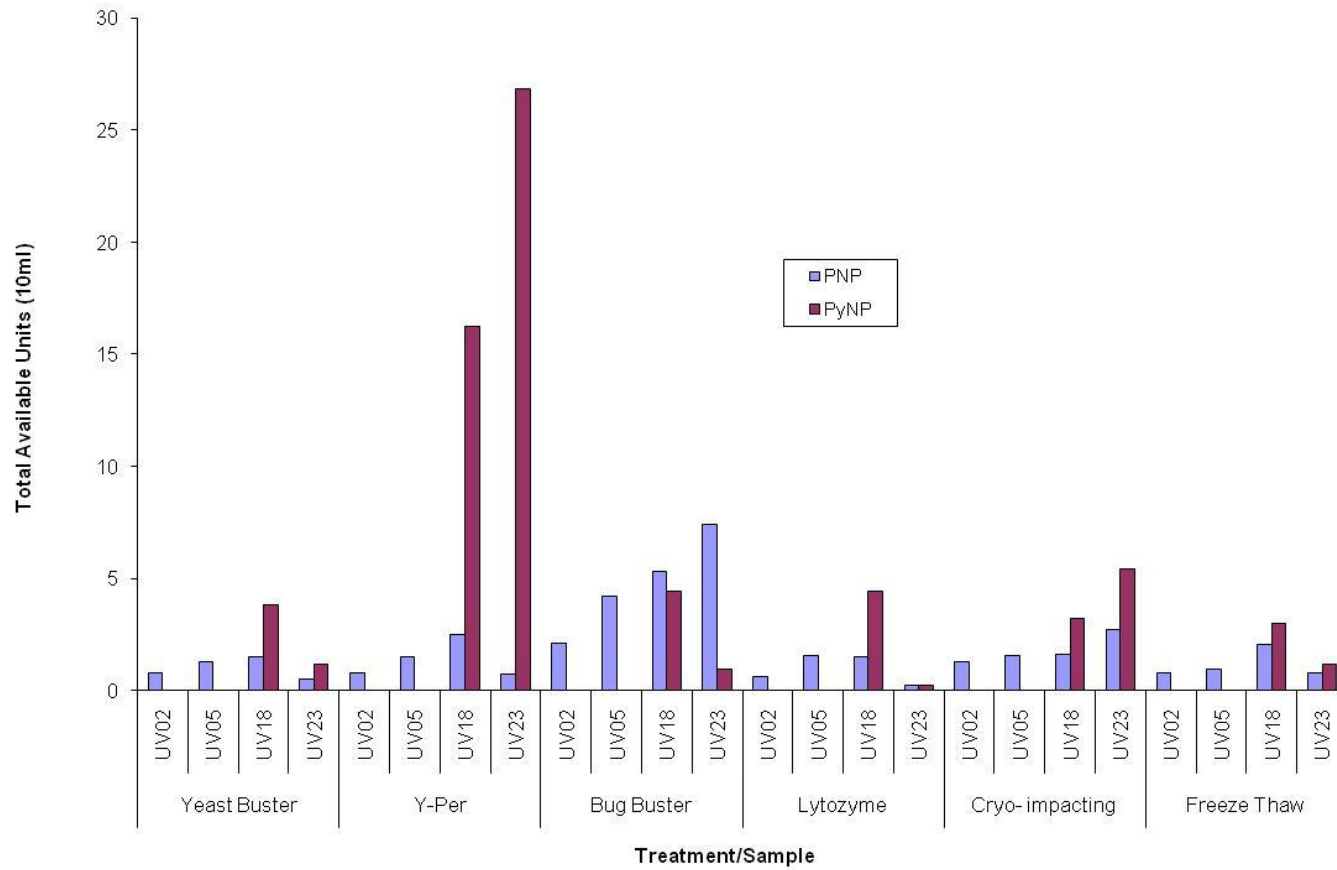


Figure A2.4 Comparison of total units of enzyme available in the extracted cytosolic fraction after different protein extraction methods.

Appendix 3

Creation and validation of working cell banks of *E. coli* JM109 (DE3)[pMSPNP] and *E. coli* BL21(DE3)[pETUP]

A3.1 Growth and cryopreservation of clones

Fifty millilitres of GMO Broth (Table A3.1) was inoculated with a loopful of selected bacteria. Strains were grown at 37°C until an OD_{600nm} of 1.0. The culture broth was aseptically mixed with 50 ml of 25 % sterile glycerol solution, and 1.0 ml aliquots of this mixture was transferred into sterile cryovials and stored at -70°C after an initial 24 h controlled freeze in Nalgene Cryo-containers.

Table A3.1 – Composition of GMO media

Ingredient	Amount	Unit
K ₂ HPO ₄	14.6	g/L
(NH ₄) ₂ SO ₄	2	g/L
Na ₂ HPO ₄	3.6	g/L
Citric Acid	2.5	g/L
MgSO ₄ .7H ₂ O	0.25	g/L
NH ₄ NO ₃	5	g/L
Yeast Extract (Biolab)	10	g/L
Glucose	30	g/L
Trace element solution	5	ml/L
Antifoam	1	ml/L
Antibiotic (Ampicillin)	100	ug/ml
IPTG	1.0	mM
Trace Element Solution		
CaCl ₂ .2H ₂ O	0.4	g/L
FeCl ₃ .6H ₂ O	16.7	g/L
MnCl ₂ .4H ₂ O	0.15	g/L
ZnSO ₄ .7H ₂ O	0.18	g/L
CuCl ₂ .2H ₂ O	0.125	g/L
CoCl ₂ .6H ₂ O	0.18	g/L
Na ₂ EDTA	20.1	g/L

A3.2 Culture viability

Three cryovials from each cell bank were randomly selected. Viable cell counts were determined by plating the cultures (by serial dilutions) on to LA-Amp plates. Culture purity was determined by plating on nutrient agar plates and microscopic analysis (Table A3.2). Cultures (5 ml) of each of the three clones were grown at 37°C overnight.

Table A3.2 – Total viable cell counts of random cell bank cryovials

	CFU/ml
<i>E. coli</i> JM109 [pMSPNP]	$2.57 \times 10^7 \pm 1.27 \times 10^7$
<i>E. coli</i> JM109 [pETUP]	$1.432 \times 10^8 \pm 1.59 \times 10^7$

No apparent contamination was noted on any of the dilutions plated out for either of the clones.

A3.3 Growth curves and growth rates

Three cryovials were randomly selected from each cell bank and used to inoculate each of 3 x 50 ml flasks. Flasks were incubated at 37°C overnight with shaking at 200 rpm. The inoculum was subsequently used to inoculate Fernbach flasks to a total volume of 700 ml. OD_{600nm} values were determined every hour. Plots of the natural log of OD_{600nm} against time (Figure A3.1) were used to determine growth rates and doubling times according to the following equations:

Growth Rate: $\mu = d \ln (OD_{600})/dt$

Doubling Time: $DT = \ln (2)/\mu$

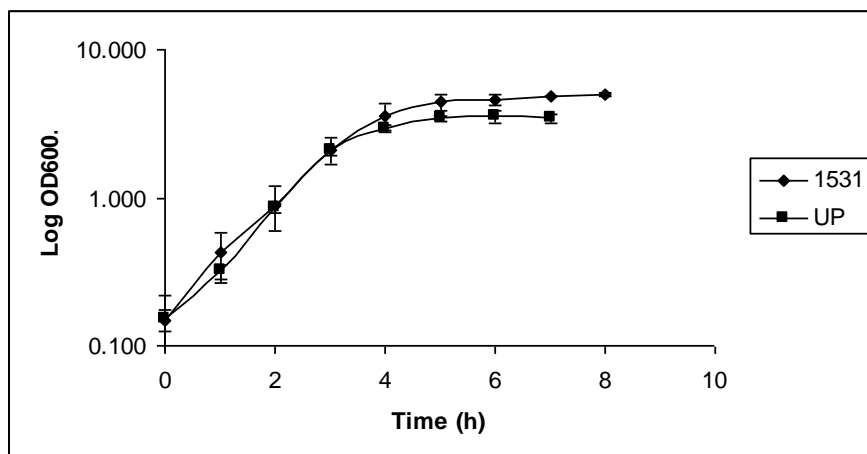


Figure A3.1 Growth curves of *E. coli* [pMSPNP] and *E. coli* [pETUP].

Results shown are composites of 3 replicate cultures for each clone.

Growth curves (Figure A3.1) show that both cultures reach stationary phase between 4 and 5 h under the growth conditions defined in the methods section. Mid-log phase is reached at approximately 2 h. Maximum growth rates (μ_{\max}) of 0.7945 and 0.782 and doubling times (DT) of 0.87 h and 0.89 h were determined for *E. coli* [pMSPNP] and *E. coli* [pETUP] respectively.

A3.4 Induction profiles and plasmid stability

Three cryovials were randomly selected from each cell bank and used to inoculate each of 3 x 50 ml flasks. Flasks were incubated at 37°C overnight with shaking at 200 rpm. The inoculum was used to inoculate Fernbach flasks to a total volume of 700 ml. OD_{600nm} values were determined every hour. A further 1 ml sample was taken every hour to determine protein and activity. Samples were sonicated and then cell debris removed by centrifugation (13000 rpm, 5 min). The supernatant was analysed for protein content according to Bradford method using BSA as a standard (Biorad method according to manufacturer's instructions) and nucleoside phosphorylase activity (measured according to standard colorimetric methods described in Chapter 2).

Based on the growth curves, cultures were induced with 1.0 mM IPTG between mid and late log growth phase. Growth and sampling was continued for a further 2 hours. Plots of protein concentration ($\text{mg}\cdot\text{ml}^{-1}$), volumetric activity ($\text{U}\cdot\text{ml}^{-1}$) and specific activity ($\text{U}\cdot\text{mg}^{-1}$) against time were determined (Figure A3.2 – A3.4). A 5 ml sample of the initial and final broth was used to determine plasmid stability. The plasmids were extracted using QIAprep Spin Miniprep Kit (Qiagen) according to the manufacturer's instructions. Restricted and unrestricted samples of each plasmid were analysed on an agarose gel to determine plasmid integrity (Figure A3.5 and Figure A3.6).

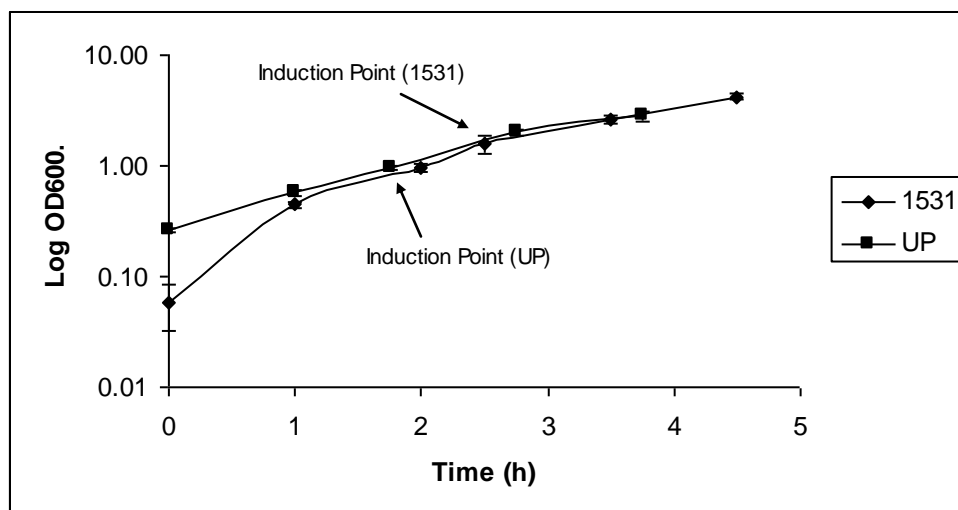


Figure A3.2 Growth characteristics of production strains during induction

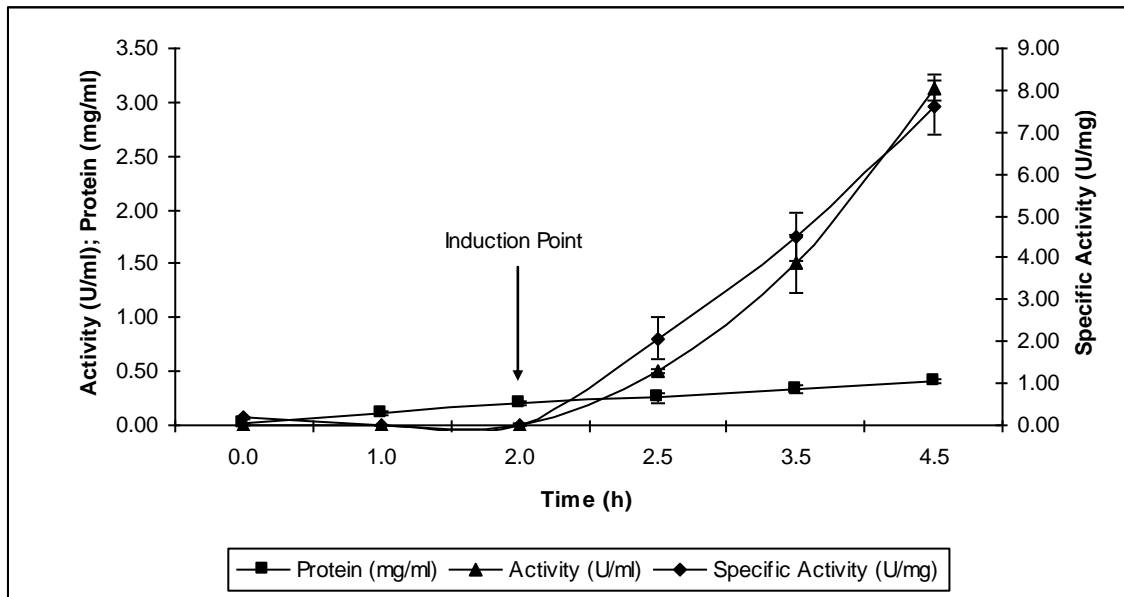


Figure A3.3 Profiles of protein concentration, activity and specific activity obtained during the induction of *E. coli* [pMSPNP].

Results shown are the composites of three separate experiments. Protein and activity trends are related to the primary (left axis), specific activity to the secondary (right) axis.

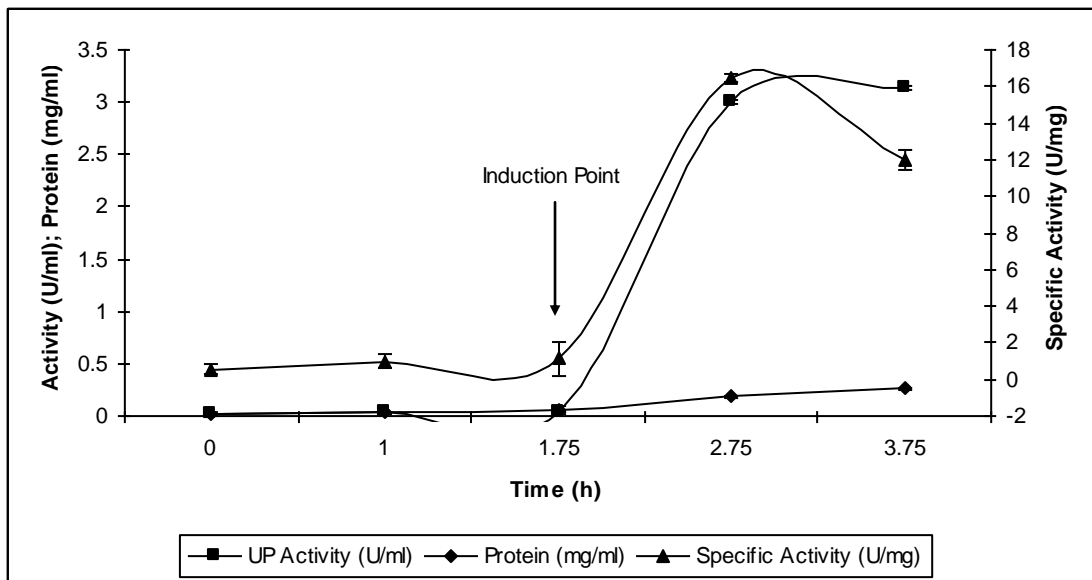


Figure A3.4 Profiles of protein concentration, activity and specific activity obtained during the induction of *E. coli* [pETUP].

Results shown are the composites of three separate experiments. Protein and activity trends are related to the primary (left axis), specific activity to the secondary (right) axis.

Visual analysis of the restricted plasmids (Figures A3.5 and A3.6) indicated a minimal loss in plasmid integrity in the case of pMSPNP and negligible loss in plasmid integrity for pETUP.

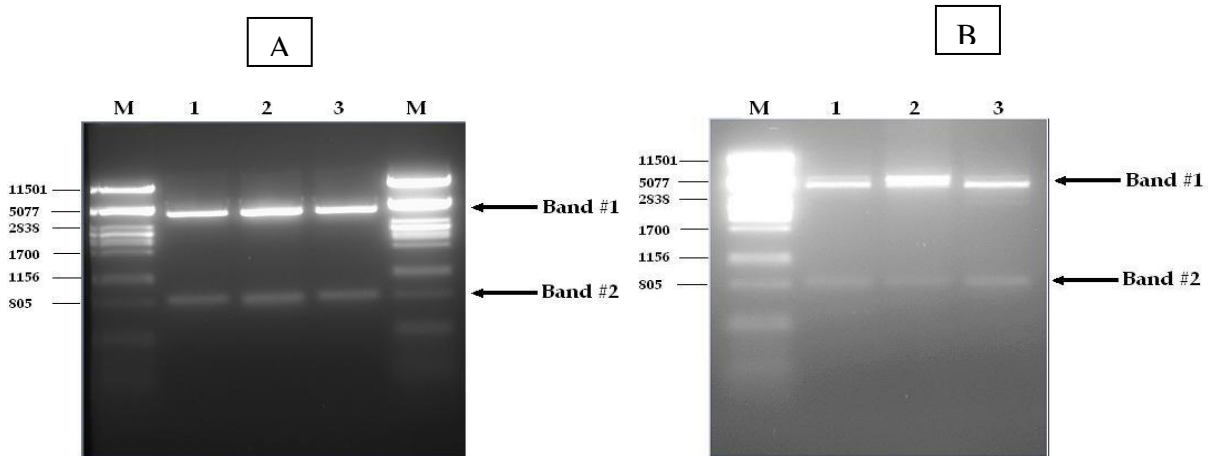


Figure A3.5 A 1% agarose gel was used to resolve pMSPNP restricted with *HindIII* and *NdeI*.

(A) indicates plasmid isolated before induction, and (B) indicates plasmid isolated after induction. Lanes: M - DNA Marker (λ DNA digested with *PstI*); 1 - Flask A plasmid digest; 2- Flask B plasmid digest; 3 - Flask C plasmid digest. Band #1 indicates the pMS Vector. Band #2 shows the release of the BH1531 gene sequence.

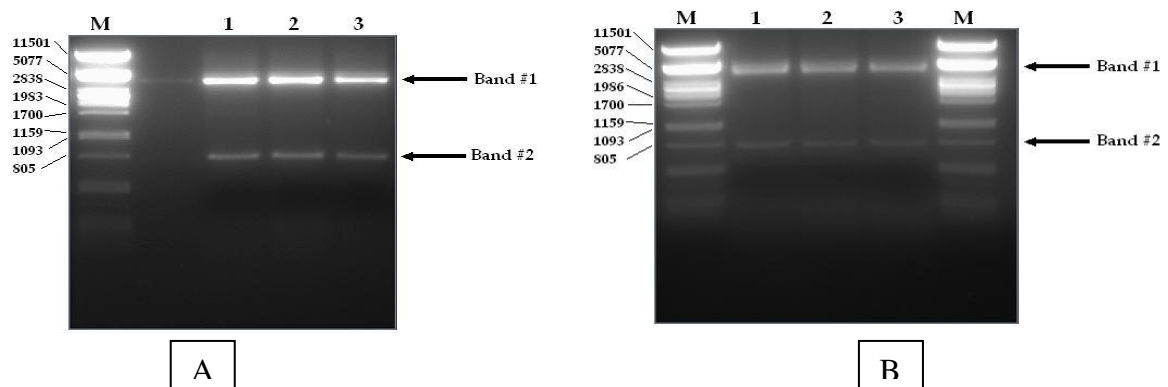


Figure A3.6 A 1 % agarose gel was used to resolve pETUP restricted with *HindIII* and *NdeI*.

(A) indicates plasmid isolated before induction, and (B) indicates plasmid isolated after induction. Lanes: M - DNA Marker (λ DNA digested with *PstI*); 1 - Flask A plasmid digest; 2- Flask B plasmid digest; 3 - Flask C plasmid digest. Band #1 indicates the pET Vector. Band #2 shows the release of the UP gene sequence after restriction cleavage.

Appendix 4

Determining growth parameters and induction point for *E. coli* batch fermentations

A4.1 Methods and Materials

Cell banking and validation

E. coli BL21 [pETUP] was grown and cell banked according to the methods described in Appendix 2.

Fermentation Part A – Determination Of Growth Parameters And Background Activity

Inoculum Train

Two Erlenmeyer flasks (250 ml) containing 50 ml LB medium were autoclaved for 15 minutes at 121°C and allowed to cool to ambient temperature. Subsequently 100 µl of ampicillin (1 mg.ml⁻¹) was added aseptically to each flask before being inoculated with 100 µl of *E. coli* BL21 [pETUP] suspension from the cell bank. The inoculated flasks were incubated at 37°C and 200 rpm overnight. The full 50 ml culture was used as the inoculum for the 1.5 L fermentations (3.3% inoculum). The monoculture status of the flasks was checked microscopically on LB and LB amp (100 µg.ml⁻¹ ampicillin).

Batch fermentations

Two batch fermenters (InFors HT) containing GMO 20 medium (Appendix 2) were inoculated with 50 ml inocula.

Glucose, Trace element solution and ampicillin were added separately after sterilization as a 99 ml charge containing: 90 ml of 50% m/v glucose solution (54.5 g glucose monohydrate per 100 ml dH₂O); 7.5 ml Trace element solution (see appendix 2 for composition); and 1.5 ml of 100 mg.ml⁻¹ ampicillin.

The pH was controlled at pH 7.2 with 33% m.v⁻¹ NH₄OH or 10% m.v⁻¹ H₂SO₄. The temperature was controlled at 37°C and the aeration was set to 1 v.v.m⁻¹. The starting agitation was set at 300 rpm and ramped up through cascade control to maintain the pO₂ above 30% saturation. Samples (10 ml) were taken at hourly intervals for determination of growth, enzyme activity and glucose utilisation.

Analysis

Growth was measured by determining the optical density at 600 nm and dry cell weight (DCW) in triplicate. A volume of 2 ml of the sample was centrifuged and the pellet was used for dry cell weight determination by drying to constant weight at 110°C. Glucose concentration was measured by Accutrend[®] (Boehringer Mannheim). Triplicate samples of 1 ml were centrifuged and resuspended at a minimum volume of B-Per (Pierce) and vortexed briefly to resuspend pellet. After incubation at room temperature for 5 min the samples were centrifuged and the supernatant analysed for nucleoside phosphorylase activity by uridine phosphorolysis. Selected samples were also visualised by SDS-PAGE.

Fermentation Part B – Investigation Of Early- And Mid-Log Phase Induction

Inoculum train

Two inoculum flasks were prepared as described above.

Batch fermentations

Two batch fermenters (InFors HT), prepared as above, were inoculated with the 50 ml inocula and operated under the same conditions as described previously.

Target induction times are early and mid late log-phase, based on results obtained in Part A. UP expression was induced by adding IPTG to a final broth concentration of 0.5 mM. Fermentations were run for a further 5 h after induction.

Analysis

As described above.

A4.2 Results

Fermentation Part A – growth curves and background activity

Un-induced duplicate fermentations of *E. coli* BL21 [pETUP] were performed to determine the growth curve of the clone under fermentation conditions (Figure A4.1). The clone entered logarithmic growth 2 h after inoculation and entered stationary phase after 7 h. Glucose analysis indicated that the strain utilises very little of the glucose until mid log phase (4 h) after which there is a rapid utilisation, with full depletion of the glucose after 7 h, coinciding with end of log phase growth. Due to this rapid depletion of glucose, it was decided to use the OD_{660nm} (growth) measurements as an indicator of induction time rather than residual glucose level, as there is no clear distinction in glucose levels between early and mid log phase. For Part B of this study, it was decided to induce the fermentations after 2 h and 3.5 h, reflecting early and mid log-phase growth. *E. coli* BL21 [pETUP] showed a high level of background activity during the un-induced fermentations (Figure A4.2). Final activity levels of ~9.0 U.ml⁻¹ were noted with a specific activity of ~2.2 U.mg⁻¹ protein.

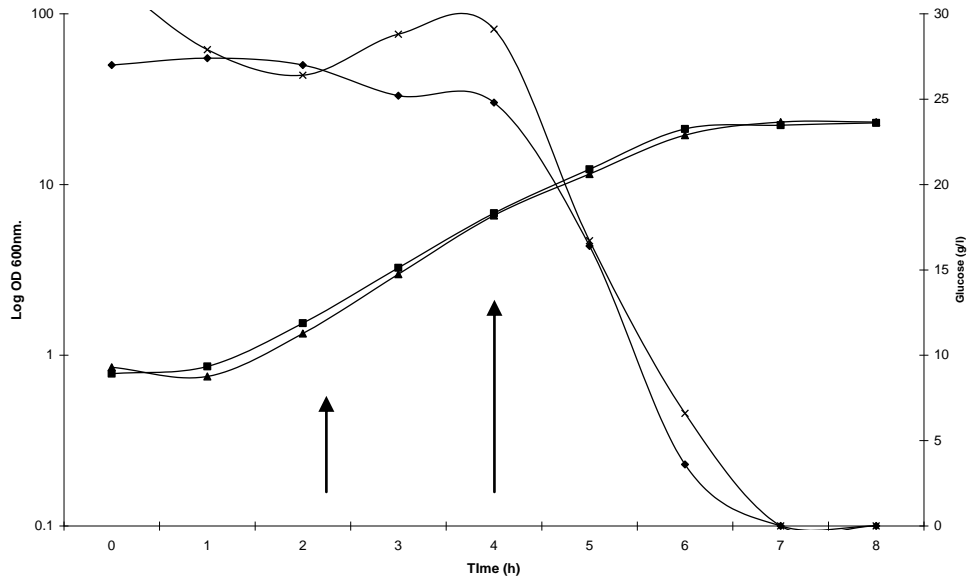


Figure A4.1 Growth profiles from duplicate fermentations from un-induced fermentations.

Arrows indicate proposed induction times (Early and mid log-phase) for Part B (induced fermentations). (-■-) IN1-07 OD_{660nm}; (-◆-) IN1-07 [glucose]; (-▲-) IN2-07 OD_{660nm}; (-×-) IN2-07 [glucose].

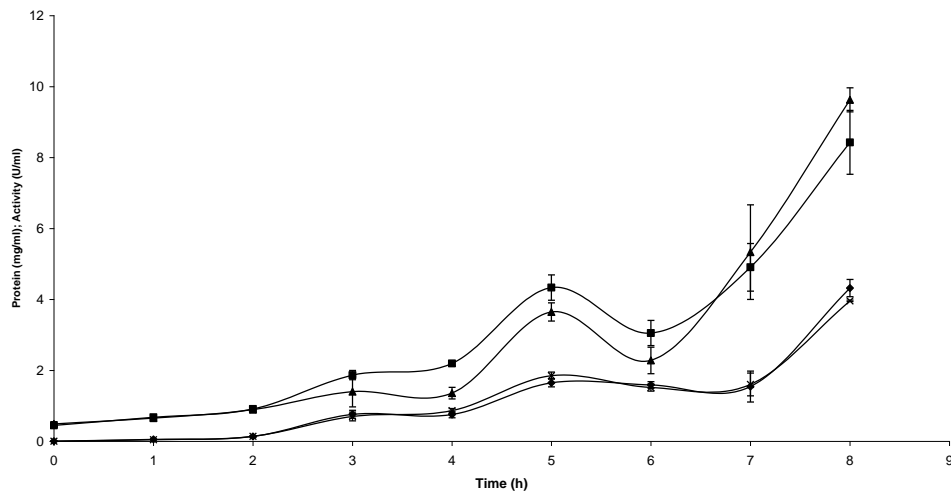


Figure A4.2 Activity and protein profiles from duplicate un-induced fermentations.

(-■-) IN1-07 UP activity; (-◆-) IN1-07 [Protein]; (-▲-) IN2-07 UP activity; (-×-) IN2-07 [Protein].

Fermentation Part B –Early and Mid log phase induction

Comparison of early and mid log phase induction (Figure A4.3 and Table A1.1) indicates that higher yield is achieved when inducing at mid-log phase.

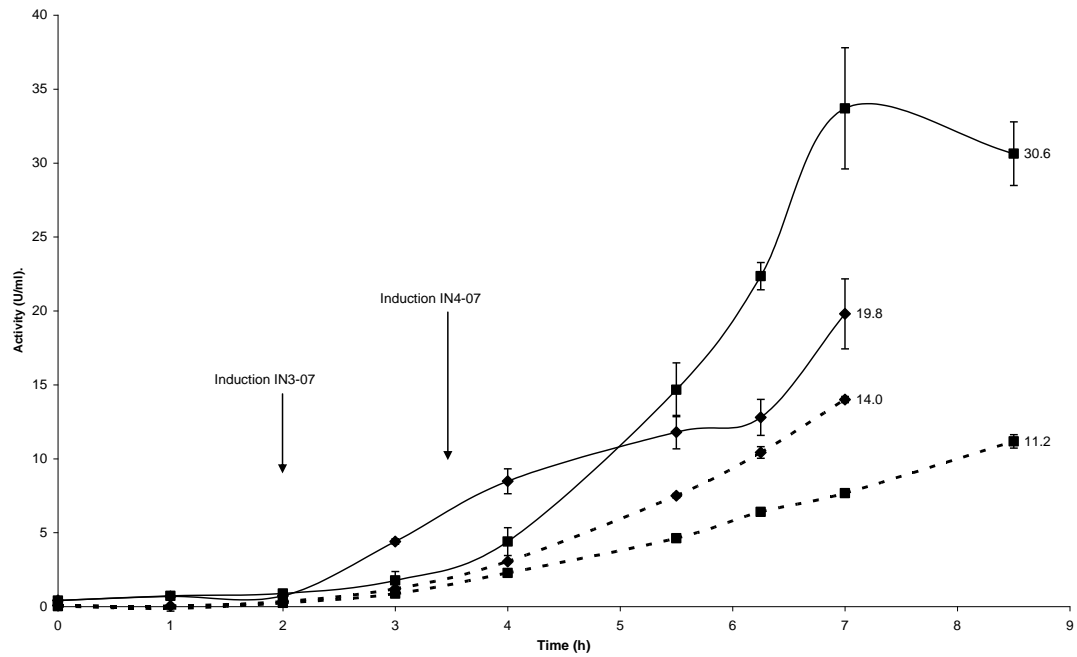


Figure A4.3 UP activity and biomass trends from fermentations IN3-07 (early-log phase induction) and IN4-07 (mid-log phase induction).

(-◆-) IN3-07 UP Activity (--◆--) IN3-07 Biomass (-■-) IN4-07 UP Activity (--■--) IN4-07 Biomass.

Table A1.1 Summary of induced fermentation results

	IN3-07 (early-log phase induction)	IN4-07 (mid-log phase induction)
Maximal OD (660nm)	26.7	21.93
μ_{\max} (exponential)	0.71	0.69
Yield (g DCW.gC ⁻¹)	0.57	0.49
Biomass Yield (DCW.l ⁻¹)	14.0	11.18
Productivity (g DCW.l ⁻¹ .h ⁻¹)	2.0	1.39
Enzyme Yield (U.l ⁻¹)	19,800	30,600
Enzyme productivity (U.l ⁻¹ .h ⁻¹)	2,828.6	3,600

A4.3

Conclusion

Growth trends and glucose analysis indicated that using OD_{660nm} as an indicator for growth phase as opposed to glucose concentration (as in previous batch fermentations) may be more accurate. Early and mid-log phase induction studies showed that mid-log phase induction is more effective. A final yield of 30,600 U.l⁻¹ was achieved at a productivity of 3,600 U.l⁻¹.h⁻¹. The maximum productivity however was achieved after 3.5 h of induction (7 h fermentation) where the yield was 33,700 U.l⁻¹ giving a productivity of 4,800 U.l⁻¹.h⁻¹.

Appendix 5

NMR spectra

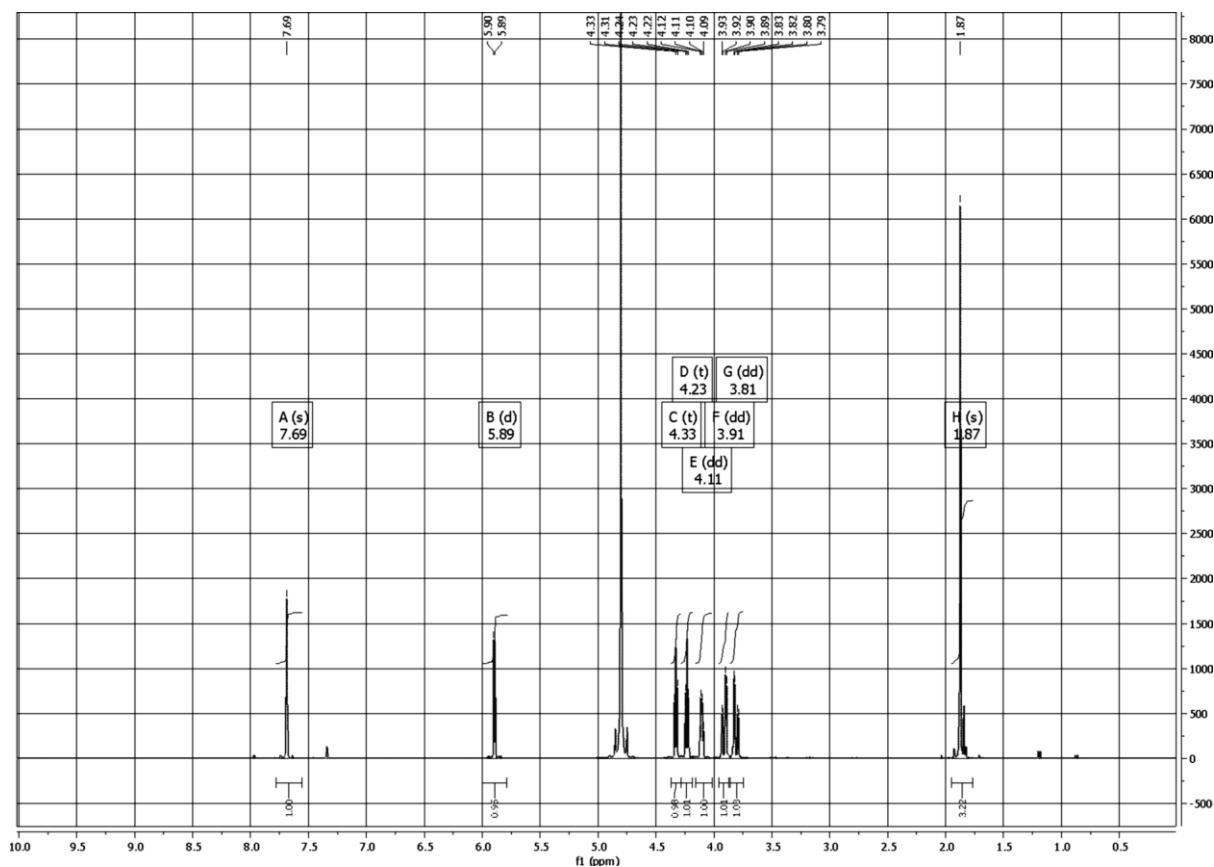


Figure A5.1 400 MHz proton NMR spectrum of 5-MU produced by the biocatalytic method described (Chapters 2, 3 and 5) (one-step purification using hot isopropyl alcohol followed by filtration).

^1H NMR (400 MHz, D_2O), δ (ppm): 7.69 (^1H , s); 5.89 (^1H , d, $J_{4.7}$ Hz); 4.33 (^1H , t, $J_{5.1}$ Hz); 4.23 (^1H , t, $J_{5.4}$ Hz); 4.11 (^1H , dd, $J_{4.2}$ and 8.2 Hz); 3.91 (^1H , dd, $J_{2.9}$ and 12.8 Hz); 3.81 (^1H , dd, $J_{4.2}$ and 12.8 Hz); 1.87 (^3H , s).

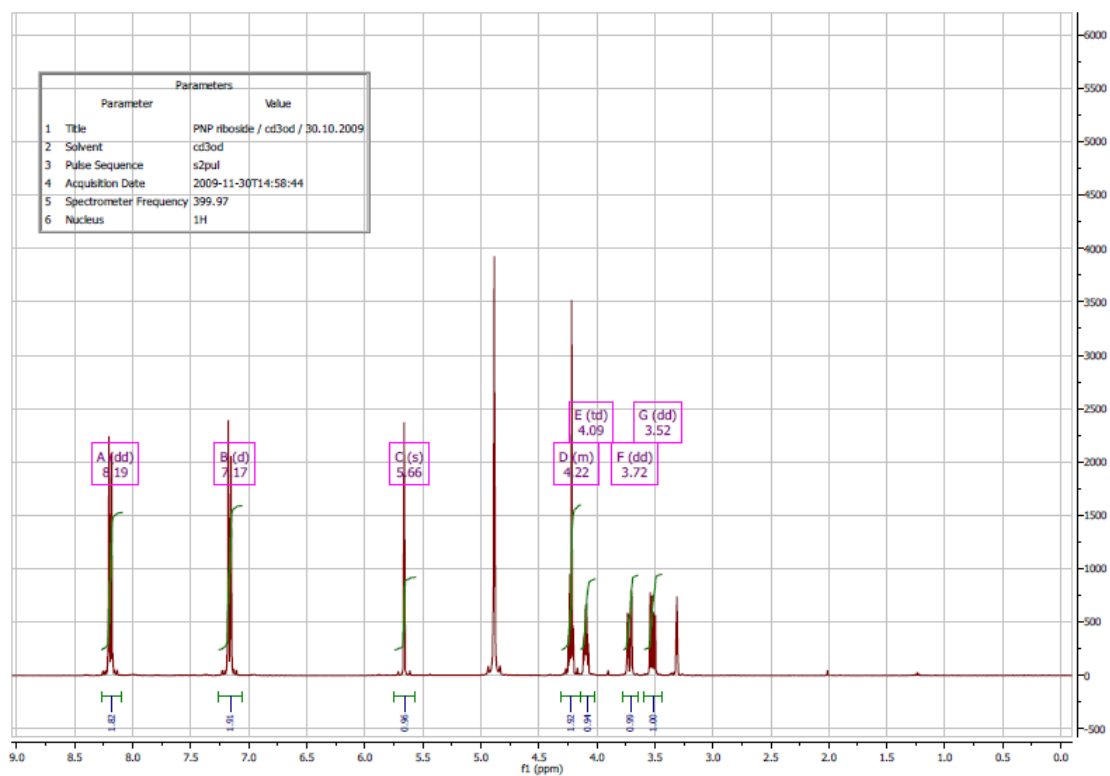


Figure A5.2 400 MHz proton NMR spectrum of *p*-nitrophenol ribofuranoside produced by the method described (Chapter 4)

δ_{H} (400 MHz, cd₃od) 8.19 (2 H, dd, J 0.5, 9.3), 7.17 (2 H, d, J 9.2), 5.66 (1 H, s), 4.31 – 4.14 (2 H, m), 4.09 (1 H, td, J 3.5, 6.1), 3.72 (1 H, dd, J 3.5, 12.0), 3.52 (1 H, dd, J 6.1, 12.0).

REFERENCES

1. **Almendros, M; Gago, JV; and Carlos, JB** (2009) *Thermus thermophilus* strains active in purine nucleoside synthesis. *Molecules*. **14**(3) 1279 - 1287.
2. **Altschul, SF; Gish, W; Miller, W; Myers, EW; and Lipman, DJ** (1990) Basic local alignment search tool. *J Mol. Biol* **215**(3) 403 - 410.
3. **Antikainen, NM and Martin, SF** (2005) Altering protein specificity: techniques and applications. *Bioorg. Med. Chem* **13**(8) 2701 - 2716.
4. **Araki, T; Ikeda, I; Matoishi, K; Abe, R; Oikawa, T; Matsuba, Y; Ishibashi, H; Nagahara, K; and Fukuiri, Y.** Method for producing cytosine nucleoside compounds. [US20030207405A1]. 2003.
5. **Arnold, FH and Georgiou, G.**(2003). Directed Enzyme Evolution - Screening and Selection Methods. Humana Press. Totowa, New Jersey.
6. **Avraham, Y; Yashphe, J; and Grossowicz, N** (1988) Thymidine phosphorylase and uridine phosphorylase of *Lactobacillus casei*. *FEMS. Lett.* **56**(1) 29 - 33.
7. **Balzer, D; Ziegelin, G; Pansegrau, W; Kruft, V; and Lanka, E** (1992) KorB protein of promiscuous plasmid RP4 recognizes inverted sequence repetitions in regions essential for conjugative plasmid transfer. *Nucleic Acids Res.* **20**(8) 1851 - 1858.
8. **Bennett, EM; Li, C; Allan, PW; Parker, WB; and Ealick, SE** (2003) Structural basis for substrate specificity of *Escherichia coli* purine nucleoside phosphorylase. *J. Biol. Chem.* **278**(47) 47110 - 47118.
9. **Bestetti, G; Cali, S; Ghisotti, D; Orsini, G; Tonon, G; and Zuffi, G.** Recombinant Bacterial Strains for the production of natural nucleosides and analogues thereof. [WO 00/39307]. 2000.
10. **Brady, D and Jordaan, J** (2009) Advances in enzyme immobilisation. *Biotechnol. Lett.* **31**(11) 1639 - 1650.
11. **Brady, D; Jordaan, J; Simpson, C; Chetty, A; Arumugam, C; and Moolman, FS** (2008) Spherezymes: a novel structured self-immobilisation enzyme technology. *BMC. Biotechnol.* 88 - 93
12. **Burling, FT; Kniewel, R; Buglino, JA; Chadha, T; Beckwith, A; and Lima, CD** (2003) Structure of *Escherichia coli* uridine phosphorylase at 2.0 Å. *Acta Crystal. D.* **59**(1) 73 - 76.
13. **Burton, SG; Cowan, DA; and Woodley, JM** (2002) The search for the ideal biocatalyst. *Nat. Biotech.* **20**(1) 37 - 45.
14. **Butler, T and Alcalde, M** (2003) Preparing libraries in *Saccharomyces cerevisiae*. (3) 17-23.

15. **Bzowska, A** (2002) Calf spleen purine nucleoside phosphorylase: complex kinetic mechanism, hydrolysis of 7-methylguanosine, and oligomeric state in solution. *Biochim. Biophys. Acta* **1596**(2) 293 - 317.
16. **Bzowska, A; Koellner, G; Wielgus-Kutrowska, B; Stroh, A; Raszewski, G; Holy, A; Steiner, T; and Frank, J** (2004) Crystal structure of calf spleen purine nucleoside phosphorylase with two full trimers in the asymmetric unit: important implications for the mechanism of catalysis. *J. Mol. Biol.* **342**(3) 1015 - 1032.
17. **Bzowska, A; Kulikowska, E; and Shugar, D** (2000) Purine nucleoside phosphorylases: properties, functions, and clinical aspects. *Pharmacol. Ther.* **88**(3) 349 - 425.
18. **Bzowska, A; Luic, M; Schroder, W; Shugar, D; Saenger, W; and Koellner, G** (1995) Calf spleen purine nucleoside phosphorylase: purification, sequence and crystal structure of its complex with an N(7)-acycloguanosine inhibitor. *FEBS Lett.* **367**(3) 214 - 218.
19. **Bzowska, A; Tebbe, J; Luic, M; Wielgus-Kutrowska, B; Schroder, W; Shugar, D; Saenger, W; and Koellner, G** (1998) Crystallization and preliminary X-ray studies of purine nucleoside phosphorylase from *Cellulomonas* sp. *Acta Crystallogr. D. Biol. Crystallogr.* **54**(5) 1061 - 1063.
20. **Cacciapuoti, G; Forte, S; Moretti, MA; Brio, A; Zappia, V; and Porcelli, M** (2005) A novel hyperthermostable 5'-deoxy-5'-methylthioadenosine phosphorylase from the archaeon *Sulfolobus solfataricus*. *FEBS J.* **272**(8) 1886 - 1899.
21. **Cacciapuoti, G; Gorassini, S; Mazzeo, MF; Siciliano, RA; Carbone, V; Zappia, V; and Porcelli, M** (2007) Biochemical and structural characterization of mammalian-like purine nucleoside phosphorylase from the Archaeon *Pyrococcus furiosus*. *FEBS J.* **274**(10) 2482 - 2495.
22. **Cacciapuoti, G; Porcelli, M; Bertoldo, C; De Rosa, M; and Zappia, V** (1994) Purification and characterization of extremely thermophilic and thermostable 5'-methylthioadenosine phosphorylase from the archaeon *Sulfolobus solfataricus*. Purine nucleoside phosphorylase activity and evidence for intersubunit disulfide bonds. *J. Biol. Chem.* **269**(40) 24762 - 24769.
23. **Caradoc-Davies, TT; Cutfield, SM; Lamont, IL; and Cutfield, JF** (2004a) Crystal structures of *Escherichia coli* uridine phosphorylase in two native and three complexed forms reveal basis of substrate specificity, induced conformational changes and influence of potassium. *J. Mol. Biol.* **337**(2) 337 - 354.
25. **Castilho, MS; Postigo, MP; Pereira, HM; Oliva, G; and Andricopulo, AD** (2010) Structural basis for selective inhibition of purine nucleoside phosphorylase from *Schistosoma mansoni*: kinetic and structural studies. *Bioorg. Med. Chem* **18**(4) 1421 - 1427.
26. **Chaikuad, A and Brady, RL** (2009) Conservation of structure and activity in *Plasmodium* purine nucleoside phosphorylases. *BMC. Struct. Biol* **9**42 -

27. **Chantry, D** (2004) HIV entry and fusion inhibitors. *Expert. Opin. Emerg. Drugs* **9**(1) 1 - 7.
28. **Chebotaev, DV; Gul'ko, LB; and Veiko, VP** (2001) Protein engineering of uridine phosphorylase from *Escherichia coli* K-12. II. A comparative study of the properties of hybrid and mutant forms of uridine phosphorylases. *Russ. J. Bioorg. Chem.* **27**(3) 160 - 166.
29. **Chen, BC; Quinlan, SL; Stark, DR; Gregory Reid, J; Audia, VH; George, JG; Eisenreich, E; Brundidge, SP; Racha, S; and Spector, RH** (1995) 5'-Benzoyl-2'[alpha]-bromo-3'-O-methanesulfonylthymidine: A superior nucleoside for the synthesis of the anti-AIDS drug D4T (Stavudine). *Tet. Lett.* **36**(44) 7957 - 7960.
30. **Chen, K and Arnold, FH** (1993) Tuning the activity of an enzyme for unusual environments: sequential random mutagenesis of subtilisin E for catalysis in dimethylformamide. *Proc. Natl. Acad. Sci. U. S. A* **90**(12) 5618 - 5622.
31. **Chien, CV** (2007) HIV/AIDS drugs for Sub-Saharan Africa: How do brand and generic supply compare? *PLoS ONE* **2**(3) e278 -
32. **Cihlar, T and Ray, AS** (2010) Nucleoside and nucleotide HIV reverse transcriptase inhibitors: 25 years after zidovudine. *Antiviral Res.* **85**(1) 39 - 58.
33. **Cirino, PC; Mayer, KM; and Umeno, D** (2003) Generating mutant libraries using error-prone PCR. **1**(1) 3-9.
34. **Crampton, M; Berger, E; Reid, S; and Louw, M** (2007) The development of a flagellin surface display expression system in a moderate thermophile, *Bacillus halodurans* Alk36. *Appl. Microbiol. Biotechnol.* **75**(3) 599 - 607.
35. **Cutayar, JM and Poillon, D** (1989) High cell density culture of *E. coli* in a fed-batch system with dissolved oxygen as substrate feed indicator. *Biotechnol. Lett.* **11**(3) 155 - 160.
36. **Dandanell, G; Szczepanowski, RH; Kierdaszuk, B; Shugar, D; and Bochtler, M** (2005) *Escherichia coli* purine nucleoside phosphorylase II, the product of the xapA gene. *J. Mol. Biol.* **348**(1) 113 - 125.
37. **de Bethune, MP** (2010) Non-nucleoside reverse transcriptase inhibitors (NNRTIs), their discovery, development, and use in the treatment of HIV-1 infection: a review of the last 20 years (1989-2009). *Antiviral Res.* **85**(1) 75 - 90.
38. **De Clercq, E** (1998) The role of non-nucleoside reverse transcriptase inhibitors (NNRTIs) in the therapy of HIV-1 infection. *Antiviral Res.* **38**(3) 153 - 179.
39. **De Clercq, E** (2001) Antiviral drugs: current state of the art. *J Clin. Virol.* **22**(1) 73 - 89.
40. **Domagala, JM; Bader, JP; Gogliotti, RD; Sanchez, JP; Stier, MA; Song, Y; Prasad, JV; Tummino, PJ; Scholten, J; Harvey, P; Holler, T; Gracheck, S; Hupe, D; Rice, WG; and Schultz, R** (1997) A new class of anti-HIV-1 agents targeted

- toward the nucleocapsid protein NCp7: the 2,2'-dithiobisbenzamides. *Bioorg. Med. Chem* **5**(3) 569 - 579.
41. **Dontsova, MV; Gabdoukhakov, AG; Molchan, OK; Lashkov, AA; Garber, MB; Mironov, AS; Zhukhlistova, NE; Morgunova, EY; Voelter, W; Betzel, C; Zhang, Y; Ealick, SE; and Mikhailov, AM** (2005) Preliminary investigation of the three-dimensional structure of *Salmonella typhimurium* uridine phosphorylase in the crystalline state. *Acta Crystallogr. Sect. F. Struct. Biol Cryst. Commun* **61**(Pt 4) 337 - 340.
 42. **Doskoil, J and Holý, A** (1977) Specificity of purine nucleoside phosphorylase from *Escherichia coli*. *Coll Czech Chem Commun* **42**370 - 382.
 43. **Douek, DC; Roederer, M; and Koup, RA** (2009) Emerging concepts in the immunopathogenesis of AIDS. *Annu. Rev. Med.* **60**471 - 484.
 44. **Ealick, SE; Rule, SA; Carter, DC; Greenhough, TJ; Babu, YS; Cook, WJ; Habash, J; Helliwell, JR; Stoeckler, JD; Parks, RE, Jr.; and .** (1990) Three-dimensional structure of human erythrocytic purine nucleoside phosphorylase at 3.2 Å resolution. *J. Biol. Chem.* **265**(3) 1812 - 1820.
 45. **Eijsink, VG; Gaseidnes, S; Borchert, TV; and van den, BB** (2005) Directed evolution of enzyme stability. *Biomol. Eng* **22**(1-3) 21 - 30.
 46. **Erion, MD; Stoeckler, JD; Guida, WC; Walter, RL; and Ealick, SE** (1997) Purine nucleoside phosphorylase. 2. Catalytic mechanism. *Biochemistry* **36**(39) 11735 - 11748.
 47. **Esipov, RS; Gurevich, AI; Chuvikovskiy, DV; Chupova, LA; Muravyova, TI; and Miroschnikov, AI** (2002) Overexpression of *Escherichia coli* genes encoding nucleoside phosphorylases in the pET/BI21(DE3) system yields active recombinant enzymes. *Protein Expr. Purif.* **24**(1) 56 - 60.
 48. **Gao, XF; Huang, XR; and Sun, CC** (2006) Role of each residue in catalysis in the active site of pyrimidine nucleoside phosphorylase from *Bacillus subtilis*: a hybrid QM/MM study. *J Struct. Biol* **154**(1) 20 - 26.
 49. **Ge, C; OuYang, L; Ding, Q; and Ou, L** (2009) Co-expression of recombinant nucleoside phosphorylase from *Escherichia coli* and its application. *Appl. Biochem Biotechnol.* **159**(1) 168 - 177.
 50. **Gordon, GER; Visser, DF; Brady, D; Raseroka, N; and Bode, ML** (2010) Defining a process operating window for the synthesis of 5-methyluridine by transglycosylation of guanosine and thymine. *J. Biotechnol.* **Submitted**.
 51. **Haag, R and Lewis, RA** (1994) The partial purification and characterization of purine nucleoside phosphorylase from mammalian mitochondria. *Mol. Cell Biochem.* **135**(2) 129 - 136.
 52. **Hamamoto, T; Noguchi, T; and Midorikawa, Y** (1997a) Cloning of purine nucleoside phosphorylase II gene from *Bacillus stearothermophilus* TH 6-2 and characterization of its gene product. *Biosci. Biotechnol. Biochem.* **61**(2) 276 - 280.

53. **Hamamoto, T; Okuyama, K; Noguchi, T; and Midorikawa, Y** (1997b) Cloning and expression of purine nucleoside phosphorylase I gene from *Bacillus stearothermophilus* TH 6-2. *Biosci. Biotechnol. Biochem.* **61**(2) 272 - 275.
54. **Hammer-Jespersen, K; Munch-Petersen, A; Schwartz, M; and Nygaard, P** (1971) Induction of enzymes involved in the catabolism of deoxyribonucleosides and ribonucleosides in *Escherichia coli* K 12. *Eur. J Biochem* **19**(4) 533 - 538.
55. **Hanrahan, JR and Hutchinson, DW** (1992) The enzymatic synthesis of antiviral agents. *J. Biotechnol.* **23**(2) 193 - 210.
56. **Hori, N; Watanabe, M; Sunagawa, K; Uehara, K; and Mikami, Y** (1991) Production of 5-methyluridine by immobilised thermostable purine nucleoside phosphorylase and pyrimidine nucleoside phosphorylase from *Bacillus stearothermophilus* JTS 859. *J. Biotechnol.* **17**(2) 121 - 131.
57. **Hori, N; Watanabe, M; Yamazaki, Y; and Mikami, Y** (1989a) Purification and characterization of thermostable purine nucleoside phosphorylase of *Bacillus stearothermophilus* JTS-859. *Agri. Biol. Chem.* **53**(8) 2205 - 2210.
58. **Hori, N; Watanabe, M; Yamazaki, Y; and Mikami, Y** (1989b) Synthesis of 5-methyluridine by a thermophile, *Bacillus stearothermophilus* JTS-859. *Agri. Biol. Chem.* **53**(1) 197 - 202.
59. **Huff, JR and Kahn, J** (2001) Discovery and clinical development of HIV-1 protease inhibitors. *Adv. Protein Chem* **56**213 - 251.
60. **Hwang, WI and Cha, S** (1973) A new enzymatic method for the determination of inorganic phosphate and its application to the nucleoside diphosphatase assay. *Anal. Biochem* **55**(2) 379 - 387.
61. **Ichikawa, E and Kato, K** (2001) Sugar-modified nucleosides in past 10 years, A review. *Curr. Med. Chem.* **8**385 - 423.
62. **Ishii, M; Shirae, H; and Yokozeki, K** (1989) Enzymatic production of 5-methyluridine from purine nucleosides and thymine by *Erwinia carotovora* AJ-2992. *Agric. Biol. Chem.* **53**(12) 3209 - 3218.
63. **Ivanova, N; Sorokin, A; Anderson, I; Galleron, N; Candelon, B; Kapatral, V; Bhattacharyya, A; Reznik, G; Mikhailova, N; Lapidus, A; Chu, L; Mazur, M; Goltsman, E; Larsen, N; D'Souza, M; Walunas, T; Grechkin, Y; Pusch, G; Haselkorn, R; Fonstein, M; Dusko Ehrlich, S; Overbeek, R; and Kyrpides, N** (2003) Genome sequence of *Bacillus cereus* and comparative analysis with *Bacillus anthracis*. *Nature* **423**(6935) 87 - 91.
64. **Johnson, AA; Marchand, C; and Pommier, Y** (2004) HIV-1 integrase inhibitors: a decade of research and two drugs in clinical trial. *Curr. Top. Med. Chem* **4**(10) 1059 - 1077.
65. **Jordaan, J; Mathye, S; Simpson, C; and Brady, D** (2009) Improved chemical and physical stability of laccase after spherezyme immobilisation. *Enz. Micro. Tech.* **45**(6-7) 432 - 435.

66. **Koellner, G; Luic, M; Shugar, D; Saenger, W; and Bzowska, A** (1998) Crystal structure of the ternary complex of *E. coli* purine nucleoside phosphorylase with formycin B, a structural analogue of the substrate inosine, and phosphate (sulphate) at 2.1 Å resolution. *J. Mol. Biol.* **280**(1) 153 - 166.
67. **Koshland, DE** (1998) Conformational changes: how small is big enough? *Nat. Med.* **4**(10) 1112 - 1114.
68. **Krenitsky, TA; Koszalka, GW; and Tuttle, JV** (1981) Purine nucleoside synthesis, an efficient method employing nucleoside phosphorylases. *Biochemistry* **20**(12) 3615 - 3621.
69. **Larkin, MA; Blackshields, G; Brown, NP; Chenna, R; McGettigan, PA; McWilliam, H; Valentin, F; Wallace, IM; Wilm, A; Lopez, R; Thompson, JD; Gibson, TJ; and Higgins, DG** (2007) Clustal W and Clustal X version 2.0. *Bioinformatics.* **23**(21) 2947 - 2948.
70. **Larson, ET; Mudeppa, DG; Gillespie, JR; Mueller, N; Napuli, AJ; Arif, JA; Ross, J; Arakaki, TL; Lauricella, A; Detitta, G; Luft, J; Zucker, F; Verlinde, CL; Fan, E; Van Voorhis, WC; Buckner, FS; Rathod, PK; Hol, WG; and Merritt, EA** (2010) The crystal structure and activity of a putative *Trypanosoma* nucleoside phosphorylase reveal it to be a homodimeric uridine phosphorylase. *J Mol. Biol* **396**(5) 1244 - 1259.
71. **Lee, HC; Kim, JH; Kim, JS; Jang, W; and Kim, SY** (2009) Fermentative production of thymidine by a metabolically engineered *Escherichia coli* strain. *Appl. Environ. Microbiol.* **75**(8) 2423 - 2432.
72. **Lee, J; Filosa, S; Bonvin, J; Guyon, S; Aponte, RA; and Turnbull, JL** (2001) Expression, purification, and characterization of recombinant purine nucleoside phosphorylase from *Escherichia coli*. *Protein Expr. Purif.* **22**(2) 180 - 188.
73. **Leer, JC; Hammer-Jespersen, K; and Schwartz, M** (1977) Uridine phosphorylase from *Escherichia coli*. Physical and chemical characterization. *Eur. J Biochem* **75**(1) 217 - 224.
74. **Lewandowicz, A; Shi, W; Evans, GB; Tyler, PC; Furneaux, RH; Basso, LA; Santos, DS; Almo, SC; and Schramm, VL** (2003) Over-the-barrier transition state analogues and crystal structure with *Mycobacterium tuberculosis* purine nucleoside phosphorylase. *Biochemistry* **42**(20) 6057 - 6066.
75. **Lewkowicz, ES and Iribarren, AM** (2006) Nucleoside Phosphorylases. *Curr. Org. Chem.* **10**1197 - 1295.
76. **Lewkowicz, ES; Martinez, N; Rogert, MC; Porro, S; and Iribarren, AM** (2000) An improved microbial synthesis of purine nucleosides. *Biotechnol. Lett.* **22**1277 - 1280.
77. **Li, N; Smith, TJ; and Zong, MH** (2010) Biocatalytic transformation of nucleoside derivatives. *Biotechnol. Adv.* **28**(3) 348 - 366.
78. **Ling, F; Inoue, Y; and Kimura, A** (1990) Purification and characterization of a novel nucleoside phosphorylase from a *Klebsiella sp.* and its use in the enzymatic production of adenine arabinoside. *Appl. Environ. Microbiol.* **56**(12) 3830 - 3834.

-
79. **Louw, ME; Reid, SJ; and Watson, TG** (1993) Characterization, cloning and sequencing of a thermostable endo-(1,3-1,4) beta-glucanase-encoding gene from an alkalophilic *Bacillus brevis*. *Appl. Microbiol. Biotechnol.* **38**(4) 507 - 513.
 80. **Lovett, PS and Keggins, KM** (1979) *Bacillus subtilis* as a host for molecular cloning. *Meth. Enzymol.* **68** 342 - 357.
 81. **Luli, GW and Strohl, WR** (1990) Comparison of growth, acetate production, and acetate inhibition of *Escherichia coli* strains in batch and fed-batch fermentations. *Appl. Environ. Microbiol.* **56**(4) 1004 - 1011.
 82. **Mao, C; Cook, WJ; Zhou, M; Koszalka, GW; Krenitsky, TA; and Ealick, SE** (1997) The crystal structure of *Escherichia coli* purine nucleoside phosphorylase: a comparison with the human enzyme reveals a conserved topology. *Structure.* **5**(10) 1373 - 1383.
 83. **Medici, R; Porro, MT; Lewkowicz, ES; Montserrat, E; and Iribarren, AM** (2004) Coupled biocatalysts applied to the synthesis of nucleosides. *Nucleic Acids Symp Ser 2008* 541 - 542.
 84. **Mikhailopulo, IA** (2007) Biotechnology of nucleic acid constituents - state of the art and perspectives. *Curr. Org. Chem.* **11** 317 - 333.
 85. **Miyazaki, K and Takenouchi, M** (2002) Creating random mutagenesis libraries using megaprimer PCR of whole plasmid. *Biotechniques* **33**(5) 1033 - 1038.
 86. **Montgomery, JA** (1993) Purine nucleoside phosphorylase: a target for drug design. *Med. Res. Rev.* **13**(3) 209 - 228.
 87. **Montgomery, JA; Niwas, S; Rose, JD; Secrist, JA, III; Babu, YS; Bugg, CE; Erion, MD; Guida, WC; and Ealick, SE** (1993) Structure-based design of inhibitors of purine nucleoside phosphorylase. 1. 9-(arylmethyl) derivatives of 9-deazaguanine. *J. Med. Chem.* **36**(1) 55 - 69.
 88. **Morgunova, EY; Mikhailov, AM; Popov, AN; Blagova, EV; Smirnova, EA; Vainshtein, BK; Mao, C; Armstrong, S; Ealick, SE; Komissarov, AA.** (1995) Atomic structure at 2.5 Å resolution of uridine phosphorylase from *E. coli* as refined in the monoclinic crystal lattice. *FEBS Lett.* **367**(2) 183 - 187.
 89. **Myers, RM; Lerman, LS; and Maniatis, T** (1985) A general method for saturation mutagenesis of cloned DNA fragments. *Science* **229**(4710) 242 - 247.
 90. **Narayana, SV; Bugg, CE; and Ealick, SE** (1997) Refined structure of purine nucleoside phosphorylase at 2.75 Å resolution. *Acta Crystallogr. D. Biol. Crystallogr.* **53**(Pt 2) 131 - 142.
 91. **Niedballa, U and Vorbru'eggen, H** (1974) A general synthesis of N-glycosides. I. Synthesis of pyrimidine nucleosides. *J Org. Chem.* **39**(25) 3654 - 3660.
 92. **Niedzwicki, JG and M.H.el Kouni** (1983) Structure-activity relationship of ligands of the pyrimidine nucleoside phosphorylases. *Biochem Pharmacol* **32**(3) 399 - 415.

93. **Norman, RA; Barry, ST; Bate, M; Breed, J; Colls, JG; Ernil, RJ; Luke, RW; Minshull, CA; McAlister, MS; McCall, EJ; McMiken, HH; Paterson, DS; Timms, D; Tucker, JA; and Pauptit, RA** (2004) Crystal structure of human thymidine phosphorylase in complex with a small molecule inhibitor. *Structure* **12**(1) 75 - 84.
94. **Ogawa, T and Matsui, M** (1978) A stannyl modification of the Hilbert-Johnson method for the synthesis of pyrimidine nucleosides. *J Organomet. Chem.* **145**(3) C37 - C40.
95. **Okamoto, H; Cujec, TP; Okamoto, M; Peterlin, BM; Baba, M; and Okamoto, T** (2000) Inhibition of the RNA-dependent transactivation and replication of human immunodeficiency virus type 1 by a fluoroquinoline derivative K-37. *Virology* **272**(2) 402 - 408.
96. **Okuyama, K; Hamamoto, T; Noguchi, T; and Midorikawa, Y** (1996) Molecular cloning and expression of the pyrimidine nucleoside phosphorylase gene from *Bacillus stearothermophilus* TH 6-2. *Biosci. Biotechnol. Biochem.* **60**(10) 1655 - 1659.
97. **Oliva, I; Zuffi, G; Orsini, G; Tonon, G; De Gioia, L; and Ghisotti, D** (2004) Mutagenesis of *Escherichia coli* uridine phosphorylase by random pentapeptide insertions. *Enz. Micro. Tech.* **35**(4) 309 - 314.
98. **Pal, S and Nair, V** (1997) Enzymatic synthesis of thymidine using bacterial whole cells and isolated purine nucleoside phosphorylase. *Biocat. Biotrans.* **5**(2) 147 - 158.
99. **Palella, FJ, Jr.; Delaney, KM; Moorman, AC; Loveless, MO; Fuhrer, J; Satten, GA; Aschman, DJ; and Holmberg, SD** (1998) Declining morbidity and mortality among patients with advanced human immunodeficiency virus infection. HIV Outpatient Study Investigators. *N. Engl. J Med.* **338**(13) 853 - 860.
100. **Pollard, DJ and Woodley, JM** (2007) Biocatalysis for pharmaceutical intermediates: the future is now. *Trends Biotechnol.* **25**(2) 66 - 73.
101. **Prasad, AK; Trikha, S; and Parmar, VS** (1999) Nucleoside Synthesis Mediated by Glycosyl Transferring Enzymes. *Bioorg. Chem.* **27**(2) 135 - 154.
102. **Pugmire, MJ and Ealick, SE** (1998) The crystal structure of pyrimidine nucleoside phosphorylase in a closed conformation. *Structure.* **6**(11) 1467 - 1479.
103. **Pugmire, MJ and Ealick, SE** (2002) Structural analyses reveal two distinct families of nucleoside phosphorylases. *Biochem. J.* **361**(Pt 1) 1 - 25.
104. **Ramchuran, S; Nordburg Karlsson, E; Velut, S; de Mare, L; Hagander, P; and Holst, O** (2002) Production of heterologous thermostable glycoside hydrolases and the presence of host-cell proteases in substrate limited fed-batch cultures of *Escherichia coli* BL21(DE3). *Appl. Microbiol. Biotechnol.* **60**(4) 408 - 416.
105. **Razzell, WE and Casshyap, P** (1964) Substrate specificity and induction of thymidine phosphorylase in *Escherichia Coli*. *J Biol Chem* **239**1789 - 1783.

106. **Reetz, MT; Bocola, M; Carballeira, JD; Zha, DX; and Vogel, A** (2005) Expanding the range of substrate acceptance of enzymes: Combinatorial active-site saturation test. *Ange. Chem. Int. Ed.* **44**(27) 4192 - 4196.
107. **Reetz, MT and Carballeira, JD** (2007) Iterative saturation mutagenesis (ISM) for rapid directed evolution of functional enzymes. *Nature Prot.* **2**(4) 891 - 903.
108. **Reetz, MT; Carballeira, JD; Peyralans, J; Hobenreich, H; Maichele, A; and Vogel, A** (2006a) Expanding the substrate scope of enzymes: Combining mutations obtained by CASTing. *Chem. Euro. J.* **12**(23) 6031 - 6038.
109. **Reetz, MT; Carballeira, JD; and Vogel, A** (2006b) Iterative saturation mutagenesis on the basis of B factors as a strategy for increasing protein thermostability. *Ange. Chem. Int. Ed.* **118**7909 - 7915.
110. **Reetz, MT; Wang, LW; and Bocola, M** (2006c) Directed evolution of enantioselective enzymes: Iterative cycles of CASTing for probing protein-sequence space (vol 45, pg 1236, 2006). *Ange. Chem. Int. Ed.* **45**(16) 2494 - 2494.
111. **Rey, MW; Ramaiya, P; Nelson, BA; Brody-Karpin, SD; Zaretsky, EJ; Tang, M; Lopez, dL; Xiang, H; Gusti, V; Clausen, IG; Olsen, PB; Rasmussen, MD; Andersen, JT; Jorgensen, PL; Larsen, TS; Sorokin, A; Bolotin, A; Lapidus, A; Galleron, N; Ehrlich, SD; and Berka, RM** (2004) Complete genome sequence of the industrial bacterium *Bacillus licheniformis* and comparisons with closely related *Bacillus* species. *Genome Biol* **5**(10) R77 -
112. **Rinaldo-Matthis, A; Wing, C; Ghanem, M; Deng, H; Wu, P; Gupta, A; Tyler, PC; Evans, GB; Furneaux, RH; Almo, SC; Wang, CC; and Schramm, VL** (2007) Inhibition and structure of *Trichomonas vaginalis* purine nucleoside phosphorylase with picomolar transition state analogues. *Biochemistry* **46**(3) 659 - 668.
113. **Rocchietti, S; Ubiali, D; Terreni, M; Albertini, AM; Fernandez-Lafuente, R; Guisan, JM; and Pregnotato, M** (2004) Immobilisation and stabilization of recombinant multimeric uridine and purine nucleoside phosphorylases from *Bacillus subtilis*. *Biomacromolecules.* **5**(6) 2195 - 2200.
114. **Rogert, MC; Trelles, JA; Porro, S; Lewkowicz, ES; and Iribarren, AM** (2002) Microbial synthesis of antiviral nucleosides using *Escherichia coli* BL21 as biocatalyst. *Biocat. Biotrans.* **20**(5) 347 - 351.
115. **Roosild, TP; Castronovo, S; Fabbiani, M; and Pizzorno, G** (2009) Implications of the structure of human uridine phosphorylase 1 on the development of novel inhibitors for improving the therapeutic window of fluoropyrimidine chemotherapy. *BMC. Struct. Biol* **9**14 -
116. **Saen-Oon, S; Ghanem, M; Schramm, VL; and Schwartz, SD** (2008) Remote mutations and active site dynamics correlate with catalytic properties of purine nucleoside phosphorylase. *Biophys. J.* **94**(10) 4078 - 4088.
117. **Sambrook, J and Russell, DW.**(2001). *Molecular Cloning: A Laboratory Manual*. Cold Spring Harbor Laboratory Press. New York.

118. **Saunders, PP; Wilson, BA; and Saunders, GF** (1969) Purification and comparative properties of a pyrimidine nucleoside phosphorylase from *Bacillus stearothermophilus*. *J. Biol. Chem.* **244**(13) 3691 - 3697.
119. **Schimandle, CM; Tanigoshi, L; Mole, LA; and Sherman, IW** (1985) Purine nucleoside phosphorylase of the malarial parasite, *Plasmodium lophurae*. *J. Biol. Chem.* **260**(7) 4455 - 4460.
120. **Schramm, V; Furneaux, RH; Tyler, PC; and Clinch, K** (2002) Enzyme detection/assay method and substrates. *US Patent* (US20020132263A1)
121. **Schuch, R; Garibian, A; Saxild, HH; Piggot, PJ; and Nygaard, P** (1999) Nucleosides as a carbon source in *Bacillus subtilis*: characterization of the *drm-pupG* operon. *Microbiology* **145** (Pt 10)2957 - 2966.
122. **Sheldon, RA** (2007) Cross-linked enzyme aggregates (CLEAs): stable and recyclable biocatalysts. *Biochem Soc. Trans.* **35**(Pt 6) 1583 - 1587.
123. **Shimizu, B; Asai, M; and Nishimura, T** (1965) A convenient synthesis of nucleotides. *Chem. Pharm. Bull.* **13**(2) 230 - 232.
124. **Shimizu, K and Kunishima, N** (2007) Purification, crystallization and preliminary X-ray diffraction study on pyrimidine nucleoside phosphorylase TTHA1771 from *Thermus thermophilus* HB8. *Acta Crystallogr. Sect. F. Struct. Biol. Cryst. Commun.* **63**(Pt 4) 308 - 310.
125. **Shirae, H and Yokozeki, K** (1991) Purifications and properties of orotidine-phosphorolyzing enzyme and purine nucleoside phosphorylase from *Erwinia carotovora* AJ 2992. *Agric. Biol. Chem.* **55**(7) 1849 - 1857.
126. **Shiragami, H; Amino, Y; Honda, Y; Arai, M; Tanaka, Y; Iwagami, H; Yukawa, T; and Izawa, K** (1996) Synthesis of 2',3'-dideoxypurinenucleosides via the palladium catalyzed reduction of 9-(2,5-Di-O-acetyl-3-bromo-3-deoxy- β -D-xylofuranosyl)purine derivatives. *Nucleosides and Nucleotides* **15**(1) 31 - 45.
127. **Spoldi, E; Ghisotti, D; Cali, S; Grisa, M; Orsini, G; Tonon, G; and Zuffi, G** (2001) Recombinant bacterial cells as efficient biocatalysts for the production of nucleosides. *Nucleosides Nucleotides Nucleic Acids* **20**(4-7) 977 - 979.
128. **St Clair, NL and Navia, MA** (2008) Cross-linked enzyme crystals as robust biocatalysts. *J. Am. Chem. Soc.* **114**7314 - 7316.
129. **Stemmer, WP** (1994) Rapid evolution of a protein in vitro by DNA shuffling. *Nature* **370**(6488) 389 - 391.
130. **Stoeckler, JD; Bell, CA; Parks, RE, Jr.; Chu, CK; Fox, JJ; and Ikehara, M** (1982) C(2')-substituted purine nucleoside analogs. Interactions with adenosine deaminase and purine nucleoside phosphorylase and formation of analog nucleotides. *Biochem. Pharmacol.* **31**(9) 1723 - 1728.
131. **Straathof, AJJ; Panke, S; and Schmid, A** (2002) The production of fine chemicals by biotransformations. *Curr. Op. Biotechnol.* **13**(6) 548 - 556.

-
132. **Tahirov, TH; Inagaki, E; Ohshima, N; Kitao, T; Kuroishi, C; Ukita, Y; Takio, K; Kobayashi, M; Kuramitsu, S; Yokoyama, S; and Miyano, M** (2004) Crystal structure of purine nucleoside phosphorylase from *Thermus thermophilus*. *J. Mol. Biol.* **337**(5) 1149 - 1160.
133. **Takami, H; Nakasone, K; Takaki, Y; Maeno, G; Sasaki, R; Masui, N; Fuji, F; Hirama, C; Nakamura, Y; Ogasawara, N; Kuhara, S; and Horikoshi, K** (2000) Complete genome sequence of the alkaliphilic bacterium *Bacillus halodurans* and genomic sequence comparison with *Bacillus subtilis*. *Nucleic Acids Res.* **28**(21) 4317 - 4331.
134. **Taran, SA; Verevkina, KN; Feofanov, SA; and Miroshnikov, AI** (2009) Enzymatic transglycosylation of natural and modified nucleosides by immobilised thermostable nucleoside phosphorylases from *Geobacillus stearothermophilus*. *Bioorg. Khim.* **35**(6) 822 - 829.
135. **Taylor, EA; Rinaldo-Matthis, A; Li, L; Ghanem, M; Hazleton, KZ; Cassera, MB; Almo, SC; and Schramm, VL** (2007) *Anopheles gambiae* purine nucleoside phosphorylase: catalysis, structure, and inhibition. *Biochemistry* **46**(43) 12405 - 12415.
136. **Titti, F; Cafaro, A; Ferrantelli, F; Tripiciano, A; Moretti, S; Caputo, A; Gavioli, R; Ensoli, F; Robert-Guroff, M; Barnett, S; and Ensoli, B** (2007) Problems and emerging approaches in HIV/AIDS vaccine development. *Expert. Opin. Emerg. Drugs* **12**(1) 23 - 48.
137. **Tobias, AV** (2003) Preparing Libraries in *Escherichia coli*. (2) 11-16.
138. **Tonon, G; Capra, E; Orsini, G; and Zuffi, G.** Novel immobilised biocatalysts usable for the production of natural nucleosides and modified analogues by enzymatic transglycosylation reactions. [US20040142438]. 2004.
139. **Trelles, JA; Bentancor, L; Grasselli, M; Lewkowicz, ES; and Iribarren, AM** (2008) Nucleoside synthesis using a novel macroporous grafted polyethylene as biocatalyst support. *J Mol. Cat. B: Enz.* **52-53** 189 - 193.
140. **Trelles, JA; Bentancor, L; Schoijet, A; Porro, S; Lewkowicz, ES; Sinisterra, JV; and Iribarren, AM** (2004) Immobilised *Escherichia coli* BL21 as a catalyst for the synthesis of adenine and hypoxanthine nucleosides. *Chem Biodivers.* **1**(2) 280 - 288.
141. **UNICEF; WHO; and UNAIDS** (2009) Towards Universal Access: Scaling up Priority HIV/AIDS interventions in the health sector.
142. **Utagawa, T** (1999) Enzymatic preparation of nucleoside antibiotics. *J Mol. Cat. B: Enz* **6**(3) 215 - 222.
143. **van de, WM and Shiloach, J** (1998) Proposed mechanism of acetate accumulation in two recombinant *Escherichia coli* strains during high density fermentation. *Biotechnol. Bioeng.* **57**(1) 71 - 78.
144. **Venkata, RR; Mukund, KG; and Sista, VS.** Method for the production of 5-methyluridine. [US 5596087]. 1997.

145. **Visser, DF; Hennessy, F; Rashamuse, K; Gordon, GER; Bode, ML; and Brady, D.** A biocatalytic method for synthesis of 5-methyluridine. [WO2010055369]. 2009.
146. **Visser, DF; Hennessy, F; Rashamuse, K; Louw, ME; and Brady, D** (2010a) Cloning, purification and characterisation of a recombinant purine nucleoside phosphorylase from *Bacillus halodurans* Alk36. *Extremophiles*. **14**(2) 185 - 192.
147. **Visser, DF; Rashamuse, KJ; Hennessy F; Gordon, GER; Van Zyl, PJ; Mathiba, K; Bode, ML; and Brady, D.** (2010b) High-yielding cascade enzymatic synthesis of 5-methyluridine using a novel combination of nucleoside phosphorylases. *Biocat. Biotrans.* **28** 245-253.
148. **Walter, MR; Cook, WJ; Cole, LB; Short, SA; Koszalka, GW; Krenitsky, TA; and Ealick, SE** (1990) Three-dimensional structure of thymidine phosphorylase from *Escherichia coli* at 2.8 Å resolution. *J Biol Chem* **265**(23) 14016 - 14022.
149. **Walton, L; Richards, CA; and Elwell, LP** (1989) Nucleotide sequence of the *Escherichia coli* uridine phosphorylase (*udp*) gene. *Nucleic Acids Res.* **17**(16) 6741 -
150. **Weiss, RA** (1993) How does HIV cause AIDS? *Science* **260**(5112) 1273 - 1279.
151. **Wielgus-Kutrowska, B; Bzowska, A; Tebbe, J; Koellner, G; and Shugar, D** (2002) Purine nucleoside phosphorylase from *Cellulomonas sp.*: physicochemical properties and binding of substrates determined by ligand-dependent enhancement of enzyme intrinsic fluorescence, and by protective effects of ligands on thermal inactivation of the enzyme. *Biochim. Biophys. Acta* **1597**(2) 320 - 334.
152. **Williams, SR; Goddard, JM; and Martin, DW, Jr.** (1984) Human purine nucleoside phosphorylase cDNA sequence and genomic clone characterization. *Nucl. Acids Res.* **12**(14) 5779 - 5787.
153. **Wilson, L; Betancor, L; Fernandez-Lorente, G; Fuentes, M; Hidalgo, A; Guisan, JM; Pessela, BC; and Fernandez-Lafuente, R** (2004) Cross-linked aggregates of multimeric enzymes: a simple and efficient methodology to stabilize their quaternary structure. *Biomacromolecules*. **5**(3) 814 - 817.
154. **Woodley, JM** (2006a) Choice of biocatalyst form for scalable processes. *Biochem Soc. Trans.* **34**(Pt 2) 301 - 303.
155. **Woodley, JM** (2006b) Microbial biocatalytic processes and their development. *Adv. Appl. Microbiol.* **60**1 - 15.
156. **Zaks, A and Dodds, DR** (1997) Application of biocatalysis and biotransformations to the synthesis of pharmaceuticals. *Drug Discovery Today* **2**(12) 513 - 531.
157. **Zhao, H; Giver, L; Shao, Z; Affholter, JA; and Arnold, FH** (1998) Molecular evolution by staggered extension process (StEP) in vitro recombination. *Nat. Biotechnol.* **16**(3) 258 - 261.
158. **Zoref-Shani, E; Bromberg, Y; Lilling, G; Gozes, I; Brosh, S; Sidi, Y; and Sperling, O** (1995) Developmental changes in purine nucleotide metabolism in cultured rat astroglia. *Int. J. Dev. Neurosci.* **13**(8) 887 - 896.

159. **Zuffi, G; Ghisotti, D; Oliva, I; Capra, E; Frascotti, G; Tonon, G; and Orsini, G** (2004) Immobilised biocatalysts for the production of nucleosides and nucleoside analogues by enzymatic transglycosylation reactions. *Biocat. Biotrans.* **22**(1) 25 - 33.

Published Journal Articles

(See Next Page)

Cloning, purification and characterisation of a recombinant purine nucleoside phosphorylase from *Bacillus halodurans* Alk36

Daniel F. Visser · Fritha Hennessy ·
Konanani Rashamuse · Maureen E. Louw ·
Dean Brady

Received: 22 September 2009 / Accepted: 16 December 2009 / Published online: 9 January 2010
© The Author(s) 2010. This article is published with open access at Springerlink.com

Abstract A purine nucleoside phosphorylase from the alkaliphile *Bacillus halodurans* Alk36 was cloned and overexpressed in *Escherichia coli*. The enzyme was purified fivefold by membrane filtration and ion exchange. The purified enzyme had a V_{\max} of $2.03 \times 10^{-9} \text{ s}^{-1}$ and a K_m of 206 μM on guanosine. The optimal pH range was between 5.7 and 8.4 with a maximum at pH 7.0. The optimal temperature for activity was 70°C and the enzyme had a half life at 60°C of 20.8 h.

Keywords Nucleoside phosphorylase · Biocatalysis · Guanosine · 5-Methyluridine · *Bacillus halodurans*

Abbreviation

BHPNP1 *Bacillus halodurans* purine nucleoside phosphorylase 1

Introduction

5-Methyluridine is a non-natural nucleoside that can be used as an intermediate in the synthesis of thymidine, and

in the synthesis of nucleoside analogues AZT and stavudine, both of which are used in highly active antiretroviral treatment of HIV/AIDS patients. As the compound needs to be formed as a single isomer, 5-methyluridine can be synthesised through the transglycosylation of D-ribose-1-phosphate, using guanosine as a donor, and thymine as receptor (Ge et al. 2009; Medici et al. 2008; Rocchietti et al. 2004). Enzymes provide regio- and stereoselectivity, and hence are an ideal option for nucleoside transglycosylation (Prasad et al. 1999; Utagawa 1999). The hydrolysis reaction for the ribose decoupling reaction can be achieved using purine nucleoside phosphorylase (PNPase; EC 2.4.2.1) (Fig. 1).

However, the reagents guanosine and thymine are relatively insoluble, and are particulate substrates with poor reaction kinetics. The most effective method of solubilising these materials is in hot aqueous solutions. Therefore, it would be preferable to utilise thermostable enzymes to catalyse these reactions. Enzymes that can be used in this transglycosylation reaction include PNPase, thymidine phosphorylase (TPase; EC 2.4.2.4) and uridine phosphorylase (UPase; EC 2.4.2.3) (Bzowska et al. 2000; Pugmire and Ealick 2002). TPase and UPase are functionally both pyrimidine nucleoside phosphorylases (PyNPase; EC 2.4.2.2.), although UPase is closer in sequence identity to PNPase than PyNPase (Lewkowicz and Iribarren 2006). PNPases are divided into two different classes depending on their tertiary and quaternary structures (Bzowska et al. 2000). Type I PNPases tend to be bacterial in origin and, based on sequence and structural information, appear to have a hexameric structure. Type II PNPases tend to be found in eukaryotes and, based on the sequence and structural information, are trimeric in structure (Bzowska et al. 2000; Pugmire and Ealick 2002). Bzowska et al. (2000) refer to type I PNPases as high molecular mass

Communicated by L. Huang.

D. F. Visser · F. Hennessy (✉) · K. Rashamuse · D. Brady
Enzyme Technologies Group, CSIR Biosciences,
Private Bag X2, Modderfontein,
Johannesburg 1645, South Africa
e-mail: fhennessy@csir.co.za

M. E. Louw
Microbial Expression Systems, CSIR Biosciences,
PO Box 395, Pretoria 0001, South Africa

DNA sequencing

The insert was sequenced at Inqaba Biotechnology (Pretoria, South Africa) using the PCR primers described above. The sequence was compared with the known nucleotide and amino acid sequence of the BH1531 gene from *B. halodurans* C-125 (protein sequence—BAB05250) and has been submitted to GenBank under the accession number GQ390428.

Homology modelling

Multiple sequence alignments were performed using ClustalW (Larkin et al. 2007). Homology modelling was performed using Accelrys Discovery Studio 2.0. A trimeric model was based on the bovine structure 1LVU (Bzowska et al. 2004). A second model was based on the monomeric structure 1VFN (Koellner et al. 1997). Bovine PNPase and BHPNP1 have 49% sequence identity and 61% sequence similarity (Table 1).

Growth and induction

Recombinant *E. coli* strains were grown in 50 ml LB medium with 100 µg/ml ampicillin, at 37°C with shaking at 200 rpm. Cultures were induced with 0.25 mM IPTG when they had reached an OD₆₀₀ between 0.05 and 0.1. Cultures were subsequently grown at 30°C with shaking at 150 rpm overnight for enzyme expression.

Batch fermentations

A 1.5 l InFors HT batch fermentor (Labfors, Switzerland) containing 1 l of GMO 20 medium was inoculated with a 50 ml inoculum (overnight culture of *E. coli* JM109 [pMSPNP] in LB medium). The composition of the GMO 20 medium was as follows: 14.6 g/l K₂HPO₄, 2 g/l (NH₄)₂SO₄, 3.6 g/l Na₂HPO₄, 2.5 g/l citric acid, 1.2 g/l MgSO₄, 5 g/l NH₄NO₃, and 20 g/l yeast extract. Glucose (17.5 g/l) and trace element solution (5 ml/l) was sterilized separately and added to the fermenters before inoculation.

Ampicillin (100 µg/ml) was aseptically added to the flasks containing the glucose and trace element solution. The trace element solution consisted of the following: 0.4 g/l CaCl₂·2H₂O, 16.7 g/l FeCl₃·6H₂O, 0.15 g/l MnCl₂·4H₂O, 0.18 g/l ZnSO₄·7H₂O, 0.125 g/l CuCl₂·2H₂O, 0.18 g/l CoCl₂·6H₂O, and 20.1 g/l Na₂EDTA. The pH of the fermentations was controlled at pH 7.2 with 33% *m/v* NH₄OH or 20% *m/v* H₂SO₄. The temperature was controlled at 37°C and the aeration set to 1 *v/v/m*. The starting agitation was set at 300 rpm and ramped up manually to control the pO₂ above 30% saturation. PNPase expression was induced at mid-log phase by adding IPTG to a final broth concentration of 0.5 mM. Fermentations were run for a further 4 h after induction.

Preparation of crude extract

After induction, the bacteria were harvested by centrifugation (15,000g, 20 min). The pellet was re-suspended in minimal sterile deionised water, and subjected to a freeze–thaw cycle alternating between +20 and –20°C. Liberated protein was separated by centrifugation (14,000g, 10 min) and stored. The pellet was re-suspended in 1 l sterile deionised water and further disrupted using a cell disruptor (2 Plus, Constant Systems, UK) with 1 pass at 40 kpsi. Cellular debris was removed by centrifugation (15,000g, 10 min). The resultant protein solution (supernatants from freeze–thaw and cell disruption processes) were concentrated and washed once with sterile deionised water by ultrafiltration using an Amicon (Millipore, USA) stirred cell ultrafiltration unit (30 kDa cut-off polyethersulfone membrane). The final preparation was lyophilised in the presence of 1% maltose and 1% PEG 8000 (Vertis Genesis 25 l). A portion of the lyophilised product, equivalent to 200 ml original fermentation broth, was re-suspended in 20 mM Tris–HCl buffer (pH 7.5) for further purification.

Column chromatography

Anion exchange chromatography of each sample was performed on an AKTA Prime (Amersham Biosciences,

Table 1 Comparison of various PNPases to BHPNP1

Protein	Percentage of protein identity	Percentage of protein similarity	PNPase type	Accession number
<i>E. coli</i> PNP	17.0	33.0	I	P0ABP8
<i>E. coli</i> XapA	44.0	61.0	II	NP_416902
<i>G. stearothermophilus</i> PNP1	74.9	86.2	II	P77834
Bovine PNP	47.1	61.1	II	P55859
Human PNP	45.2	58.5	II	P00491
<i>B. halodurans</i> BH1532	57.1	75.6	II	BAB05251
<i>B. subtilis</i> PNP	69.6	78.8	II	P46354
<i>G. stearothermophilus</i> PNP2	18.3	32.2	I	P77835

UK) using Toyopearl SuperQ650m anion exchange resin (Tosoh BioSep, USA). Protein was first eluted from the column using a salt gradient of between 50 and 500 mM NaCl in 20 mM Tris–HCl pH 7.2, over 400 ml at a flow rate of 4 ml/min. PNPase activity was assayed in all fractions (5 ml fractions collected) and those containing activity were separately pooled and concentrated by ultrafiltration (30 kDa membrane, Millipore USA). This sample was then re-applied to the anion exchange column and eluted over a salt gradient of 150–400 mM NaCl. Active fractions were pooled and concentrated by ultrafiltration as above.

Tertiary conformation

Denatured (5 min, 95°C) and non-denatured preparations of the enzyme were analysed on a 12% SDS-PAGE gel. The gel was overlaid with a 0.5% agarose solution to determine the position of active subunits. The agarose solution contained 10 mM inosine, 0.2 U/ml xanthine oxidase and 10 mM INT (iodonitrotetrazolium violet) in 20 mM sodium phosphate buffer, pH 7.5. Active PNPase is indicated by a red/pink band on the gel due to the cascade action of the PNPase and xanthine oxidase leading to the reduction of INT to its tetrazolium salt. Positions of active and non-active units were then confirmed by staining the gel with Coomassie brilliant blue G-250.

PNPase assay

A volume (10 µl) of suitably diluted sample was added to 190 µl of 50 mM sodium phosphate buffer containing 0.5 mM inosine and 0.2 U/ml of xanthine oxidase in UV compatible microtitre plates (Thermomix) (Erion et al. 1997). The change in absorbance at 293 nm due to the liberation of uric acid was measured on a Powerwave HT microplate spectrophotometer (Biotek, USA). One unit of PNPase is defined as the amount of enzyme required to liberate 1 µmol of uric acid from inosine, in the presence of an excess of xanthine oxidase, in 1 min. The extinction coefficient (ϵ) under these conditions was determined to be 7,454 cm²/mol.

Physical characteristics

A pH profile was performed using reaction mixtures (1 ml) containing 1 mM guanosine in 50 mM universal buffer (50 mM Tris, 50 mM boric acid, 33 mM citric acid 50 mM Na₂PO₄), adjusted to pH values between 3 and 11 with either HCl or NaOH. PNPase (0.025 U) was added to initiate the reaction. After 10 min of incubation at 40°C, the reaction was stopped by the addition of 0.5 ml of a 5 M NaOH solution. Guanosine conversion and guanine

formation were analysed by HPLC on a Waters 2690 HPLC (interfaced with Waters Millennium Software) equipped with Waters 996 Photodiode Array Detector at 260 nm and a Phenomenex Synergi 4u Max-RP 80A, 150 × 4.60 mm column at 22°C. The mobile phase was 25 mM ammonium acetate (pH 4.0), at a flow rate of 1.0 ml/min.

The temperature optimum was determined with reaction mixtures (1 ml) containing 1 mM guanosine in 50 mM sodium phosphate buffer, pH 8.0. PNPase (0.025 U) was added to initiate the reaction. After 10 min of incubation at temperatures between 30°C and 90°C, the reaction was stopped by the addition of 0.5 ml of a 5 M NaOH solution. Guanosine conversion and guanine formation were analysed by HPLC as above. For temperature stability, enzyme solutions were incubated at temperatures between 40 and 70°C. Samples were removed and analysed every 30 min for the first 2 h, followed by less frequent sampling for a further 18 h.

Kinetic parameters

The kinetic parameters for PNPase were determined for both inosine (standard assay) and guanosine (assay as described for temperature optimum study) as starting substrates. Initial substrate concentrations were varied between 0.05 and 1.0 mM. The reaction was stopped at 1, 2, 3, 4, 6 and 10 min to ensure measurements remained in the linear range. Michaelis–Menten plots and the linear transformations (Lineweaver–Burk, Hanes–Woolf and Eadie–Hofstee) were used to determine kinetic parameters.

Results and discussion

Sequence analysis and homology modelling

Bacillus halodurans is unusual amongst the *Bacilli* that have been completely sequenced so far in that it contains two type II PNPases as opposed to the types I and II PNPases present in other *Bacillus* species (unpublished data). The gene sequence of BHPNP1 was identical to that of BH1531 from *B. halodurans* C-125 except for a silent substitution at nucleotide 519 (C–T), and hence the protein sequence was identical to that expressed by *B. halodurans* C-125. BLAST analysis indicated that the closest related structure deposited in the protein data base (PDB) was that of the bovine PNP (Table 1; Fig. 2) which is 47% identical to BHPNP1. On the basis of sequence identity, BH1531 is a member of the type II PNPases.

BHPNP1 has low levels of identity to type I PNPases, such as *E. coli* PNP and *G. stearothermophilus* PNP2 (17 and 18.3% identity, respectively). It has higher levels of identity to type II PNPases. Selected type II PNPases were

Fig. 2 Multiple sequence alignment comparing BHPNP1 to other type II PNPases. BHPNP1 was aligned with *G. stearothermophilus* PNP1 (P77834) (Hamamoto et al. 1997a), bovine PNP (P55859) (Bzowska et al. 1995), human PNP (P00491) (Williams et al. 1984), *B. subtilis* PNP (P46354) (Schuch et al. 1999), the second *B. halodurans* PNP (BH1532, BAB05251) (Takami et al. 2000) and *E. coli* XapA (NP_416902) (Dandaneil et al. 2005). The alignment was generated using ClustalW (Larkin et al. 2007; <http://www.ebi.ac.uk/clustalw>). Residues shown to be important in the binding site of bovine and human PNPases are underlined (Mao et al. 1997, 1998; Montgomery et al. 1993; Narayana et al. 1997). Dots (.) and asterisks (*) indicate partial similarity and asterisks (*) indicate a 100% match

Bovine	MANGYTYEDYQDTAKWLLSHTEQ---- <td>55</td>	55
Human	MENGYTYEDYKNTAEWLLSHTKH---- <td>55</td>	55
<i>B. halodurans</i>	---MLNVTLQEQEATTFIQQQIET-----KPTIGLILGSGGLGLADEIEQPVKVPSDIIPN	52
<i>G. stearothermophilus</i>	----MNRTAIEQAAQFLKEKFFP-----SQPIGLILGSGGLVLADEIEQAIKIPYSDIIPN	51
<i>B. subtilis</i>	----MKDRIERAAAFIKQNLPE-----SPKIGLILGSGGLGLADEIENPVKLYEDIPE	50
BH1532	---MENIREKVKQSAEYLLGKIKN-----KPAIGLILGSGGLGELANEIEEAVHIPPYEQIPN	53
<i>E. coli</i>	---MSQVQFSHNPLFCIDIKTYPDFTPRVAFILGSGGLGALADQIENAVASPYEKPLG	56
	: : : : : : : : : : * : : * : : * : : * : : * : : * : : *	
Bovine	FPFESTVPGHAGRLVFGILNGRACVMMQGRFHMVYCYFPWKVTFPVRVFRLLGVETLVVIN	115
Human	FPRSTVPGHAGRLVFGFLNGRACVMMQGRFHMVYCYPLWKVTFPVRVFRLLGVDTLVVIN	115
<i>B. halodurans</i>	FPVSTVQGHAGQLVIGMLEGKQVIAMQGRFHFYCYGSLVVTFPVRVVKALGVEQLIVIN	112
<i>G. stearothermophilus</i>	FPVSTVQGHAGQLVIGMLEGKQVIAMQGRFHFYCYGSLVVTFPVRVVKALGVEQLIVIN	111
<i>B. subtilis</i>	FPVSTVQGHAGQLVIGMLEGKQVIAMQGRFHFYCYGSLVVTFPVRVVKALGVEQLIVIN	110
BH1532	FPVSTVQGHAGQLVIGMLEGKQVIAMQGRFHFYCYGSLVVTFPVRVVKALGVEQLIVIN	113
<i>E. coli</i>	FPVSTVQGHAGQLVIGMLEGKQVIAMQGRFHFYCYGSLVVTFPVRVVKALGVEQLIVIN	116
	* * * * * : : : * : : * : : * : : * : : * : : * : : * : : *	
Bovine	AAGGLNPNFVGDIMLIRDHINLPGFSGENPLRGPNEERFVGRFAMSDAYDRDMRQKAH	175
Human	AAGGLNPNKFEVGDIMLIRDHINLPGFSGENPLRGPNEERFVGRFAMSDAYDRDMRQRAL	175
<i>B. halodurans</i>	AAGGVNE SFEAGDLMII RDHINN---MAQNPFLIGPNDEAFGVRFPDM SNAYSERLRRLAK	169
<i>G. stearothermophilus</i>	AAGGVNE SFEAGDLMII SDHINN---MCGNPFLIGPNDSALGVRFPM SNAYSERLRRLAK	168
<i>B. subtilis</i>	AAGGVNTEFRAGDLMII TDHINF---MGTNPFLIGPNDEAFGARFPDM SNAYSERLRRLAK	167
BH1532	ACGGMNRNFA PGDLMII TDHLMN---TGDNPFLIGPNVEWGFPRFPDM SNAYSERLRRLAK	170
<i>E. coli</i>	AAGSLRPEVAGSLSVALKDHIINT---MPGTPMVGILNDDRFGRFFSLANAYDAEYRALLQ	173
	* : : * : : * : : * : : * : : * : : * : : * : : * : : * : : *	
Bovine	STWQMGQRELEQEGTYVMVAGPSSFEIVAECLRLLRN LGADAVGMS TVPEVIVARHCGLRV	235
Human	STWQMGQRELEQEGTYVMVAGPSSFEIVAECLRLLRN LGADAVGMS TVPEVIVARHCGLRV	235
<i>B. halodurans</i>	EKGNLML--LKLQEGVYVANTGPVYETPAEVRMI RKLGGDAVGMSTVPEVIVARHAGLEV	227
<i>G. stearothermophilus</i>	DVANDIG--LRVREGVYVANTGPVYETPAEVRMI RKLGGDAVGMSTVPEVIVARHAGLEV	226
<i>B. subtilis</i>	KIARDLN--IPIQKGVYVANTGPVYETPAEVRRLRMSDAVGMSTVPEVIVANHAGMVR	225
BH1532	ETANRLD--IKVQKGVYAGITGPTVYMTGAELIMLRNLGGDVIGMSTVPEVIVARHAGMVR	228
<i>E. coli</i>	KVAKKEG--PPLTEGVYVSYPGPNFEAEEIRMMQIIGGDVVGMSTVPEVIVARHCGLRV	231
	: : : * : : * : : * : : * : : * : : * : : * : : * : : *	
Bovine	FGFSLITNKVIMDYESQKANKHEEVL EAGKQAQKLEQFVSLMASIPVSGHT	289
Human	FGFSLITNKVIMDYESLEKANKHEEVL AAGKQAQKLEQFVSLMASIPVSGHT	289
<i>B. halodurans</i>	LGISCSISNAAGILDQP--LSHDEVIEETTERVQDFLNLVKAIVKDM-----	272
<i>G. stearothermophilus</i>	LGISCSISNAAGILDQP--LTHDEVIEETTERVQDFLNLVKAIVRNMKN----	274
<i>B. subtilis</i>	LGISCSISNAAGILDQP--LTHDEVMEVTEKVKAGFLKLVKAIVAQYE-----	271
BH1532	IGISCSITDMAIGEEIAG--ITHEVAVANKTKPKF IKLVKEIVANVNV-----	275
<i>E. coli</i>	VAVSAITNMAEGLSDVK--LSHAQTALAAELSKQNF INLICGFLRKA-----	277
	... * : : : * : : * : : * : : * : : * : : * : : * : : * : : *	

aligned using ClustalW (Larkin et al. 2007). Amino acids known to be involved in the activity of the bovine and human enzymes (Lewkowicz and Iribarren 2006; Ealick et al. 1990) were generally conserved, with the exception of Tyr¹⁹², Ser²³⁴, Met²³⁶ and Ala²³⁷ in BHPNP1 and Cys¹¹⁵, Tyr¹⁹³, Met¹⁹⁴, Ile²¹⁰, Asp²³⁶, Met²³⁷ and Ala²³⁸ in BH1532. These were all conservative substitutions with the exception of Met²³⁶ (BHPNP1), Cys¹¹⁵, Met¹⁹⁴ and Met²³⁷ (BH1532). The position and orientation of these residues are shown in Fig. 3. Hence, it is likely that the active site, and overall tertiary structure, of BHPNP1 should resemble the bovine and human PNPases and is, therefore, likely to be a homotrimer. The structure of BHPNP1 was, hence, modelled based on the structure of the bovine PNPase (Fig. 3). This structure shows the modelled monomer, including a putative substrate, namely hypoxanthine. Residues that are known to be important in structure and function of the mammalian proteins and are conserved in BHPNP1 are indicated in yellow. Residues that are known to be important in structure and function of the mammalian proteins and are not conserved in BHPNP1 are indicated in red.

Tertiary conformation

BHPNP1 and *G. stearothermophilus* PNP1 are 74.9% identical. These proteins are likely to have similar

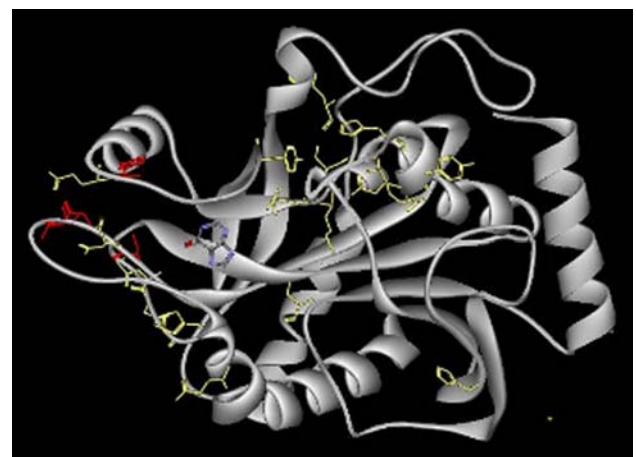


Fig. 3 Homology modelled three-dimensional structure of BHPNP1. Homology modelling of the BHPNP1 structure was performed using the bovine structure 1VFN (Koellner et al. 1997) as a template. The monomer was modelled along with the substrate, hypoxanthine

structural characteristics. As already mentioned by Hamamoto et al. (1997b), the high level of sequence identity between the *G. stearothermophilus* PNP1 and the eukaryotic PNPases strongly suggest structural similarity. This would also apply to the BHPNP1 protein. However, gel filtration analysis of the *G. stearothermophilus* PNP1 gave

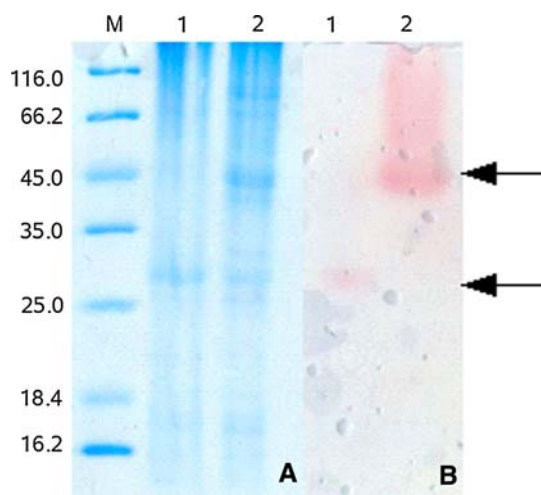


Fig. 4 12% SDS PAGE gel (a) and corresponding activity gel overlay (b). *M* marker, lane 1 heat-treated PNPase preparation (95°C, 5 min); lane 2 non-heat-treated PNPase preparation. Arrows indicate the position of the monomer and the dimer

an apparent molecular weight of 68,000, potentially indicating a dimeric protein (Hori et al. 1989b).

To confirm whether BHPNP1 is a trimer, which the sequence data suggests, or a dimer based on information about *G. stearothermophilus* PNP1 an overlay experiment was performed. The stained gel and overlay are shown in Fig. 4. The experiment indicated that the predominant tertiary confirmation was a dimer. The expected monomeric subunit was visible in both the heat-treated and non-heat-treated samples at approximately 27 kDa. Another dominant band at approximately 50 kDa on the Coomassie stained gel (lane 2, Fig. 4a) was related to the active band on the overlay (lane 2, Fig. 4b). Hence, in contrast to the mammalian system, this enzyme appears to be dimeric.

Enzyme expression and purification

The productivity of *B. halodurans* Alk36 BHPNP1 heterologously expressed in *E. coli* JM109 (DE3) was 700 U/l/h in shake flasks, but increased to 3,007 U/l/h under the controlled fermentation conditions. PNPase was purified to 42% purity (by density analysis in SDS-PAGE, Fig. 5) and a specific activity of 30.2 U/mg total protein with a fold purification of 5.0 from the culture broth (Table 2).

Physical characteristics

PNPase showed a pH optimum of 7.0, retaining 60% activity between pH 5.7 and 7.4 (Fig. 6). PNPase had optimum activity at 70°C and a broad activity range, retaining 60% activity between 30 and 74°C (Fig. 7). Although the optimum temperature of PNPase was shown to be 70°C, only 7.2% activity remained after 30 min

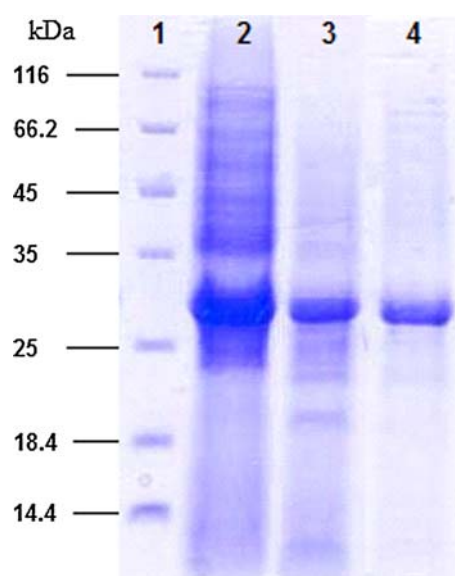


Fig. 5 Denaturing SDS-PAGE gel (12%) showing successive purification steps. Various fractions from a purification of BHPNP were resolved using 12% SDS-PAGE. Lane 1 protein marker sizes in kilodaltons, lane 2 crude extract, lane 3 concentrated sample after anion exchange column 1, lane 4 final sample after anion exchange column 2

incubation at this temperature ($t_{1/2}$ – 15.2 min). PNPase did, however, show good stability at 60°C ($t_{1/2}$ – 20.8 h) and excellent stability at 40°C, with no change in activity over the time period (19 h).

Kinetic characterisation

Linear transformation of velocity data obtained for varying initial substrate concentrations showed good linear regression fit where inosine was used ($R^2 > 99\%$ for all plots) and adequate fit for guanosine experiments ($R^2 > 94\%$). From the plots (Lineweaver–Burk, Eadie–Hofstee and Hanes–Wolf), K_m and V_{max} were determined with <7% deviation in the values calculated from the three plots. Subsequently, the turnover number (k_{cat}) and the specificity constant were calculated. These values are summarised in Table 3.

The PNP1 from the thermophile *G. stearothermophilus* has been previously expressed and characterised (Hori et al. 1989a; Hamamoto et al. 1997a). The *G. stearothermophilus* enzyme has a *pI* of 4.7, with an optimal pH range between 7.5 and 11, in contrast to the optimal pH range of BHPNP1 of between 5.7 and 8.4 and a predicted *pI* of 5.1. The *G. stearothermophilus* PNPase is more thermostable than BHPNP1 as it is stable at 70°C for greater than 30 h. In contrast, the half life of PNPase BHPNP1 at 60°C is 20 h. *G. stearothermophilus* PNPase K_m for inosine was similar at 0.22 mM, but had a greater affinity for guanosine at K_m of 0.14 mM.

Table 2 Fold purification table for the purification of recombinant BHPNP1

	Total units	Specific activity	Percentage of recovery (%)	Fold purification
Initial culture (intracellular)	4,840	6.93	100.00	1.00
Lyophilised crude extract	732	20.65	15.12	2.97
Ion exchange 1 (0–500 mM NaCl gradient)	541	22.24	11.17	3.73
Ion exchange 2 (150–400 mM NaCl gradient)	110	30.23	2.27	4.99

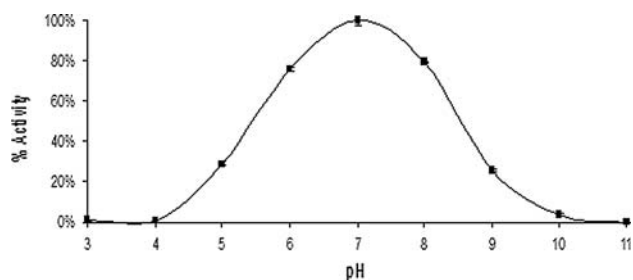


Fig. 6 pH optimum profiles of BHPNP1. A pH profile was performed using reaction mixtures (1 ml) containing 1 mM guanosine in 50 mM universal buffer (50 mM Tris, 50 mM boric acid, 33 mM citric acid; 50 mM Na₂PO₄), adjusted to pH values between 3 and 11 with either HCl or NaOH. PNPase (0.025 U) was added to initiate the reaction. After 10 min of incubation at 40°C, the reaction was stopped by the addition of 0.5 ml of a 5 M NaOH solution. Guanosine conversion and guanine formation were analysed by HPLC at 260 nm. The mobile phase was 25 mM ammonium acetate (pH 4.0), at a flow rate of 1.0 ml/min

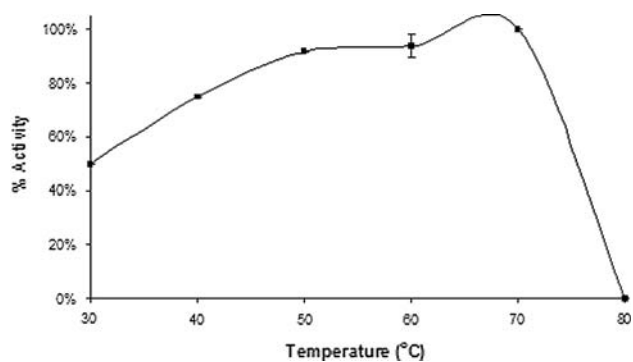


Fig. 7 Temperature optimum profile of BHPNP1. The temperature optimum of BHPNP1 was determined with reaction mixtures containing 1 mM guanosine in 50 mM sodium phosphate buffer, pH 8.0. PNPase (0.025 U) was added to initiate the reaction. After 10 min of incubation at temperatures between 30 and 90°C, the reaction was stopped by the addition of 0.5 ml of a 5 M NaOH solution. Guanosine conversion and guanine formation were analysed by HPLC

Conclusions

The thermostable type II nucleoside phosphorylase from the bacterium *B. halodurans* Alk36 was expressed heterologously in *E. coli*, purified, and functionally characterised.

Table 3 Physical and kinetic characteristics of BHPNP1

Parameter (units)	Inosine	Guanosine
Specific activity (U mg ⁻¹)	30.23	ND
K_m (μM)	236	206
V_{max} (mol s ⁻¹)	4.76×10^{-6}	2.03×10^{-9}
k_{cat} (s ⁻¹)	2.8×10^4	1.2×10^1
Specificity constant (M ⁻¹ s ⁻¹)	1.2×10^8	5.87×10^4
pH Opt	7	
pH range (60%)	5.7–8.4	
Temp Opt (°C)	70	
Temp range (60%) (°C)	32–74	
Temp stability ($t_{1/2}$ at 60°C) (h)	20.8	
Temp stability ($t_{1/2}$ at 40°C) (h)	>200	

The enzyme was capable of phosphorolysis of guanosine to yield guanine and ribose-1-phosphate, the latter of which may be used in the enzymatic glycosylation of nucleosides.

Acknowledgments We would like to thank Dr D. R. Walwyn (CEO of Arvir Technologies) for support for this project, as well as Zimkhitha Sotenjwa, Dr Anu Idicula and Dr Neeresh Rohitlall who helped lay the foundations for this research. We gratefully acknowledge the financial support, and resources from CSIR Biosciences, LIFElab and Arvir Technologies in funding this project, without which this work would not have been possible.

Open Access This article is distributed under the terms of the Creative Commons Attribution Noncommercial License which permits any noncommercial use, distribution, and reproduction in any medium, provided the original author(s) and source are credited.

References

- Altschul SF, Gish W, Miller W, Myers EW, Lipman DJ (1990) Basic local alignment search tool. *J Mol Biol* 215:403–410
- Balzer D, Ziegelin G, Pansegrau W, Kruft V, Lanka E (1992) KorB protein of promiscuous plasmid RP4 recognizes inverted sequence repetitions in regions essential for conjugative plasmid transfer. *Nucl Acids Res* 20:1851–1858
- Bzowska A, Luić M, Schröder W, Shugar D, Saenger W, Koellner G (1995) Calf spleen purine nucleoside phosphorylase: purification, sequence and crystal structure of its complex with an *N*(7)-acycloguanosine inhibitor. *FEBS Lett* 367:214–218

- Bzowska A, Kulikowska E, Shugar D (2000) Purine nucleoside phosphorylases: properties, functions, and clinical aspects. *Pharmacol Therapeut* 88:349–425
- Bzowska A, Koellner G, Wielgus-Kutrowska B, Stroh A, Raszewski G, Holý A, Steiner T, Frank J (2004) Crystal structure of calf spleen purine nucleoside phosphorylase with two full trimers in the asymmetric unit: important implications for the mechanism of catalysis. *J Mol Biol* 342:1015–1032
- Crampton M, Berger E, Reid S, Louw M (2007) The development of a flagellin surface display expression system in a moderate thermophile, *Bacillus halodurans* Alk36. *Appl Microbiol Biotechnol* 75:599–607
- Dandanell G, Szczepanowski RH, Kierdaszuk B, Shugar D, Bochtler M (2005) *Escherichia coli* purine nucleoside phosphorylase II, the product of the *xapA* gene. *J Mol Biol* 348:113–125
- Ealick SE, Rule SA, Carter DC, Greenhough TJ, Babu YS, Cook WJ, Habash J, Helliwell JR, Stoeckler JD, Parks RE Jr (1990) Three-dimensional structure of human erythrocytic purine nucleoside phosphorylase at 3.2 Å resolution. *J Biol Chem* 265:1812–1820
- Erion MD, Takabayashi K, Smith HB, Kessi J, Wagner S, Hönger S, Shames SL, Ealick SE (1997) Purine nucleoside phosphorylase. 1. Structure–function studies. *Biochemistry* 36:11725–11734
- Ge C, Ouyang L, Ding Q, Ou L (2009) Co-expression of recombinant nucleoside phosphorylase from *Escherichia coli* and its application. *Appl Biochem Biotechnol* 159:168–177
- Hamamoto T, Noguchi T, Midorikawa Y (1996) Purification and characterization of purine nucleoside phosphorylase and pyrimidine nucleoside phosphorylase from *Bacillus stearothermophilus* TH 6-2. *Biosci Biotechnol Biochem* 60:1179–1180
- Hamamoto T, Okuyama K, Noguchi T, Midorikawa Y (1997a) Cloning and expression of purine nucleoside phosphorylase I gene from *Bacillus stearothermophilus* TH 6-2. *Biosci Biotechnol Biochem* 61:272–275
- Hamamoto T, Noguchi T, Midorikawa Y (1997b) Cloning of purine nucleoside phosphorylase II gene from *Bacillus stearothermophilus* TH 6-2 and characterization of its gene product. *Biosci Biotechnol Biochem* 61:276–280
- Hori N, Watanabe M, Yamazaki Y, Mikami Y (1989a) Purification and characterisation of thermostable purine nucleoside phosphorylase of *Bacillus stearothermophilus* JTS 859. *Agric Biol Chem* 53:2205–2210
- Hori N, Watanabe M, Yamazaki Y, Mikami Y (1989b) Purification and characterization of second thermostable purine nucleoside phosphorylase in *Bacillus stearothermophilus* JTS 859. *Agric Biol Chem* 53:3219–3224
- Hori N, Watanabe M, Yamazaki Y, Mikami Y (1989c) Synthesis of 5-methyluridine by a thermophile, *Bacillus stearothermophilus* JTS 859. *Agric Biol Chem* 53:197–202
- Hori N, Watanabe M, Sunagawa K, Uehara K, Mikami Y (1991) Production of 5-methyluridine by immobilized thermostable purine nucleoside phosphorylase and pyrimidine nucleoside phosphorylase from *Bacillus stearothermophilus* JTS 859. *J Biotechnol* 17:121–131
- Koellner G, Luić M, Shugar D, Saenger W, Bzowska A (1997) Crystal structure of calf spleen purine nucleoside phosphorylase in a complex with hypoxanthine at 2.15 Å resolution. *J Mol Biol* 265:202–216
- Larkin MA, Blackshields G, Brown NP, Chenna R, McGettigan PA, McWilliam H, Valentin F, Wallace IM, Wilm A, Lopez R, Thompson JD, Gibson TJ, Higgins DG (2007) Clustal W and Clustal X version 2.0. *Bioinformatics* 23:2947–2948
- Lewkowicz E, Iribarren A (2006) Nucleoside phosphorylases. *Curr Org Chem* 10:1197–1215
- Louw ME, Reid SJ, Watson TG (1993) Characterization, cloning and sequencing of a thermostable endo-(1, 3-1, 4) beta-glucanase-encoding gene from an alkaliphilic *Bacillus brevis*. *Appl Microbiol Biotechnol* 38:507–513
- Lovett PS, Keggins KM (1979) *Bacillus subtilis* as a host for molecular cloning. *Method Enzymol* 68:342–357
- Mao C, Cook WJ, Zhou M, Koszalka GW, Krenitsky TA, Ealick SE (1997) The crystal structure of *Escherichia coli* purine nucleoside phosphorylase: a comparison with the human enzyme reveals a conserved topology. *Structure* 5:1373–1383
- Mao C, Cook WJ, Zhou M, Federov AA, Almo SC, Ealick SE (1998) Calf spleen purine nucleoside phosphorylase complexed with substrates and substrate analogues. *Biochemistry* 37:7135–7146
- Medici R, Porro MT, Lewkowicz E, Montserrat J, Iribarren AM (2008) Coupled biocatalysts applied to the synthesis of nucleosides. *Nucleic Acids Symp Ser* 2008:541–542
- Montgomery JA, Niwas S, Rose JD, Secrist JA, Babu YS, Bugg CE, Erion MD, Guida WC, Ealick SE (1993) Structure-based design of inhibitors of purine nucleoside phosphorylase. 1. 9-(aryl-methyl) derivatives of 9-deazaguanine. *J Med Chem* 36:55–69
- Narayana SV, Bugg CE, Ealick SE (1997) Refined structure of purine nucleoside phosphorylase at 2.75 Å resolution. *Acta Crystallogr D* 53:131–142
- Prasad A, Trikha S, Parmar V (1999) Nucleoside synthesis mediated by glycosyl transferring enzymes. *Bioorg Chem* 27:135–154
- Pugmire MJ, Ealick SE (2002) Structural analyses reveal two distinct families of nucleoside phosphorylases. *Biochem J* 361:1–25
- Rocchetti S, Ubiali D, Terreni M, Albertini AM, Fernández-Lafuente R, Guisán JM, Pregnolato M (2004) Immobilization and stabilization of recombinant multimeric uridine and purine nucleoside phosphorylases from *Bacillus subtilis*. *Biomacromolecules* 5:2195–2200
- Saunders PP, Wilson BA, Saunders GF (1969) Purification and comparative properties of a pyrimidine nucleoside phosphorylase from *Bacillus stearothermophilus*. *J Biol Chem* 244:3691–3697
- Schuch R, Garibian A, Saxild HH, Piggot PJ, Nygaard P (1999) Nucleosides as a carbon source in *Bacillus subtilis*: characterization of the *drm-pupG* operon. *Microbiology* 145:2957–2966
- Takami H, Nakasone K, Takaki Y, Maeno G, Sasaki R, Masui N, Fuji F, Hiramata C, Nakamura Y, Ogasawara N, Kuhara S, Horikoshi K (2000) Complete genome sequence of the alkaliphilic bacterium *Bacillus halodurans* and genomic sequence comparison with *Bacillus subtilis*. *Nucleic Acids Res* 28:4317–4331
- Tonon G, Capra E, Orsini G, Zuffi G (2004) Novel immobilized biocatalysts usable for the production of natural nucleosides and modified analogues by enzymatic transglycosylation reactions. US Patent Number 20040142438
- Utagawa T (1999) Enzymatic preparation of nucleoside antibiotics. *J Mol Catal B Enzym* 6:215–222
- Williams SR, Goddard JM, Martin DW (1984) Human purine nucleoside phosphorylase cDNA sequence and genomic clone characterization. *Nucleic Acids Res* 12:5779–5787

ORIGINAL ARTICLE

High-yielding cascade enzymatic synthesis of 5-methyluridine using a novel combination of nucleoside phosphorylases

DANIEL F. VISSER, KONANANI J. RASHAMUSE, FRITHA HENNESSY,
GREGORY E. R. GORDON, PETRUS J. VAN ZYL, KGAMA MATHIBA,
MOIRA L. BODE & DEAN BRADY

CSIR Biosciences, Private Bag X2, Modderfontein, 1645, South Africa

Abstract

A novel combination of *Bacillus halodurans* purine nucleoside phosphorylase (BhPNP1) and *Escherichia coli* uridine phosphorylase (EcUP) has been applied to a dual-enzyme, sequential, biocatalytic one-pot synthesis of 5-methyluridine from guanosine and thymine. A 5-methyluridine yield of >79% on guanosine was achieved in a reaction slurry at a 53 mM (1.5% w/w) guanosine concentration. 5-Methyluridine is an intermediate in synthetic routes to thymidine and the antiretroviral drugs zidovudine and stavudine.

Keywords: Purine nucleoside phosphorylase, uridine phosphorylase, biocatalysis, 5-methyluridine, fermentation, transglycosylation

Introduction

Nucleoside analogs are widely used as antiviral and anticancer drugs, where they act as inhibitors of viral replication or cellular DNA replication. The traditional synthetic routes for these compounds are often complex and inefficient multi-stage processes (Lewkowicz & Iribarren 2006). Zidovudine (AZT) and stavudine (d4T) are thymidine analogs that are approved by regulatory bodies such as the South African Medicines Control Council as part of an HIV/AIDS treatment regimen. Due to the current high cost of antiretrovirals and high incidence of HIV/AIDS in southern Africa, low-cost syntheses are needed. Chemical synthesis of both zidovudine and stavudine can be achieved using 5-methyluridine (5-MU) as a precursor (Chen et al. 1995; Shiragami et al. 1996).

Early 5-MU syntheses used toxic thymine-mercury and tri-*O*-acetyl-*D*-ribofuranosyl chloride in toluene, and subsequent deacetylation using methanolic hydrogen chloride gave low product yields (5–25%). An alternative coupling protocol using tri-*O*-benzoyl-*D*-ribofuranosyl halide (chloride or bromide) and dithymine-mercury, followed by quantitative debenzoylation using alcoholic ammonia, resulted

in enhanced yields of 50% and 36%, respectively (Fox et al. 1956; Stepanenko et al. 1973). Subsequently, in the 1980s, alternative biocatalytic syntheses for nucleosides became the focus of research (Hanrahan & Hutchinson 1992; Prasad et al. 1999; Utagawa 1999; Lewkowicz & Iribarren 2006; Mikhailopulo 2007). 5-MU can be synthesized by means of selective biocatalytic transglycosylation of guanosine and thymine (Utagawa 1999; Figure 1). Biocatalytic transglycosylation reactions between purines and pyrimidines require the combination of pentosyltransferases such as a purine nucleoside phosphorylase (PNPase; EC 2.4.2.1) and a pyrimidine nucleoside phosphorylase (PyNPase; EC 2.4.2.2), both of which catalyze the reversible phosphorylation of nucleosides. Other enzymes that have a similar catalytic function to PyNPases (and can be referred to as PyNPases) are uridine phosphorylase (UPase; EC 2.4.2.3) and thymidine phosphorylase (TPase; EC 2.4.2.4). A particular benefit of nucleoside synthesis by enzymatic transglycosylation is the *in situ* activation of the 1' position by phosphorylation with an anomeric selectivity that results in formation of only the β -anomer of the nucleoside.

Correspondence: D. F. Visser, CSIR Biosciences, Private Bag X2, Modderfontein, 1645, Johannesburg, South Africa, 1645, Tel: +27-11-605-2748. Fax: +27-11-608-3020. E-mail: dvisser@csir.co.za

(Received 25 January 2010; revised 18 March 2010; accepted 11 May 2010)

ISSN 1024-2422 print/ISSN 1029-2446 online © 2010 Informa UK Ltd. (Informa Healthcare, Taylor & Francis AS)
DOI: 10.3109/10242422.2010.493210

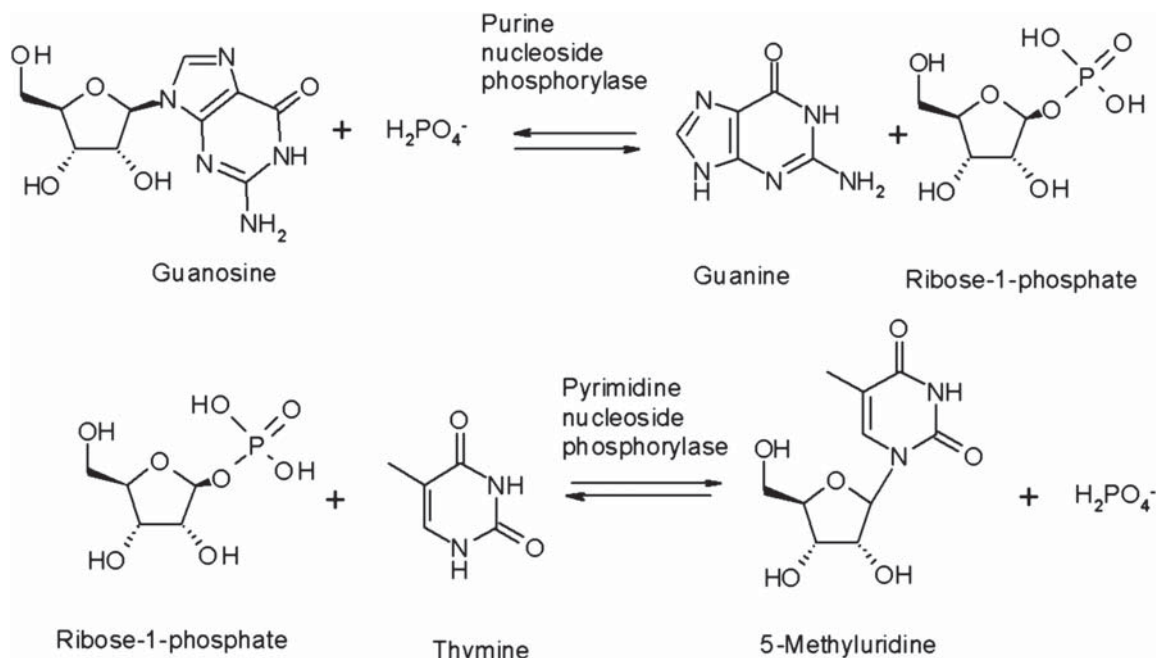


Figure 1. The component reactions in the synthesis of 5-MU from guanosine and thymine.

Other synthetic methods typically yield a mixture of the α - and β -anomers (Freskos et al. 1990; Lewkowicz & Iribarren 2006), which then need to be chromatographically separated. The equilibrium for PNPase is towards nucleoside formation for natural substrates, while PyNPase favors the phosphorolysis reaction (Erion et al. 1997; Bzowska et al. 2000; Lewkowicz & Iribarren 2006; Figure 1), and hence the majority of the work to date has focused on synthesis of purine nucleosides from pyrimidine nucleosides.

The anticipated adverse reaction equilibrium and the very low solubility of the starting substrates would suggest that synthesis of 5-MU (a pyrimidine nucleoside) would suffer from low yield and productivity. Studies using inosine as the glycosyl donor, thymine and crude enzyme were performed by Hori et al. (1989a,b), but the reaction yielded only 22% 5-MU at low substrate concentrations. Further work by the same group (Hori et al. 1991a) using immobilized enzymes showed improvements, with a continuous conversion of inosine and thymine at an initial concentration of 75 mM in the feed to give a 5-MU yield of 33%. The poor equilibrium constant of 0.24 of the overall transglycosylation reaction limited the conversion to 5-MU (Hori et al. 1991b), indicating that the reaction lacks an overall driving force towards pyrimidine synthesis. However the potential of transglycosylation was demonstrated by Ishii et al. (1989), who showed that by using guanosine in combination with thymine and whole cells of *Erwinia carotovora* it was possible to produce 5-MU at a yield of 74% from

high starting substrate concentrations (300 mM), albeit over a 48 h period. Another potentially limiting factor for enzymatic conversion is that the substrates guanosine and thymine are only sparingly soluble in aqueous solutions. As heating the aqueous solution improves the solubility, it would be preferable to utilize moderately thermostable nucleoside phosphorylases in heated reactions. In general prokaryotic PyNPase and PNPase tend to be more thermostable and have broader specificity than their mammalian counterparts (Tonon et al. 2004). A few thermostable PNPase enzymes from extremophiles have been reported and applied to the production of nucleosides (Hori et al. 1991a; Cacciapuoti et al. 2005, 2007).

Previously, we have expressed and isolated the purine nucleoside phosphorylase (BhPNP1) from the thermotolerant alkalophile *Bacillus halodurans* (Visser et al. 2010), formerly *Bacillus brevis* (Louw et al. 1993). Here we report on the combination of that enzyme with the *Escherichia coli* UPase in a one-pot cascade reaction to produce 5-MU in high yield.

Materials and methods

Assessment of nucleoside phosphorylases for production of 5-methyluridine

Demonstration of 5-methyluridine synthesis by enzymatic transglycosylation. Reactions (3 mL) with nucleoside and/or base at concentrations of 2.5 mM (Table I) were performed in phosphate buffer, pH

7.4, at 25°C over 3 h with agitation. TPase (Sigma catalog no. T2807), bacterial PNPase (Sigma catalog no. N8264) and xanthine oxidase (XO) (Sigma catalog no. X2252) were evaluated, as well as a freshly prepared crude enzyme extract of *E. coli* containing both PNPase and UPase activity.

Native enzyme production. A strain of *E. coli* was used to provide a crude native enzyme solution for initial experiments. An inoculum culture of *E. coli* JM109 was grown in 100 mL Luria broth (LB) (NaCl 10 g L⁻¹, tryptone 10 g L⁻¹, yeast extract 5 g L⁻¹) overnight at 37°C with shaking at 200 rpm. Fifteen milliliters of this culture was used to inoculate 5 × 400 mL LB in Fernbach flasks. These cultures were grown for 4 h at 37°C with shaking at 220 rpm. Two liters of culture broth were centrifuged for 10 min at 17 000g. The resultant pellet was re-suspended in 100 mL sonication buffer (20 mM Tris-HCl, pH 7.2, 5 mM ethylenediamine-*N,N,N',N'*-tetraacetic acid, 1 mM dithiothreitol) and chilled on ice for 20 min. This suspension was sonicated for 10 min at 4°C and then centrifuged for 10 min at 17 000g. Ammonium sulfate was added to the supernatant to a saturation of 40% (w/v) and stirred at 4°C for 20 min. This was centrifuged as before and additional ammonium sulfate was added to the supernatant to obtain 70% (w/v) saturation, which was again stirred on ice for 20 min. After centrifugation the pellet containing the enzymes of interest was re-suspended in 100 mL Tris-HCl buffer at pH 7.2. This preparation was desalted by ultrafiltration through a 10 kDa filtration membrane. The concentrated sample was washed with water and filtered to aid desalting. The resulting solution was lyophilized (50 mL) and a total of 710 mg of lyophilized material was obtained, which constituted the crude extract sample.

Similarly *B. halodurans*, *Klebsiella pneumoniae* and *Bacillus licheniformis* were cultivated in TYG medium (tryptone 5 g L⁻¹, yeast extract 2 g L⁻¹, glucose 1 g L⁻¹) at 40°C with shaking at 200 rpm overnight for isolation of native PyNPase (BhPyNP, KpPyNP and BIPyNP, respectively). *K. pneumoniae* and *B. licheniformis* had been identified as good PyNPase producers in a previous screening experiment (unpublished).

Biocatalytic screening. Enzyme stock solutions (0.02 U mL⁻¹) of the enzymes described above were prepared in water. Each of the enzymes was tested for the ability to produce 5-MU. The total enzyme concentration was maintained at 0.004 U mL⁻¹ for each of the experiments. Enzyme solutions and assay reagent (100 µL containing 5 mM guanosine and 5 mM thymine in 50 mM phosphate

buffer, pH 8.0) were aliquoted into a 96-well microtiter plate using an EpMotion 5075 liquid handler (Eppendorf, Hamburg, Germany). The microtiter plate was incubated for 1 h at 40°C with shaking at 900 rpm (Labsystems shaker; Thermomix, Helsinki, Finland). Results were analyzed by TLC (5 µL spot, mobile phase chloroform-methanol, 85:15 (v/v), UV₂₅₄ Silica plates (Merck, Darmstadt, Germany)).

Over-expression and preparation of selected nucleoside phosphorylases

Isolation of E. coli DNA

E. coli XL1 blue was grown overnight at 37°C in a 10 mL culture volume. A 1.5 mL aliquot of this was pelleted by centrifugation, and genomic DNA was isolated using a genomic DNA isolation kit (Fermentas Canada, Inc., Burlington, ON, Canada).

Oligonucleotides, plasmids and microbial strains

E. coli JM109 (DE3) was used as the expression host for *E. coli* PNPase1 (EcPNP1), PNPase2 (EcPNP2) and *B. halodurans* PNPase (BhPNP1). *E. coli* BL21 (DE3) was used as the production host for *E. coli* UPase (EcUP).

The PNPase gene designated *BhPNP1* was amplified and cloned as described previously (Visser et al. 2010). Isolation and cloning of the *E. coli* genes encoding PNPase and UPase was carried out as described by Lee et al. (2001) and Spoldi et al. (2001), respectively. The *E. coli* PNP2 (EcPNP2, product of the *xapA* gene) was cloned according to the methods of Dandanell et al. (2005). The amplified PCR products were subcloned initially into pGEM-T Easy and subsequently into pMS470 (EcPNP1, EcPNP2, BhPNP1) and pET20b (EcUP). The expression plasmids were then transformed into their respective expression hosts by heat shock (Sambrook & Russell 2001).

Preparation of extracts of over-expressed enzymes

Recombinant strains producing selected nucleoside phosphorylases were prepared at 700 mL scale using defined growth medium (K₂HPO₄ 14.6 g L⁻¹, (NH₄)₂SO₄ 2 g L⁻¹, Na₂HPO₄ 3.6 g L⁻¹, citric acid 2.5 g L⁻¹, MgSO₄ 0.25 g L⁻¹, NH₄NO₃ 5 g L⁻¹, yeast extract 10 g L⁻¹, glucose 30 g L⁻¹, ampicillin 100 µg mL⁻¹). Overnight cultures (100 mL) of each strain were used as the inocula for 600 mL media in 2L Fernbach flasks. Cultures were grown for 4 h at 37°C with shaking at 200 rpm before enzyme expression was induced with a final concentration of 1 mM isopropyl β-D-thiogalactopyranoside (IPTG).

Cultures were then harvested after a further 2 h growth under the same conditions.

Culture broth was centrifuged for 10 min at 17 000g. The resultant pellet was re-suspended in Bugbuster HT (Novagen, Merck KGaA, Darmstadt, Germany) containing lysozyme (USB, Cleveland, OH, USA) at 3 mg mL⁻¹ and incubated for 2 h at 30°C. Cell debris was removed by centrifugation (16 000g, 10 min). The supernatant was diluted with 20 mM Tris-HCl buffer, pH 7.2, containing 50 mM NaCl. Samples were dialyzed against the same buffer overnight. Anion-exchange chromatography of each sample was performed on an AKTA Prime (Amersham Biosciences, Bucks, UK) using Tosoh BioSep SuperQ650m resin (Tosoh, Tokyo, Japan). Proteins were eluted using a gradient of 50 to 350 mM NaCl in 20 mM Tris-HCl, pH 7.2, over 400 mL (4 mL min⁻¹). PNPase and UPase activity was assayed on all fractions (5 mL fractions collected). Fractions identified in this step for UPase and PNPase activity were separately pooled and concentrated to 2 mL by ultrafiltration (30 kDa membrane).

Enzyme production by fermentation

Organism maintenance

E. coli JM109 (pMSPNP) and *E. coli* BL21 (pETUP) were maintained as cryopreserved cultures at -70°C.

Inoculum train

Fernbach flasks containing 650 mL LB medium with 100 µg ampicillin mL⁻¹ were inoculated with 2 mL of cell bank cultures. The cultures were grown overnight and used as inocula for the fermentations. The production strain had a maximum growth rate of between 0.80 and 0.88 in the exponential phase.

Batch fermentations

Batch fermentors (B. Braun Biotech International GmbH, Melsungen, Germany) containing 10 L of GMO 20 medium were inoculated with 650 mL inoculum. The composition of the GMO 20 medium was according to Visser et al. (2010). The temperature was controlled at 37°C and the aeration set to 1 vvm (volume of air per volume of reactor per minute). The starting agitation was set at 300 rpm and ramped up manually to control the pO₂ above 30% saturation. Growth, enzyme activity and glucose utilization were measured using 10 mL samples taken at hourly intervals.

Initially *E. coli* JM109 (pMSPNP) fermentations were induced at a residual glucose concentration of between 1 and 3 g L⁻¹ at an IPTG concentration of 1.0 mM. Upon further investigation at 1L scale (data not shown), it was determined that targeting induction at mid-log growth phase based on measurements of

optical density at 660 nm ($OD_{660} \approx 7$) and at an IPTG concentration of 0.5 mM was more effective. Induction using 0.5 mM IPTG of *E. coli* BL21 (pETUP) in fermentations was at an OD_{660} of approximately 13, which was reached at 4 h.

Enzyme recovery

After fermentation, the broth was harvested and allowed to settle overnight at 4°C. The biomass was separated from the supernatant by decanting, and subjected to a freeze-thaw cycle alternating between +20°C and -20°C. Liberated soluble protein was stored at 4°C, after separation by centrifugation (14 000g, 10 min, Beckman Avante; Beckman Coulter, Inc., Fullerton, CA, USA). The pelleted biomass was re-suspended in 1 L deionized water and further disrupted using a pressure-based cell disruptor (2 Plus; Constant Systems, Daventry, UK) with one pass at 276 MPa (40 ksi) to release additional enzyme. Cellular debris was again removed by centrifugation. The combined resultant protein solutions (supernatants from freeze-thaw and cell disruption processes) were concentrated and simultaneously washed with water by ultrafiltration using a Prostack cross-flow filtration unit (30 kDa cut-off membrane; Waters Corp., Milford, MA, USA). The final preparation was lyophilized in the presence of 1% w/w maltose and 1% w/w PEG 8000 (Vertis Genesis 25 L freeze drier, Gardiner, NY, USA).

Biocatalytic reactions

Except where stated otherwise, reactions were carried out at 40°C with agitation in sodium phosphate buffer (50 mM, pH 7.4) using equivalent molar concentrations of thymine and guanosine (53 mM) and incorporating appropriate amounts of PNPase and UPase.

Analytical

Biocatalysis reaction samples were prepared by dissolving the required amount of sample in sodium hydroxide (10 M, 0.5–1 mL) and samples were then made up to the required volume so as to ensure the sample concentration was within the linear region of the calibration curve. Reaction components were quantitatively analyzed by HPLC, using a Waters Alliance model 2609 instrument (Waters Corp.) with a Synergi 4 µm Max-RP 150 mm × 4.6 mm column. Components were detected using a UV detector at 260 nm. The eluent was ammonium acetate (NH₄OAc, 25 mM), pH 4.00, flow rate 1 mL min⁻¹ and run time of 20–30 min at 25°C. Elution times were 6.5, 9.4, 17.2 and 16.7 min for guanine, thymine, 5-MU and guanosine, respectively, using authentic materials as reference standards. Guanine (98% pure, catalog no. G11950) and guanosine

(99% pure, catalog no. G-6752) were supplied by Sigma-Aldrich (St Louis, MO, USA). 5-MU (98% pure) and thymine (99% pure) were supplied by NSTU Chemicals (Hangzhou, China).

An indirect method of ribose-1-phosphate (R-1-P) analysis was used based on the acidic decomposition of R-1-P to ribose and phosphate ion. Released ribose was measured by ion chromatography at ambient temperature and run time of 10 min on a CarboPac PA10 column (4 mm×250 mm; Dionex, Bannockburn, IL, USA) using a Dionex GP40 pump fitted with a TSP AS 3500 autosampler (ThermoFinnigan, San Jose, CA, USA) and a Dionex ED40 electrochemical detector. To validate the method, the released ribose was compared with the molar concentration of guanine released in the same reaction since guanine and R-1-P are produced in equimolar concentrations during the phosphorolysis reaction.

Fermentation sampling, growth and analysis

Growth was measured by determining the optical density at 660 nm and dry cell weight (dcw) in triplicate. A volume of 2 mL of the sample was centrifuged, washed with 0.1 M HCl to remove precipitated salts, and the pellet was then used for dry cell weight determination by drying to constant weight at 110°C. Glucose concentration was measured using an Accutrend sensor (Boehringer Mannheim, Mannheim, Germany).

For determination of the enzyme activity of the biomass, triplicate samples of 1 mL were centrifuged, re-suspended in a minimum volume of the cell disruption solution B-Per (Pierce, Rockford, IL, USA) and vortexed briefly to re-suspend the pellet. After incubation at room temperature for 5 min the samples were centrifuged and the supernatant analyzed for nucleoside phosphorylase activity using the standard enzyme assays.

Enzyme assays. The method of Hwang & Cha (1973) was modified for PNPase determination wherein a suitably diluted sample (10 µL) was added to 190 µL of 50 mM sodium phosphate buffer containing 0.5 mM inosine and 0.2 U XO mL⁻¹ in UV-compatible, 96-well microtiter plates (Thermo-mix). The change in absorbance at 293 nm due to the liberation of uric acid was measured on a PowerWave HT microplate spectrophotometer (Biotek Instruments, Inc., Winooski, VT, USA). One unit of PNPase was defined as the enzyme liberating 1 µmol of uric acid from inosine per minute, in the presence of excess XO. The extinction coefficient under these conditions was determined to be 7454 cm² mol⁻¹.

The method of Hammer-Jespersen et al. (1971) was modified for UPase determination, wherein a suitably diluted sample (10 µL) was added to

190 µL of 50 mM sodium phosphate buffer containing 2.5 mM uridine in 96-well polypropylene microtiter plates. After 10 min incubation time at 40°C, the reaction was stopped by addition of 100 µL of 0.5 N perchloric acid. The samples were then incubated on ice for 20 min and centrifuged for a further 20 min (7000g) to remove residual protein. Samples (100 µL) were then transferred to a UV-compatible microtiter plate and combined with 100 µL of 1 N NaOH. The change in absorbance at 290 nm due to the liberation of uracil was measured on a PowerWave HT microplate spectrophotometer (Biotek Instruments, Inc.). One unit of UPase was defined as the enzyme required for liberation of 1 µmol of uracil from uridine. The extinction coefficient under these conditions was determined to be 3240 cm² mol⁻¹. Nucleosides were purchased from Sigma-Aldrich.

Results and discussion

Assessment of nucleoside phosphorylases for production of 5-methyluridine

The aim of the research was to develop an enzyme-based high-yielding synthesis for 5-MU. To this end initial reactions were performed to confirm the relevant enzyme activities and demonstrate the transglycosylation reaction. Results were analyzed by HPLC (Table I).

Reactions 1 and 2 were performed to confirm the reversibility and direction of equilibrium of the pyrimidine phosphorolysis, while reaction 3 confirmed purine nucleoside phosphorolysis when using PNPase in the presence of XO. XO was used to convert the co-product hypoxanthine to uric acid to prevent the reverse reaction. Reaction 4 successfully demonstrated transglycosylation using commercial enzyme preparations with transfer of deoxyribose from thymidine to hypoxanthine. However, use of the same commercial enzyme preparations for transglycosylation involving ribose transfer failed (reactions 5 and 6). This failure was presumably due to the strict requirement of TPase for deoxyribose-1-phosphate rather than R-1-P, a result that was anticipated, but required confirmation. The enzyme UPase can utilize R-1-P, but was not commercially available, and on this basis we decided to isolate UPase from *E. coli*. Through the use of native *E. coli* cell extract (which contained both PNPase and UPase activities of 0.017 and 0.012 U mg⁻¹), it was possible to generate 5-MU (reactions 7 and 8).

Combinations of partially purified nucleoside phosphorylases were screened for 5-MU production. While all combinations tested demonstrated 5-MU production (Figure 2), reactions containing either EcPNP1 or BhPNP1 combined with EcUP showed the highest production levels (lanes 1, 5, 9).

Table I. Demonstration of 5-MU synthesis by enzymatic transglycosylation (data extracted from Visser et al. 2009).

Reaction	Expected product	Starting reagents	Enzymes	Product peak (% of total peak area)
1	Thymine	Thymidine	TPase	78.5
2	Thymidine	Thymine, deoxyribose-1-phosphate	TPase	19.5
3	Hypoxanthine, xanthine	Inosine	XO, PNPase	61.7
4	2-deoxyinosine	Hypoxanthine, thymidine	TPase, PNPase	33.4
5	5-methyluridine	Thymine, Guanosine	TPase, PNPase	0
6	5-methyluridine	Inosine, thymine	XO, TPase, PNPase	0
7	5-methyluridine	Inosine, thymine	Crude extract, XO	21.8
8	5-methyluridine	Guanosine, thymine (16 h)	Crude extract	8.7

A series of experiments was then conducted to identify which enzyme system (EcPNP1/EcUP or BhPNP1/EcUP) provided the best 5-MU yield. The enzymes were over-expressed as stated in the Materials and methods section by shake-flask cultivation. EcPNP (0.85 U mg⁻¹), EcUP (0.52 U mg⁻¹) and BhPNP1 (1.41 U mg⁻¹) at final concentrations of 0.15 U mL⁻¹ each were tested in 75 mL reactions at 40°C for 25 h. 5-MU yields of 51% on guanosine were observed for the combination of the *E. coli* UPase and PNPase. However, a combination of the *B. halodurans* PNPase (BhPNP1) and the *E. coli* UPase (EcUP) gave a dramatically improved yield of 80% (Figure 3). This enzyme combination was used in all subsequent reactions.

Influence of the second reaction on the reaction equilibrium: Effect of decoupling the first reaction step

Transglycosylation can in theory occur as either a one-pot or a two-pot process, and it was of interest to determine the influence of the second reaction on overall reaction equilibrium. A phosphorolysis experiment was conducted using 53 mM guanosine, sodium

Enzyme	EcPNP1	EcPNP2	BhPNP1
EcUP	Lane 1	Lane 5	Lane 9
BhPyNP	Lane 2	Lane 6	Lane 10
BiPyNP	Lane 3	Lane 7	Lane 11
KpPyNP	Lane 4	Lane 8	Lane 12

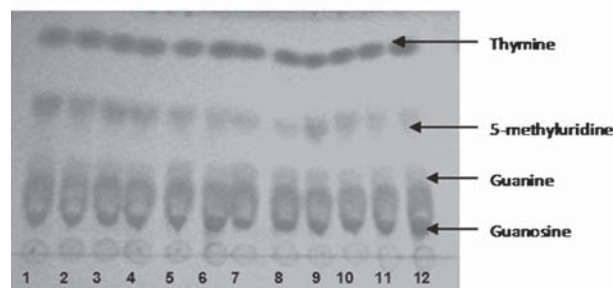


Figure 2. Comparative efficiencies of combinations of purine and pyrimidine nucleoside phosphorylases in the production of 5-MU (combinatorial enzyme reactions listed in table insert; adapted from Visser et al. 2009).

phosphate buffer and PNPase enzyme (200 U, 5.14 U mg⁻¹) to investigate the decoupling of the biocatalytic reaction.

The precipitation of guanine due to low solubility, approximately 0.01% w/v at 40°C, was expected to drive the phosphorolysis reaction to completion. However the results (Figure 4) show that a guanosine conversion of only 37% occurred. The utilization of R-1-P in the coupled reaction system thus plays a far greater role in driving the phosphorolysis reaction to completion than was anticipated. The conclusion based on these results is that the only practical means of conducting the reaction is as a coupled process. The results also indicated that ribose-1-phosphate was relatively stable under the biocatalytic reaction conditions for the duration of the reaction.

Effect of co-solvents and surfactants

At 53 mM (1.5% w/w) the substrates are well above their solubilities and therefore form slurries. The low solubility of guanosine and thymine, both around 0.1% w/v at 40°C, was considered to be a possible limiting factor in the success of the reaction. The rate of conversion of substrates in aqueous suspensions may be increased by the addition of co-solvents to increase substrate solubility. Co-solvents

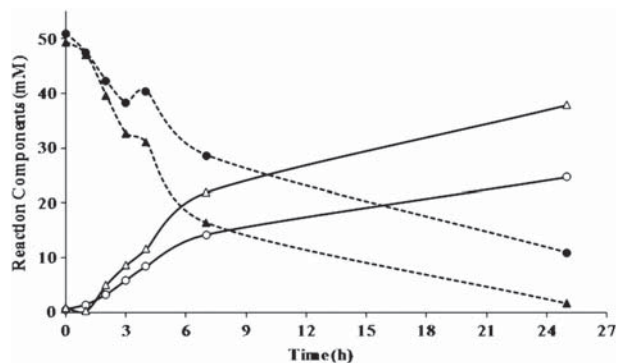


Figure 3. Guanosine conversion (●, ▲) and 5-MU production (○, △) for a combination of *E. coli* PNPase and UPase (●, ○) and *B. halodurans* PNPase and *E. coli* UPase (▲, △).

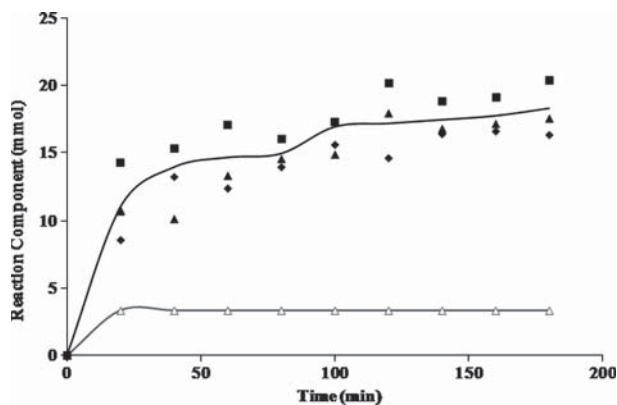


Figure 4. Guanosine phosphorolysis by PNPase in a decoupled reaction. (—) Average of guanosine converted (■), guanine (◆) and total ribose (▲). No increase in free ribose (△) in the suspension indicates that R-1-P remains stable throughout the reaction.

and surfactants have previously been demonstrated to improve reaction yields in nucleoside (Hori et al. 1991b) as well as in slurry-based reactions (Brady et al. 2004; Steenkamp & Brady 2008). Hydrophilic solvents such as methanol and ethanol, which showed moderate guanosine wetting properties, were tested. These solvents are of interest owing to their ease of removal with boiling points of 64.7°C (methanol) and 78°C (ethanol). At 53 mM, guanosine was completely soluble in 20% v/v DMSO in water, indicating that this could be a suitable reaction medium. However DMSO is generally difficult to remove from the product as high distillation temperatures are required (DMSO boiling point 189°C).

The use of non-miscible hydrophobic solvents such as toluene was not considered since this would further increase the complexity of the biocatalytic reaction, resulting in both biphasic liquids (water and toluene) and solids (guanosine, guanine and thymine).

These reactions (3 mL) were tested by adding guanosine and thymine to mixtures of co-solvent (20%

Table II. Effect of co-solvents and surfactants on the transglycosylation reaction.

Co-solvent	Guanosine conversion (%)	5-MU yield ^a (%)	Mole balance ^b (%)
Aqueous	95.1±1.3	56.4±1.7	92.3±7.4
20% v/v MeOH	90.7±2.5	61.4±4.4	92.2±7.5
20% v/v EtOH	87.7±2.3	59±9.8	87.2±14.9
20% v/v DMSO	94.3±1.1	63.3±14.0	84.4±18.4
2.5% Triton X-100	97.2±0.3	46.4±1.1	78.5±6.9
2.5% Tween 80	96.7±0.8	50.8±10.0	80.8±16.5

Experimental conditions: 53 mM guanosine, 122 mM thymine, sodium phosphate buffer (50 mM, pH 7.5–8.0), 40°C. The triplicate reactions were catalyzed by BhpNP1 0.27 U (5.14 U mg-protein⁻¹) and EcUP 0.27 U (0.2 U mg-protein⁻¹).

^a5-MU yield on guanosine at 24 h reaction.

^bMole balance for reaction, including guanosine, guanine, thymine and 5-MU.

v/v in water) or surfactant (2.5% v/v in water). The reaction mixtures were stirred at room temperature for 1 h before addition of enzyme, and then incubated for 24 h. However, addition of co-solvent or surfactant did not significantly improve the conversion of guanosine (Table II), while the influence on the 5-MU analytical results obscured any marginal increase in 5-MU yield. What is obvious is that although the guanine was completely soluble in the DMSO solution the conversion was similar to the control reaction, again indicating that precipitation of this co-product is not the main driving force of the coupled reaction.

Enzyme production

In order to prepare sufficient enzyme for larger-scale reactions, optimized fermentations (10 L) were performed for the production of BhpNP1 and EcUP (Figure 5). High levels of enzyme were produced within 8 to 10 h of fermentation. The fermentation results are summarized in Table III. Data

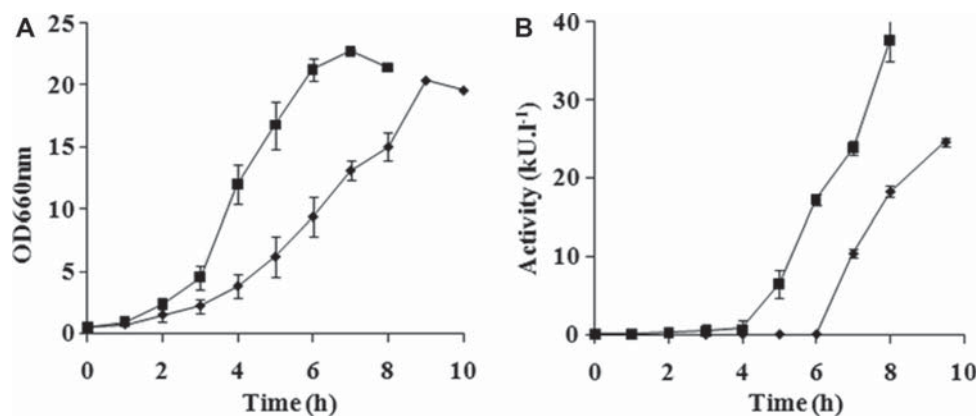


Figure 5. Growth (A) and enzyme activity (B) profiles of *E. coli* (pMSPNP) (◆) and *E. coli* (pETUP) (■) in duplicate batch fermentations.

presented are averages of duplicate fermentations. The lyophilized BhPNP1 activity (5.41 U mg^{-1}) was similar to that of the preparation used earlier (5.14 U mg^{-1}), while the EcUP preparation (4.3 U mg^{-1}) showed a more than 20-fold improvement in purity when compared to the previous preparation (0.2 U mg^{-1} used in the screening experiments).

Bench-scale biocatalytic reaction

To demonstrate the biocatalysis at bench scale, a 650 mL reaction was performed. The results obtained showed a guanosine conversion of 94.7% and a 5-MU yield of 79.1% (Figure 6) within 7 h, at a 5-MU productivity of $1.37 \text{ g L}^{-1} \text{ h}^{-1}$. The yield of this non-optimized reaction was comparable to the 74% reported by Ishii et al. (1989) using whole cells of an *Erwinia* wild-type organism, but in a much shorter time. This also demonstrated that cell free extracts are tolerant of high substrate concentrations as slurries, using starting substrate concentrations in excess of 0.1 M, which has previously only been applied in whole-cell biocatalytic reactions (Ishii et al. 1989).

Finally, to confirm the structure of the reaction product, a sample was washed with hot isopropyl alcohol, filtered and vacuum dried. NMR data for this compound: ^1H NMR (400 MHz, D_2O), δ (ppm) 7.69 (1H, s), 5.89 (1H, d, $J=4.7$ Hz), 4.33 (1H, t, $J=5.1$ Hz), 4.23 (1H, t, $J=5.4$ Hz), 4.11 (1H, dd, $J=4.2$ and 8.2 Hz), 3.91 (1H, dd, $J=2.9$ and 12.8 Hz), 3.81 (1H, dd, $J=4.2$ and 12.8 Hz), 1.87 (3H, s); ^{13}C NMR (100 MHz, D_2O), δ (ppm) 166.3, 151.6, 137.2, 111.2, 88.8, 84.0, 73.4, 69.2, 60.5, 11.4. Spectroscopic data were identical to that of a commercial standard (see Supplementary Figure S1 for ^1H NMR spectrum).

Conclusions

The biocatalytic reaction described here shows that a novel combination of nucleoside phosphorylases

Table III. Summary of fermentation data for the production of BhPNP1 and EcUP.

Value	BhPNP1	EcUP
Maximum OD (660 nm)	14.4	20.59
μ_{max}	0.43	0.60
Yield (g-dcw g-glucose $^{-1}$)	0.53	0.55
Biomass (g L $^{-1}$)	9.45	12.37
Productivity (g-dcw L $^{-1}$ h $^{-1}$)	1.16	1.62
Enzyme yield (kU L $^{-1}$)	26.9	37.7
Enzyme productivity (kU L $^{-1}$ h $^{-1}$)	3.3	5.8
Enzyme yield (kU) ^a	215	211
Specific activity (kU g $^{-1}$) ^b	5.41	4.30

^aTotal recovered units after downstream processing.

^bUnits per gram dry product after lyophilization.

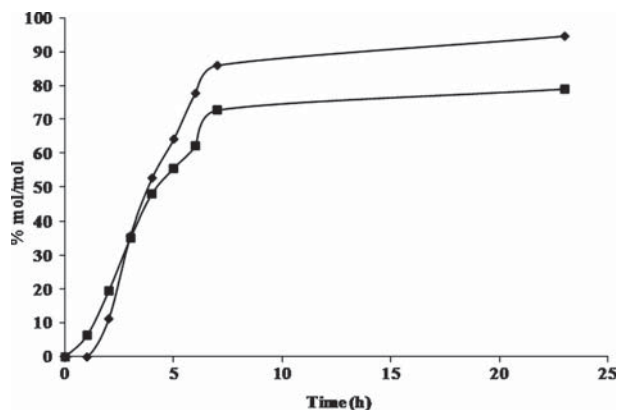


Figure 6. Bench-scale (650 mL) biocatalytic production of 5-MU containing 127 mM thymine (1.6% w/w), 53 mM guanosine (1.5% w/w), BhPNP1 (105 U) and EcUP (75 U) in 50 mM sodium phosphate buffer (pH 7.8) at 40°C. Guanosine conversion (◆) and 5-MU yield (■) are shown.

(*B. halodurans* PNPase and *E. coli* UPase) can facilitate the production of pyrimidine nucleosides from purine nucleosides in high yields. Partially purified enzyme preparations were applied in a two-step one-pot transglycosylation reaction for the production of 5-MU in a synthesis step with a molar yield of 79.1% on guanosine. Reaction engineering is anticipated to improve yield and productivity further.

Acknowledgements

The authors would like to thank N. Gumede, S. Ramchuran (LIFELab), R. Lalloo, C. van der Westhuyzen, V. Moodley, K. Pillay, D. Mabena, S. Machika and H. Manchidi (CSIR Biosciences) for technical assistance. They gratefully acknowledge Dr D. R. Walwyn (CEO of Arvir Technologies) and Dr H. Roman (CSIR) for management of the project. Financial support for this work was provided by CSIR Biosciences, LIFELab, DST and Arvir Technologies. Thanks also go to Professor D. Litthauer (University of the Free State) for the *K. pneumoniae* and *B. licheniformis* cultures. This paper is dedicated to the analytical chemist and colleague Mr Simon Machika, who passed away during this research.

Declaration of interest: The authors report no conflicts of interest. The authors alone are responsible for the content and writing of the paper.

References

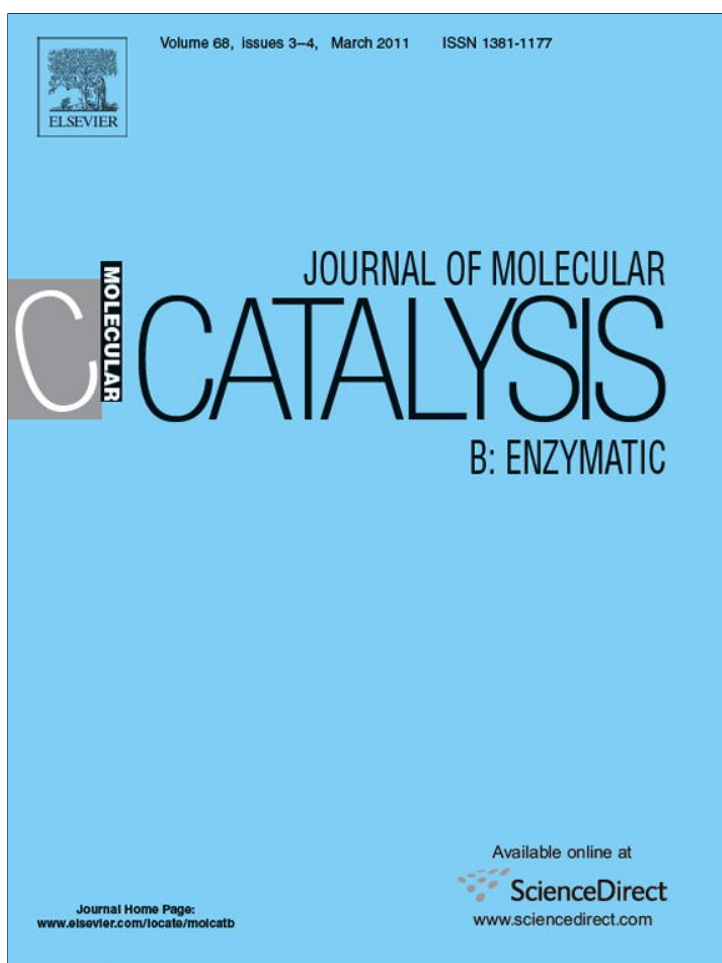
Brady D, Steenkamp L, Skein E, Chaplin JA, Reddy S. 2004. Optimisation of the enantioselective biocatalytic hydrolysis of

- naproxen ethyl ester using ChiroCLEC-CR. *Enzyme Microb Technol* 34:283–291.
- Bzowska A, Kulikowska E, Shugar D. 2000. Purine nucleoside phosphorylases: properties, functions, and clinical aspects. *Pharmacol Ther* 88:349–425.
- Cacciapuoti G, Forte S, Moretti MA, Brio A, Zappia V, Porcelli M. 2005. A novel hyperthermostable 5'-deoxy-5'-methylthioadenosine phosphorylase from the archaeon *Sulfolobus solfataricus*. *FEBS J* 272:1886–1899.
- Cacciapuoti G, Gorassini S, Mazzeo MF, Siciliano RA, Carbone V, Zappia V, Porcelli M. 2007. Biochemical and structural characterization of mammalian-like purine nucleoside phosphorylase from the archaeon *Pyrococcus furiosus*. *FEBS J* 274:2482–2495.
- Chen B-C, Quinlan SL, Gregory Reid J. 1995. A new synthesis of the anti-AIDS drug AZT from 5-methyluridine. *Tetrahedron Lett* 36:7961–7964.
- Dandanell G, Szczepanowski RH, Kierdaszuk B, Shugar D, Bochtler M. 2005. *Escherichia coli* purine nucleoside phosphorylase II, the product of the *xapA* gene. *J Mol Biol* 348:113–125.
- Erion MD, Takabayashi K, Smith HB, Kessi J, Wagner S, Hönger S, Shames SL, Ealick SE. 1997. Purine nucleoside phosphorylase. 1. Structure–function studies. *Biochemistry* 36:11725–11734.
- Fox JJ, Yung N, Davoll J, Brown GB. 1956. Pyrimidine nucleosides. I. A new route for the synthesis of thymine nucleosides. *J Am Chem Soc* 78:2117–2122.
- Freskos JN, Senaratne K, Pushpananda A. 1990. Synthesis of beta-thymidine. US patent 4,914,233.
- Hammer-Jespersen K, Munch-Petersen A, Schwartz M, Nygaard P. 1971. Induction of enzymes involved in the catabolism of deoxyribonucleosides and ribonucleosides in *Escherichia coli* K 12. *Eur J Biochem* 19:533–538.
- Hanrahan JR, Hutchinson DW. 1992. The enzymatic-synthesis of antiviral agents. *J Biotechnol* 23:193–210.
- Hori N, Watanabe M, Yamazaki Y, Mikami Y. 1989a. Synthesis of 5-methyluridine by a thermophile, *Bacillus stearothermophilus* JTS 859. *Agric Biol Chem* 53:197–202.
- Hori N, Watanabe M, Yamazaki Y, Mikami Y. 1989b. Purification and characterization of thermostable purine nucleoside phosphorylase from *Bacillus stearothermophilus* JTS 859. *Agric Biol Chem* 53:2205–2210.
- Hori N, Watanabe M, Sunagawa K, Uehara K, Mikami Y. 1991a. Production of 5'-methyluridine by immobilized thermostable purine nucleoside phosphorylase and pyrimidine nucleoside phosphorylase from *Bacillus stearothermophilus* JTS 859. *J Biotechnol* 17:121–131.
- Hori N, Watanabe M, Mikami Y. 1991b. The effects of organic solvent on the ribosyl transfer reaction by thermostable purine nucleoside phosphorylase and pyrimidine nucleoside phosphorylase from *Bacillus stearothermophilus* JTS 859. *Biocatal Biotransform* 4:297–304.
- Hwang WI, Cha S. 1973. A new enzymatic method for the determination of inorganic phosphate and its application to the nucleoside diphosphatase assay. *Anal Biochem* 55:379–387.
- Ishii M, Shirae H, Yokozeki K. 1989. Enzymatic production of 5-methyluridine from purine nucleosides and thymine by *Erwinia cartovora* AJ-2992. *Agric Biol Chem* 53:3209–3218.
- Lee J, Filosa S, Bonvin J, Guyon S, Aponte R, Turnbull J. 2001. Expression, purification, and characterization of recombinant purine nucleoside phosphorylase from *Escherichia coli*. *Protein Expr Purif* 22:180–188.
- Lewkowicz ES, Iribarren AM. 2006. Nucleoside phosphorylases. *Curr Org Chem* 10:1197–1215.
- Louw ME, Reid SJ, Watson TG. 1993. Characterization, cloning and sequencing of a thermostable endo-(1,3-1,4) β -glucanase-encoding gene from an alkalophilic *Bacillus brevis*. *Appl Microbiol Biotechnol* 38:507–513.
- Mikhailopolu IA. 2007. Biotechnology of nucleic acid constituents – state of the art and perspectives. *Curr Org Chem* 11:317–335.
- Prasad AK, Trikha S, Parmar VS. 1999. Nucleoside synthesis mediated by glycosyl transferring enzymes. *Bioorg Chem* 27:135–154.
- Sambrook J, Russell DW. 2001. *Molecular cloning: A laboratory manual*. Cold Spring Harbor (NY): Cold Spring Harbor Press.
- Shiragami H, Ineyama T, Uchida Y, Izawa K. 1996. Synthesis of 1-(2,3-dideoxy- β -D-glycero-pent-2-enofuranosyl)thymine (d4t; stavudine) from 5-methyluridine. *Nucleosides Nucleotides Nucleic Acids* 15:47–58.
- Spoldi E, Ghisotti D, Cali S, Grisa M, Orsini G, Tonon G, Zuffi G. 2001. Recombinant bacterial cells as efficient biocatalysts for the production of nucleosides. *Nucleosides Nucleotides Nucleic Acids* 20:977–979.
- Steenkamp L, Brady D. 2008. Optimisation of stabilised carboxylesterase NP for enantioselective hydrolysis of naproxen methyl ester. *Process Biochem* 43:1419–1426.
- Stepanenko BN, Kaz'mina EM, Dubinkina ZS. 1973. Methods of synthesis of pyrimidine nucleosides. *Russ Chem Rev* 42:494–508.
- Tonon G, Capra E, Orsini G, Zuffi G. 2004. Novel immobilized biocatalysts usable for the production of natural nucleosides and modified analogs by enzymatic transglycosylation reactions. US Patent Application 20040142438.
- Utagawa T. 1999. Enzymatic preparation of nucleoside antibiotics. *J Mol Catal B: Enzym* 6:215–222.
- Visser DF, Gordon G, Bode ML, Hennessy F, Rashamuse K, Louw ME, Brady D. 2009. A biocatalytic method for synthesis of 5-methyluridine. Patent number: WO2010055369.
- Visser DF, Hennessy F, Rashamuse K, Louw M, Brady D. 2010. Cloning, purification and characterisation of a recombinant purine nucleoside phosphorylase from *Bacillus halodurans* Alk36. *Extremophiles* 14:185–192.

Supplementary material available online

Supplementary Figure S1. Proteon NMR spectrum of 5-MU produced by the biocatalytic method described in this paper.

Provided for non-commercial research and education use.
Not for reproduction, distribution or commercial use.



This article appeared in a journal published by Elsevier. The attached copy is furnished to the author for internal non-commercial research and education use, including for instruction at the authors institution and sharing with colleagues.

Other uses, including reproduction and distribution, or selling or licensing copies, or posting to personal, institutional or third party websites are prohibited.

In most cases authors are permitted to post their version of the article (e.g. in Word or Tex form) to their personal website or institutional repository. Authors requiring further information regarding Elsevier's archiving and manuscript policies are encouraged to visit:

<http://www.elsevier.com/copyright>



Contents lists available at ScienceDirect

Journal of Molecular Catalysis B: Enzymatic

journal homepage: www.elsevier.com/locate/molcatbStabilization of *Escherichia coli* uridine phosphorylase by evolution and immobilizationDaniel F. Visser^{a,b,*}, Fritha Hennessy^a, Justice Rashamuse^a, Brett Pletschke^b, Dean Brady^a^a CSIR Biosciences, Pvt Bag X2, Modderfontein, Johannesburg 1645, South Africa^b Department of Biochemistry, Microbiology and Biotechnology, Rhodes University, PO Box 94, Grahamstown 6140, South Africa

ARTICLE INFO

Article history:

Received 14 September 2010

Received in revised form

24 November 2010

Accepted 26 November 2010

Available online 2 December 2010

Keywords:

Biocatalysis

Transglycosylation

Directed evolution

Immobilization

Spherezyme

5-Methyluridine

ABSTRACT

Mutation and immobilization techniques were applied to uridine phosphorylase (UP) from *Escherichia coli* in order to enhance its thermal stability and hence productivity in a biocatalytic reaction. UP was evolved by iterative saturation mutagenesis. Compared to the wild type enzyme, which had a temperature optimum of 40 °C and a half-life of 9.89 h at 60 °C, the selected mutant had a temperature optimum of 60 °C and a half-life of 17.3 h at 60 °C. Self-immobilization of the native UP as a Spherezyme showed a 3.3 fold increase in thermostability while immobilized mutant enzyme showed a 4.4 fold increase in thermostability when compared to native UP. Combining UP with the purine nucleoside phosphorylase from *Bacillus halodurans* allows for synthesis of 5-methyluridine (a pharmaceutical intermediate) from guanosine and thymine in a one-pot transglycosylation reaction. Replacing the wild type UP with the mutant allowed for an increase in reaction temperature to 65 °C and increased the reaction productivity from 10 to 31 g l⁻¹ h⁻¹.

© 2010 Elsevier B.V. All rights reserved.

1. Introduction

Nucleoside analogues are widely used as antiviral and anti-cancer drugs, where they act as inhibitors of viral replication or cellular DNA replication. The antiviral compounds stavudine and AZT (azidothymidine) can be synthesized from β-thymidine, which can in turn be synthesized from 5-methyluridine (5-MU). The traditional synthetic routes for these compounds are often complex and inefficient multi-stage processes [1]. We have previously demonstrated that a combination of the purine nucleoside phosphorylase (PNP, EC 2.4.2.1) from the thermotolerant alkalophile *Bacillus halodurans* (BHPNP1) with the *Escherichia coli* uridine phosphorylase (EcUP, EC 2.4.2.3) in a one-pot cascade reaction can produce 5-MU in high yield [2,3] (Fig. 1). The optimal operating conditions, with loadings based on mass of substrate per reaction mass (m m⁻¹), were found to be 9% guanosine (378 mM) and 4.7% thymine (439 mM) at 60 °C with an enzyme loading of 2000 U l⁻¹

operating in a low shear environment. Under these conditions, a final product concentration of 84 g l⁻¹, a guanosine conversion of >95% and a 5-MU yield of 85% were achieved. An overall productivity of 10 g l⁻¹ h⁻¹ 5-MU was possible, approaching the figure of 15.5 g l⁻¹ h⁻¹ that Straathof et al. [4] indicate is the average for economic viability.

This reaction productivity could be significantly improved by increasing reaction temperature. Due to the low solubility of the reaction components the biocatalytic reaction medium is a slurry with limited solid–liquid mass transfer [3]. However, the current optimal reaction temperature of 60 °C is constrained by the low thermostability of the UP at 60 °C and higher enzyme loading is required to offset the rate of thermal deactivation. Hence it is desirable to improve the volumetric productivity of the transglycosylation reaction by enhancing the thermostability of EcUP by mutation or immobilization.

Of particular interest for rapid evolution of enzyme stability is the method developed by Reetz and co-workers [5–7] known as iterative saturation mutagenesis (ISM). The method combines the randomization of saturation mutagenesis with rational design in that the saturation is targeted at or areas of the protein that are likely to create an enhanced phenotype based on structural or catalytic information. In addition, this method represents a “rapid” form of evolution in that the libraries created are small and focused and therefore do not require extensive screening programs. Analysis of mesophilic and thermophilic enzymes shows

Abbreviations: PNP, purine nucleoside phosphorylase; PyNP, pyrimidine nucleoside phosphorylase; UP, uridine phosphorylase; BHPNP1, *Bacillus halodurans* PNP; 5-MU, 5-methyluridine; SZ, Spherezyme; EcUP, *Escherichia coli* UP; ISM, iterative saturation mutagenesis; NP-4, Nonoxyl 4.

* Corresponding author at: CSIR Biosciences, Enzyme Technologies, Pvt Bag X2, Modderfontein, Johannesburg, Gauteng 1645, South Africa. Tel.: +27 877509748; fax: +27 116083020.

E-mail address: dvisser@csir.co.za (D.F. Visser).

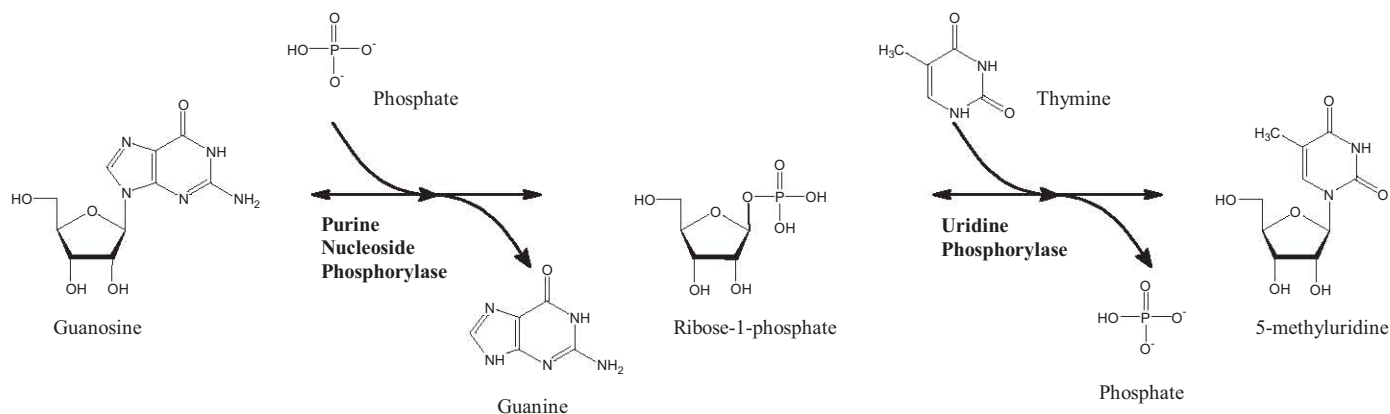


Fig. 1. Transglycosylation reaction for the production of 5-methyluridine from guanosine and thymine.

that extremophilic enzymes have a higher degree of surface rigidity. Reetz et al. [6] therefore targeted amino acids with the highest degree of flexibility indicated by atomic displacement parameters available from X-ray data, namely B-factors. The B-Factor Iterative Test (B-FIT) highlights the amino acids with the highest flexibility and thereby creates targets for mutagenesis. EcUP is a good candidate for directed evolution through ISM as the crystal structure has been determined [8,9], which simplifies the process of determining saturation targets and, as a native *E. coli* enzyme, expression of EcUP mutants is well suited for an *E. coli* expression system. Previous research of mutagenesis on pyrimidine nucleoside phosphorylases (PyNP), of which EcUP is a sub-class, was directed at discovering residues critical to folding [10] and for determining active site residues [11]. To date no mutagenesis studies have been reported for the specific enhancement of physical or catalytic characteristics of PyNP.

An alternative route to stabilization is through immobilization [12,13]. The *E. coli* UP and PNP have been co-immobilized previously by covalent linkage to epoxy-activated Sepabeads for the biocatalytic preparation of a variety of natural and modified purine nucleosides [14]. Similarly, the nucleoside phosphorylase from *Geobacillus stearothermophilus* was covalently immobilized on aminopropylated macroporous glass [15]. These preparations showed increased thermal stability and high levels of activity retention (>80%) when immobilized. Of particular interest is the work of Hori and co-workers, who immobilized PNP and PyNP from *G. stearothermophilus* by ionic binding to DEAE-Toyopearl 650 M anion exchange resin [16]. Using the immobilized biocatalysts, they were able to design a continuous reaction for the production of 5-methyluridine from inosine and thymine which was run for 17 days at 60 °C. Self-immobilization techniques, such as the Spherezyme method, are particularly suited to multimeric enzymes as they eliminate the potential of only one of the monomers binding to a carrier [12]. This study aims to show that stabilization of EcUP, through either enzyme evolution, immobilization or a combination thereof, can lead to increased reaction productivity for the synthesis of 5-MU.

2. Experimental

2.1. Materials

Thymine, guanosine, 5-methyluridine and guanine standards were purchased from Sigma (Missouri, USA). The enzymes purine nucleoside phosphorylase from *B. halodurans* (BHPNP1), uridine phosphorylase from *E. coli* (EcUP) and mutant *E. coli* UP (UPL8) were expressed in *E. coli* as *E. coli* JM109[pMSPNP], *E. coli* BL21(DE3)[pETUP] and *E. coli* BL21(DE3)[pETUPL8], respectively.

The enzymes were produced by fermentation as according to methods previously described [2,3].

2.2. Choice of saturation mutagenesis targets

The crystal structure of *E. coli* UP (1LX7) [17] was used to determine surface residues with the highest degree of flexibility, indicating potential areas of structural instability [6]. Target amino acids were identified using “B-fitter” [6]. Six regions of interest (mutant libraries 1–6) were identified for saturation mutagenesis (Fig. 2).

2.3. Mutagenesis

A QuikChange II Mutagenesis Kit (Stratagene, USA) was used to perform plasmid based mutagenesis. Primers were obtained from Inqaba Biotech (Pretoria, South Africa). To initiate the reaction, 1 μ l of *PfuTurbo* DNA polymerase (2.5 U μ l⁻¹) was added to the reaction mixes. The PCR reaction was as follows. A single hold at 95 °C for 1 min was followed by 18 cycles at 95 °C for 50 s, 55 °C for 50 s, and 68 °C for 5 min, followed by a hold at 68 °C for 7 min. *DpnI* restriction enzyme (5 μ l) was then added to each reaction and incubated for 5 h at 37 °C to digest the parental (i.e., the nonmutated) supercoiled dsDNA. The mutated plasmid was then cleaned and concentrated (Zymogen DNA clean up kit, Fermentas). Between 100 and 250 ng of this material was used to transform competent *E. coli* XL1 blue cells by heat shock (42 °C, 45 s).

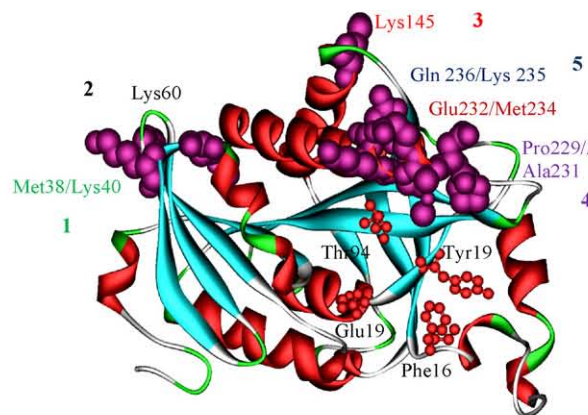


Fig. 2. Ribbon representation of *E. coli* uridine phosphorylase based on the 1LX7 structure [9]. Catalytic residues are shown in ball and stick format and sites targeted for saturation mutagenesis (1–6) based on high B-factors are in CPK format.

2.4. Preparation of mutant screening libraries

Mutant libraries were plated onto Luria agar ($100 \mu\text{g ml}^{-1}$ ampicillin) in Q-trays (Genetix, UK) and incubated overnight at 37°C . Colonies were picked and inoculated into Luria Bertani (LB) medium ($60 \mu\text{l}$, 384 well microtitre plates) using the QPix2 colony picker (Genetix, UK). The number of colonies picked ranged from 600 to 3500 per library depending on the number of colonies required to obtain coverage of all the possible mutations. A total of 12,300 clones were picked across the 6 initial libraries. After an overnight incubation, duplicate plates were prepared using the replication function of the QPix2. The replicate microtitre plates were incubated overnight and served as the back-up cultures. To the master plates, IPTG was added to a final concentration of 1 mM. These plates were incubated for a further 20 h to facilitate mutant protein expression. Cells were then harvested by centrifugation ($3000 \times g$, 20 min). The cells were broken by the addition of 15 μl B-Per (Pierce, USA) directly to the cell pellet followed by 60 min incubation at room temperature. Cell debris was removed by centrifugation ($3000 \times g$, 20 min).

2.5. Library screening

p-Nitrophenol- β -D-ribofuranoside, prepared according to the methods of Schramm et al. [18], was used as the substrate for UP screening. For 96 and 384 well microtitre plates a volume of 240 μl or 40 μl , respectively, was added to an aliquot of crude cell extract. The change in absorbance due to the release of *p*-nitrophenol was measured at 410 nm using a Powerwave HT microtitre plate reader (Biotek, USA).

Primary screening (set point residual activity): Activity of the samples was measured before and after incubation at 70°C for 15 min. The wild type *E. coli* UP showed 10% residual activity under these conditions. Hits from each of the libraries were selected based on the highest percentage residual activity.

Secondary screening (thermostability profile): Primary hits were re-inoculated into 5 ml LB broth and incubated overnight. The plasmid harboring the mutated gene was then extracted (QIAprep Spin Miniprep Kit, Qiagen, USA). This plasmid was used to transform *E. coli* XL1 blue. This new culture was then grown (50 ml LB $100 \mu\text{g ml}^{-1}$ ampicillin) and protein expression induced (0.1 mM IPTG, 3.5 h). Cells were harvested by centrifugation ($3000 \times g$, 20 min) and disrupted by addition of B-Per (4 ml per gram wet weight). After removal of cellular debris, the expressed protein was further purified by ultrafiltration through a 100 kDa membrane (Amicon, USA). The resultant protein solutions were then incubated at temperatures between 40 and 80°C for 60 min to determine the temperature at which 50% of the initial activity was retained ($T_{50}^{60(\text{min})}$ value).

2.6. Iterative mutagenesis

The plasmid expressing the mutated enzyme showing the highest stability after the first round of mutagenesis was used as the template for the second round of mutagenesis. In this case a strain from library 5 showed the highest residual activity after a 15 min incubation at 70°C (95% activity retained). The plasmid harboring this mutated gene was used in a PCR with the mutation primers for library 4 and library 1, which had given the next two best hits, respectively. The second round of saturation mutagenesis and subsequent screening was performed as described above. Plasmid DNA from the best results from each of the mutation experiments was isolated and sequenced as before (Inqaba Biotech).

The plasmid for the best mutant (UPL8 from library 8) was isolated from the *E. coli* XL1 blue strain (QIAprep Spin Miniprep Kit,

Qiagen, USA) and retransformed by heat shock (45°C , 45 s) into competent *E. coli* BL21 (DE3) for over expression and production of the mutant enzyme. This strain was designated *E. coli* BL21 (DE3)[pETUPL8].

2.7. Production and characterization of UPL8

The mutant enzyme was produced in two 10 l fermentations and purified as described previously [3]. Characterization of UPL8 was performed according to a modified method of Hammer-Jespersen et al. [20] wherein a suitably diluted broth sample (10 μl) was added to 190 μl of 50 mM sodium phosphate buffer containing 2.5 mM uridine, in 96 well polypropylene microtitre plates. After 10 min incubation at 40°C , the reaction was stopped by addition of 100 μl of 0.5 M perchloric acid. The samples were then incubated on ice for 20 min and centrifuged for 20 min ($7000 \times g$) to remove residual protein. Sample (100 μl) was then transferred to a UV compatible microtitre plate and combined with 100 μl of 1 N NaOH. The change in absorbance at 290 nm due to the liberation of uracil was measured on a Powerwave HT microplate spectrophotometer. One unit (U) of UPase was defined as the enzyme required for liberation of 1 μmol of uracil from uridine. The extinction coefficient under these conditions was determined to be $3240 \text{ M}^{-1} \text{ cm}^{-1}$. For pH profiling the phosphate buffer in the standard assay was replaced with Universal buffer [21] (50 mM Tris, 50 mM boric acid, 33 mM citric acid, 50 mM Na_2PO_4 , adjusted with either HCl or NaOH to pH values between 3 and 11). Temperature profiling was performed using the standard assay between temperatures of 30°C and 90°C . Thermostability was determined by incubating enzyme solutions (wild type UP and UPL8) at 60°C or 70°C . Samples were analyzed for activity over a 6 h period. UPL8 kinetic parameters were determined using the standard assay, with uridine initial concentrations varying between 0.1 mM and 5.0 mM. The reaction was stopped at 1, 2, 3, 4, 6 and 10 min for selection of data within the linear range. Michaelis–Menten plots and the linear transformations (Lineweaver–Burk, Hanes–Woof and Eadie–Hofstee) were used to determine kinetic parameters.

2.8. Enzyme immobilization

The enzymes were immobilized as Spherezymes [22]. This technique uses a water in oil emulsion and addition of a protein cross-linking agent to generate spherical self-immobilized macromolecular biocatalysts. Solutions (2 ml) of EcUP (100 mg ml^{-1}), UPL8 (100 mg ml^{-1}) and BHPNP1 (70 mg ml^{-1}) were prepared. In addition, mixtures (2 ml) of EcUP and BHPNP1 (60 and 70 mg, respectively) as well as UPL8 and BHPNP1 (85 and 70 mg, respectively) were prepared for co-immobilization studies. Active site protectants (50 mM inosine and/or 50 mM uridine) were combined to the solution directly prior to cross linking. To these solutions, 320 μl of the cross linker, which consisted of equal volumes of glutaraldehyde (25% solution) and polyethyleneimine (5% solution), was added, mixed and then directly added to 20 ml of the oil phase (mineral oil with 0.05% NP-4). The solutions were stirred at 700 rpm with a magnetic stirrer for 1 min to ensure a proper emulsion. Stirring was then decreased and the emulsion was allowed to incubate overnight at 4°C . The emulsion was then broken and the particles recovered by centrifugation (Beckman J-21, $1000 \times g$, 10 min). Immobilized enzyme particles were washed 4 times with 50 mM Tris–HCl, pH 8.0, containing 1 mM ethanolamine. Excess ethanolamine was washed off with the same Tris buffer. Finally, the immobilized enzyme particles were recovered by filtration under vacuum (Whatman No. 1). The immobilized enzyme particles were then dried at room temperature under high vacuum (Virtis Genesis 25L freeze dryer, USA).

Table 1
Best hits from libraries UP 7 and UP 8 based on residual activities observed after incubation of the enzyme preparations for 1 h at 75 °C.

Library	Mutant	Observed mutation	% Residual activity
Control	n/a	n/a	3.70%
7	UPL7	Met38Val; Lys40Asp Lys235Arg; Gln236Ala	88.5%
8	UPL8	Lys235Arg; Gln236Ala	80.2%

2.9. Transglycosylation by stabilized enzyme preparations

A series of transglycosylation experiments were performed to compare various combinations of biocatalysts. Reactions (100 ml) contained 1.5% m m⁻¹ loading of guanosine and thymine in 50 mM sodium phosphate buffer (pH 8.0) with 200 U l⁻¹ of each of the biocatalysts. Reactions were performed at 60 °C and 70 °C in round bottomed flasks immersed in an oil bath controlled at the set temperatures. Flasks were fitted with condensers to negate the effects of evaporation. Mixing was achieved with magnetic stirrers at 500 rpm.

2.10. Synthesis of 5-MU

The reaction (65 °C, 100 ml) contained 9.0% m m⁻¹ guanosine and 4.7% m m⁻¹ thymine suspended in 50 mM sodium phosphate buffer, pH 8.0, in a round bottomed flask fitted with a condenser. A 1000 U l⁻¹ biocatalyst loading was used. Samples (100 µl) were removed (in triplicate) hourly. The sample was diluted in 900 µl of 10 M NaOH to stop the reaction and fully dissolve the nucleosides. This solution was then further diluted in 1 M NaOH for analysis so as to ensure that the sample concentration was within the linear region of the calibration curve. Guanosine, guanine, thymine and 5-MU were quantitatively analyzed by HPLC, using a Waters Alliance Model 2609 instrument with a Synergi 4 µm Max-RP 150 mm × 4.6 mm column and compared to pure standards (Sigma–Aldrich). Components were detected using a UV detector at 260 nm. The eluent was 25 mM ammonium acetate (pH 4.0), at a flow rate of 1 ml min⁻¹ and a run time of 20–30 min at 25 °C. Elution times for guanine, thymine, 5-MU and guanosine were 6.53, 9.38, 17.20 and 19.66 min, respectively.

3. Results and discussion

3.1. Mutagenesis

The *E. coli* UP was mutated using iterative saturation mutagenesis guided by the B-Fit method [5–7], with the aim of improving thermal stability, and hence permitting application at higher temperatures with the intention of enhancing biocatalytic reaction productivity. The best hits after the primary screening were from libraries 1, 4 and 5 based on their retained activity after incubation at 70 °C for 1 h (32%, 51% and 96%, respectively). Mutation of the best hit from library 5 (Lys235Arg; Gln236Ala) with the primers for library 4 (giving library 7) and library 6 (giving library 8) again resulted in positive results in initial screening (Table 1), now performed at the elevated temperature of 75 °C for 15 min.

Determination of residual activities after incubating the mutant enzymes at set temperature for 1 h (Fig. 3) showed good stability at 70 °C for both mutants but no activity at 80 °C, skewing the final stability values. The mutant from library 8 (UPL8) showed better activity retention at 70 °C and it was therefore decided to determine the stability of that enzyme at 60 and 70 °C to get a better indication of improved thermostability (Fig. 4). These results showed marked improvements in stability at both 60 and 70 °C compared to the wild type UP.

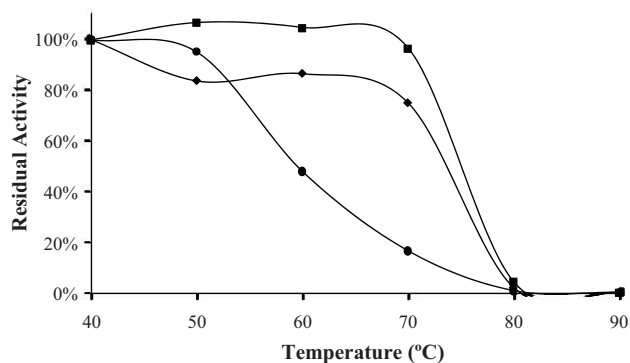


Fig. 3. Plot of residual activity for mutants UPL7 (◆) and UPL8 (■) compared to wild type UP (●). Residual activity was determined after incubation for 60 min at the set temperatures.

The characterization we performed previously [19] indicated that BHPNP1 would operate most effectively between 60 °C and 70 °C for the duration of the biocatalytic reaction. The target for directed evolution was therefore to enhance EcUP thermostability to match that of the BHPNP1. The results in Fig. 4 clearly show that this was achieved with UPL8. Although further stabilization could possibly be obtained by further rounds of mutation, it was unnecessary since further enhancements in stability would then outperform BHPNP1. It was decided therefore to continue with characterization of this mutant.

3.2. Characterization of the mutant UPL8

UPL8 showed a pH optimum of 7.0, retaining 60% activity between pH 5.6 and 8.4 which is similar to the wild type UP (optimum of 7.0, retaining 60% activity between pH 6.0 and 8.2). UPL8 has a significantly improved temperature optimum (60 °C) and a broader activity range, retaining 60% activity between 37 and 67 °C. In contrast, native UP had an optimum of 40 °C with a narrow activity range (retaining 60% activity) between 30 and 52 °C. The thermal characteristics of the modified enzyme were now similar to those of BHPNP (optimum of 70 °C, range of 30–74 °C). Wild type UP showed a half life of 9.9 h at 60 °C and inactivated almost instantaneously at 70 °C. The mutant enzyme had a half life at 60 °C of 17.3 h and 3.3 h at 70 °C (Table 2). The thermal characteristics of the modified enzyme were now similar to those of BHPNP1 (optimum of 70 °C, range of 30–74 °C) [17].

Data obtained for varying uridine concentrations also showed good linear regression fit ($R^2 \geq 0.95$). From the plots (Lineweaver–Burk, Eadie–Hofstee and Hanes–Wolf), K_M and V_{max} were determined with less than 5% deviation in the values cal-

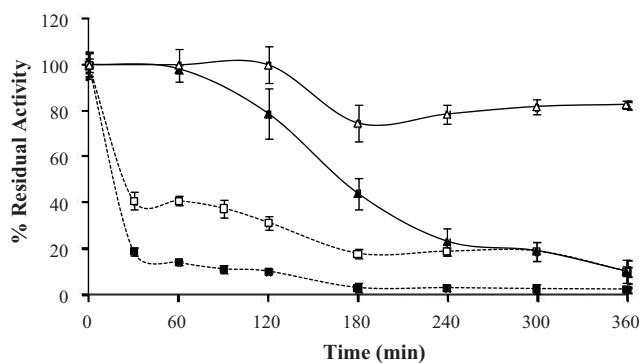


Fig. 4. Thermostability comparison for EcUP (■) and mutant UPL8 (▲). Enzyme preparations were incubated at 60 °C (open symbols) and 70 °C (closed symbols) for 6 h. Data averaged from triplicate results.

Table 2
Physical and kinetic characteristics of UPL8 and EcUP characterized using uridine as the substrate at 40 °C.

Parameter	Unit	EcUP	UPL8
Specific activity	U mg ⁻¹	30.69	19.18
K_M	μM	233.9	464.3
V_{max}	mol s ⁻¹	4.57×10^{-5}	6.46×10^{-5}
k_{cat}	s ⁻¹	2.73×10^7	2.81×10^7
Specificity constant	M ⁻¹ s ⁻¹	1.17×10^{11}	6.28×10^{10}
pH optimum	–	7.0	7.0
pH range	–	6.0–8.2	5.6–8.4
Temp optimum	°C	40	60
Temp range	°C	30–52	38–67
Temp stability ($t_{1/2}$ at 60 °C)	h	9.9	17.3
Temp stability ($t_{1/2}$ at 70 °C)	h	–	3.3

culated from the three plots. Subsequently the turnover number (k_{cat}) and the specificity constant were calculated. The data is summarized in Table 2.

3.3. Sequence and homology model analysis of the mutant UPL8

The best mutant identified from the first round of mutation was from library UP5, which targeted Lys235 and Gln236. The subsequent mutations (those from libraries UP4 and UP6) targeted Pro229, Asn230, Ala231; and Glu232, Met234 in two separate experiments, respectively. The expectation therefore would be to achieve between 2 and 7 mutations in the final mutants. The best mutant from library UP7 showed a total of 4 mutations (Table 1). These additional mutations were not necessarily beneficial as the UPL8 mutant showed only the original mutations at position 235 (Lys → Arg) and 236 (Gln → Ala), yet UPL8 was shown to be the superior mutant. This was unexpected as the Lys235Arg mutation is an exchange of similar, basic amino acids. The larger arginine should also have increased flexibility (and therefore decrease stability) at the site due to it being a longer side chain. This longer side chain may however be interacting with the neighboring α-helix, thereby conferring rigidity to the overall structure. The Gln236Ala mutation does fit with the theory of decreased flexibility due to alanine having a smaller side chain and being non-polar as opposed to the polar glutamine. Why just these two amino acid changes should have such a marked effect on the stability of the protein is unknown. Both are positioned on the α-helix leading to the N-terminal of

the protein. This entire domain may have created instability in the native protein and it is plausible that these mutations stabilized that region. This is further confirmed by the mutation in library 4, where removal of the entire α-helix yielded good thermostability characteristics. The mutations are also situated in close proximity to the entrance of the binding pocket and not associated with subunit binding, indicating that this enzyme is thermally denatured due to distortion of the active site rather than dissociation of the subunits. To prove this, an experiment was performed to determine the primary mode of thermal inactivation of the native enzyme by incubating different concentrations of the enzyme at 60 °C. Results of this experiment (data not shown) showed that the rate of inactivation is independent of enzyme concentration, indicating that distortion (and not subunit dissociation) is the primary mode of thermal inactivation. Mutations that decrease distortion would therefore show the improvement in stability noted in this research.

This mutant UP is compared in Table 3 to the few characterized wild type enzymes reported in the literature. Additionally PyNP from *B. subtilis* [23] and *T. thermophilus* [24] have been purified for crystallography studies, but no characterization was reported. The PyNP from *G. stearothermophilus* has the highest temperature optimum and thermal stability reported to date. *E. coli* UPL8 is then the next most stable PyNP. The substrate affinity of the mutant enzyme ($K_M = 0.46$ mM) is lower than both the native *E. coli* and the *G. stearothermophilus* enzymes, but is still within the micromolar range, making it significantly active towards uridine.

3.4. Enzyme immobilization

Immobilization of enzymes can lead to enhanced thermal stability [15], and hence could result in improved reactor productivity at higher temperatures where the enzyme would otherwise denature. As the enzymes EcUP, UPL8 and BHPNP1 are all multimeric, it was decided to use an immobilization method that could provide both inter-subunit bonds (to enhance multimer stability) and inter-enzyme bonds. The method used was the Spherezyme self-immobilization technique that does not require any carrier. EcUP, UPL8 and BHPNP1 were all successfully immobilized with varying degrees of activity retention using this method (Table 4). Both the immobilized EcUP (EcUP-SZ) and the EcUP co-immobilized with BHPNP1 (EcUP/BHPNP1-SZ) showed improved temperature

Table 3
Physical and kinetic characteristics of reported prokaryotic UP.

Organism	K_M (mM) (uridine)	pH optimum	Temperature optimum	Ref.
<i>E. coli</i>	0.15	7.5	37	[25]
<i>L. casei</i>	3.8	7.0	–	[26]
<i>E. carotovora</i>	–	–	60	[27]
UPL8	0.46	7.0	60	This study
<i>E. aerogenes</i>	0.7	8.52	65	[28]
<i>G. stearothermophilus</i>	0.19	7.2	70	[29,30]

Table 4
Characteristics of free and immobilized (Spherezyme) forms of EcUP, UPL8 and BHPNP1. Data for co-immobilized enzymes was determined using the uridine phosphorylase assay.

Biocatalyst	Specific activity (U mg ⁻¹)	Activity retention (%)	pH optimum	Temp optimum (°C)	Temp range (°C)
EcUP	18.3	–	7.0	40.0	30–52
EcUP-SZ	2.7	4.5	7.0	60.0	40–67
EcUP-BHPNP1-SZ	2.4	13.9	7.0	60.0	40–80
UPL8	12.3	–	7.0	60.0	40–67
UPL8-SZ	1.8	2.2	7.0	60.0	40–80
UPL8/BHPNP1-SZ	3.2	40.9	7.0	60.0	40–80
BHPNP1 ^a	8.7	–	7.0	70.0	32–74
BHPNP1-SZ ^a	1.0	25.4	7.0	50.0	40–80

^a Data determined using guanosine as the substrate.

optima and had activity at 70 and 80 °C, which had not been noted with the free enzyme. UPL8-SZ did not show an increase in the temperature optimum but did exhibit a broader thermal range, maintaining significant activity at 70 and 80 °C. Both preparations maintained the pH optimum profiles seen for the free enzymes. No significant changes were noted in either the temperature or pH optimum for BHPNP1, although the preparation did show greater activity at 80 °C than that noted for the free enzyme. In addition to the single enzyme preparations, co-immobilized combinations were also evaluated. Co-immobilizing UP with BHPNP1 seemed to increase the cross-linking efficiency and activity retention of the UP, with UPL8 and EcUP showing increase to 13.9% and 40.9% in activity retention, respectively, when immobilized with BHPNP1. The physical characteristics of the co-immobilized enzymes were similar to that of the single-immobilized preparations.

Hori and co-workers [16] immobilized 0.42 units of crude cell extract (containing PNP and PyNP) from *G. stearothermophilus* on an anion exchange resin for production of 5-MU and showed no loss on activity through immobilization. The PNP and PyNP from *G. stearothermophilus* were immobilized on a glass solid support [15] with only 30% loss in initial activity. Similar activity loss was noted for the immobilization of *E. coli* PNP and PyNP on Sepabeads [14]. In contrast, between 51 and 86% of the activity was lost on Spherezyme formation although this figure may be improved upon further optimization of the immobilization process. The advantage of immobilization by Spherezymes, however, is the high specific activity compared to other preparations. In the study by Zuffi and co-workers, specific activities (per mg of immobilized biocatalyst) were 0.18 and 0.04 U mg⁻¹ for PNP and UP, respectively. In comparison, co-immobilized BHPNP1 and UPL8 showed specific activities (per mg Spherezyme) of 0.6 and 2.6 U mg⁻¹, respectively.

3.5. Production of 5-MU by transglycosylation using free enzyme preparations

The control reaction (using BHPNP1 and EcUP at 60 °C) showed similar results to those obtained previously [2], indicating that the reaction conditions were similar (Fig. 5). Use of the mutant uridine phosphorylase (UPL8), however, showed a marked improvement in reaction productivity (5.0 g l⁻¹ h⁻¹ compared to 1.29 g l⁻¹ h⁻¹ for the control) while maintaining the same yield (73% yield compared to 75% for the control, Table 5).

Table 5
Comparative figures for guanosine conversion, 5-MU yield and reaction productivity for transglycosylation reactions using free enzyme, immobilized enzyme and co-immobilized enzyme combinations.

Rxn ^a	Biocatalysts ^b		Temp (°C)	Reaction time (h)	Guanosine conversion (% mol/mol)	5-MU yield (% mol/mol)	5-MU productivity (g l ⁻¹ h ⁻¹)
	PNP	PyNP					
1	BHPNP1	EcUP	60	8	88.9	75.6	1.29
2	BHPNP1	EcUP	70	8	44.4	0.0	0.00
3	BHPNP1	UPL8	60	2	91.1	73.1	5.00
4	BHPNP1	UPL8	70	8	44.4	0.0	0.00
5	BHPNP1-SZ	EcUP-SZ	60	7	86.7	76.8	1.50
6	BHPNP1-SZ	EcUP-SZ	70	8	57.8	29.2	0.50
7	BHPNP1-SZ	UPL8-SZ	60	8	93.3	69.5	1.19
8	BHPNP1-SZ	UPL8-SZ	70	8	75.6	70.6	1.21
9	BHPNP1-SZ	UPL8-SZ	60	2	85.7	62.7	4.16
10	BHPNP1-EcUP-SZ		60	7	82.2	65.8	1.29
11	BHPNP1-EcUP-SZ		70	8	53.3	41.4	0.71
12	BHPNP1-UPL8-SZ		60	8	86.7	80.4	1.38
13	BHPNP1-UPL8-SZ		70	8	57.8	51.2	0.88
14	BHPNP1	UPL8	65	2	79.8	76.8	31.50

^a Reactions 1–12 contained 1.5% m m⁻¹ (53 mM) guanosine and 1.5% m m⁻¹ (119 mM) thymine. Reactions 13 and 14 contained 9.0% m m⁻¹ (378 mM) Guanosine and 4.6% m m⁻¹ (439 mM) thymine.

^b Biocatalyst loading for Reactions 1–12 was 200 U l⁻¹ of each. For reactions 9, 13 and 14, 1000 U l⁻¹ was used.

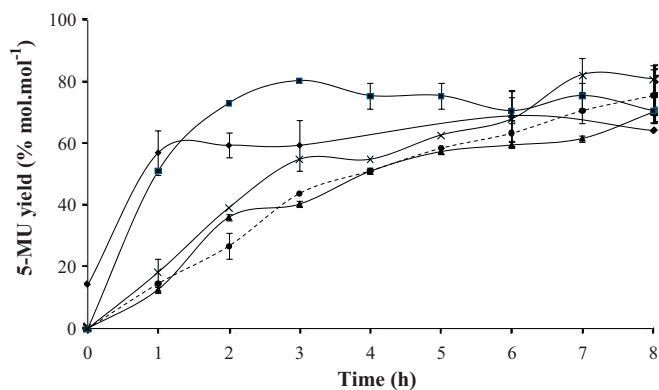


Fig. 5. Selected transglycosylation experiment showing the 5-MU yield obtained over time when using 200 U l⁻¹ free EcUP (●) or free UPL8 (■) in combination with free BHPNP1; 200 U l⁻¹ separately immobilized EcUP and BHPNP1 (×) and co-immobilized UPL8 and BHPNP1 (▲); and 1000 U l⁻¹ separately immobilized EcUP and BHPNP1 (◆). All reactions were performed using 1.5% m m⁻¹ substrate loading at 60 °C. Data averaged from triplicate samples.

3.6. Production of 5-MU by transglycosylation using immobilized preparations

The use of immobilized enzymes for this reaction could potentially have two advantages, namely an increase in stability of mesophilic enzymes allowing a higher reaction temperature, and the ability to recycle the biocatalyst to decrease the catalyst cost. The results obtained for the use of single immobilized enzymes demonstrated increased stability compared to the native EcUP, indicated by the production of 5-MU at 70 °C (Table 5). This increased stability however did not lead to a significant increase in reaction productivity at 60 °C (1.50 g l⁻¹ h⁻¹ compared to 1.29 g l⁻¹ h⁻¹ for the free enzyme control. Higher 5-MU yield was noted when using UPL8-SZ (70%, Reaction 8) compared to using EcUP-SZ (29%, Reaction 6) at 70 °C.

Co-immobilizing enzymes could be advantageous in that the proximity of the two enzymes could enhance the mass transfer characteristics of the system, thereby increasing the reaction rate while maintaining the other potential advantages discussed above. Using Spherezyme technology it was indeed possible to co-immobilize two multimeric enzymes. However similar yields and reaction productivities were seen for the co-immobilized enzymes (Reactions 10–13) when compared to the single immobilized preparations. Immobilized preparations did show higher yields at

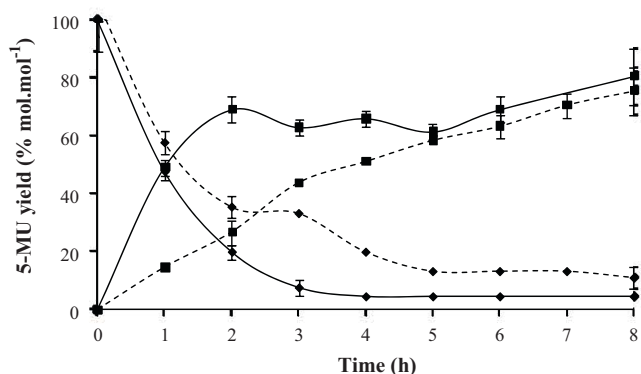


Fig. 6. Yield of 5-MU (■) and guanosine conversion (◆) over time by transglycosylation using either 2000 U l⁻¹ EcUP (broken lines) or 1000 U l⁻¹ UPL8 with equivalent amounts of BHPNP1. Reactions were performed at 60 °C (EcUP) or 65 °C (UPL8) in 50 mM sodium phosphate buffer, pH 7.5, with 9% m m⁻¹ guanosine and 4.6% m m⁻¹ thymine as the starting substrate concentrations. Data averaged from triplicate samples.

70 °C compared to free enzyme systems indicating that immobilization improved the thermal stability of the enzymes. The lower productivity observed is likely due to mass transfer limitations. An experiment was therefore performed at 1.5% m m⁻¹ substrate loading using 5 fold higher loading of UPL8-SZ and BHPNP1-SZ (1000 U l⁻¹ compared to 200 U l⁻¹) to prove that the low productivities could be improved by higher enzyme loading. This resulted in an increase in productivity to 4.16 g l⁻¹ h⁻¹ compared to 1.19 for the same reaction using 200 U l⁻¹ (Reactions 7 and 9 in Table 5, respectively).

Free UPL8 with BHPNP1 were then tested under the optimum reaction conditions determined for this process [3], namely using 9% m m⁻¹ guanosine and 4.6% m m⁻¹ thymine as starting substrate concentrations. In this experiment, however, the temperature was increased slightly to 65 °C as previous results had shown that all the biocatalysts would be stable at this temperature. In addition, the enzyme load was decreased to 1000 U l⁻¹ (compared to optimized reaction described in [3] where 2000 U l⁻¹ was used) as it was felt that the high enzyme load used in the optimized reaction was not necessary due to the increased stability of the mutant enzyme. The results in Fig. 6 and Table 5 (Reaction 14) show that use of UPL8 as free enzyme biocatalysts leads to similar 5-MU yields (76.8%) at much higher reactor productivities. The reaction was essentially complete within 2 h leading to a productivity of 31.5 g l⁻¹ h⁻¹, which is a 3-fold improvement on the optimized reaction using the native EcUP (10 g l⁻¹ h⁻¹).

4. Conclusions

Increasing the temperature of the reaction could increase productivity of 5-MU production. This required a catalyst that was more thermostable. This stability enhancement was attempted through mutagenesis and immobilization. We have shown here that it is possible to increase the thermal stability of *E. coli* UP by directed evolution, without the need for extensive screening. The mutation shown here increased the thermostability of the enzyme two-fold at 60 °C and gave a ten-fold improvement at 70 °C. This was achieved after screening fewer than 20000 clones. Small scale experiments showed that the mutant enzyme UPL8 is a superior catalyst for the production of 5-MU. The increase in stability of the mutant enzyme lead to a significant (three-fold) increase in reactor productivities while maintaining the high yields (75–80%) in the free enzyme system.

Immobilization of the enzyme led to an increase in stability for EcUP and a further increase in stability for UPL8. The yields obtained with immobilized enzymes were similar to the free enzyme preparations at 60 °C and higher than the free enzymes at 70 °C. Co-immobilized enzymes (PNP and UP), provided higher yields at 70 °C. Reactor productivity was not equivalent to the free enzyme systems at equal enzyme loading, indicating a potential mass transfer limitation. Increasing the immobilized enzyme loading however resulted in the high productivity observed in the free enzyme reaction. Considering the possibility of recycling the immobilized catalysts, such a system would then be more cost-effective than the use of free enzymes. Optimization of the immobilization method with the aim of improving activity retention will be performed in future work.

Acknowledgements

We would like to thank Dr. Moira Bode, Dr. Greg Gordon, Dr. Petrus van Zyl, Mr. Kgama Mathiba and Dr. Dave Walwyn (ARVIR) for their inputs. The research was financially supported by the CSIR Young Researchers Establishment Fund.

References

- [1] E.S. Lewkowicz, A.M. Iribarren, *Curr. Org. Chem.* 10 (2006) 1197.
- [2] D.F. Visser, K.J. Rashamuse, F. Hennessy, G.E.R. Gordon, P.J. Van Zyl, K. Mathiba, M.L. Bode, D. Brady, *Biocatal. Biotransformation* 28 (2010) 245.
- [3] G.E.R. Gordon, D.F. Visser, D. Brady, N. Raseroka, M.L. Bode, J. *Biotechnol.*, doi:10.1016/j.jbiotec.2010.11.013.
- [4] A.J.J. Straathof, S. Panke, A. Schmid, *Curr. Opin. Biotechnol.* 13 (2002) 548.
- [5] M.T. Reetz, J.D. Carballeira, J. Peyralans, H. Hobenreich, A. Maichele, A. Vogel, *Chem.: Eur. J.* 12 (2006) 6031.
- [6] M.T. Reetz, J.D. Carballeira, A. Vogel, *Angew. Chem. Int. Ed. Engl.* 118 (2006) 7909.
- [7] M.T. Reetz, J.D. Carballeira, *Nat. Protoc.* 2 (2007) 891.
- [8] E.Y. Morgunova, A.M. Mikhailov, A.N. Popov, E.V. Blagova, E.A. Smirnova, B.K. Vainshtein, C. Mao, S. Armstrong, S.E. Ealick, A.A. Komissarov, *FEBS Lett.* 367 (1995) 183.
- [9] T.T. Caradoc-Davies, S.M. Cutfield, I.L. Lamont, J.F. Cutfield, *J. Mol. Biol.* 337 (2004) 337.
- [10] I. Oliva, G. Zuffi, G. Orsini, G. Tonon, L. De Gioia, D. Ghisotti, *Enzyme Microb. Technol.* 35 (2004) 309.
- [11] D.V. Chebotayev, L.B. Gul'ko, V.P. Veiko, *Russ. J. Bioorg. Chem.* 27 (2001) 160.
- [12] D. Brady, J. Jordaan, *Biotechnol. Lett.* 31 (2009) 1639.
- [13] R. Fernandez-Lafuente, *Enzyme Microb. Technol.* 45 (2009) 405.
- [14] G. Zuffi, D. Ghisotti, I. Oliva, E. Capra, G. Frascotti, G. Tonon, G. Orsini, *Biocatal. Biotransformation* 22 (2004) 25.
- [15] S.A. Taran, K.N. Verevkin, S.A. Feofanov, A.I. Miroshnikov, *Bioorg. Khim.* 35 (2009) 822.
- [16] N. Hori, M. Watanabe, K. Sunagawa, K. Uehara, Y. Mikami, *J. Biotechnol.* 17 (1991) 121.
- [17] F.T. Burling, R. Kniewel, J.A. Buglino, T. Chadha, A. Beckwith, C.D. Lima, *Acta Crystallogr. D: Biol. Crystallogr.* 59 (2003) 73.
- [18] V. Schramm, R.H. Furneaux, P.C. Tyler, K. Clinch, *US Patent US2002/0132263 A1* (2002).
- [19] D.F. Visser, F. Hennessy, K. Rashamuse, M.E. Louw, D. Brady, *Extremophiles* 14 (2010) 185.
- [20] K. Hammer-Jespersen, A. Munch-Petersen, M. Schwartz, P. Nygaard, *Eur. J. Biochem.* 19 (1971) 533.
- [21] D.D. Perrin, B. Dempsey, *Buffers for pH and Metal Ion Control*, Halsted Press, New York, 1974, p. 38.
- [22] D. Brady, J. Jordaan, C. Simpson, A. Chetty, C. Arumugam, F.S. Moolman, *BMC Biotechnol.* 8 (2008) 8.
- [23] X.F. Gao, X.R. Huang, C.C. Sun, *J. Struct. Biol.* 154 (2006) 20.
- [24] K. Shimizu, N. Kunishima, *Acta Crystallogr. F: Struct. Biol. Cryst. Commun.* 63 (2007) 308.
- [25] J.C. Leer, K. Hammer-Jespersen, M. Schwartz, *Eur. J. Biochem.* 75 (1977) 217.
- [26] Y. Avraham, J. Yashphe, N. Grossowicz, *FEMS Microbiol. Lett.* 56 (1988) 29.
- [27] A. Zaks, D.R. Dodds, *Drug Discov. Today* 2 (1997) 513.
- [28] T. Utagawa, H. Morisawa, S. Yamanaka, A. Yamazaki, F. Yoshinaga, Y. Hirose, *Agric. Biol. Chem.* 49 (1985) 3239.
- [29] N. Hori, M. Watanabe, Y. Yamazaki, Y. Mikami, *Agric. Biol. Chem.* 53 (1989) 2205.
- [30] T. Hamamoto, T. Noguchi, Y. Midorikawa, *Biosci. Biotechnol. Biochem.* 60 (1996) 1179.